U.PORTO
UNIVERSIDADE NOVA DE LISBOA
NOVA SCHOOL OF SCIENCE & TECHNOLOGY
DEPARTAMENT OF CHEMISTRY
universidade de aveiro
theoria poiesis praxis

Integrated manufacture of liposomal dry powder formulations

Clarinda Isabel da Silva e Costa Sequeira

Master in Chemical and Biochemical Engineering

NOVA University of Lisbon
March, 2023

DEPARTAMENT OF
CHEMISTRY

Integrated manufacture of liposomal dry powder formulations

CLARINDA ISABEL DA SILVA E COSTA SEQUEIRA

Master in Chemical and Biochemical Engineering

Adviser: Ana Isabel Nobre Martins Aguiar de Oliveira Ricardo
Full Professor, NOVA School of Science and Technology of NOVA University Lisbon

Co-advisers: Maria Luísa Teixeira de Azevedo Rodrigues Corvo
Principal Investigator, Faculty of Pharmacy of University of Lisbon

Eduarda das Graças Rodrigues Fernandes
Associate Professor, Faculty of Pharmacy of University of Porto

Examination Committee:

Chair: Susana Filipe Barreiros
Full Professor, NOVA School of Science and Technology of NOVA University of Lisbon

Rapporteurs: Hermínio José Cipriano de Sousa
Associate Professor, Faculty of Sciences and Technology of University of Coimbra

Luís Miguel Borges Padrela
Lecturer, Bernal Institute of University of Limerick

Adviser: Ana Isabel Nobre Martins Aguiar de Oliveira Ricardo
Full Professor, NOVA School of Science and Technology of NOVA University of Lisbon

Members: Manuel Luís de Magalhães Nunes da Ponte
Retired Full Professor, NOVA School of Science and Technology of NOVA University of Lisbon

Maria de La Salette de Freitas Fernandes Hipólito Reis Dias Rodrigues
Full Professor, Faculty of Pharmacy of University of Porto

Eunice Margarida Santos Costa
Director of Inhalation and Advanced Drug Delivery, Hovione

DOCTORATE IN SUSTAINABLE CHEMISTRY

NOVA University of Lisbon
March, 2023

Integrated Manufacture of Liposomal Dry Powder Formulations

For those who will always be in my heart

Erikson, Matias, António & Benedita

ACKNOWLEDGMENTS

One day, someone told me that it takes a village to raise a child. She was completely right, but I would say more “It takes also a village to develop and deliver a doctoral dissertation”. Therefore, this section is dedicated to all who were "my village" during these years.

First, I would like to acknowledge my supervisors Professor Ana Aguiar-Ricardo, Doctor Luísa Corvo, and Professor Eduarda Fernandes. Professor Ana Aguiar-Ricardo, thank you so much for having believed in that 21 years old girl that applied for a small internship in your laboratory. I am grateful for the years working with you. Thank you for all the learning, and trust, for all the times you cheered me up in less good times, for the rides, for listening to me, and in moments of uncertainty for hugging me. A 'thank you' will always be too little to acknowledge you. Doctor Luísa, thank you for these years of learning and growth. If anyone helped me grow, it was you. Pharmaceutical technology was a new world for me, and I thank you for helping me with the fundamental concepts, and for tirelessly explaining the entire liposomal world to me. Professor Eduarda, unfortunately, we were not able to work as much as we would have liked, but I want to thank you for the ideas and suggestions you gave me throughout the Ph.D.

I would also like to acknowledge all my colleagues and friends at NOVA University of Lisbon. Teresa, thank you so much for all the kindness, and help with the SASD, for being always available to help me when something went wrong, and for teaching me so much about the supercritical and SASD worlds. I’m truly grateful to you. Raquel, you were like a big sister to me. You heard me, cleaned my tears, supported me, and gave me wise advice. Thank you so much. “Duplo trio da alegria” also known as Catarina, Maria, Messi, Filipa, Ana, Paninho. You are outstanding. I am so grateful for having you in my life. Thank you so much for every moment, every laugh, every lunch, every song “Mas a Pipa nos chama loucas”, thank you for all the crazy moments. I would like also to acknowledge all my colleagues and friends from the Faculty of Pharmacy: Catarina, Manuela Colla, Margarida, Jacinta, Sandra, and Manuela Gaspar. You were

incredible to me. Thank you for all your support, advice, help, and kindness in babysitting Matias in the last months so I could develop work in the lab. Catarina thank you for all the moments you worked with organic solvent and washed my HPLC vials in my turn when I was pregnant.

To Professor Manuel Nunes da Ponte, thank you for all the support and trust, especially in the first years of my Ph.D.

To Professor Madalena Dionísio for all the support and great discussions about DSC thermograms.

To Maria José Carapinha, Bárbara Costa, Isabel Rodrigues, Inês Santos, and Alexandra Carapinha thank you for all the assistance and availability to help.

To Nuno Costa and Luz Fernandes, a big, big thank you for the analytical characterization and discussions of the results. To Isabel Nogueira for being always available to perform SEM image acquisitions.

I would like also to acknowledge Professor Hélder Santos and the incredible Santos' Lab group. Professor Hélder a big thank you for having believed in my Ph.D. work and having received me in the first months of my Ph.D. You gave me incredible support during the months in Helsinki, I am so grateful. Alexandra "my Fin mother", you were incredible to me. I am grateful for the efforts you made for helping me, all the weekends you spent with me in the lab, and for teaching me how to work with HPLC and cells. To Zehua for all the learning, and support and for being a fan of my chocolate cake. Antti, Patrícia, João, Shiqi, Giulia, Wei, and Flavia thank you so much for the support and guidance.

To all my friends. Carol, Filipe, Kika, Becas, and Ana you are amazing. Thank you for all the babysitting times, the dinners, and the holidays, and thank you so much for your friendship. To Cristiana, Edson, Zénia, Eduardo, Balbina, Denis, Tasha, and Melissa, all of you will always be in my heart. Cris and Edson, thank you so much for the godson that you gave me.

To Paulo e Mariete Muginga, Águeda Jamais e João Ramires for being my mentors. A part of this thesis belongs to you.

I cannot finish these acknowledgments without thanking my family. To my parents, António and Benedita. *Pai e mãe, obrigada por tudo! Obrigada por todo o esforço, carinho, amor que me deram ao longo destes anos.*

To my beloved big sister, my brothers-in-law, nephews and nieces, my aunt Bárbara and uncle Zé, and my mother-in-law, thank you for all your love and support.

Last but not the least, for my boys: Erikson and Matias. Erikson, I have no words to thank you. You are an incredible person. Thank you for being at my side in the bad and good moments, and for celebrating with me the victories. Thank you for all the late nights you stayed at my side to help me not fall asleep during the writing and for all the time you picked me up in the lab at late hours. Thank you so much for supporting and sharing my dreams. This thesis is as much yours as mine. I am so grateful for your love, friendship, and communion. Finally, to my beloved son, Matias. In two years, you changed my life. I am grateful for being your mother. I hope someday you can be proud of me as I am proud of you little boy.

As a person of faith, I cannot finish without thanking God, for the strength, trust, and capacity over these years.

To conclude this acknowledgments section, I would also like to express my gratitude to the financial support from FCT (Fundação para a Ciência e Tecnologia) and ESF (European Social Fund) through POCH (Programa Operacional Capital Humano) for my Ph.D. grant ref. PD/BD/142880/2018, travel grant, COVID/BD/152744/2022 and Project PD/00184/2012-PDQS, respectively. I would like also to acknowledge the Doctoral Program in Sustainable Chemistry, LAQV-Requimte and CA18224 GREENERING ("Green Chemical Engineering Network towards upscaling sustainable processes"). COST Actions are funded within the EU Horizon 2020 Programme.

"Esforça-te, e tem bom ânimo; não temas, nem te espantes; porque o Senhor teu Deus é contigo, por onde quer que andares."
Josué. 1:9

"Para ser grande, sê inteiro: nada
Teu exagera ou exclui.
Sê todo em cada coisa. Põe quanto és
No mínimo que fazes.
Assim em cada lago a lua toda
Brilha, porque alta vive."
Fernando Pessoa.

ABSTRACT

Chronic respiratory diseases (CRDs) affect the airways and other structures of the lungs. CRDs are not curable, and it is estimated by the World Health Organization, 70 % of deaths under 70 years of age occur in low- and middle-income countries. Anti-inflammatory-based therapies may result in several adverse side effects. To address this problem, a synergy between pharmaceutical and supercritical carbon dioxide techniques is established for the manufacturing of inhaled enzyme and natural products-based anti-inflammatory therapies. In this work, enzyme (SOD)/quercetin (Quer) - loaded liposomal formulations were converted into liposomal dry powder formulations (Lip-DPFs) for the treatment of inflammatory lung diseases, using supercritical CO_2-assisted spray-drying (SASD). First, liposomal formulations were produced using distinct methods - microfluidics and thin-film method hydration. Microfluidics showed to be able to encapsulate both low and high molecular weight proteins, while preserving the conformational structure and enzyme activity. Secondly, a quality-by-design approach was applied towards the Lip-DPFs optimization using a low molecular weight hydrophilic dye as a model molecule. Stability studies proved that powders remain stable for 30 days at a relative humidity of 4 %. Translating the knowledge, the optimized parameters and formulations were applied to the production of SOD-loaded liposomal dry powder formulations (SOD_Lip-DPFs) for inhalation. Resuspended SOD-loaded liposomes showed structural maintenance and enzyme protection, regarding the SOD encapsulation efficiency and enzyme activity retention. SOD_Lip-DPFs showed to be able to inhalation, reaching the respiratory region, namely terminal bronchi. Finally, hydrophobic molecule-loaded liposomal dry powder formulations (Quer_Lip-DPFs) were produced with suitable aerodynamic properties. Overall, the work herein detailed represents an innovative, robust, upscaling, and time-efficient technique for drying liposomes, keeping them stable during storage and overcoming the common drawbacks of current drying and storage methods.

Keywords: biopharmaceuticals, flavonoids, liposomes, solid dosage forms, pulmonary delivery, supercritical CO_2-assisted spray-drying.

RESUMO

As doenças respiratórias crónicas (DRCs) afetam as vias aéreas e outras estruturas dos pulmões. Terapias baseadas em anti-inflamatórios podem resultar em vários efeitos colaterais adversos. Para resolver este problema, uma sinergia entre a tecnologia farmacêutica e processos de dióxido de carbono supercrítico é estabelecida para a produção de terapias anti-inflamatórias inaláveis baseadas em enzimas e produtos naturais. Neste trabalho, converteram-se as formulações lipossomais carregadas com enzima (SOD) ou quercetina (Quer) em formulações lipossomais em pó seco (Lip-DPFs) para o tratamento de doenças pulmonares inflamatórias, usando o processo de secagem por pulverização assistida pelo CO_2 supercrítico. Primeiro, as formulações lipossomais foram produzidas usando métodos distintos - microfluídica e o método de hidratação do filme fino. A microfluídica mostrou ser capaz de encapsular proteínas de baixo e alto peso molecular, preservando a estrutura conformacional e a atividade enzimática. Em segundo lugar, usando o desenho de experiências e os princípios de qualidade-por-design optimizou-se o processo de produção de Lip-DPFs usando um corante hidrofílico de baixo peso molecular como molécula modelo. Os estudos de estabilidade dos pós mostraram que o SOD_Lip-DPF manteve a estabilidade lipossomal e enzimática, por 50 dias, a uma humidade relativa de 40%. De seguida, considerando os parâmetros operacionais e as formulações otimizadas, produziram-se Lip-DPFs encapsulando SOD (SOD_Lip-DPFs). Depois de serem ressuspensos, os lipossomas contendo SOD mantiveram as cartacterísticas estruturais e capacidade de proteção da atividade enzimática. SOD_Lip-DPFs apresentaram propriedades aerodinâmicas adequadas para inalação, atingindo a região respiratória, ou seja, os brônquios terminais. Finalmente, produziram-se formulações lipossomais em pó seco carregadas com moléculas hidrofóbicas (Quer_Lip-DPFs) as quais também apresentaram propriedades aerodinâmicas adequadas. No geral, o trabalho aqui apresentado demonstra que a secagem usando a tecnologia supercrítica é inovadora, robusta, facilita o aumento de escala, é eficiente em termos de tempo para secagem dos lipossomas, mantendo-os estáveis durante o armazenamento e superando as desvantagens comuns dos métodos atuais de secagem e armazenamento.

Palavras-chave: Biofarmacêuticos, flavonoides, lipossomas, formas farmacêuticas sólidas, administração pulmonar, secagem por pulverização assistida por CO_2 supercrítico.

CONTENTS

LIST OF FIGURES

List of Tables

ACRONYMS

ANOVA	Analysis of variance
API	Active pharmaceutical ingredient.
ASES	Aerosol solvent extraction
ATR-FTIR	Attenuated total reflectance Fourier transform infrared
BCS	Biopharmaceutical classification system
CAN-BD	Carbon Dioxide-Assisted Nebulization with a Bubble Dryer
CF	5(6) – carboxyfluorescein
CF_Lip	5(6) – carboxyfluorescein- loaded liposomes
CF_Lip-DPFs	5(6) – carboxyfluorescein- loaded liposomal dry powder formulations
Chol	Cholesterol
CHT	Chitosan
CLSM	Confocal laser scanning microscopy
CO_2	Carbon dioxide.
COPD	Chronic obstructive pulmonary disease
CPP	Critical process parameter
CQA	Critical quality attribute
CysFib	Cystic fibrosis
DDS	Drug delivery system
DELOS	Depressurization of an Expanded Liquid Organic Solution

DoE	Design of experiments
DPFs	Dry powder formulations
DPI	Dry powder inhaler
DSC	Differential scanning calorimetry
DSPE-PEG$_{2000}$	Distearoylphosphatidylethanolamine-poly(ethyleneglycol)$_{2000}$
Dv$_{50}$	Mean volumetric diameter
EE	Encapsulation efficiency
E-PC	Egg-phosphatidylcholine
EPR	Enhanced permeability and retention
EtOH	Ethanol
ESCA	Electron Spectroscopy for Chemical Analysis
FDA	Food and drug administration
FD	Freeze-drying
FPF	Fine particle fraction
GSD	Geometric standard deviation
HFA	Hydrofluoroalkanes
HPMCAS-MF	Hydroxypropyl methylcellulose acetate succinate
IE	Incorporation efficiency
ICS	Inhaled corticosteroids
i.p.	Intraperitoneal
i.v.	Intravenous
Ins	Insulin
Ins_Lip	Insulin-loaded liposomes
Ins_Lip-CHT	Chitosan-coated liposomes
Ins@MPs	Insulin-loaded pH-responsive nano-in-microparticles

Leu	L-Leucine.
Lip-DPFs	Liposomal dry powder formulations
MMAD	Mass median aerodynamic diameter
N_2	Nitrogen
OOS	Optimal operating space
PCA	Precipitation with a compressed fluid anti-solvent
PdI	Polydispersity index
PDMS	Polydimethylsiloxane
PGSS	Particles from Gas-Saturated Solutions
pMDI	Pressurized metered dose inhaler
p_{SM}	Pressure at static-mixer
QbD	Quality-by-design
QTP	Quality target product profile.
Quer	Quercetin
Quer_Lip	Quercetin-loaded liposomes
Quer_Lip-DPFs	Quercetin-loaded liposomal dry powder formulations
RCTs	Randomized controlled trials
RESS	Rapid Expansion of Supercritical Solvent
Ret.Act.	Retained enzymatic activity
RF	Respirable fraction
RH	Relative humidity
SA	Stearylamine
SAA	Supercritical CO_2- assisted atomization
SAS	Supercritical anti-solvent
SASD	Supercritical CO_2- assisted spray-drying

SEDS	Solution-enhanced dispersion by supercritical fluids
SFEE	SCF-assisted extraction of emulsions
$scCO_2$	Supercritical CO_2.
SEM-EDS	Scanning electron microscopy with energy dispersive X-ray spectroscopy
SD	Spray-drying.
SFD	Spray freeze-drying
SMI	Soft mist inhaler
SOD	Cu, Zn- superoxide dismutase
SOD_Lip	Cu, Zn- superoxide dismutase - loaded liposomes
SOD_Lip- DPFs	Cu, Zn- superoxide dismutase - loaded liposomal dry powder formulations
T_{CO_2}	Carbon dioxide temperature
TFFD	Thin-film freeze-drying
T_{out}	Outlet temperature.
T_{SM}	Temperature at static mixer
XRD	X-ray powder diffraction.
WHO	World health organization
ZP	ζ-potential

THESIS OUTLINE

This Ph.D. project is focused on the development of a green integrated manufacturing process to produce liposomal dry powder formulations (Lip-DPFs) for encapsulation of high-and-low molecular weight anti-inflammatory drugs for the treatment of lung inflammatory diseases. Two model bioactive agents, an antioxidant therapeutic enzyme- Cu, Zn-superoxide dismutase (SOD)- as a water-soluble macromolecule, and quercetin, a low molecular weight hydrophobic flavonoid with anti-inflammatory properties, were studied. Nanoformulations of the enzyme were prepared by microfluidics and thin-film hydration followed by extrusion, whereas nanoformulations of quercetin were prepared only by the latter. Then, both nanoformulations were processed in the supercritical CO_2-assisted spray-drying (SASD) for continuous production of dry powder formulations for pulmonary delivery. To produce Lip-DPFs two industrial challenges must be gripped. First, there is a need to further develop new sustainable technologies that can overcome the problems of conventional bulk methods and circumvent the time, complexity, and cost of present liposome preparation. Second, the need to ensure the ability to produce Lip@DPFs preserving liposomal integrity with optimal aerodynamics for pulmonary delivery. To improve the powder *in-vitro* performance without compromising the product manufacturability, a systematic quality-by-design approach, and design-of-experiments tool, followed by statistical analysis, was implemented to carefully perform a balance between the process optimization and powder requirements in terms of enzyme and drug functionality and formulation stability. *In vivo*, histopathological, and cellular assays were performed to study the effectiveness of the drug delivery systems.

The main body of this Ph.D. dissertation is based on six manuscripts (listed below) that are presented in chapters (2 to 6). Five of them have already been published in peer-reviewed international journals, whereas the remaining one is submitted for publication at the time this thesis was concluded. The chapters were organized so that they followed a rational order considering the objectives delineated for this Ph.D. work. Each chapter is preceded by a title page containing the reference of the publication, the specific contribution of the author, and, if

applicable, the alteration regarding style adjustments, referred to as "minor changes" or the structure of the paper, referred to as "major changes". Besides the manuscript-based chapters, the present Ph.D. dissertation included a preamble (chapter 1) and a conclusion overview, including future perspectives (chapter 7). Briefly, each chapter includes the following contents:

Chapter 1 – This chapter consists of a preamble to provide the reader with the context and the motivation of this doctoral dissertation, addressing the state of the art, including the specific research questions. It ends with the hypothesis that drove the investigations carried out on behalf of each chapter presented.

Chapter 2 – This chapter is an introduction section that describes the basic concepts of pulmonary drug delivery and particle engineering, particularly supercritical CO_2-based techniques. State-of-the-art related liposomal dry powder formulations are also provided. Lastly, a resumed introduction to Quality-by-Design principles (QbD) and the Design of Experiments (DoE) tool is presented.

C. Costa, T. Casimiro, and A. Aguiar-Ricardo. Optimization of Supercritical CO_2 -Assisted Atomization: Phase Behavior and Design of Experiments, J. Chem. Eng. Data, **2018**, 63, 4, 885–896.

C. Costa, T. Casimiro, M. L. Corvo, and A. Aguiar-Ricardo. Solid Dosage Forms of Biopharmaceuticals in Drug Delivery Systems Using Sustainable Strategies, Molecules, **2021**, 26, 24, 7653.

Chapter 3- In this chapter, the study of liposome production using microfluidics is presented in two distinct works. First, we introduce the assembly of insulin-loaded pH-responsive nano-in-microparticles (Ins@MPs) for oral insulin delivery. Secondly, we proposed a one-step microfluidics production of enzyme-loaded liposomes (SOD_Lip). In this chapter, several microfluidic process variables were studied to optimize the encapsulation efficiency of the protein and enzyme, considering the challenges faced by the encapsulation of biopharmaceuticals with a significant difference in their molecular weights. *In vitro, in vivo*, and histopathological studies were performed to testify to the cytotoxicity and the anti-inflammatory properties of the processed micro and nanoparticles.

C. Costa,* Z. Liu,* J.P. Martins, A. Correia, P. Figueiredo, A. Rahikkala, W. Li, J. Seitsonen, J. Ruokolainen S.-P. Hirvonen, A. Aguiar-Ricardo, M. Luísa Corvo, H. A. Santos. All-in-one microfluidic assembly of insulin-loaded pH-responsive nano-in-microparticles for oral insulin delivery, Biomater. Sci., **2020**, 8, 12,3270–3277.

* *These two authors equally contributed to this work.*

C. Costa, Z. Liu, S. Simões, A. Correia, A. Rahikkala, J. Seitsonen, K. Ruokolainen, A. Aguiar-Ricardo, H. A. Santos, M. Luísa Corvo. One-step microfluidics production of enzyme-loaded liposomes for the treatment of inflammatory diseases, Colloids and Surfaces B: Biointerfaces, **2021**, 199, 111556.

Chapter 4- Here, we first apply SASD to the liposomes, producing Lip-DPFs. To monitor the process, a hydrophilic dye, 5(6)-carboxyfluorescein (CF), is encapsulated in PEGylated liposomes (CF_Lip), that were then dried in the SASD (CF_Lip-DPFs). CF is used as a model molecule for hydrophilic compounds and enables process optimization. A QbD approach used the DoE tool and then statistical analyses were carried out. Finally, powder storage stability is assessed at different relative humidity to evaluate moisture impact on the CF_Lip and CF_Lip-DPFs, first at one week and then at a month.

C. Costa, B. Nobre, A.S. Matos, A.S. Silva, T. Casimiro, M. Luisa Corvo, A. Aguiar-Ricardo. Inhalable hydrophilic molecule-loaded liposomal dry powder formulations using supercritical CO_2 – assisted spray-drying. Journal of CO_2 Utilization, **2021**, 53, 101709.

Chapter 5- In this chapter, considering the optimization from the previous work, the production of SOD-loaded liposomal dry powder formulations (SOD_Lip-DPFs) is proposed. Here, the encapsulation efficiency and the enzymatic activity retention after SASD processing are evaluated. Moreover, stability assays are assessed at a relative humidity of 40 ± 5% to evaluate moisture impact on the SOD_Lip and SOD_Lip-DPFs, for 50 days.

C. Costa, T. Casimiro, M. Luisa Corvo, A. Aguiar-Ricardo. Cu,Zn - Superoxide dismutase liposomal dry powder formulations production using supercritical CO_2-assisted spray-drying: a proof-of-concept. Submitted in The Journal of Supercritical Fluids

Chapter 6- This chapter consists of producing liposomal dry powder formulations for the delivery of a hydrophobic molecule - quercetin. Like the last chapter, quercetin is incorporated into liposomes and then dried using SASD. In the end, incorporation efficiency is assessed, and *in vitro* cytotoxicity assays are performed. This chapter is still on-going work.

Chapter 7- Conclusion overview and future work perspectives. This chapter provides an overall summary of the subjects addressed through the chapters, highlighting the main results and

conclusions achieved in the Ph.D. dissertation. Prospects and research questions raised with this work that can be addressed in the future are also presented.

1 PREAMBLE

1.1 General introduction

Chronic obstructive pulmonary disease (COPD), asthma and cystic fibrosis (CysFib) are the most common chronic neutrophilic inflammatory lung diseases [1,2]. In 2019, COPD led the third leading cause of mortality worldwide, claiming 3.2 million lives [3]. Despite the high costs related to treatment and patient hospitalization, these diseases represent a worldwide public health challenge. Therefore, anti-inflammatory therapies, like the use of corticosteroids and bronchodilators, represent a particular interest in the treatment of chronic lung diseases [4]. However, severe inflammatory diseases require high doses of anti-inflammatory drugs, which is a long-term systemic therapy that may result in adverse effects such as osteoporosis, cataracts, diabetes, and cardiovascular diseases [5,6]. There is a crescent need for alternative therapeutics, such as enzyme-based therapies and natural products. Flavonoids, natural compounds present in dietary plants and vegetables, have been recognized for their anti-inflammatory and antioxidant properties, protecting the cells against oxidative stress [7]. Similarly, enzymes, such as the Cu, Zn- superoxide dismutase (SOD) have antioxidant properties and represent an alternative therapy for the treatment of inflammatory diseases [8,9]. However, these drugs have not shown therapeutic outputs as expected due to poor bioavailability [10,11], premature metabolization, or poor pharmacokinetic profile. This can be overcome with its association with well-designed and tailor-made drug delivery systems (DDS) [12–14]. Liposomes, introduced in the 1960s by Bangham [15], are concentric lamellar vesicles made with phospholipids organized in bilayers forming an inner aqueous core [16]. They have been extensively studied due to their nontoxicity, non-immunogenicity, high biocompatibility,

biodegradability, and their many exceptional features in drug delivery [14,17]. Due to their propellant-free nature and high dose-carrying capacity, liposomes have a great interest in the targeted delivery of hydrophilic and hydrophobic drugs, namely therapeutic enzymes, and flavonoid-like compounds, respectively. Companies in the liposome drug delivery market are increasing their R&D activities to unlock new lipid compositions and strategies that optimize the stability and drug vehiculation capabilities of liposomes. The liposome drug delivery market is expected to experience favorable growth, with an estimated revenue of ~US$ 8 Bn by 2027 [18]. Currently, functional liposomes are prepared by conventional methods based on bulk synthesis (e.g. freeze-drying, thin-film hydration) which require post-processing steps to homogenize their sizes (e.g. extrusion, sonication), limiting their batch-to-batch-reproducibility, which is a critical requirement [19]. To overcome these limitations, reported studies on the microfluidic field have gained substantial attention for their use in liposomal preparation. The microfluidic assembling method presents some advantages when compared to the bulk method, such as a continuous control of particle size, surface properties, and size distribution [20]. In addition, microfluidic devices allow the use of small amounts of reagents and samples in fast high throughput portable platforms that have the potential for automation and high-level integration, associated with decreased cost and easy scale-up [21]. The fast-mixing capability provided by the microfluidic method enables fine control of nucleation and growth processes, which yields a narrow particle size distribution, turns this method into a promising technology for the manufacture of liposomes for a broad range of applications. The Microfluidics market is expected to increase to ~US$ 58.8 Bn by 2026 [22].

Despite being thermodynamically stable, after long-term storage, biopharmaceutical-loaded lipid-based nanoparticles in solution can suffer instability due to physical and chemical events, such as fusion or aggregation of the nanoparticles, or hydrolysis and oxidation of the phospholipids and/or the biopharmaceuticals [23,24]. This leads to the demand for cold supply and distribution chains. For these reasons, it is fundamental to ensure the stability of the drug-loaded liposomes via storage methods accessible to people of all social and geographical conditions. The most common liposome stabilization techniques are based on drying processes, in which liposomes are converted into dry liposome powder formulations (Lip-DPFs). Additionally, as a medicine, the powder can be administered after being reconstituted into a solution or a suspension just before i.v. administration and/or in powder form by non-invasive route [23,24]. In the case of pulmonary delivery, Lip@DPFs must fulfill specific demanding requisites (mass median aerodynamic diameter ~ 2 μm, fine particle fraction >70 %), to have the

necessary aerodynamic performance [25–27]. Traditional techniques, such as freeze-drying, need low operating temperatures and show difficulties in producing powders with narrow and controlled particle size distributions, restricting their application. Spray freeze-drying and spray-drying are associated with high costs and energy consumption [28–30]. In addition, they might also induce heat, cold or shear stress on the liposomes, possibly affecting their integrity. These drawbacks can be overcome using the supercritical CO_2-assisted spray-drying [31]. The 2018 FDA draft guidance on Products Quality Considerations refers to supercritical fluid technology as an alternative pharmaceutical engineering approach in micronizing pharmaceuticals and in ensuring uniform final formulations [32]. Using mild temperatures, liposomal formulations may be produced by SASD assuring the complete removal of solvents, the improved control of microparticle morphology and size distribution, while preserving the structures of nanoliposomal systems [23]. The $scCO_2$ technology enables the use of mild conditions for processing thermolabile drugs and biologics [27,33], the production of particles with controllable morphology and narrow size distribution, the complete removal of organic solvents and an easy scale-up. Considering the similarity of process yields and throughputs, SASD is a good alternative technology to conventional SD for the processing of sensitive drugs into stable particles suitable for different administration via. There is a need to improve the understanding of the stabilization of the liposomes during the SASD process to ensure a high quality of the final inhalable liposomal product. The mechanistic insight on the $scCO_2$ technique in terms of droplet and particle formation mechanism in correlation with studies in terms of liposome structure, lipids composition, the stabilizing effects of excipients (carbohydrates) [34] and the final outcome in terms of powder aerodynamic performance will be the key to guarantee the applicability of this technology for the production of Lip-DPFs. A quality-by-design approach [31] to construct a design space available for manufacturing Lip-DPFs (encapsulating the flavonoid or SOD) will enable a deeper understanding of the interrelations of operational critical parameters and the critical quality attributes of the Lip-DPFs and at the same time the optimization of the integrated supercritical-microfluidic combined process. Thus, this strategy provides a more rational design for the development of the Lip-DPFs and ensures high-quality liposomal dry formulations. Finally, as this development is based on the innovative technology of $scCO_2$, the studies carried out throughout this Ph.D. work could contribute to a scale-up of technology with a consequent increase in sustainability due to the low carbon footprint and low energy consumption of the process.

1.2 Aims and general research plan

According to the described background, the major aims of this thesis can be pointed out as follows:

1. To produce enzyme/flavonoid-loaded liposomes using microfluidics.
2. To convert enzyme/flavonoid-loaded liposomal suspensions into liposomal dry powder formulations, keeping their structural, physical, and chemical properties.
3. To obtain liposomal dry powder formulations able to be inhaled, reaching the respiratory region.
4. To obtain liposomal dry powder formulations stable upon storage.
5. To integrate microfluidics into SASD
6. To link the critical formulation and critical process parameters (CPPs) to critical quality attributes (CQAs) using the design of experiments, an optimal operating space (OOS) be identified.

To pursue these general objectives, we carried out several studies attempting to answer the following main research questions:

1. Is it possible to process a biopharmaceutical using microfluidics, while the conformational structure and enzymatic activity are preserved? (Chapter 3)
2. Is it possible to obtain empty Lip-DPFs using SASD? Does their structure remain? What are the variables that must be considered? (Chapter 4)
3. Can hydrophilic molecules with high and low molecular weight present similar encapsulation efficiency? (Chapters 4 and 5)
4. Can Lip-DPFs keep liposomes and hydrophilic molecules stable upon storage? (Chapters 4 and 5)
5. Is it possible to process liposomal dry powder formulations with hydrophilic and hydrophobic loaded molecules, while keeping their size, encapsulation/incorporation efficiency, and activity retention? (Chapter 6)

In this context, this doctoral dissertation includes cumulative reports from several investigations (which can be read separately) continuously marked by insights into the manufacture of liposomal dry powder formulations for encapsulation of hydrophilic and hydrophobic molecules.

2 INTRODUCTION

The contents of this chapter (with major modifications) were published in a peer reviewed international journal:

(1) C. Costa, T. Casimiro, and A. Aguiar-Ricardo. Optimization of Supercritical CO_2 -Assisted Atomization: Phase Behavior and Design of Experiments, J. Chem. Eng. Data, **2018**, 63, 4, 885–896.
(https://pubs.acs.org/doi/full/10.1021/acs.jced.7b00820)
(2) C. Costa, T. Casimiro, M. L. Corvo, and A. Aguiar-Ricardo. Solid Dosage Forms of Biopharmaceuticals in Drug Delivery Systems Using Sustainable Strategies, Molecules, **2021**, 26, 24, 7653
(https://www.mdpi.com/1420-3049/26/24/7653)
Reproduced with the authorization of the editor and subjected to the copyrights imposed.

Personal contribution
CC contributed to the design of the study and wrote most of the manuscript.

2.1 Pulmonary drug delivery

Despite inhaled therapy being traced to India 4000 years ago, pulmonary drug delivery has upsurged scientific interest in the nineteenth-century industrial age [35]. When searching for "pulmonary drug delivery" in the database *Web of Science*, it is possible to observe a growing tendency of published articles over the last 40 years (Figure 2.1).

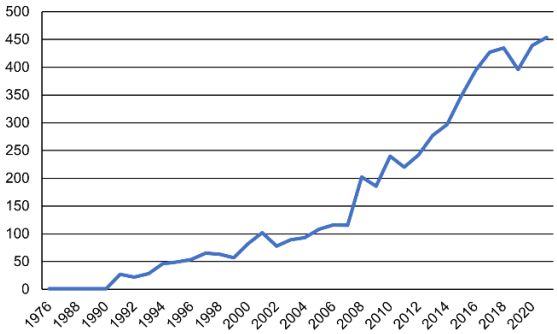

Figure 2.1- Evolution of the number of articles published from 1976 to 2021, according to the databank *Web of Science*.

Lungs physiology shows attractive and unique features like i) thin blood-barrier membrane (0.1 - 0.2 μm); ii) large absorption area (> 100 m^2) from a highly vascularized alveolar epithelium constituted by a single layer of cells; and iii) elevated blood flow (5 L/min) [36,37]. The physiological pH and reduced mucociliary clearance in the deep lungs avoid rapid clearance, poor absorption, and exposure to digestive enzymes [38]. Moreover, pulmonary administration bypasses the hepatic first-pass of metabolism, decreasing the total dose required in the formulation for an effective local and systemic treatment and, consequently, decreasing the medical costs and adverse side effects, improving patient compliance and the therapy efficacy [39]. Therefore, pulmonary administration is an interesting and attractive alternative to oral, intravenous, and intraperitoneal routes, especially for people suffering from pulmonary diseases such as lung cancer or chronic inflammatory diseases [40]. Formulations for pulmonary drug delivery can be administered by i) a nebulizer [41]; ii) a pressurized metered dose inhaler (pMDI) [42]; iii) a dry powder inhaler (DPI) [43]; iv) a soft mist inhaler (SMI) [44]. Nebulizers are the oldest device for inhalation therapy. They consist in dispersing a drug-containing aqueous formulation (solution or suspension) into aerosol droplets, using compressed air or piezoelectric

vibrations [43]. The main advantage is the capacity to generate aerosols using diverse water-soluble drugs; no need for a proper 'press and breathe' technique, and the absence of propellants [45]. However, these devices are known to present low efficiency, poor reproducibility, great variability, and time consumption (approximately 30 min) [37], and they require deep cleaning to avoid contamination with microorganisms. pMDI was introduced in the 1950s. The first devices contained a solution or suspension of drug particles in pressurized liquefied chlorofluorocarbon (CFC) propellant sealed in a canister. These devices were banned by the Montreal Protocol (1989) due to their ozone depletion effect. As an alternative, hydrofluoroalkanes (HFA) were selected as alternative propellants, although they contribute to the greenhouse effect [43,46]. The main advantage of pDMI is being easily portable and low cost. However, it is necessary coordination between the patient inhalation and action, resulting in a higher drug deposition at the mouth and oropharynx area and inconsistent dose delivery [47]. DPIs were developed to overcome these drawbacks. DPIs are propellant-free and, consequently, more environmentally friendly, present higher stability due to the solid state of the medicine, and can be used as a single or multiple doses or even in multiple blister packs [27,37]. Stegemann *et al.* [46] defended that DPI products maintain their cost advantage in delivering efficient medicines to emerging markets compared to pMDIs. Finally, SMI is a portable device that actively generates an aerosol independently of the patient's inhalation effort, with a slow velocity (1-3 seconds) and prolonged duration (approximately, 1.5 seconds), which facilitates the coordination of actuation and inhalation [44].

Successful pulmonary drug delivery in the deep lungs can face some challenges depending on the respiratory airway tract, particle diameter, and breathing pattern [27]. Lungs are, in general, divided into two main regions: conducting airways (composed of nose, mouth, trachea, bronchi, bronchioles, and terminal bronchioles) and respiratory regions that comprise the respiratory bronchioles, alveolar ducts, and alveolar sacs [48]. The main objective of the conducting airways is the humidification and filtration of inhaled air through the mucociliary escalator (formed by layered two different epithelial and goblet cells). In this way, insoluble inhaled particles are entrapped and swept out of the lungs. On the other hand, the respiratory region is composed of epithelial cells to synthesize and secrete surfactants, which form the surface-active film at the respiratory air-liquid interface [49]. These secretions are mainly composed of approximately 90 % of lipids and cholesterol and 10 % of proteins [50]. Therefore, a drug delivery system (DDS) must overcome the challenges of being exhaled or mucociliary cleared out before reaching the underlying epithelia. Besides, DDS also faces the possibility of

phagocytosis by alveolar macrophages. For this reason, DDS's particle diameter is an important factor in pulmonary drug delivery. Three main mechanisms can describe the particle deposition mechanism in the lung: inertial impaction, gravitational sedimentation, and Brownian diffusion [51]. These mechanisms are closely related to particle size. Particles with a mass median aerodynamic diameter (MMAD) of more than 5 µm are subject to inertial impaction during the passage through the oropharynx and large conducting airways. Usually, these particles deposit in the upper and conducting airways and especially in bifurcation points, where there is a sudden change in the direction of the flow [52]. In contrast, particles ranging between 1 and 5 µm, reach out to respiratory bronchioles due to the sedimentation mechanism influenced by the gravitational force. This phenomenon is closely related to breath-holding [51]. Finally, for particles smaller than 0.5 µm deposited the dominant mechanism is Brownian diffusion. Brownian diffusion is inversely proportional to particle size. This mechanism is based on random motions of the particles caused by their collisions with gas molecules and is most effective in the acinar region of the lung where air velocities are low [52]. To improve mucus diffusion and cellular uptake by the epithelial cells, nanocarriers represent an advantageous strategy for the delivery of small molecules and biopharmaceuticals [27]. The size of nanocarriers of approximately 100 nm up to 150 nm promotes drug delivery and capitalizes on the enhanced permeability and retention (EPR) effect as the nanocarrier extravasates through the inflamed cell vasculature [53]. Therefore, considering all the factors for a successful pulmonary drug delivery, a microparticle that comprises a size between 0.5 and 5 µm, avoids the mucociliary clearance and, upon deposition on the deep lung and swelling, enables the release of the nanoparticle that interacts with the lung epithelial cells, releasing the small molecule or biopharmaceutical represents a complex particle engineering.

2.2 Nano-in-micro particle engineering for pulmonary delivery

Particle engineering is defined by Albert Chow and co-workers as an *alternative strategy, which is synonymous with the controlled production of drug particles in pure physical forms or with carriers as composite materials of optimized size, morphology, and structure* [54]. Considering pulmonary drug delivery, the principal objective of this strategy is to obtain particles with desirable attributes such as narrow particle size distribution, improved dispersibility, enhanced API stability, optimized bioavailability, sustained release, and/or specific targeting. For this reason, several techniques (top-down and bottom-up) have been applied to produce nano-in-

microparticles with specific attributes for inhalation. In this section, the most common techniques such as milling, spray-drying, spray freeze-drying, and supercritical fluids will be addressed considering pulmonary drug delivery.

2.2.1 Milling

Milling is the common *Top-down* technique to micronize APIs and excipients. Co-milling is also widely used to achieve a homogenous powder blend [55] of two or more components. There are several milling techniques, such as vibration milling, ball milling, and jet-milling (fluid-energy) [54]. However, the most used for pulmonary delivery is ball milling and jet-milling [37]. Ball milling consists of moving the mill body, to transfer grinding energy to materials through balls or pebbles [56]. The main disadvantage of ball milling is the powder compaction on the milling walls, the need for multiple processing steps, and the use of solvents in wet ball milling [55]. In jet-milling, the injection pressure, generated by the flow of compressed gas through the venturi system, forces the particles to accelerate at high velocities into the grinding chamber of the jet mill, where the material is submitted to high pressure and velocities generated from airflow introduced via the two "grinding" nozzles. Subsequently, particles undergo multiple particle-particle and particle-wall impactions, which induce particle fracture and subsequent size reduction [55,56]. Relenza®, the commercial name for Zanamivir, is an example of commercialized inhalation powder produced via air-jet milling [57]. Brunaugh *et al.* [58] obtained clofazimine microparticles with a D_{50} of 1.81 µm and an FPF of 80 % with significant improvement of the drug dissolution and anti-bacterial effect. Desai *et al.* [59] produced liposomes in dry powder form using jet-milling, obtaining MMAD values from 2.55 µm to 4.80 µm and FPF from approximately 10 % to 50 %. Milling is also widely used as a post-freeze-drying (FD) step [28,60]. Hickey and co-workers [28] reported the production of aerosolizable β-glucuronidase- loaded liposomal dry powder. Dry powders were produced by freeze-drying and then were milled to achieve the particle size suitable for inhalation. However, a decrease in enzyme retained activity from 100 % to 20 % was observed, being one of the process disadvantages. Moreover, some authors have defended that micronization of liposomal dry powder by milling is ineffective, due to particle aggregation from recrystallization and poor control of the size distribution, favoring spray-drying [55,61,62].

2.2.2 Spray-drying

Spray-drying (SD) was developed in the 1980s as an alternative to milling techniques. SD is a one-step continuous technique that consists of converting a solution/suspension or emulsion into dry powders, by atomizing the liquid feed into an air/nitrogen heated flow [63]. This process consists mainly of four stages: i) atomization of the liquid solution; ii) contact between the hot stream and nebulized liquid; iii) solvent's evaporation and iv) powder recovery/collection. The first stage occurs in the nozzle where the surface area is increased by the breaking up of the initial solution into many droplets. This surface area increases lead to heat and mass transfer between the heated stream (usually N_2) and the droplet, resulting in fast moisture evaporation (in seconds). In the drying chamber occurs the third stage. After atomization, droplets are in contact with the inlet drying gas (heated compressed air) and the solvent evaporates. Finally, dried particles are collected throughout a bag or a cyclone [64,65]. SD is a scalable technique, being possible to manipulate the characteristic of the final product (particle size, density, morphology, and residual moisture) by adjusting the process parameters [66]. Several works in pulmonary drug delivery have been published, concerning the use of SD. Cai *et al.* [62] processed inhalable zanamivir microparticles, whereas Fernandes *et al.* [26] investigated the effect of SD process parameters on the drying of a biopharmaceutical (Cu, Zn- superoxide dismutase). Pardeshi and co-workers [67] obtained pirfenidone-loaded microparticles for the treatment of idiopathic pulmonary fibrosis. They obtained microparticles with an MMAD of 4.25 μm and an FPF of 47.47 %. SD has been also widely applied to the production of liposomal dry powder formulations [30,68,69,69–71]. Charnvanich *et al.* [68] investigated the effect of ethanol in the liposomal bilayer on the properties of inhalable protein-loaded liposomal powders prepared by SD, whereas van den Hoven and co-workers [30] performed a benchmarking between FD and SD. They observed a dramatic increase in liposomes' size, PdI, and drug leakage of 70 % when the internal sugar was trehalose or sucrose, for both SD and FD. However, no changes were observed for hydroxypropyl- β -cyclodextrin, retaining completely the drug. More recently, Huck *et al.* [71] produced dry-powder microparticles of spray-dried bedaquiline-loaded liposomes with an FPF over 70%, as well as preserved liposomal integrity and targeting function. Notwithstanding, the use of solvents, thermal and shear stress may be not suitable for sensitive biomolecules [27].

2.2.3 Spray freeze-drying

Spray freeze-drying (SFD) is a technology that overcomes the drawbacks of spray-drying, in the processing of thermolabile compounds, like biopharmaceuticals. In SFD the liquid solution is sprayed through a nozzle, which is in contact with a low-temperature fluid. Therefore, the droplet is frozen and it is transferred into a freeze-dryer to remove water and obtain a solid formulation [29]. Powders from SFD commonly present good fluidity, high specific surface area, and fast dissolution. Sweeney and co-workers [72] manufactured a liposomal powder formulation containing ciprofloxacin. They observed an MMAD of 2.8 μm and an FPF over 60 %. A drug encapsulation efficiency of 50 % of the drug was obtained for those powders reconstituted in water. Ali *et al.* [73] compared the SFD and SD techniques on the production of polymers and lipid-based nanoparticles. They observed smaller diameters of those particles produced via SD. However, particles from SFD presented higher specific surface area and a slight increase in the FPF values. Liang *et al.* [74] produced siRNA and DNA dry powder formulations, using mannitol as an excipient. They observed an FPF of 28 % for DNA-loaded microparticles and 20 % for siRNA-loaded microparticles. Bi and co-workers [75] proposed dry powders of insulin-loaded liposomes using SFD, with an MMAD of 5.07 μm and an FPF of 31.40 % SFD is a time-consuming and hard scalable technique. Therefore, over the last few years, many efforts have been applied to improve and optimize the SFD technique from computational approaches and mathematical modeling [76] to modifications to the SFD apparatus [77].

2.2.4 Supercritical fluids

Recent decades have seen an upsurge of interest in dry powder formulations using supercritical fluids (SCF) since first reported in 1879 by Hannay and Hogarth [78]. The advantages include the ability to operate at mild conditions, their cost-effectiveness, the ability to produce microparticulate protein powders, and their scaling up feasibility [79]. Supercritical CO_2 ($scCO_2$) is the most common SCF, with a low critical temperature and moderate critical pressure at 31.1 °C and 7.38 MPa, respectively, making them suitable for processing heat-sensitive compounds [27,80]. Moreover, CO_2 is non-flammable, non-toxic, recyclable, inert, chemically stable, and, as it is a gas at normal conditions, it can be removed by simply lowering the pressure [81]. At supercritical conditions, CO_2 has liquid-like density and gas-like transport properties. Thus, its polarity and solvation power are superior, and it offers the mass transfer properties of a low viscosity gas in association with high associated diffusivity [82]. For this reason, $scCO_2$ use also

respects some of the Twelve principles of green chemistry, outlined by Anastas in 1991 [83], rating in fifth place Safer solvents and auxiliaries. $scCO_2$ properties are easily tunable near the critical point via minor temperature or pressure changes [84]. For this reason, $scCO_2$ can be used with different technologies, depending on its solvating behavior. In fact, these processes can be classified into different groups depending on the $scCO_2$ processing role: acting as a solvent, co-solvent, anti-solvent, or as a co-solute [85].

2.2.4.1 Rapid Expansion of Supercritical Solution (RESS)

The rapid expansion of supercritical solution (RESS) is a 1987 technique by Peterson, Matson, and Smith [86–88] which consists of saturating supercritical fluids with a solid substrate (and the coating agent), without any organic solvents. Upon depressurization to subcritical pressure using a heated nozzle, the substrate precipitates into a lower pressure precipitation chamber as the solution density drops (Table 2.1; page 57) (usually near atmospheric pressure) [86,87,89]. The morphology and physicochemical properties of the resulting powders are related to the processing parameters (temperature, pressure, nozzle geometry) and the chemical structure of the material [90,91]. RESS has been applied mainly to the production of micronized poor water-soluble compounds. In 1993, Reverchon *et al.* [92] reported the micronization of salicylic acid. The first particles were in needle form, but the work was optimized, and spherical particles resulted. Years later, Yildiz and co-authors [93] reported the micronization of salicylic acid and paclitaxel, using ethanol as a co-solvent to improve salicylic acid's solubility in CO_2. This highlights, in fact, one of the technique's limitations. On the one hand, scCO2 presents low solubility for most polymers and pharmaceuticals. On the other, the addition of a second component influences phase behavior. Unfortunately, there is little data available for the multicomponent systems involved in real processes [94].

Years later, a variation in a non-solvent RESS method (RESS-N), introduced by Mishima and co-authors, aroused considerable interest [95]. An organic solvent which does not, in its pure form, solubilize the polymer was added as a co-solvent. Nevertheless, in the presence of those organic solvents, the polymer solubility in CO_2 in-creased significantly. In sum, a suspension of a drug in the ternary system composed by CO_2, the non-toxic organic solvent (such as ethanol, isopropanol), and the dissolved polymer was sprayed through the nozzle. The polymer excipient then precipitated around the drug, producing core–shell structured microparticles [96]. Another process modification involved the rapid expansion of a supercritical solution into a liquid solvent (RESOLV) in order to obtain nanoscale particles [97,98]. In this case, however, the

supercritical solution was expanded into a liquid solvent instead of a lower pressure precipitation chamber, and particles with a diameter less than 50 nm were obtained [97].
RESS is more often used with poor water-soluble compound processing, yet it (and its derivatives) has been also applied to encapsulating biopharmaceuticals in drug de-livery microsystems. In fact, the processing of water-soluble compounds using RESS can be quite challenging due to CO_2's poor solubility in water.

2.2.4.2 Particles from Gas-Saturated Solutions (PGSS)

The PGSS technique [99] was introduced in 1994 by Weidner, Knez, and Novak and uses CO_2 as a solute. $ScCO_2$ is dissolved into a melted material, consisting of drugs, polymers, biopolymers, oils, or fatty acids in a stirred high-pressure vessel until saturation is achieved [85]. The gas saturated liquid is then expanded through the nozzle to an expansion chamber at ambient pressure and lower temperature where the particles precipitate (Table 2.1; page 57). PGSS can be more effective than RESS insofar as the compound (drug or polymer) does not need to be dissolved in $scCO_2$ [100] and no organic solvents are necessary. Moreover, PGSS enables polar and water-soluble compounds to be processed. For this reason, this technique has been widely used in the pharmaceutical field with different compounds. Initially, compounds were processed without carriers. In 1999, Kerč and co-workers [100] used the technique to micronize nifedipine and felodipine (commonly used in hypertension treatment) in order to increase the dissolution rate and their bioavailability. Using temperatures between 150 °C and 185 °C, nifedipine and felodipine microparticles with an irregular shape showed a mean size between 15 and 30 μm and 42 μm, respectively. Smaller microparticles showed an increased dissolution rate. However, the effective surface area was reduced by the drug's hydrophobicity and agglomeration. Thus, to reduce agglomeration, PEG_{4000} was added. Microparticles were produced between 50 and 70 °C since the polymer decreased the drug's melting point. It was found that the size reduction and the drug/ PEG_{4000} interaction contributed for an enhanced dissolution rate against the pure micronized drugs. Interestingly, this study allowed the further micronization of drug delivery systems with different carriers. Hao *et al.* [101] produced poly($_{DL}$-lactic acid) ($P(_{DL}LA)$) microparticles, affirming that solid drug particles can be mixed into the plasticized polymer. Figure 2.2 shows that $scCO_2$ dissolves into and plasticizes the polymer at temperatures significantly below its glass transition temperature [102,103].

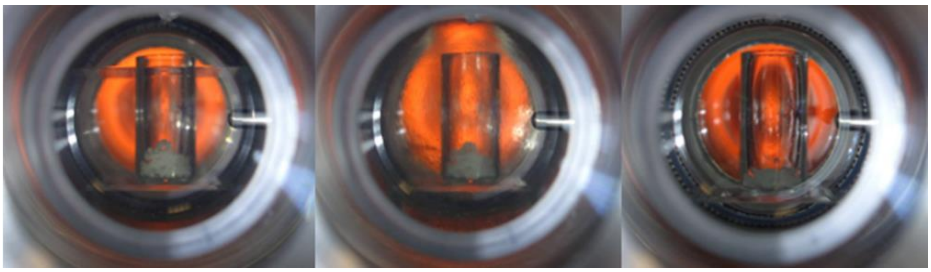

Figure 2.2- Plasticization of the P(LLA)-PEG1500-P(LLA) copolymers by $scCO_2$, with rise in working tempera-ture and pressure, from *Perinelli et al.* [103]. Left- Stage conditions at 29 °C and 71 bar; Center- conditions at 35 °C and 85 bar; and Right- plasticization point at 47 °C and 140 bar. Reproduced with permission. Copyright 2014, Elsevier.

A year later, Hao *et al.* [104] applied PGSS to produce PEG microparticles and observed that the temperature increase and the pressure decrease favored the production of spherical particles. These works contributed to the development of the CriticalMix™—a solvent-free encapsulation process based on PGSS [105]. Rodrigues *et al.* [106] reported the encapsulation of theophylline—a bronchodilator—in hydrogenated palm oil, yielding microparticles sized between 2 and 3 µm. Higher working pressures (*P*) were found to lead to a more spherical size and a more limited distribution. Lower *P* of 120 or 140 bar led to agglomerated structures. Theophylline encapsulation was lower since the drug was mostly located on the carrier's surface. More recently, Tokunaga *et al.* [107] reported the encapsulation of an amino acid, phenylalanine, in Eudragit L100. The work was carried out at 50 °C, between 80 and 120 bar. Microparticles sized from 200 µm to 140 µm were obtained for the respective pressures. At 100 bar, an encapsulation efficiency (*EE*) of 68.7% was achieved. In fact, the PGSS technique produced microparticles with a wide range of diameters, depending on the working parameters.

2.2.4.3 Carbon Dioxide-Assisted Nebulization with a Bubble Dryer (CAN-BD)

In 1997, Sievers *et al.* [108] proposed a PGSS improvement: the carbon dioxide-assisted nebulization with a bubble dryer (CAN-BD). This technique enables the use of any water-soluble compound, as well as the nebulization of inorganic salts or proteins [109]. Here, CO_2 serves as a co-solute. An aqueous stream containing the drug and any excipients or stabilizers (typically 1 to 10% of the total solids dissolved [85]) is mixed with supercritical CO_2 in a low-dead-volume mixing tee, forming a gas–liquid emulsion. This is then rapidly decompressed through a flow

restrictor, forming an aerosol of droplets containing dissolved CO_2. Upon expanding the dissolved CO_2, the droplets rupture, and a fine aerosol, usually of diameters below 5 μm, is produced (Table 2.1; page 57). It is important to point out that the expansion is enhanced since CO_2 is one of the most soluble gases in water (1.6 mole% at 63 °C and 1500 psi). Dry particles are obtained in a furnace [110], and micronized particles are then collected on a filter. Due to the use of the aqueous stream, CAN-BD has been widely applied to processing water-soluble compounds. In 2001, Sellers *et al.* [111] reported the encapsulation of proteins (lysozyme and lactate dehydrogenase) using sucrose and mannitol as excipients for pulmonary delivery. A buffer was used to neutralize any potential acidification of the solution upon the addition CO_2 to avoid damaging the protein. The proteins were also found to maintain their activity after rehydration due to the excipients and surfactant. Years later, Sievers *et al.* [112] reported the encapsulation of hepatitis B sur-face antigen (HBsAg) and a live-attenuated measles virus by trehalose and sucrose. In addition to achieving powder stability after 43 days of storage, they were also able to provide pulmonary administration. CAN-BD has been also used to produce vaccines, such as the Edmonston-Zagreb live-attenuated measles virus vaccine [113–115], and inhalable antibiotics [116]. To our knowledge, no data on biopharmaceuticals in solid dosage forms have been reported.

2.2.4.4 Supercritical Assisted Atomization (SAA)/Supercritical CO_2-Assisted Spray-Drying (SASD)

Supercritical assisted atomization (SAA) is based on the PGSS and CAN-BD techniques. First patented by Reverchon in 2001, it consists of the production of nano and microparticles from liquid formulations [117]. This one-step process is very similar to spray-drying but is aided by $scCO_2$ and it can also be called supercritical CO_2-assisted spray drying (SASD) [84,95,118]. $scCO_2$ acts as a co-solute and is solubilized into a liquid solution containing the drug and/or a carrier system. The resulting near-equilibrium mixture flowing out of the saturator is atomized using a nozzle in a precipitation chamber at near atmospheric pressure, where it is dried with a hot air/nitrogen flow [94,119] which serves to avoid the Joule–Thomson effect upon decompression. Two atomization processes take place: (i) droplets at the nozzle are produced by pneumatic atomization; and (ii) CO_2 is quickly released from inside the droplets [118]. A series of SAA/SASD (Table 2.1; page 57) studies have been published over the years reporting microparticle production, even for poorly water-soluble compounds. In 2002, Reverchon and co-authors reported the micronization of various compounds using SAA, from salts to

corticosteroids [120]. Next, several demonstrated the micronization of antibiotics for inhalation [121–123]. The research continued, and later polymeric microparticles (chitosan [124], poly(methyl methacrylate), and poly-L-lactide [125]) were produced using the technique. Reverchon, in 2007, proposed to produce a composite, in which ampicillin tri-hydrate and chitosan were selected as a model drug and carrier, respectively, upscaling the technique to produce a drug delivery system [126]. Several projects have developed drug delivery systems for inhalation. Cabral *et al.* [127] reported the production of inhalable ibuprofen-loaded chitosan microparticles. Nano-in-microparticles were also developed for effective pulmonary drug delivery using dendrimers [128] and gold nanoparticles [129] as well as gold-coated magnetite nanocomposites [130]. As in the case of RESS, SAA/SASD has also undergone modifications, such as the introduction of a hydrodynamic cavitation mixer (HCM) [131], to improve mass transfer. Smaller diameter microparticles were reported with a narrower particle size distribution than those produced without HCM.

An adaptation of SAA to produce liposomes was recently reported [132]. Supercritical assisted Liposome formation (SuperLip) is a continuous operative process, in which biopharmaceuticals can be encapsulated in liposomes, with high reproducibility [133,134]. It is important to point out that these vesicles are obtained in aqueous bulk instead of solid dosage forms.

2.2.4.5 Depressurization of an Expanded Liquid Organic Solution (DELOS)

Ventosa and co-workers [135] reported the depressurization of an expanded liquid organic solution (DELOS) crystallization technique twenty years ago, and it has been commonly used for producing nano- and micro-sized crystalline particles. In this process, at certain temperature and pressure conditions, a compressed gas, e.g., CO_2, is completely miscible with the organic solvent, acting as a co-solvent, unlike in other techniques [136]. This is a three-step process. First, the solute is dissolved in the organic solvent, below the saturation limit, at working temperature and atmospheric pressure. Then, an expanded liquid mixture is obtained by adding the compressed fluid, at high working pressure, which should not exceed the critical point of the CO_2/solvent mixture. Finally, depressurization takes place by way of using a non-returning valve upon the rapid reduction of the pressure of the expanded liquid mixture, leading to the precipitation of nano- or microparticles [85,136] (Table 2.1; page 57).

Since 2001, DELOS has been applied to the micronization of polymers, surfactants, [108] and poorly water-soluble compounds such as naproxen and ibuprofen [137–139]. This process uses less CO_2; the filtration takes place at atmospheric pressure, and the lack of nozzles improves

scalability [140]. A technique for developing unilamellar nanovesicles based on DELOS was developed that was like the above-mentioned SuperLip [141]. Depressurization of an expanded liquid organic solution into aqueous solution (DELOS-susp) is mainly applied to produce nanovesicles to carry nucleic acids and enzymes [142,143]. However, loaded liposomes are obtained in aqueous bulk rather than in the dried form.

2.2.4.6 Supercritical CO_2 as Anti-Solvent

Since $scCO_2$ is a poor solvent for most pharmaceutical compounds and polymers, some approaches use it as an anti-solvent. In a supercritical anti-solvent (SAS), a solute is dissolved into an organic solvent and precipitates when $scCO_2$ is added. In fact, the precipitation occurs by the diffusion of CO_2 in the organic solvent, expanding the liquid mixture, decreasing its density, and consequently, its solvation power, until nucleation and precipitation occur [144]. The mass transfer between the CO_2 and the organic solution decreases the surface tension, which is strong enough to control droplet shape [145]. In the Table 2.1 (page 57) a schematic illustration of this process is represented. The CO_2 is pumped until a desired pressure in the heated precipitator is achieved. The organic solvent with the solute(s) is then injected by nozzle. In the case of a drug/polymer system, both precipitate under supersaturation and the drug are trapped into the polymer matrix [146]. The loaded polymer precipitates on a filter and the organic solvent/CO_2 are recovered for further separation [147]. Impressive reviews related to pharmaceutical encapsulation using the SAS and SAS-based methods have been published [145,147]. However, the use of organic solvents to dissolve the solute may represent an obstacle to biopharmaceutical applications [146]. Even so, some research has reported successful biopharmaceutical drying with the SAS technique. In 1993, Yeo *et al.* [148] reported the first production of microparticulate insulin powders using SAS, obtaining powders with diameters mostly less than 4 μm. The blood glucose level decreased with the administration of the insulin microparticles. Further results showed that SAS can compromise proteins' secondary structure, although precipitated insulin recovered its native structure upon redissolution in aqueous media [149]. Some modifications of the SAS process have been proposed to overcome this drawback, where CO_2 also acts as an anti-solvent. However, this review reported little focused attention on this aerosol solvent extraction system (ASES) [150] using solution-enhanced dispersion by supercritical fluids (SEDS) [151], precipitation with a compressed fluid anti-solvent (PCA)[152] and SCF-assisted extraction of emulsions (SFEE) [147,153].

Table 2.1- Schematic representations of $scCO_2$-based techniques.

Technique	Scheme of the process
RESS, adapted from Aguiar-Ricardo *et al.* **[90]**	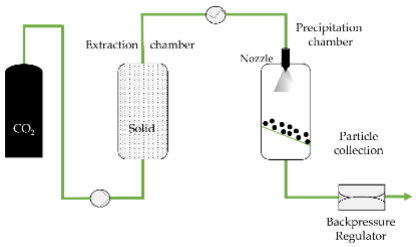
PGSS adapted from Kerč *et al.* **[100]**.	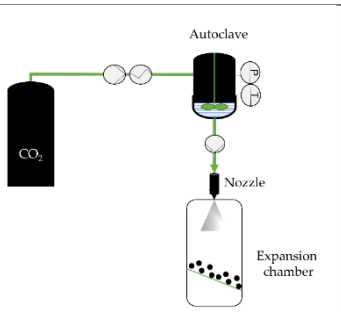
CAN-BD adapted from Sievers *et al.* **[109]**.	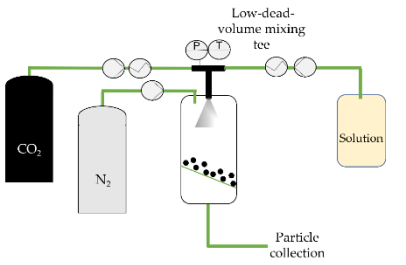
SASD apparatus at NOVA's laboratory.	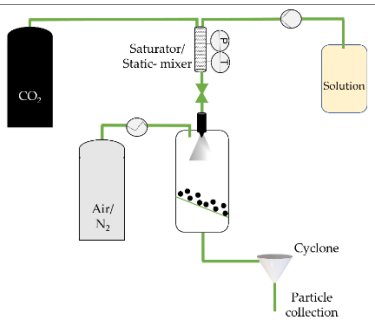

DELOS adapted from Ventosa *et al.* **[135]**.	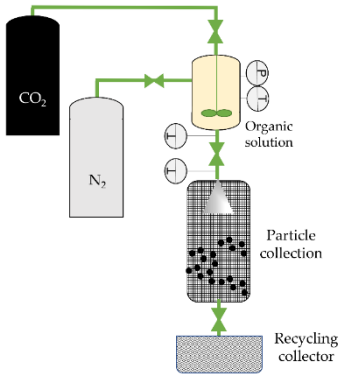
SAS adapted from Aguiar-Ricardo *et al.* **[90]**.	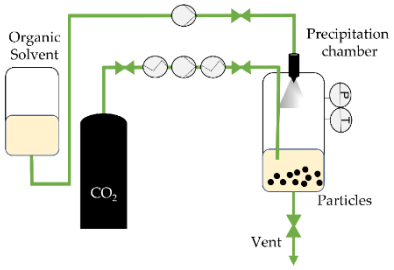

P and *T*–Pressure and temperature indicator and controller, respectively.

2.2.5 Thin-film freeze-drying

Thin-film freeze-drying (TFFD) was introduced by Evans *et al.* [154] in 2006, with the objective of enhancing the dissolution rates and bioavailability of poorly water-soluble drugs. In this process, droplets of drug formulation are frozen upon impact with a cryogenically cooled substrate (*e.g.,* a metal surface) to form a thin film in less than a second. Then, the thin film is freeze-dried to sublimate the solvents from the formulation [155]. Since the supercooling is fast, the nucleation of drug crystals is prevented, forming an amorphous morphology and increasing the surface area [156]. Engstrom *et al.* [157] studied the processing of lysozyme and lactate dehydrogenase (LDH) by TFFD. Protein particles with an average diameter of 300 nm were obtained. Upon reconstitution, LDH microparticles presented 100 % of enzyme activity. Li *et al.* [158] proposed to convert vaccine containing aluminum salts into dry powder. The authors did not observe particle aggregation, nor decreased the immunogenicity of the vaccines. More recently, AboulFotouh and co-workers [159] converted vaccines adjuvants into dry powder formulations for inhalation purposes. The obtained microparticles showed an FPF of 66.3 % and an MMAD of 2.4 µm. Vaccine immunogenicity was maintained in the dry powders.

2.3 Dry powder formulations for pulmonary drug delivery

The advantages of a treatment based on dry powder formulations (DPFs) over nebulized solutions and aerosols due to regulatory limitations and environmental issues have aroused scientific research over the last decades. DPFs do not require the use of propellant, it is easy to handle, and due to their relative chemical stability, cold chain storage can be avoided [160,161], being also promising as an inhaled vaccine [162]. Besides the particle size, an efficient pulmonary drug delivery must have also into account the excipients' properties; particle release behavior, and targeting delivery [163].

2.3.1 Excipients

Inactive inert ingredients (mostly referred to as excipients) are normally added to the formulation to i) improve the physical and chemical stability of the active pharmaceutical ingredient (API); ii) provide mechanical and aerodynamic properties to the API iii) enable an accurate dosage of the drug [37] and iii) improve its pharmacokinetics behavior [164], as most of drugs and biopharmaceuticals present lack of solubility and/or permeability, being classified in the classes II, III or IV of the Biopharmaceutical Classification System (BCS). Lungs are very sensitive to external irritants, so Food and Drug Administration (FDA) has limited the approval of excipients to pulmonary delivery. The most common excipients are sugars (such as mannitol, lactose, or glucose). Beclophar®, Flixotide®, Relenza®, Seretide®, Spiriva®, and Symbicort® are some of the commercial DPI products that have lactose as the carrier [62]. Ultibro® Breezhaler® used lactose and magnesium stearate as excipients. Exubera®, withdrawn from the market in 2007, was a commercial example of an insulin-based solid dosage form mostly made up of mannitol, glycine, and sodium citrate [165,166]. Usually, the resultant DPFs are amorphous, which is an advantage as it improves the drug solubility in water and has a higher dissolution rate than in crystalline form [161]. However, the physical stability of the amorphous powders is limited as they are more hygroscopic and might return to crystalline form. For this reason, amino acids, such as leucine and trileucine, are often added to the formulation to improve the physical stability of the powder [164,167]. Hydrophobic additives, like magnesium stearate, are also added to protect the powder from moisture [37]. Magnesium stearate is the magnesium salt of the fatty acid, stearic acid [168], found in various animal and vegetable fats. The choice of lipids as excipients is related to the search for use of so-called natural and bioinspired excipients (NBEs) [164]. Phospholipids are cell membranes' constituents and the main component

of pulmonary surfactant (approximately 90 %). Therefore, they are biodegradable and present high biocompatibility. PulmoSphere™ is a commercial example of a spray-dried formulation which comprise small porous particles with characteristic spongelike particle morphology. It is constituted by a phospholipid - distearoylphosphatidylcholine (DSPC) - and $CaCl_2$, in a 2:1 molar ratio [169]. More recently, lipid-based nanoparticles have been used as mRNA carriers in currently available vaccines against the severe acute respiratory syndrome Coronavirus 2 (SARS-CoV-2) [170]. The amphiphilic nature of phospholipids (composed of lipophilic chains and a polar head group) makes them form lipid bilayers, in which the polar heads are prone to interact with the aqueous medium, whereas the long aliphatic tails interact with one another, forming liposomes. In fact, hydrophobic interactions are responsible for the formation of the lipid bilayers and Van der Waals forces maintain the long hydrocarbon chains together. The lipophilic compartment is constituted by the hydrophobic chains of each layer facing each other. Additionally, between the polar groups (of the phospholipids) and the water molecules (of the aqueous medium) hydrogen bonds, that stabilize the structure, are established.

2.3.2 Liposomal dry powder formulations

Liposomes, vesicles formed by phospholipid bilayers that enclose an aqueous medium, are a well-known, non-toxic, biodegradable, and biocompatible drug delivery systems (DDS) [17,171]. Due to their physical and chemical features, liposomes can carry hydrophilic biopharmaceuticals in an inner aqueous medium, whereas hydrophobic small molecules are inserted into the lipidic bilayer [12]. Liposome size can vary from the nano to the micro-scale [8], which is an important factor in tailoring the formulations to treat specific diseases or pathologies. In fact, liposomes up to 150 nm can escape from circulation and can accumulate at sites of inflammation, infection, or even tumors, thus taking advantage of their EPR effect [172] and resulting in passive targeting. These lipid-based nanosystems can be produced through different techniques, such as film hydration [11,172], reverse phase evaporation [173,174], ethanol injection [175], and, more recently, microfluidics [176,177], and supercritical fluids [178,179]. Despite being thermodynamically stable, after long-term storage, biopharmaceutical-loaded lipid-based nanoparticles in solution can suffer instability due to physical and chemical events, such as fusion or aggregation of the nanoparticles, or hydrolysis and oxidation of the phospholipids and/or the biopharmaceuticals [180,181]. This leads to the demand for cold supply and distribution chains. In fact, one of the disadvantages of the current mRNA-based SARS-CoV-2 vaccines is the need for cold supply chains (temperatures approximately - 80 ºC or even

2 - 8 °C) [182]. For these reasons, it is fundamental to ensure the stability of the drug-loaded liposomes via storage methods accessible to people of all social and geographical conditions. Thereby, liposome stabilization upon storage has been studied over the last 40 years to increase the shelf-life of liposomal formulations [183,184]. Moreover, the administration of the liposomes' solid form through a DPI can significantly improve drug delivery to the lungs [185]. The most common techniques to convert liposomes into dry powder formulations (Lip-DPFs) are i) freeze-drying (FD) [183], SFD [29], and SD [186]. However, if on the one hand, these techniques improve storage stability, on the other, they are associated with high costs and energy consumption. In addition, they might also induce heat, cold or shear stress on the liposomes, possibly affecting their integrity [23,187]. In contrast to the FD technique, which requires post-additional processes to reduce the particle size, the SD and SFD enable particle engineering, where it is possible to precisely design the size and morphology of the resulting powder [54]. Even so, these techniques are controversial. While Gomez-Estaca *et al.* [188] prefer SD rather than FD, Chun *et al.* [189] and Zhu *et al.* [190] reported SD disadvantages including high-temperature requirements. Within the last decades, supercritical carbon dioxide ($scCO_2$) has been studied as an alternative means of producing Lip-DPFs. There are few reports in the literature about the $scCO_2$-based liposome drying process. Kunastitchai *et al.* [191] reported the production of dried liposomes using an aerosol solvent extraction system. Dried liposomes with sizes ranging from 2.7 μm to 40 μm were obtained, losing their effectiveness as a DDS. Moreover, the technique uses methanol and dichloromethane to solubilize the lipids. The final microparticles present residual content of up to 86 ppm of methanol and 30 ppm of dichloromethane. The solvent extraction takes 3 - 4 hours, making the process more expensive and not scalable. Lévai *et al.* [192] produced quercetin suspensions using soybean lecithin and Pluronic L64® using Supercritical Fluid Extraction of Emulsion (SFEE). Then, microparticles of quercetin suspensions were produced through Particles from Gas Saturated Solutions (PGSS)-drying technology.

As a matter of fact, during the drying process, the absence of stabilizing agents can lead to liposome fusion, aggregation, or even drug leakage [23]. For this reason, one of the most important factors is the presence of a liposome membrane protectant, carbohydrates being the most used. So far, a few theories have been proposed to explain the stabilizing effect of the carbohydrates, such as the water replacement theory, vitrification, and kosmotropic effects [24], [193]. The water replacement theory is the oldest theory for the liposome's stabilization upon drying. The theory suggests that during dehydration and in the solid-state, the

surrounding water molecules are replaced by hydrogen bonds with carbohydrates [24]. The vitrification theory states that in the highly viscous vitrified state of the surrounding sugar, the molecular mobility during the process decreases and constitutes a barrier between adjacent liposomal bilayers [194,195]. The kosmotropic effect theory states that carbohydrates act like kosmotropes, displacing the water molecules in the bulk phase, and persevering the three-dimensional structure of the liposomes [196].

Several works have studied the efficacy of liposomal dry powder formulations for the treatment of diverse lung diseases, such as lung cancer, tuberculosis, chronic obstructive pulmonary diseases, and cystic fibrosis, among others, as observed in Table 2.2.

Table 2.2- Liposomal dry powder formulations reported in the literature from 2001 to 2022.

Liposomes composition	Excipients	API	Technique	Observations	Year	Ref.
E-PC Cholesterol	-	Budesonide	Freeze-drying	Entrapped drug values of 91.79% to 78.99% After 24h, 63.54% of budesonide remained retained within liposomes Higher targeting factor in liposomes	2001	[60]
DPPC DMPC DMPG E-PC + DMPG DMPC + DMPG	Pharmatose 325 M (Lactose monohydrate)	Ciprofloxacin Cationic peptide (CM3) Salbutamol sulfate (SS)	Jet-milling	The Andersen cascade impactor was coupled to jet-milling **Ciprofloxacin:** 2.55 µm < MMAD <4.67 µm 10 % < FPF < 50% ; 5 % < Encapsulation < 30% **CM3:** 3.17 µm < MMAD <4.80 µm 30 % < FPF < 60%; 20 % < Encapsulation < 40% **SS**: 2.91 µm < MMAD <4.72 µm 20 % < FPF < 60% ; 15 % < Encapsulation < 35%	2003	[59]
E-PC + Chol α-tocopherol	Lactose	Ketotifen fumarate	Freeze-drying followed by planetary ball mill	65 % < Entrapped drug < 89% 1.62 µm < $D_{[4,3]}$ < 2.00 µm *In vivo* studies performed with reconstituted liposomes	2003	[197]
DPPC	Sucrose	Superoxide dismutase	Spray-drying	SOD activity of 98 % Wrinkled and raisin-like appearance particles. ED of 71 %; d_A = 2 µm and RF of 72% ESCA analysis of this formulation suggested the absence of SOD on the surface region of the powders	2004	[198]
DMPG	Lactose	Ciprofloxacin	Spray freeze-drying	FPF > 60 %; MMAD: 2.78 µm Ciprofloxacin's encapsulation efficiency in: Water: 50 %; isotonic saline: 93.5 % bovine mucin: 80 %; porcine mucus: 73 %	2005	[72]

DPPC DMPC DOPC DOTAP DOPG Chol	Mannitol Sucrose	β-Glucuronidase	Freeze-drying followed by jet-milling	Encapsulation efficiency of 40 % and retained activity above 20 % after jet-milling FPF < 15 %	2005	[28]
HSPC + Chol	Lactose Sucrose Mannitol Glycine	Amiloride Hydrochloride	Spray-drying	6.7 µm < Ps < 9.3 µm Drug retention > 97 % 50 % < FPF < 70 % Prolonged release in in vitro studies	2006	[69]
HSPC+ Chol	Trehalose L-Leucine	Tacrolimus	Spray-drying	Ps: 9.46 µm; MMAD: 2.2 µm; FPF: 71.1% *In vivo* studies show drug residence up to 24 h within the lungs and slow systemic dilution of tacrolimus	2007	[199]
DPPC+Chol	Lactose Sucrose Hydrolyzed gelatin L-leucine	Dapsone	Spray-drying	Hydrolyzed gelatin based DPFs: PS: 7.9 µm; MMAD: 2.2µm; FPF: 75.6 %; 97.8 % < Drug retention < 98.5 % Prolonged in vitro drug release up to 16 h	2008	[70]
Soya lecithin + Chol	Lactose Sucrose Mannitol Glucose	Insulin	Spray-freeze-drying	FPF: 31.4 %; MMAD: 5.07 µm 14.87 µm < Mean diameter <19.48 µm Encapsulation efficiency of 35.9 %	2008	[75]
HSPC + Chol	Mannitol (M)	Lysozyme (LSZ)	Spray-drying	$D_{[4,3]}$ of reconstituted liposomes: HPC/M/LSZ: 14.34 µm HPC/Chol9:1/M/LSZ: 9.43 µm HPC/Chol8:2/M/LSZ: 7.39 µm HPC/Chol7:3/M/LSZ: 5.15 µm Lysozyme kept their biological enzymatic activity	2010	[68]

DPPC+DSPE-PEG$_{2000}$+Chol	Sucrose Trehalose hydroxypropyl-ß -cyclodextrin (HP-ß-CD)	Prednisolone sodium phos-phate	Spray-drying Freeze-drying	**Sucrose-based DPFs**: Size increased from 104 nm to 503 nm (SD) and 95 nm (FD) **Trehalose-based DPFs**: Size increased from 98 nm to 1159 nm (SD) and 101 nm (FD) **HP-ß-CD-based DPFs**: Size increased from 104 nm to 132 nm (SD) and 108 nm (FD)	2012	[200]
CAF01	Lactose Trehalose Mannitol	-	Spray-drying	Trehalose and lactose preserve the liposome size better than mannitol. 2.48 µm < MMAD <3.33 µm Spray drying of CAF01 with trehalose resulted in the preserva-tion of the adjuvant activity *in vivo*	2013	[201]
SPC + Chol	Lactose	N-acetylcysteine	Spray-drying	$D_{[4,3]}$: 2.72 µm; MMAD: 7.3 µm; RF: 35.34%; After SD, relative antioxidant activity remained constant	2014	[185]
HSPC **DSPG** **Chol** **DSPE-PEG$_{2000}$**	Trehalose Sucrose Lactose L-Leucine	Gemcitabine-HCl	Freeze-drying fol-lowed by sized through #240 sieves	**Lactose-based DPFs:** FPF: 40.20 %; MMAD: 5.52 µm **Sucrose-based DPFs:** FPF: 34.45 %; MMAD: 6.04 µm **Trehalose-based DPFs:** FPF: 56.12 %; MMAD: 3.91 µm Better uptake of liposomal DPI formulation than plain DPI for-mulation	2016	[202]
SPC + Chol	Mannitol + Sucrose	Clarithromycin	Ultrasonic spray freeze drying	Reconstituted liposome suspension entrapment efficiency up to 80% Liposomes size increased from 196.5 nm to 398.5 nm. FPF: 53.78 % Stable after storage at RH of 60 %, 25 °C, for 3 months	2017	[203]
SPC + Chol	Mannitol	Curcumin	Freeze-drying	FPF: 46.71 %; MMAD: 5.81 µm; D_{50}: 15.02 µm Increase of anti-proliferation effect Higher anti-oxidation effect observed for curcumin liposomes	2018	[204]

DPPG HSPC Chol	Mannitol + Glycine	Colchicine Budesonide	Freeze-drying followed by sized through #120 and #240 sieves	97.9 % <Entrapment efficiency < 98.6 % 44.45 % < FPF < 48.62 % 4.09 µm < MMAD < 4.68 µm Prolonged drug retention at targeted site and reduced the systemic exposure	2018	[205]
PC + Chol DSPE-PEG_{2000}-FA DESP-PEG_{2000}-COOH	Mannitol Leucine	Docetaxel	Spray-Drying	PS: 3.94 µm; MMAD: 3.10 µm; FPF: 10 % Redispersed liposomes increase their size from 100 nm to 346 nm They display an anti-tumor activity comparable to that of initial liposome	2019	[190]
SPC + Chol	Mannitol	Vincristine	Spray-drying	2.5 µm < Ps < 5.4 µm; 6.31 % < FPD < 14.99 % D_{50}: 2.92 µm; IC_{50} values of spray-dried powder were much lower than the values of free-VCR in both MCF-7 and A549 cells; The tumor clearance was decreased by 83.2%	2019	[206]
SPC + Chol	Maltodextrin Lactose	Salbutamol sulphate	Spray-drying	**Maltodextrin-based DPFs:** D_{v50}: 6.82 µm; MMAD: 3.72 µm. Drug retention: 97.87 % **Lactose-based DPFs:** D_{v50}: 6.35 µm; MMAD: 3.42 µm Drug retention: 98.36 %; FPF: 64 %	2019	[207]
Not available	Sucrose Lactose Magnesium stearate Isoleucine	Ciprofloxacin	Spray-drying	**Sucrose-based DPFs:** FPF: 61.7 %; ED: 85.0 %; MMAD: 2.48 µm After 6 months at RH of 20 %: FPF decreased to 47.3 % and MMAD increase to 4.11 µm. **Lactose-bases DPFs:** FPF: 76.2 %; ED: 84.3 %; MMAD: 1.75 µm No modifications observed after 6 months at RHs of 4 and 20 %	2021	[208]
Not available	Lactose Leucine	Levofloxacin	Spray-drying	FPF > 50 %:	2021	[209]

				Liposomal membrane fusion occurred Increasing of the liposomes size and PdI		
Lecithin	Lactose Leucine L-fucose	Bedaquiline	Spray-drying	FPF > 70 %; 2.6 µm < D_{v50} < 3.0 µm Fucosylated liposomes increased 20 nm of their size after SD Enhanced killing of intracellular respiratory pathogen was observed	2022	[71]
HSPC **DPPC** **DSPE-NA-PEG$_{2000}$** **DAPI** **Chol**	Trehalose L-Leucine	Afatinib dimaleate	Freeze-drying followed by sized through #240 sieves	PSD: 9.6 ± 1.4 µm; Drug content of 72.56 ± 1.04% ED: 85 %	2022	[210]
DOPC + Chol	Trehalose Mannitol	AS01$_B$ adjuvant (MPL + QS-21) Ovalbumin	Thin-film freeze-drying	FPF: 66.3 %; MMAD: 2.4 µm The liposome integrity and vaccine immunogenicity were maintained in the dry powders. To aerodynamic characterization the collection cups are coated with 1.5% w/v Tween 20 in methanol to prevent bounce and re-entrapment and then left t dry before	2022	[159]

From *Web of Science* database (Keywords: liposomes AND dry powder AND pulmonary drug delivery)

Cationic adjuvant formulation 01 (CAF01): Composed of the cationic surfactant dimethyldioctadecylammonium bromide and α,α′-trehalose-6,6′-dibehenate); Chol: Cholesterol; CM3: amino acid with the sequence KWKKFIKSLTKSAAKTVVKTAKKPLIV; DAPI: dihydrochloride (2-(4-Amidinophenyl)-6-indolecarbamidine dihydrochloride; DMPC: dimyristoyl phosphatidylcholine; DOPC: 1,2-dioleoyl-sn-glycero-3-phosphocholine; DOPG: dioleoyl phosphatidylglycerol; DPPC: Dipalmitoylphosphatidylcholin; DPPG: 1,2-Dipalmitoyl-sn-glycero-3- phosphoglycerol sodium; DOTAP: Dioleoyl trimethylammonium propane; DSPE-PEG$_{2000}$: 1, ,2-distearoyl-sn-glycero-3-phosphoethanolamine-N-[amino(polyethylene glycol)-2000] ; FA: Folic acid; MPL: 3-O-desacyl-4′-monophosphoryl lipid A; HSPC: Hydrogenated soybean phosphatidylcholine. SPC: soybean phosphatidylcholine; QS-21: acylated 3, 28-bisdesmodic triterpene glycosides (1,3); RH: Relative humidity; ED: Emitted dose; RF: Respirable fraction; FPD: Fine particle deposition; PS: particle size; PSD: particle size distribution; $D_{[4,3]}$: mean diameter over volume

2.4 Quality-by-design towards an efficient pulmonary drug delivery

Both EMA and the FDA regulatory authorities, recommend the application of a Quality-by - Design (QbD) approach for the development of pharmaceutical products. According to EMA, *Quality by design is an approach that aims to ensure the quality of medicines by employing statistical, analytical and risk-management methodology in the design, development and manufacturing of medicines* [211]. The QbD takes into account the quality target product profiles (QTPPs), identifies the critical process parameters (CPPs) and, via the design of experiments (DoE) tool, establishes a relationship between them and the critical quality attributes (CQAs) and then identifies an optimal operating space (OOS) [186]. DoE is a well-established statistical method for improving the efficiency of the optimization process [127,212], and its use in the domain of the optimization of supercritical CO_2-assisted spray drying technique has been proven to be effective to obtain composite dry powder formulations (DPFs) with good aerodynamic performance and appreciable yields [82,213]. The optimization of the SASD is complex and there are other variables that, while do not contribute directly to achieving the near equilibrium state at the saturator, play a key role in the final particles' properties, such as the nozzle diameter, drying efficiency, or cyclone efficiency. Thus, a combination of thermodynamics and engineering contributions is needed for process optimization. Phase equilibria data for the binary systems CO_2+solvent is available in the literature, but as stated above no data are available for the multi-component systems involved in the atomization processes. Hence empirical studies on the effect of the operational conditions are necessary for process optimization. These studies can be very time and resource-consuming if a suitable plan of experiments is not designed. The saturator pressure, the inlet drying gas temperature, and the feed solution flow rate are common variables studied either for conventional or supercritical-assisted spray drying. Temtem *et al.* [213] reported a case study on the use of SASD benchmarked against a conventional spray-drying process for trehalose-leucine composite powders. The SASD technology enabled the successful production of inhalation powders with FPF values as high as 86% by manipulating feed solution flow rate and inlet temperature, while regardless of the process conditions, presented particles with a more homogeneous morphology maintaining a high process throughput and yield. Regarding the development of carrier-free dry powder

formulations, including the formation of nanoparticle agglomerates, the most significant operational conditions affecting the process, apart from the inlet temperature and the gas and feed flows, are the type of excipients, especially the selection of the stabilizer and the ratios of stabilizer and each excipient to drug weight [214]. These selections will influence the downstream process of spray drying by affecting the yield and the particle size distribution of the resultant aerosolizable microsized particles and are typically optimized by DoE in the industry [215]. With a limited number of experiments, DoE enables a withdrawal of the statistically significant correlations between the operating conditions and the final particles' properties, being a powerful tool to optimize the process and reduce the time of experimental work, and hence the cost of atomization. Therefore, the combination of both tools would allow more efficient particle engineering in the SAA/SASD process, especially of more complex multifunctional particle systems.

3

MICROFLUIDICS APPLIED ON THE PRODUCTION OF PROTEINS/ENZYMES LOADED PEGYLATED LIPOSOMES

The content of this chapter was published in two peer reviewed international journals:

C. Costa,* Z. Liu,* J.P. Martins, A. Correia, P. Figueiredo, A. Rahikkala, W. Li, J. Seitsonen, J. Ruokolainen S.-P. Hirvonen, A. Aguiar-Ricardo, M. Luísa Corvo, H. A. Santos. All-in-one microfluidic assembly of insulin-loaded pH-responsive nano-in-microparticles for oral insulin delivery, Biomater. Sci., **2020**, 8, 12,3270–3277.
(https://pubs.rsc.org/en/content/articlelanding/2020/BM/D0BM00743A)
* *These two authors equally contributed to this work.*
C. Costa, Z. Liu, S. Simões, A. Correia, A. Rahikkala, J. Seitsonen, K. Ruokolainen, A. Aguiar-Ricardo, H. A. Santos, M. Luísa Corvo. One-step microfluidics production of enzyme-loaded liposomes for the treatment of inflammatory diseases, Colloids and Surfaces B: Biointerfaces, **2021**, 199, 111556.
(https://www.sciencedirect.com/science/article/pii/S0927776520309139)
Reproduced with the authorization of the editor and subjected to the copyrights imposed.

Personal contribution

CC contributed to the design of the study, co-optimized the microfluidics conditions and variables, performed the experimental work and wrote the manuscript.

In this chapter, the study of liposome production using microfluidics is presented in two distinct works. When this study started, the assembling of a glass-capillary microfluidic device and the optimization of microfluidic process parameters in terms of flow rate ratio, total flow rate, and lipid composition were performed considering the desired final properties of liposomes and encapsulation efficiency. Since Cu, Zn- superoxide dismutase is expensive, the optimization step was performed using insulin as a model protein. Facing the potential application of the results, the studies were pursued, and nano-in-microparticles were produced for oral protein delivery. After obtaining interesting results with insulin, the studies were pursued considering Cu, Zn- superoxide dismutase (SOD), an enzyme weighing 32.5 kDa, with small adaptations in the microfluidic device.

3.1 All-in-one microfluidic assembly of insulin-loaded pH-responsive nano-in-microparticles for oral insulin delivery

3.1.1 Abstract

In this study, we have developed a continuous two-step glass-capillary microfluidic technique to produce nano-in-microparticles for oral insulin delivery. The current bulk methods applied to the preparation of liposomes often required a post-processing steps to homogenize the liposome's size, being time-consuming. Microfluidics overcome these drawbacks, offering a batch-to-batch reproducibility and less time consuming. The coating with chitosan improves the mucoadhesion of the nanoparticle in the cells. Additionally, the encapsulation in an enteric polymer, through a microfluidic glass-capillary based double-emulsion, confer the total protection from the harsh gastric conditions. This work is a promising alternative for the common protein/peptide-loaded liposome formulations, using a scalable two-steps microfluidics process in the preparation of multistage microparticles aimed at the oral insulin administration
.

3.1.2 Introduction

The oral route of administration represents the most convenient way to administer drugs in terms of high patient compliance [216,217], promoting a fast and safe route, overcoming

several main disadvantages from parenteral administration namely the intravenous [218–221]. However, the oral delivery of therapeutic proteins and peptides represents a big challenge for the pharmaceutical technology field. In fact, the degradation of protein and peptides under acidic conditions in the stomach concomitantly with digestive enzyme action, as well as the poor oral bioavailability, characterized by a poor protein permeability in the intestinal epithelium [222–224] have led to the need of designing and developing alternative approaches to enhance the oral protein/peptide administration [225–227]. Over the last decade, the research for different strategies for the oral delivery of proteins and peptides, such as microemulsions [228,229], polymeric nanoparticles [229–231], silicon nanoparticles [232,233], and liposomes [234,235] has been significantly increasing. Liposomes, introduced for the first time by Bangham *et al.* [171] at the beginning of the 1960s, have been described as potential proteins and peptides drug carriers able to enhance their blood residence time and targeting [236–238]. However, even with high potential to deliver proteins, conventional liposomes are still likely to disintegrate in gastric conditions [239,240] and can show poor permeation across the intestinal epithelial cell membrane [241], thus resorting to coatings with other molecules, such as polymers [242,243] or protein corona [244,245]. Yet, liposomes are usually prepared under bulk methods such as thin-film hydration [172,246], ethanol injection [175] and reverse phase evaporation [173,174], in which some of them require a post-processing step to obtain a better control of size and polydispersity index (PdI), such as high pressure extrusion [247].

Microfluidics, a sophisticated technique for particles production, has gained substantial attention to prepare liposomes. High batch-to-batch reproducibility, reduced time and cost, and increased control on the production of nanoparticles are some of the advantages of microfluidics [21,248,249]. Polydimethylsiloxane (PDMS)-based microfluidic devices are widely used on liposome preparation. PDMS is compatible with some pharmaceuticals grade solvents, such as ethanol [177]. However, PDMS microfluidic devices have low resistance to high flow rates and pressures and, upon contact with common organic solvents, tend to swell. In addition, due to the hydrophobicity of the polymer, post-surface functionalization of the polymer is required [250–252]. Attending to these drawbacks, glass-capillary microfluidic devices are a good alternative when there is the need to use organic solvents. Besides, they can tolerate high flow rates and pressure [253]. The glass-capillary microfluidic devices enable the production of liposomes through a nanoprecipitation method [254,255]. If a central flow of a phospholipid-containing alcohol solution merge into a main channel with the aqueous solution in adequate concentrations, the lipids spontaneously self-assemble producing liposomes [256], with diameters in the

range of 73-131 nm, as described by Vladisavljevic *et al.* [176] Moreover, these devices enable the generation of monodisperse droplets via co-flow, coaxial flow-focusing geometry or via the combination of both geometries [20,253], offering an excellent control of the size of the droplets by adjusting the flows of immiscible fluids inside the microchannels and the dimensions of the orifices of the channels [257,258]. By the solidification of the monodisperse droplets, microparticles with an uniform size distribution can be produced [259]. In this way, using the glass-capillary microfluidic devices both nano- and nano-in-microparticles can be obtained, which represents a huge advantage for oral administration since microparticles have been described as preferable for this kind of administration than nano-sized systems [260]. Besides, microparticles are more attractive for oral delivery over the conventional larger capsules or pill-type vehicles due to the patient compliance and convenience, namely in children that have some difficulties to swallow the larger pills or capsules [261,262].

In this study, we present an optimized and continuous "all-in-one" two-step microfluidic production of a nano-in-micro composite system, as shown in Figure 3.1. This multistage system provides full protection from the harsh gastric conditions and improves the mucoadhesion to the intestinal epithelium, promoting the protein/peptide release across the intestinal epithelium. Firstly, the microfluidic process parameters were optimized in terms of flow rate ratio, the total flow rate and lipid composition. Secondly, through a nanoprecipitation method, insulin was encapsulated into PEGylated liposomes (Ins_Lip), using a glass-capillary microfluidic device. Then, the physical coating with chitosan was achieved to confer mucoadhesive properties to liposomes (Ins_Lip-CHT) to improve the insulin transport across the intestinal epithelium. Finally, through a double emulsion microfluidics method, the nanoparticles were an enteric coating encapsulated within the FDA approved excipient for oral administration - hydroxypropyl methylcellulose acetate succinate (HPMCAS-MF; M grade fine powders; abbreviated as MF), was prepared to protect the liposomes nanoparticles against the harsh stomach acidic conditions (Ins@MPs). The nano and microparticles were characterized in terms of particle size and ζ -potential, insulin encapsulation efficiency and loading degree. The insulin release profiles in different buffers, and the Ins@MPs cell viability and their interactions with Caco-2 and HT29-MTX cell lines were also evaluated. Finally, the insulin permeability across an in vitro model of intestinal epithelium (Caco-2/HT29-MTX cells), was evaluated. To the best of our knowledge, this is the first time that an "all-in-one" continuous microfluidic production of insulin-loaded nano-in-microparticles for oral drug delivery is reported.

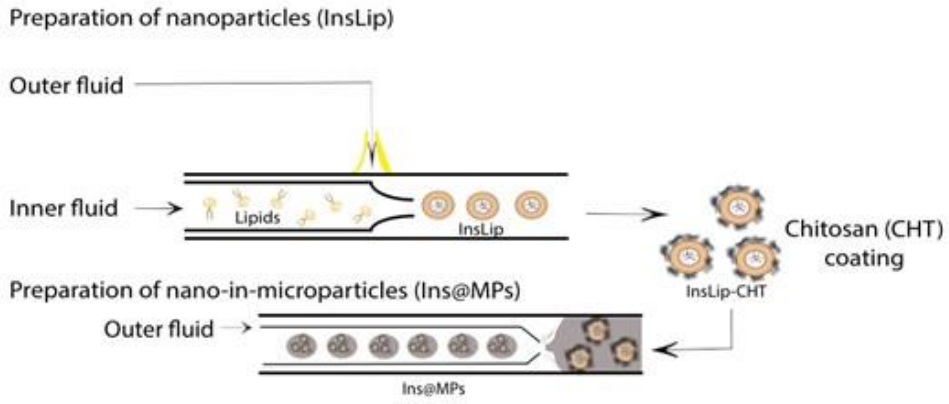

Figure 3.1- Schematic representation of the two-step microfluidics process of insulin-loaded nano-in-microparticles (not to scale), in which insulin is encapsulated in PEGylated liposomes (InsLip) through a nanoprecipitation technique, using a glass-capillary microfluidic device. The InsLip-CHT were further encapsulated in an enteric polymer (MF) using a double-emulsion microfluidic process, forming the final microcarrier system (Ins@MPs).

3.1.3 Experimental procedure

3.1.3.1 Materials

Egg-phosphatidylcholine (E-PC) and distearoylphosphatidylethanolamine-poly(ethyleneglycol)$_{2000}$ (DSPE-PEG$_{2000}$) were obtained from Lipoid (Germany). Cholesterol (Chol), recombinant human insulin (rhIns), medium viscosity chitosan (*M*w= 190 000–310 000 Da, 75–85 % deacetylated), 2-(4-(2-hydroxyethyl) piperazin-1-yl) ethanesulfonic acid (HEPES), paraformaldehyde (PFA), citric acid and sodium chloride were purchased from Sigma-Aldrich (USA). Poloxomer 407 (Kolliphor® 407) was purchased from BASF (Germany). MF grade of HPMCAS was kindly provided from ShinEtsu (Japan). Hank's balanced salt solution (HBSS) and phosphate buffer saline (PBS) were purchased from Life Technologies (USA). Fasted state simulated intestinal fluid (FaSSIF) was purchased from Biorelevant.com Ltd (London, UK). Triton® X-100 was purchased from Merck Millipore (Germany). Dulbecco's Modified Eagle medium (DMEM), L-glutamine, non-essential amino acids, penicillin (100 IU/mL) and streptomycin (100 mg/mL), ethylenediamine tetraacetic acid (EDTA) and trypsin–EDTA were purchased from HyClone (USA). Human colon carcinoma (Caco-2) and the human colorectal adenocarcinoma modified with methotrexate (HT29-MTX) cells were purchased from ATCC (USA). 4',6-Diamidino-2-phenylindole (DAPI-405), 4-[4-(dihexadecylamino)- styryl]-N-methylpyridinium iodide (DiA) and Gibco™ Versene Solution were purchased from Thermo Scientific (USA). CellMask Red® was

purchased from Invitrogen (USA). CellTiter-Glo® assay reagent was purchased from Promega Corporation (USA).

3.1.3.2 Preparation of insulin-loaded liposomes (Ins_Lip)

The recombinant human insulin was encapsulated into the inner aqueous space of liposomes by a microfluidics glass-capillary method. Briefly, E-PC, DSPE-PEG_{2000} and Chol (molar ratio 1.85:0.15:1, respectively) were dissolved in ethanol in a concentration of 43.2 µmol/mL. In parallel, rhIns was dissolved in saline citric acid solution (145 mM of NaCl, 10 mM of Citric Acid, pH 2.0) in a final concentration of 100 µg/mL. The insulin-loaded liposomes (Ins_Lip) were achieved using a co-flow microfluidic device. Briefly, a borosilicate glass capillary with an inner diameter of 70 µm was inserted into a glass capillary with an inner diameter of 1000 µm and they were coaxially aligned. The lipidic solution was injected into the inner phase, while the insulin solution was injected into the outer phase, both with flow rates of 10 mL/h and a flow rate ratio (FRR) of 1. The non-encapsulated protein was separated from the liposomes by ultracentrifugation twice, after a dilution of 20 times (Optima L-80, XP Ultracentrifuge, Beckman Coulter, CA, USA), at 135 000 *g* at 15 °C for 2 h. Then, the Ins_Lip pellet was re-suspended in a saline citric acid solution at pH 2.

3.1.3.3 Coating of Ins_Lip by chitosan (Ins_Lip-CHT):

The Ins_Lip was coated with chitosan by physical adsorption. Briefly, chitosan solution (10 mg/mL) was prepared dissolving chitosan powder in 1 % of acetic acid solution (v/v). The solution was kept under stirring overnight. Then, the pH was increased to pH 5.5 with 0.01 of NaOH and the final solution was centrifuged (Hettich EBA 21, Tuttlingen, Germany) at 4 020 *g* for 15 min [263] to remove the precipitated chitosan. Afterwards, the Ins_Lip suspension was added dropwise to the chitosan solution at the same volume ratio and kept under stirring for 6 h. Then, the dispersion containing chitosan-coated liposomes (Ins_Lip-CHT) was centrifuged (Optima MAX, Beckmann Coulter, USA) twice at 27 000 *g* for 4 min.

3.1.3.4 Preparation of insulin-loaded microparticles

The Ins_Lip-CHT nanoparticle encapsulation into MF was performed by water-in-oil-in-water (W/O/W) double emulsion, also using the microfluidic technique [264]. The nanoparticles were dispersed in a MF (10 mg/mL in ethyl acetate) in a volume ratio of 1:10 and sonicated (inner oil fluid), in order to obtain a homogeneous suspension. In parallel, the outer aqueous solution

was prepared by dissolving Poloxamer 407 in Milli-Q water (10 mg/mL, pH 4.0). Afterwards, a flow focusing microfluidic chip, as previously described [259], was used. To achieve the double emulsion, the inner and outer flow rates of 0.5 mL/h and 3.0 mL/h were employed. The formed droplets were collected in 10 mg/mL of Poloxamer 407 aqueous solution, pH 4.0. Finally, the nano-in-microparticles (Ins@MPs) were collected and were washed for three times with Milli-Q water, using the centrifuge (Hettich EBA 21, Tuttlingen, Germany) at 3 000 rpm for 5 min.

3.1.3.5 Characterization of liposomes and insulin-loaded nanoparticles

The mean size, determined as Z-average, polydispersity index as a measure of the particle size distribution that can range from 0 (monodisperse) and 1.0 (polydisperse), and the surface charge (zeta-potential, ζ) of Ins_Lip and Ins_Lip-CHT NPs dispersions were determined by Zetasizer Nano ZS (Malvern Panalytical Ltd., Malvern, UK). The morphology of the liposomes was confirmed using cryo-transmission electron microscope (Cryo-TEM, JEOL JEM-3200FSC, JEOL, Tokyo, Japan). Briefly, prior to use, vitrified specimens were prepared using an automated FEI Vitrobot device, and Quantifoil 3.5/1 holey carbon copper grids with a hole size of 3.5 μm. Then, an aliquot of liposomal suspension was applied on the grid and it was blotted twice for 5 sec and then vitrified in a 1:1 mixture of liquid ethane and propane at −180 °C. The grids with the vitrified liposomes were kept in liquid nitrogen temperature and then cryo-transferred to the microscope.

Imaging was carried out using a field emission cryo-TEM (JEOL JEM-3200FSC), operating at 200 kV. Images were taken in the bright field mode and using zero loss energy filtering (omega type) with a slit width of 20 eV. Micrographs were recorded using a Gatan Ultrascan 4000 CCD camera (Gatan Inc., Pleasanton, CA, USA). The specimen temperature was maintained at −187 °C during the imaging. The images were treated using Gatan Microscopy Suite Software (Gatan Inc).

The encapsulation efficiency (*EE*) was calculated based on the amount of insulin encapsulated into the liposomes, previously disrupted with 2 % (v/v) Triton® X-100, as follows (Eq. 1):

$$EE\ (\%) = \frac{Ins_{Liposomal}\ (\mu g)}{Ins_{Liposomal}\ (\mu g) + Ins_{free}\ (\mu g)} \times 100 \qquad (1)$$

Where the $Ins_{Liposomal}$ is the insulin encapsulated into liposomes and Ins_{free} is the insulin present in the supernatant from the ultracentrifugation, described above. Both were

determined using a high-performance liquid-chromatography (HPLC; Agilent 1260, Agilent Technologies, Santa Clara, CA, USA), using a C18 column, 15 cm × 4.6 mm, 5 µm (SUPELCO Discovery®, Sigma Aldrich, St. Louis, MO, USA), and the method as previously described [230].

3.1.3.6 Characterization of insulin-loaded microparticles

The dimensional analysis of the Ins@MPs were performed using confocal fluorescence microscopy, with a 10× objective. Briefly, an aliquot of Ins@MPs was dispersed on a 35 mm Petri-dish with a thin bottom and imaged using a confocal laser scanning microscope (Leica SP5 II HCS A, Leica, Wetzlar, Germany). The chemical modification upon encapsulation in MF was evaluated using attenuated total reflectance Fourier transformed infrared (ATR-FTIR) spectrometry. The spectra were recorded from 3 600 to 690 cm^{-1}, with a resolution of 2 cm^{-1}.

The amount of insulin loaded into the nano-in-microparticles was evaluated dissolving and disrupting them with a solution of PBS (pH 6.8) and 2% (v/v) Triton® X-100, in a ratio of 1:1 (v/v) and analyzed by HPLC, as described above. The loading degree (*LD*) was then calculated as follows (Eq. 2):

$$LD(\%) = \frac{Ins_{microparticles}\ (\mu g)}{Ins@MPs\ (\mu g)} \times 100 \quad (2)$$

Where $Ins_{microparticles}$ is the amount of insulin loaded into the microparticles and $Ins@MPs$ is the total mass of insulin-loaded nano-in-microparticles.

3.1.3.7 *In vitro* drug release studies

The insulin release profile from Ins@MPs was evaluated by mimicking the gastrointestinal tract conditions at 37 °C under stirring. First, 150 µg of Ins@MPs were dispersed in 4 mL of simulated gastric fluid (SGF) at pH 1.2. SGF solution was prepared with 0.2 % (w/v) sodium chloride and 0.7 % (v/v) hydrochloric acid, without pepsin to avoid insulin degradation, during the release studies. After 2 h, the solution was centrifuged (EBA 21, Andreas Hettich GmBH & Co, Tuttlingen, Germany) at 6 000 *g* for 15 min, the pellet was resuspended and dispersed into 4 mL of FaSSIF (pH 6.8) for the following 24 h. The studies were conducted taking 100 µL at determined time-points, being the solution replaced at the same volume in order to keep the volume constant. Then, the samples were centrifuged (Micro Centrifuge, Model 5415D, Eppendorf, Hamburg, Germany) at 16100g for 5 min. The insulin, released from the nanoparticles, was determined using the HPLC method, as described above. All the experiments were performed at least in triplicate.

3.1.3.8 Cell lines and cell culture conditions

HT29-MTX (passage #30) and Caco-2 (passages #35-40) were separately cultured in a 75 cm^2 culture flask in DMEM containing 10 % of fetal bovine serum, 1 % (v/v) of L-glutamine, penicillin, streptomycin and 1 % (v/v) of NEAA. For further cell growth, the conditions were maintained at 37 °C in 5 % of CO_2 and relative humidity of 95 %. The cell culture medium was changed every other day. Sub-culturing was performed using trypsin-PBS-EDTA when confluency reached 80 %.

3.1.3.9 *In vitro* cytotoxic studies:

The cell viability studies were carried out using CellTiter-Glo® assay reagent diluted with HBSS−HEPES buffer (pH 7.4), in a ratio of 1:1 (v/v)). Briefly, 5 × 10^4 cells of Caco-2 and HT29-MTX cell lines were individually seeded in 96-well plates (Corning Inc., USA), and left to attach for 24 h. Afterwards, the medium was discarded, and the cells were washed with HBSS-HEPES buffer at pH 7.4. Then, 100 µL of microparticles with a concentration from 50 to 1000 µg/mL were added to the cells. The cells were incubated at 6 h or 24 h, under 37 °C. After the incubation time, cells were washed twice with fresh HBSS−HEPES (pH 7.4), and 100 µL of CellTiter-Glo® was added. The plates were lightly shaken for for 2 min. HBSS−HEPES and 1 % (v/v) Triton® X-100 solutions were used as positive and negative controls, respectively. The luminescence values were measured using a Varioskan Flash Multimode Reader (Thermo Fisher Scientific, Waltham, MA, USA). All the experiments were performed at least in triplicate.

3.1.3.10 Drug permeability across Caco-2/HT29-MTX cell monolayer

The insulin permeability across the Caco-2/HT29-MTX cell monolayer was evaluated as previously described [223,230]. Briefly, Caco-2 and HT29-MTX cells were seeded on 12-Transwell™ filter membranes (3 µm pore-size; Corning Inc., USA) inserts in a ratio of 9:1 (v/v), respectively, at a seeding density of 5 × 10^4 cells per cm^2. For 21 days, the medium was replaced every other day until the complete monolayer formation. At the 21st day, the transepithelial electrical resistance (TEER) was measured using a Millicell® ERS-2 volt-ohm-meter with STX01 electrodes (Millipore, Burlington MA, USA).

The insulin permeability across the cell monolayer from the apical (donor) to basolateral (receiving) compartment was evaluated as follows. Briefly, 2.0 mg of Ins@MPs (equivalent to 15.6 µg/mL of insulin) and the equivalent concentration of free insulin (as control), were added on the apical part with FaSSIF (0.5 mL) at pH 6.8. HBSS-HEPES (1.5 mL) at pH 7.4 was added to the

basolateral compartment in order to simulate the physiological condition. The experiment was evaluated, in triplicate, at 37 °C and shaking at 100 rpm [232]. At different time-points, 200 µL of the basolateral compartment were withdrawn and replaced with the same volume of pre-warmed HBSS-HEPES (pH 7.4). The permeated insulin was then quantified by HPLC, as described above, and the apparent permeability P_{app} was calculated according to Eq. 3:

$$P_{app}\ (cm\ s^{-1}) = \frac{dQ}{dt)} \times \frac{1}{C_0 A} \quad (3)$$

Where $\frac{dQ}{dt}$ is the steady-state flux (µg s^{-1}), C_0 is the initial drug concentration on the apical compartment (µg/mL) and A is the surface area of the membrane (cm^2). The TEER values were measured in all time-points. All the experiments were performed at least in triplicate.

3.1.3.11 Cell–nanoparticle interaction studies

The interaction studies between cells and liposomes, as well as liposomes-coated chitosan were evaluated. Briefly, a hydrophobic dye, DiA, was entrapped by microfluidics into the liposomal bilayer (DiALip), in a mass ratio 100:1 (Lip:DiA), as described above. Then, the liposomes were physically coated by CHT (DiALip-CHT). The morphological properties of DiALip and DiALip-CHT were evaluated in order to keep the same properties that the Ins_Lip and Ins_Lip-CHT, respectively. Afterwards, the interactions between the Caco-2 and HT29-MTX cell lines and DiA-loaded NPs, were quantitatively and qualitatively evaluated by flow cytometry and confocal microscopy, respectively.

For evaluation by flow cytometry, 0.4 mL of the cells were seeded in 24-well plates at a density of 1×10^5 cells per well and left to attach overnight. Then, the cell culture medium was removed, and the cells were washed once with PBS buffer (pH 7.4). Afterwards, 0.3 mL of 500 µg/mL of DiALip and DiALip-CHT suspensions were incubated with the cells for 6 h at 37 °C. After removing the nanoparticles and washing the cells with PBS buffer in order to remove the non-adherent nanoparticles, the cells were detached with Gibco™ Versene Solution for 5 min (0.48 mM). The cells were then washed once with PBS buffer and suspended with PBS-EDTA (pH 7.4) for flow cytometer analysis. Then, the cells were incubated with trypan blue (0.005 %, v/v) during 4 min, washed twice with PBS-EDTA (pH 7.4), and suspended with PBS-EDTA. Flow cytometry was performed with the LSR II flow cytometer (BD Biosciences, San Jose, CA, USA), using a

laser excitation wavelength of 488 nm and a FACS Diva software. After collecting 2 × 10^4 events, the data was analyzed using FlowJo VX software (Tree Star, Ashland, OR, USA).

Regarding the confocal microscopy, 200 µL of 5 × 10^4 cells per well were seeded in Lab-Tek 8-chamber slides (Thermo Fisher Scientific, USA) and left to attach overnight. After removing the cell culture medium, 200 µL of 500 µg/mL Ins_Lip and Ins_Lip-CHT suspensions in PBS buffer (pH 7.4) were added to the cells and incubated for 6 h at 37 °C. The cells were then washed twice with PBS buffer (pH 7.4). The plasma membrane was stained by adding 200 µL of Cell-Mask Red (5 µg/mL) and incubated for 3 min at 37 °C. To remove the excess of staining solution, it was washed once with fresh PBS buffer. Afterwards, the cells were fixed using 4% paraformaldehyde (PFA), for 10 min at room temperature. Finally, the nuclei staining was done by adding 200 µL of DAPI-405 (2.8 µg/mL) and incubated for 5 min at 37 °C. The localization of nanoparticles was observed with a Leica SP5 inverted confocal microscope (Leica Microsystems, Germany), using a 63×/1.2-0.6 oil immersion objective. All the experiments were performed in triplicate.

3.1.3.12 Insulin structure stability

The structure stability of insulin, after permeability across the monolayer, was studied by J-815 (Jasco Co Ltd, Hachioji, Japan) far UV circular dichroism spectroscopy. For each experiment, quartz cuvettes with 10 mm were used. Each spectrum was recorded from 400 to 190 nm, with a data pitch of 1 nm and using a scanning speed of 100 nm min^{-1} at 20 °C. All the records were performed in triplicate.

3.1.3.13 Statistical analysis

All results are expressed as mean ± standard deviation (S.D.). To analyze the data, analysis of variance (ANOVA) followed by Bonferroni post test (GraphPadPrism, GraphPad software Inc., CA, USA) was used. The level of significance was set at the probabilities of *p< 0.05, **p< 0.01 and ***p< 0.001.

3.1.4 Results and Discussion

3.1.4.1 Influence of microfluidics parameters on liposomes morphology

Firstly, the microfluidic parameters such as flow rate ratio (FRR), initial lipid concentration and total flow rate, were optimized to prepare liposomes with a size between 100 and 150 nm and

an acceptable narrow PdI (< 0.2). To assess the influence of the FRR (the ratio between the aqueous and the organic phases) on the size and PdI of the liposomes, the microfluidic parameters outer flow rate and initial lipid concentration were kept constant (outer flow rate = 20 mL/h and initial lipid concentration = 43.2 µmol/mL). The FRR was varied between 1 and 10 (Figure 3.2A). As expected, increasing the FRR reduces the size of the liposomes [177,265]. This phenomenon can be related with the non-equilibrium kinetic model described by Zook and Vreeland [265]. This kinetic model applied to liposomes suggests that the size of the liposomes is closely related with the growth rate of the lipid planar discs (bilayered phospholipid fragments (BPFs)), and with the closing rate of the discs into spherical vesicles. In this way, the model predicts that at higher FRRs, the alcohol concentration decreases faster and the lipid disc growth rate decreases. In addition, since BPFs grow with less stabilization, the lipid discs close faster, producing smaller liposomes. In contrast, at lower FRRs, the BPFs take more time to grow, and due to the stabilization from the alcohol stream, they take more time to close, making the liposomes larger [247,265]. The optimization was pursued towards the study of the effect of the total flow rate (TFR) on the morphological properties of the liposome. The TFR was varying between 10 to 100 mL/h, while the FRR was kept at 1 and the initial lipid concentration at 43.2 µmol/mL. The Figure 3.2B shows that the TFR has no significant effect ($p>0.05$) on the size of the liposomes, which is in accordance with previous studies [266,267]. This represents an advantage of the scalable microfluidics increasing the throughput does not affect significantly the liposomes size. Likewise, it does not affect the PdI, which remained below 0.2. Thus, since the desired size and acceptable PdI were obtained with a total flow rate of 20 mL/h, the studies were pursued with a lipid concentration of 43.2 µmol/mL and a total flow rate of 20 mL/h. As the lipid concentration plays an important role on the morphology of the liposomes, the initial lipid concentration was varied from 20.8 to 54.0 µmol/mL (the total flow rate was kept at 20 mL/h and the FRR was kept at 1). The Figure 3.2C shows an increase of the size of the liposomes with the increase of lipid concentration. Upon contact with the aqueous solution, the alcohol, in which the lipids were initially solubilized, diffuses into the water leading to a lipid supersaturation [265]. Similar to the FRR, the intermediate lipid discs, described as BPFs, are formed in the ethanol/water interface and are thermodynamically less stable. When the BPFs grow, they tend to fuse and enclose into a vesicle [268] thus, higher lipid concentration can produce more BPFs, enabling the generation of larger vesicles. An initial lipid concentration of 43.2 µmol/mL was selected to pursue the experiments.

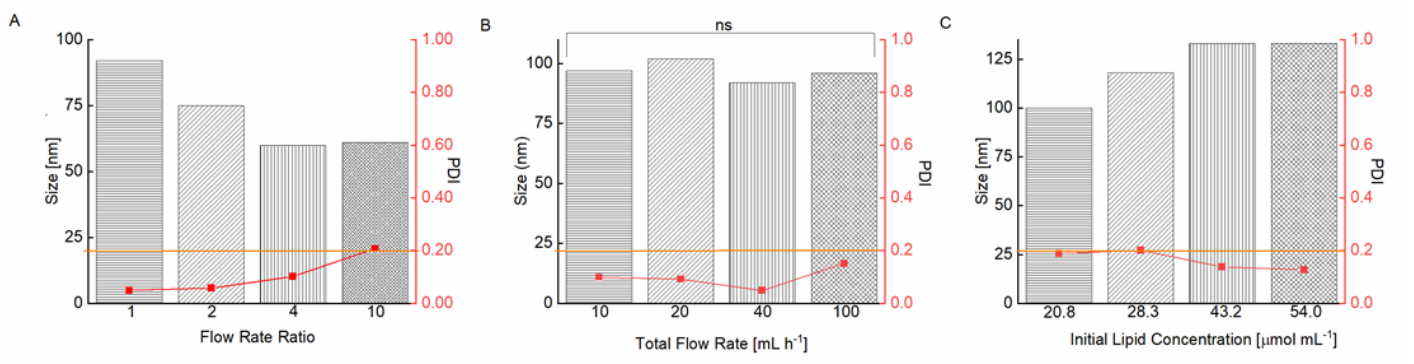

Figure 3.2- Size (bar) and PdI (red squared dots) of liposomes on the optimization of the microfluidics parameters for liposomes production: A) flow rate ratio, keeping constant the total flow rate of 20 mL/h and initial lipid concentration = 43.2 µmol/mL; B) total flow rate (mL/h), keeping fixed the FRR of 1 and initial lipid concentration = 43.2 µmol/mL and C) initial lipid concentration (µmol/mL), keeping fixed the FRR of 1 and total flow rate of 20 mL/h. The orange line represents the maximum PdI value acceptable for liposomes (0.2).

Cryo-TEM was performed in order to confirm the morphology/structure of the Ins_Lip nanoparticles. For the optimized parameters, the cryo-TEM images show a thin single-wall structure enclosing a vesicle, confirming that the structure of the nanoparticles corresponds to that of liposomes, with a mean size of 110 ± 20 nm, similarly to the values obtained by DLS (Figure 3.3). In addition, using the Gatan Microscopy Suite software, it was possible to measure the thickness of the bilayer of the liposomes, which was around 6 ± 1 nm.

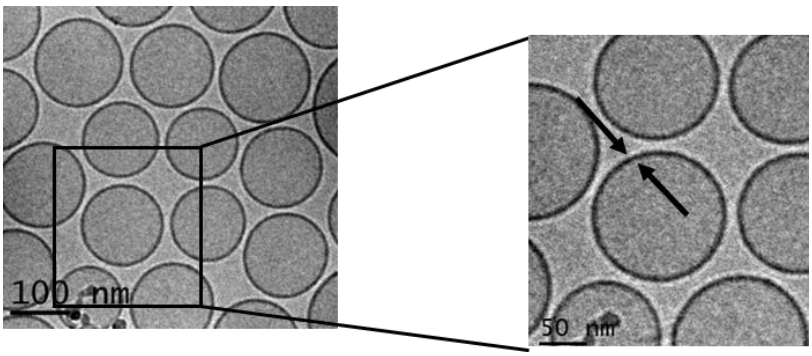

Figure 3.3- Cryo-TEM images of liposomes, using the optimized microfluidic parameters described above.

The encapsulation of insulin in liposomes was then carried out with the previous optimized parameters. Recombinant human insulin (Ins) was first dissolved in a citrate solution, at pH 2.0, at a concentration of 100 µg/mL (outer phase), whereas lipids E-PC, DSPE-PEG_{2000} and Chol were dissolved in ethanol at a concentration of 43.2 µmol/mL (inner phase). Through a nano-precipitation phenomenon [255], lipids upon contact with the citrate solution, self-assembled, forming protein-loaded PEGylated liposomes (Ins_Lip). After being collected from the glass capillary, Ins_Lip were characterized in terms of hydrodynamic size, PdI, and encapsulation efficiency (*EE*) Ins_Lip were obtained with an average size of 144 ± 23 nm, a mean PdI of 0.130 ± 0.003 and *EE* of 91 ± 4 % (Table 3.1).

Considering that this process is continuous, the *EE* was calculated from the total concentration of insulin in the liposomes and the insulin present in the supernatant after liposomes washing. During the assays, no precipitated insulin was observed. To the best of our knowledge, the *EE* obtained represents an improvement compared to previous studies, involving liposomes with same morphological properties (Niu *et al.* presented an insulin-loaded liposomes with a size of 150 nm and an *EE* of 30 % [235,241], whereas Muramatsu *et al.* reported liposomes with size between 106–108 nm with an *EE* of 21.5 % [269]).

The physical coating of chitosan on the Ins_Lip (Ins_Lip-CHT) was achieved by adding the Ins_Lip suspension in dropwise to the chitosan solution (10 mg/mL in 1 % of acetic acid solution (v/v), pH 5.5), at the same volume ratio and kept under stirring for 6 h. Then, the dispersion containing chitosan-coated liposomes (Ins_Lip-CHT) was centrifuged and washed twice. The coating was observed by the change in the Ins_Lip-CHT average size and PdI, up to a mean size of 363 ± 54 nm and a PdI of 0.315 ± 0.057. In addition, the increase of the zeta-potential from a value near to zero (–0.5 ± 0.1 mV) to positive (+23 ± 1 mV) suggests the successful chitosan coating of the liposomal surface. Since the zeta-potential of Ins_Lip was near zero

value, it is expectable that the interaction between the liposomes and chitosan might be occurred by van der Waals and hydrogen bonding forces [270].

Table 3.1- Physicochemical characterization of insulin-loaded nanoparticles and Ins_Lip-CHT.

	Size [nm]	PdI	ζ-potential [mV]	*EE* [%]
Ins_Lip	144 ± 36	0.130±0.003	- 0.5 ±0.1	91 ± 4
Ins_Lip-CHT	363 ± 54	0.315 ±0.057	+ 23 ± 1	-

The results are expressed as mean ± S.D (n = 3)
PdI: Polydispersity index

3.1.4.2 Characterization of insulin-loaded microparticles

Nano-in-microparticles are mostly used for their ability to effectively deliver higher local doses in a specific tissue [271]. In this way, through a double emulsion microfluidics method, the nanoparticles were encapsulated in the FDA approved excipient for oral administration, hydroxypropyl methylcellulose acetate succinate (HPMCAS-MF; M grade fine powders; abbreviated as MF), to protect the liposomes against the harsh stomach acidic conditions (Ins@MPs). MF is a synthetic enteric polymer with an average molecular weight around 17000 Da and a polydispersity approximately 1.3 [272] and, since it presents a pKa ~5, this polymer is widely used for oral drug delivery applications [273]. The encapsulation of the Ins_Lip-CHT in the MF matrix resulted in a batch of 15 mL of insulin-loaded nano-in-microparticles (Ins@MPs) with a size of 19 ± 1 μm. The ATR-FTIR spectra (Figure 3.4) of Ins@MPs shows a band at 1710 cm-1, which corresponds to the C=O stretching of carboxylic group from MF, as well as the band at 2900 cm-1, which belongs to the C-H stretching of the alkyl group. Nevertheless, the broad band at 3388 cm-1 and the band at 1630 cm-1 corresponding to the N-H stretching of the amine and C=O stretching of the amides groups, respectively, suggesting the presence of chitosan [274,275]. Apart from these bands, the spectrum of Ins@MPs is very similar to the MF spectra, suggesting an efficient encapsulation of Ins_Lip-CHT by MF. The microparticles were characterized in terms of loading degree, which was 0.39 ± 0.02 %.

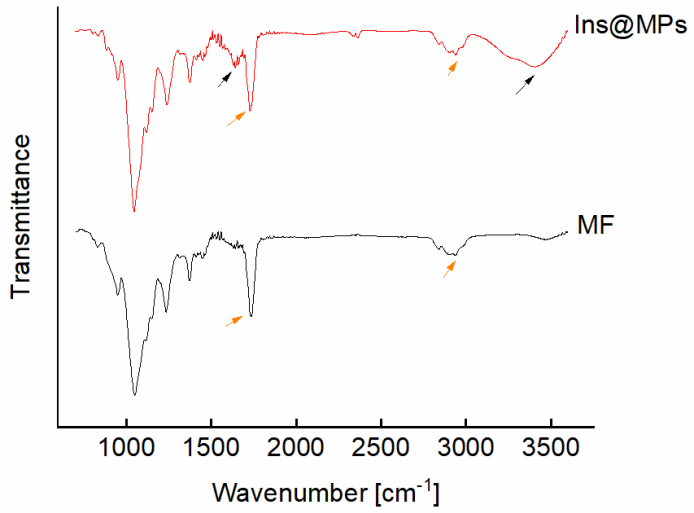

Figure 3.4 - ATR-FTIR spectra of MF and insulin-loaded nano-in-microparticles (Ins@MPs). Black arrows: bands from chitosan chemical groups; Orange arrows: bands from MF chemical groups.

3.1.4.3 In vitro drug release studies of Ins@MPs

To mimic the gastric conditions, the Ins@MPs were dispersed for 2 h in simulated gastric fluid (SGF) at pH 1.2. Afterwards, the microparticles were dispersed in fasted state simulated intestinal fluid (FaSSIF) at pH 6.8, to test their behavior after the transition from the stomach to the small intestine conditions. Regarding to the pH-responsiveness of MF-based microparticles, TEM imaging and the size measurement over the time have shown that MF microparticles keep intact at pH 1.2, but upon pH increase to 6.8, the enteric polymer starts to dissolve, releasing the CHT-based NPs, and after 2 h, the polymer is completely dissolved [263,275,276]. With respect to the pH of the small intestine on the fed or fasted state, McConner *et al.* reported that the fed state of the animal (rats or mice) had no significant effect on the pH [277]. Thus, it is hypothesized the insulin release might not be affected by food intake, although this needs to be still confirmed in the future for our particular system. The pH-responsiveness of MF was observed in the release studies. The Figure 3.5 shows that there was no release in SGF during the first 2 h, due to the successful encapsulation in the enteric polymer (MF) that is not soluble at pH below 6.0 [278]. However, MF dissolved when the pH was changed to 6.8, exposing Ins_Lip-CHT to the solution and a burst release of 7.5 % of insulin was observed in the first minutes, whereas after 24 h an insulin release up to 25 % was achieved. These results corroborate that, in this work, MF plays a relevant role in the nanoparticles protection, since previous

works have demonstrated that in the absence of MF, at pH 1.2, insulin would be released from CHT-based nanoparticles [275,276].

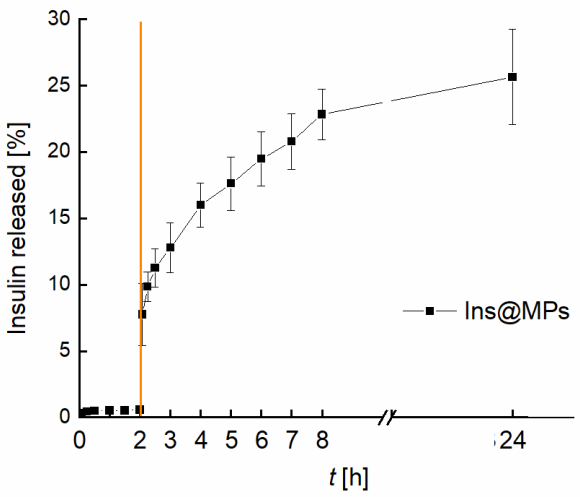

Figure 3.5- Insulin release profile from insulin-loaded nano-in-microparticles (Ins@MPs), in the first 2 h in SGF (pH 1.2) and then in FaSSIF (pH 6.8) for 24 h at 37 °C. The transition from SGF to FaSSIF is represented by the orange line. The results are expressed as mean ± S.D. (n = 3).

3.1.4.4 In vitro cytotoxic studies of Ins@MPs

Next, cell viability assays were carried out to evaluate the toxicity of the nano-in-microparticles with and without insulin. The intestinal cell lines, Caco-2 and HT29-MTX, were used in this study. Human colon carcinoma Caco-2 cells have been used over the years as a model of intestinal barrier. Upon differentiation, Caco-2 cells express similar characteristics to the small enterocytes [279]. The HT29 cells (colon adenocarcinoma) are frequently used as a model of epithelial cells of the intestinal mucosa. When they are treated with methotrexate (MTX), they become resistant to cytostatic drug and an adhesive mucus layer is formed on the apical side of a monolayer cell culture [280]. The *in vitro* cytotoxicity assay was conducted by exposing both cell lines to the nano-in-microparticles with and without insulin for 6 and 24 h, in concentrations ranging from 50 µg/mL to 1000 µg/mL of microparticles (corresponding to 0.195 µg/mL to 0.390 µg/mL of insulin, respectively) (Figure 3.6). After the first 6 h, for the Caco-2 cells, the nano-in-microparticles without insulin did not show signs of cytotoxicity, with a cell viability above 80%, for all concentrations tested. For Ins@MPs, a cell viability decrease was observed for the higher concentration used (1000 µg/mL), however, it was not statistically significant ($p<0.05$). Furthermore, after 24 h, a slight decrease in the viability of Caco-2 cells (13%

for Ins@MPs and 12% for the nano-in-microparticles) was observed at a concentration of 1000 µg/mL. Since at pH 6.8, the cells were exposed to the chitosan from Ins_Lip-CHT, this decrease in their viability can be related with the Caco-2 cytotoxicity dependence to the chitosan concentration, as reported in previous studies [281,282]. Regarding to the HT29-MTX cell line, when the nano-in-microparticles were in contact with cells, even at higher concentrations, their viability remained higher than 80 %, for both time points tested. This low cytotoxicity is in accordance with other studies reported in the literature and can be explained by the presence of mucus on the HT29-MTX surface, which acts as a barrier [223].

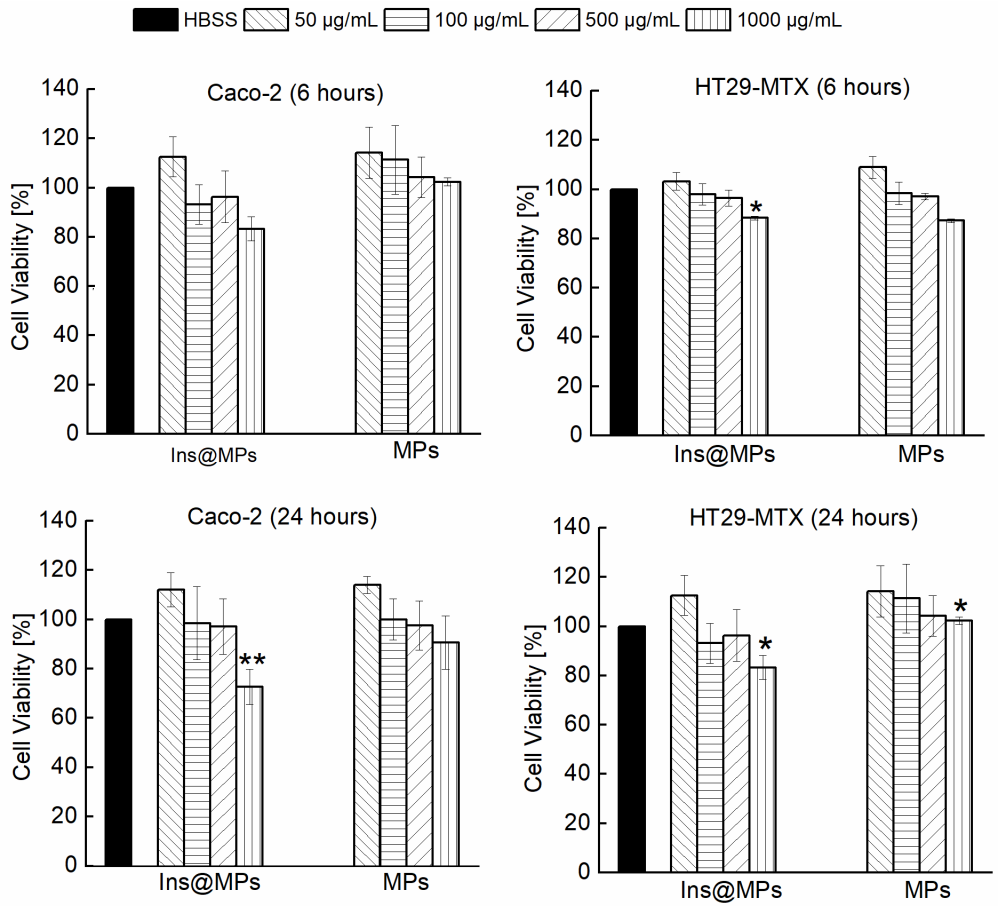

Figure 3.6- Caco-2 and HT29-MTX cells lines viability when exposed to different concentrations of nano-in-microparticles with and without insulin, after 6 h and 24 h of incubation at 37 °C. All the data were compared to the negative control (HBSS–HEPES buffer, pH 7.4). The level of significance was set at the probabilities of *p< 0.05 and **p< 0.01.
The results are expressed as mean ± S.D. (n = 3).

3.1.4.5 Drug permeability across the Caco-2/HT29-MTX cell monolayer

Once verified the cells viability, the insulin permeability across a monolayer was evaluated. To reach the bloodstream, which is mandatory for a successful insulin drug delivery, insulin must cross from the apical to the basolateral side of the intestinal epithelium. To closely mimic the *in vivo* physiological intestinal environment, Caco-2 and HT29-MTX were co-cultured for 21 days to form a monolayer [223]. The Ins@MPs were incubated with the cells for 3 h at pH 6.8 (apical compartment), whereas the pH in the basolateral compartment was kept at pH 7.4. The experiment was carried out using free insulin as a control. The permeated insulin dissolved in the basolateral compartment was quantified by HPLC. As observed in the Figure 3.7.A, a higher permeation was observed for the Ins@MPs than for free insulin (P_{app} of 2.27×10^{-5} cm s^{-1} and 1.19×10^{-7} cm s^{-1}, respectively). Since the pH in the apical compartment was 6.8, the existing enteric polymer (MF) was dissolved, exposing the chitosan-coated liposomes. These results are in accordance with the release studies, where insulin release occurred only at pH 6.8. At each time-point, transepithelial electrical resistance (TEER) was measured (Figure A1, Appendix A) to monitor the ion conductance across the monolayers. This phenomenon is characterized by the opening of the monolayer tight junctions. Once opened, the ion transport across the paracellular route [283,284] will be faster. In this nanosystem, TEER values tend to decrease faster for the Ins@MPs than for free insulin, as expectable. Some studies have reported that chitosan tends to bind with integrins from the membrane of intestinal epithelial cells activating a signal pathway that involves protein kinases, such as focal adhesion kinase (FAK) and Src tyrosine kinase [285]. In turn, these kinases induce degradation and translocation of the tight junctions proteins, such as cytoplasmic proteins, occludin and claudin (*e.g.*, CLDN4) [286,287]. This activation mechanism promotes the reversible opening of the tight junctions, enhancing the permeability of the molecules through a paracellular pathway [288]. In contrast, the decrease of the TEER values observed for free insulin, after 120 min, was not expectable, since in the drug permeability assays, no insulin was observed in the basolateral compartment. During the insulin permeation, it was important to evaluate whether its activity remains the same. Thus, far UV region circular dichroism, a tool widely used to identify the structural secondary elements of peptides [289], was performed in order to identify the α-helix and β-sheet structures of the permeated insulin and to compare them with the native form of insulin (Figure A2, Appendix A). As described elsewhere, the insulin's α-helix conformation is characterized by a valley at 208 nm and a shoulder at 223 nm [241,290]. These properties can be also clearly observed in

the permeated free insulin and insulin released from liposomes (Figure 3.7.B). In addition, when two insulin monomers associate themselves, antiparallel β-structure are created. This phenomenon can be observed through the ratio of $\theta_{208nm}/\theta_{223nm}$ [241]. The insulin dissolved in saline citric solution, at pH 2, (free insulin) presents a ratio of 0.949, whereas the insulin from Ins@MPs presents a ratio of 1.035, which is close to the value of native insulin (1.088). Therefore, regarding these observations, it is possible to conclude that the insulin's structure remained preserved after being loaded into the liposomes and permeated through the Caco-2/HT29-MTX monolayers.

3.1.4.6 Cell–nanoparticle interaction studies

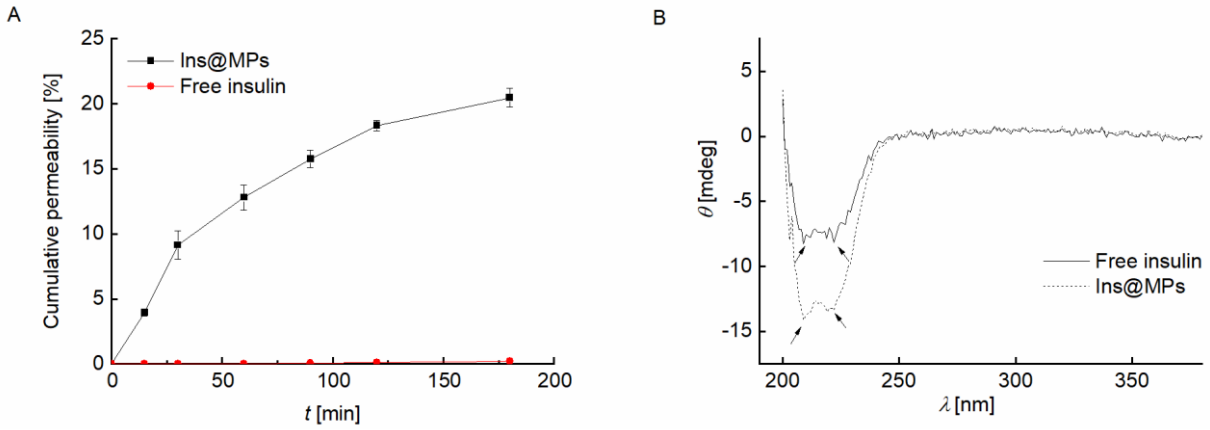

Figure 3.7- A) Insulin permeation profile across Caco-2 and HT29-MTX co-cultured (ratio of 9:1) cell monolayers. The Ins@MPs were incubated with FaSSIF (pH 6.8) in the apical compartment and HBSS–HEPES (pH 7.4) in the basolateral compartment. All the experiments were carried out for 3 h at 37 °C, using and orbital shaker at 100 rpm. B) Circular Dichroism of permeated free insulin at 2.3×10^{-2} µg/mL (solid black line) and insulin from Ins@MPs at 1.1 µg/mL (dash black line), in HBSS–HEPES (pH 7.4). The results are expressed as mean ± S.D. (n = 3).

In order to evaluate the Ins@MPs interaction with both cell lines (Caco-2 and HT29-MTX), confocal fluorescence microscopy was used for qualitative analysis, in which a fluorescent membrane dye, 4-(4-Dihexadecylaminostyryl)-N-methylpyridinium iodide (DiA), was used for imaging purposes. In this way, the experiments were carried out with 500 µg/mL of DiA-loaded liposomes (DiALip) and DiALip-loaded chitosan nanoparticles (DiALip-CHT) for 6 h. The nanoparticles coated with MF were not evaluated, since at this pH the polymer is completely dissolved, as shown in the release experiments. Figure 3.8.A shows the interaction of both nanoparticles with Caco-2 cells. It is possible to observe that DiALip were not internalized, only interacting with the cell's surface. This observation is supported by the presence of the poly(ethyleneglycol)$_{2000}$ (PEG_{2000}) in the liposomes. PEG, grafted onto the surface of the

liposomes promotes an elevated liposomes blood circulation, by the decrease of macrophages recognition and opsonization [291,292]. In addition, the slightly negative charge from DSPE-PEG_{2000} can promote a steric barrier with the cells, and thus, DiALip take more time to be internalized [293]. In contrast, the liposomes coated with chitosan were easily internalized. Regarding Figure 3.8.A, it is possible to observe a decrease of fluorescence intensity on Ins_Lip-CHT. This phenomenon might be due to the chitosan-based nanoparticles internalization whereas the DiALip were on the cell membrane. This phenomenon was also observed in the quantitative flow cytometry study, indicating the chitosan capability to enhance the cellular uptake. A difference of more than 10 % of the DiALip-CHT association with the cells show the higher interactions of this system, comparing with DiA-loaded liposomes (Figure 3.8.B). Confocal images of the HT29-MTX cells (Figure 3.8.C) did not show notable interactions between the cells and the nanoparticles. However, this difference was detected in the flow cytometry quantitative analysis (Figure 3.8.D). These different observations could be due to the confocal images show part of the sample, whereas flow cytometry quantifies all the sample. In this way, regarding the Figure3.8D, an uptake of over 40% of the chitosan-coated liposomes was observed, whereas no uptake was detected for liposomes without chitosan. This phenomenon was also observed in previous works [263,294] and it might be related to the chitosan mucoadhesion properties, driven by the electrostatic interactions between the positive charge of the chitosan and the negative charge of mucin [295].

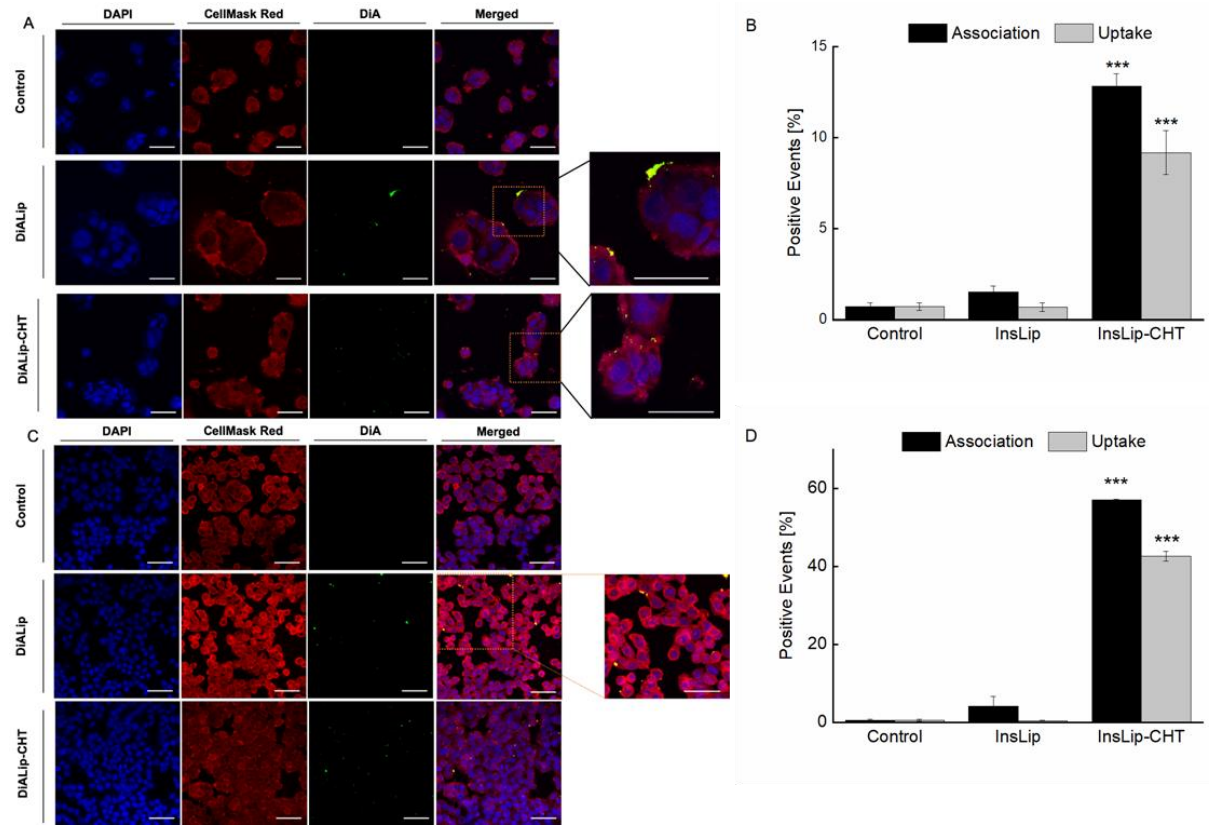

Figure 3.8- A) and C) 2D confocal fluorescence microscope images of the interactions of insulin-loaded liposomes (DiALip) and insulin-loaded liposomes coated by chitosan (DiALip-CHT) at a concentration of 500 µg/mL, with Caco-2 cells and HT29-MTX cells, respectively. Blue: Cell nucleus stained by DAPI (4',6'-diamino-2-fenil-indol); red: cell membranes stained with Cell Mask Red; green: DiA (4-(4-Dihexadecylaminostyryl)-N-methylpyridinium iodide)-encapsulated liposomes (scale bar: 50 µm). B) and D) Flow cytometry quantitative analysis of the interactions between the nanoparticles and the Caco-2 cells and HT29-MTX, respectively. The experiments were carried out at 37 °C after 6 h incubation time. The level of significance was set at a probability of ***p< 0.001.

3.1.5 Conclusions

In this work, a multistage oral insulin delivery system using a two-step microfluidics process was successfully designed and developed. Insulin was efficiently encapsulated (91 ± 4 %), into PEGylated liposomes using a microfluidics technique, overcoming the common liposome batch production drawbacks, and obtaining a narrow size distribution. This allowed the successful encapsulation of the nanoparticles in an enteric polymer, preventing their degradation upon harsh gastric conditions. *In vitro* release studies showed insulin release starting only at pH 6.8, above the pKa of MF, demonstrating an efficient protection upon gastric acidic conditions. 2D Confocal microscope images and flow cytometry analysis supported that the mucoadhesive

properties of the nanoparticles were enhanced by the physical coating with chitosan on the surface of the liposomes. In addition, insulin permeability and circular dichroism studies showed a strong improvement on the insulin permeation across the intestinal epithelium without compromising its activity, respectively. Moreover, the low cytotoxicity of the Ins@MPs in the intestinal cells was observed. Overall, we obtained a pH-responsive mucoadhesive cell-mimicked system for protein/peptides delivery that represents a promising strategy for a continuous, scalable, and high throughput method to produce oral targeted systems.

3.2 One-step microfluidics production of enzyme-loaded liposomes for the treatment of inflammatory diseases

3.2.1 Abstract

The biopharmaceuticals market is constantly growing. Despite their advantages over the conventional drugs, biopharmaceuticals have short biological half-lifes, which can be increased using liposomes. However, the common bulk methods to produce biopharmaceuticals-loaded liposomes result in loss of *EE*, resulting in an expensive process. Herein, the encapsulation of a therapeutic enzyme in liposomes is proposed, using a glass-capillary microfluidic technique. Cu,Zn- Superoxide dismutase (SOD) is successfully encapsulated into liposomes (SOD_Lip). SOD_Lip with a mean size of 135 ± 41 nm, a polydispersity index of 0.13 ± 0.01, an *EE* of 59 ± 6 % and an enzyme activity of 82 ± 3 % are obtained. *In vivo* experiments show, through an ear edema model, that SOD_Lip administered by the intravenous route enable an edema inhibition of 65 % ± 8 %, over the 20 % ± 13 % of SOD in its free form. The histopathological analyses show a higher inflammatory cell accumulation on the ear treated with SOD in its free form, than treated with SOD_Lip. Overall, this work highlights the potential of microfluidics to produce enzyme-loaded liposomes with high encapsulation efficiency, with the intrinsic advantages of the low time-consuming and easily upscaling microfluidic assembly method.

3.2.2 Introduction

Biopharmaceutical drugs, such as nucleic acids, monoclonal antibodies and therapeutic enzymes, are one of the fastest growing areas on the pharmaceutical industry [296]. Comparing with the synthetic drugs, biopharmaceuticals exhibits higher activity, selectivity and lower side

effects [297]. However, biopharmaceuticals can present low oral bioavailability , instability in biological fluids and short biological half-times, leading to a deficient systemic delivery and requiring high doses to obtain an efficient therapeutic effect [298,299]. Moreover, depending on the route of administration, biopharmaceuticals can suffer degradation and low absorption [300,301]. These issues can be easily overcome when a suitable drug delivery system (DDS) is developed to a targeted and efficient transport of the biopharmaceuticals [302]. Liposomes, introduced for the first time by Bangham and co-worker [171] at the beginning of the 1960s, have been widely used on the pharmaceutical field [254,303,304]. Liposomes are able to carry both hydrophobic and hydrophilic active compounds in the lipidic bilayer and into the inner aqueous core, respectively, enhancing the blood residence time and the targeted delivery of the drugs [236–238]. For this reason, the application of liposomes as a versatile drug delivery system has increased over the last decades. For example, the encapsulation of biopharmaceuticals in liposomes leads to a modification in their pharmacokinetics and pharmacodynamics, improving their therapeutic activity [304]. Mokhtarieh *et al.* have reported that the encapsulation of siRNA in liposomes prevented it from the RNase degradation and elimination [305]. Another example is related with the Cu,Zn-Superoxide dismutase (SOD). SOD is an enzyme with a molecular weight of 32.5 kDa that catalyzes the dismutation of anion superoxide radical in molecular oxygen and hydrogen peroxide. This enzyme is widely used on the treatment of reactive oxygen species (ROS)-mediated diseases, such as rheumatoid arthritis [9,12], inflammation [306,307] and ischemia-reperfusion injury [306,307]. However, the administration of SOD without a drug delivery system presents some disadvantages, such as the short half-life in the bloodstream (~6 min in rats and 25 min in humans) [308,309], low accumulation in affected areas and rapid renal filtration [9]. Previous studies have reported the importance of the use of PEGylated liposomes as a carrier for SOD on the improvement of the enzyme biodistribution and its therapeutic effect in inflammatory processes, increasing its half-life up to 20 h [11,12,172]. In addition, the presence of PEG on the surface of the liposomes plays an important role on the administration of SOD-loaded liposomes, since it avoids the liposomes opsonization by the mononuclear phagocyte system (MPS) [310,311]. For this reason, the application of liposomes in the delivery of biopharmaceuticals has aroused a particular interest. The common bulk techniques for the production of liposomes rely on the thin-film hydration [172,246], reverse phase evaporation [173,174] and ethanol injection [175]. Apart from the fact that post-processing steps, such as high pressure extrusion [247], are required to obtain a better control

of size and polydispersity index (PdI), these techniques also involve the use of organic solvents often resulting in an enzyme inactivation during the process [312].

Moreover, the saturation curve of the enzyme concentration in the inner aqueous space and the technical compromise between the efficient encapsulation and the small size of the liposomes [172], make reaching a stable and *EE* of macromolecules in liposomes challenging [313]. Previous works have demonstrated that bulk methods result in enzyme-loaded liposomes with low *EE* for small liposomes due to the sizing of the liposomes by extrusion, but with an efficient therapeutic effect. These works also related the effect of the sizing on the *EE,* where it is notorious that the lesser the need of sizing (less extrusion processes) of the liposomes, the higher the *EE* of SOD. For example, Corvo *et al*. obtained an *EE* of 8–21 %, 27 ± 3% and 20 % for SOD-loaded liposomes with 110 ± 10 nm [172], 230 ± 90 nm [12] and 200 ± 20 nm , respectively. York-Duran *et al*. obtained an *EE* of 3.0 ± 0.8 % for catalase-loaded liposomes size between 110 and 120 nm [314]. Moreover, Morozova *et al.* reported an *EE* about 25 % for enzyme-loaded liposomes with 218 ± 6 nm [315].

Microfluidics is an emerging technology, which enables the manipulation of fluids (in nanoliters scale) in micrometer channels [316]. Over the last years, this technique has gained a special attention on the biomedical field, since it can be widely used for the production of polymeric nano/micro-particles, due to the advantages of being a continuous process when compared to the current bulk methods [317]. High batch-to-batch reproducibility, higher process control, easy scalability and no requirement of post-processing steps are some of the advantages that microfluidics can offer [256,318]. The application of the microfluidics for the liposomes production, specifically glass-capillary microfluidic devices, has been reported [176,266,267]. Through a nanoprecipitation method [177,255] it is possible to produce liposomes in a single step process [319,320].

In this work, we propose the production of enzyme-loaded liposomes (SOD_Lip) with similar physico-chemical properties of the commonly produced ones by bulk methods, but with higher efficiency encapsulation and process yield, using a glass-capillary microfluidic device (Figure 3.9). We aimed to obtain a continuous and simple one-step method that offers a scalable, reproducible, time and cost efficient and a high throughput production of SOD-loaded PEGylated liposomes for therapeutic purposes.

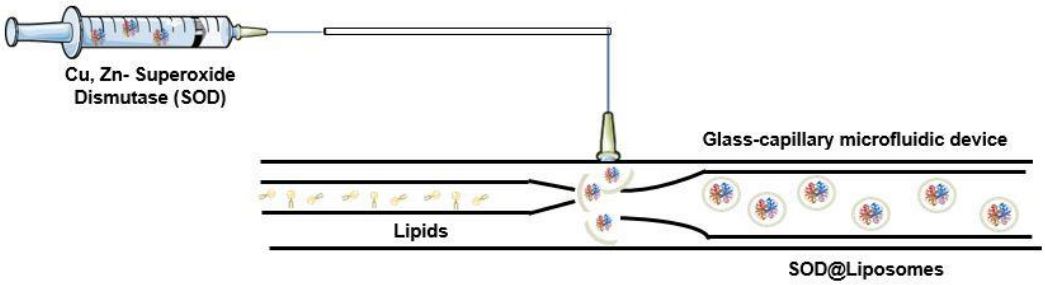

Figure 3.9- Schematic representation of the microfluidic process on the encapsulation of SOD in PEGylated liposomes (not to scale). Lipids and cholesterol were dissolved in ethanol (inner phase), whereas SOD was dissolved in a saline citric buffer at pH 6 (outer phase). Through the nanoprecipitation technique, the lipids self-assembled, enclosing the enzyme in the aqueous inner phase (SOD-Lip). SOD-Lip were then collected by the collecting capillary.

3.2.3 Experimental procedure

3.2.3.1 Materials

Egg-phosphatidylcholine (E-PC) and distearoylphosphatidylethanolamine-poly(ethyleneglycol)$_{2000}$ (DSPE-PEG$_{2000}$) were obtained from Lipoid (Germany). Cholesterol (Chol), bovine erythrocytes Cu, Zn-superoxide dismutase, 300 kU (SOD), 2-(4-(2-hydroxyethyl) piperazin-1-yl) ethanesulfonic acid (HEPES), citric acid, anthralin and sodium chloride were purchased from Sigma-Aldrich (USA). Hank's balanced salt solution (HBSS) and phosphate buffer saline (PBS) were purchased from Life Technologies (USA). Triton® X-100 was purchased from Merck Millipore (Germany). Dulbecco's Modified Eagle's medium (DMEM), L-glutamine, non-essential amino acids, penicillin (100 IU/mL) and streptomycin (100 mg/mL), ethylenediamine tetraacetic acid (EDTA) and trypsin–EDTA were purchased from HyClone (USA). Human colon carcinoma (Caco-2) and the human colorectal adenocarcinoma modified with methotrexate (HT29-MTX) cells were purchased from ATCC (USA). CellTiter-Glo® assay reagent was purchased from Promega Corporation (USA).

3.2.3.2 Preparation of liposomes and SOD-loaded liposomes (SOD_Lip)

The liposomes and SOD-loaded liposomes were prepared by the nanoprecipitation method, [47] using a modified co-flow microfluidic glass-capillary device. Briefly, a borosilicate glass capillary (inner capillary with a diameter of 100 μm) was placed in front of another glass capillary with an inner diameter of 120 μm (collecting capillary), slightly deviated. Both were inserted

into a glass capillary (outer capillary) with an inner diameter of 1000 µm. Then, a mixture of E-PC, DSPE-PEG_{2000} and Chol (molar ratio 1.85:0.15:1, respectively) was dissolved in ethanol, in a total lipid concentration of 48.0 µmol/mL and injected in the inner phase. Alike, a saline citric acid buffer (145 mM of NaCl, 10 mM of Citric Acid, pH 6.0) without and with SOD, in a final concentration of 75 µg/mL, was injected in the outer phase. Both streams were injected with flow rates of 25 mL/h and a flow rate ratio (FRR) of 1. The SOD_Lip from the collecting capillary and non-encapsulated enzyme was separated from the liposomes by ultracentrifugation twice (Optima L-80, XP Ultracentrifuge, Beckman Coulter, CA, USA), at 135 000 *g* at 4 °C for 2 h. Then, the SOD_Lip pellet was re-suspended in a saline citric acid buffer solution at pH 6.0. The experiment was performed in triplicate.

3.2.3.3 Characterization of liposomes and SOD_Lip

The liposomal formulations were characterized in terms of their morphology and phospholipid concentration. SOD_Lips were also characterized in terms of protein concentration and enzyme activity. Liposome size, determined as Z-average, the PdI, as a measure of the particle size distribution that can range from 0 (monodisperse) and 1.0 (polydisperse), and the surface charge (zeta (ζ)-potential), were determined using Zetasizer Nano ZS (Malvern Instruments Ltd., UK). The structure of the SOD_Lip was confirmed using cryo-transmission electron microscope (Cryo-TEM, JEOL JEM-3200FSC, JEOL, Tokyo, Japan). Briefly, prior to use, vitrified specimens were prepared using an automated FEI Vitrobot device, and Quantifoil 3.5/1 holey carbon copper grids with a hole size of 3.5 µm. Then, an aliquot of liposomal suspension was applied on the grid and it was blotted twice for 5 sec and then vitrified in a 1:1 mixture of liquid ethane and propane at −180 °C. The grids with the vitrified liposomes were kept in liquid nitrogen temperature and then cryo-transfered to the microscope. Imaging was carried out using a field emission cryo-TEM (JEOL JEM-3200FSC), operating at 200 kV. Images were taken in the bright field mode and using zero loss energy filtering (omega type) with a slit width of 20 eV. Micrographs were recorded using a Gatan Ultrascan 4000 CCD camera (Gatan Inc., Pleasanton, CA, USA). The specimen temperature was maintained at −187 °C during the imaging. The images were treated using Gatan Microscopy Suite Software (Gatan Inc).

The concentration of phospholipids was determined by the Rouser's method [321]. The enzyme was quantified with a modified Lowry's method [322], where liposomes were previously disrupted with 2 % (v/v) Triton® X-100 and 20 % (v/v) of sodium dodecylsulphate (SDS) [323]. The *EE* was calculated as follows (Eq. 1):

$$EE\ (\%) = \frac{\left(\frac{Prot}{Lip}\right)_f}{\left(\frac{Prot}{Lip}\right)_i} \times 100 \quad (1)$$

where, the $\left(\frac{Prot}{Lip}\right)_i$ is the initial SOD-to-lipid ratio and $\left(\frac{Prot}{Lip}\right)_f$ is the SOD-to-lipid ratio after the removal of the non-encapsulated enzyme.

The SOD enzymatic activity from SOD_Lip was evaluated using the SOD assay kit (19160-1KT-F, Sigma-Aldrich), where liposomes were previously disrupted with 2 % (v/v) Triton® X-100 and 20 % (v/v) of SDS.

3.2.3.4 Cell lines and cell culture conditions

HT29-MTX (passage #32) and Caco-2 (passages #35-40) were separately cultured in a 75 cm^2 culture flask in DMEM containing 10% of fetal bovine serum (FBS), 1 % (v/v) of L-glutamine, 1% (v/v) of penicillin and streptomycin and 1 % (v/v) of non-essential amino acids. The cells were left to grow under 37°C, in 5 % of CO_2 and relative humidity of 95 %. The cell culture medium was changed every other day. Sub-culturing was performed using trypsin-PBS-EDTA when confluency reached 80 %.

3.2.3.5 *In vitro* cytotoxic studies

The cell viability studies were carried out using CellTiter-Glo® assay reagent (previously diluted with HBSS−HEPES buffer at pH 7.4, in a ratio of 1:1 (v/v)). Briefly, 5 × 10^4 cells of Caco-2 and HT29-MTX cell lines were individually seeded in 96-well plates (Corning Inc., USA), and left to attach for 24 h. Afterwards, the medium was discarded, and the cells were washed with HBSS–HEPES buffer at pH 7.4. Then, 100 µL of liposomes with a SOD concentration ranging from 2.5 to 15 µg/mL were added to the cells. The cells were incubated at 6 h or 24 h, under 37 °C. After the incubation time, cells were washed twice with fresh HBSS−HEPES buffer, and 100 µL of CellTiter-Glo® was added. The plates were lightly shaken for 2 min. HBSS−HEPES and 1% (v/v) Triton® X-100 solutions were used as positive and negative controls, respectively. The luminescence values were measured using a Varioskan Flash Multimode Reader (Thermo Fisher Scientific, USA). All the experiments were performed at least in triplicate.

3.2.3.6 Animal experiments

NMRI female mice (6 weeks of age) were purchased from Charles River (France). The animals were used after one week for acclimatization on the laboratory environment (21 ± 1 °C and 50

± 4 % of relative humidity; 12 h day/night cycle and water and food *ad libitum*). All animal experiments were conducted according to the animal welfare organ of the Faculty of Pharmacy, Universidade de Lisboa, approved by the competent national authority Direção Geral de Alimentação e Veterinária (DGAV) and in accordance with the EU Directive (2010/63/UE) and Portuguese laws (DL 113/2013, 2880/2015, 260/2016, and 1/2019).

3.2.3.7 Anthralin induced ear edema model

The anthralin induced ear edema model was performed according to Lange *et al.* [324], modified by Ascenso *et al.* [325]. When applied onto the ear skin, anthralin provokes an ear swelling, induced by ROS in the skin. The animals were anesthetized, and the thickness of both ears was measured using a Mitutoyo® dial gage. Six groups of animals (n = 5) were tested: (i) 7.3 µg of SOD (180 µL) of SOD_Lip were administered intravenously (i.v.); (ii) 7.3 µg of SOD (180 µL) of SOD previously dissolved in citrate buffer (free SOD (i.v.)) were administered i.v.; (iii) 7.3 µg of SOD (180 µL) of SOD_Lip were administered intraperitoneally (i.p.); (iv) 7.3 µg of SOD (180 µL) of SOD previously dissolved in citrate buffer (free SOD (i.p.)), administrated by i.p.; (v) 10 µL of 0.1% betamethasone solution was applied on the right ear (positive control); and (vi) one group of animals received no treatment. Treatments were administered 1 h before the challenge for groups from (i) to (iv). Group (v) received the application 1 h after the challenge. The challenge, 10 µL of anthralin (10 mM) suspended in a mixture of 70% ethanol and olive oil (4:1), was topically applied on the pinna of both ears in all groups. Mice were kept in individual cages and, 24 h after the challenge, the resulting edema was determined through the measurement of the ears thickness (in triplicate). The percentage of the edema inhibition was determined by the comparison between the thickness of non-treated ears (negative control) and ear thickness of the treated animals.

3.2.3.8 Histopathological analysis

After the experiments, mice were euthanized with prior anesthesia with isoflurane and the ear pinna were collected. Then, the ears were fixed in formalin and submitted to histopathological analysis. Hematoxylin and eosin stain were used.

3.2.3.9 Statistical analysis

All results are expressed as mean ± standard deviation (S.D.), except the animal experiments which are expressed as mean ± standard error of the mean (SEM). To analyze the data, analysis of variance (ANOVA) followed by Bonferroni post-test (GraphPadPrism, GraphPad software

Inc., CA, USA) was used. The level of significance was set at the probabilities of *p< 0.05, **p< 0.01 and ***p< 0.001.

3.2.4 Results and Discussion

3.2.4.1 Characterization of Liposomes and SOD_Lip

The encapsulation of SOD in liposomes was achieved through a nanoprecipitation method [255]. In fact, into the glass-capillary microfluidic device, upon contact with the saline citrate buffer, the polarity of the lipid-based ethanolic solution increased. Lipids self-assembled, enclosing the buffered SOD (SOD_Lip). Previous works have demonstrated that, due to the physicochemical properties of the SOD and liposomes, SOD is exclusively encapsulated in the inner aqueous compartment [8,12,172]. In the case of empty liposomes (control), a buffered aqueous core was enclosed in spherical vesicles [256,265]. The obtained SOD_Lips were characterized, and the results are shown in Table 3.2. SOD_Lip presented an average size of 135 ± 41 nm, and a PdI of 0.128 ± 0.010, whereas liposomes without SOD presented an average size of 171 ± 14 nm and a PdI of 0.140 ± 0.016. Even though it would be expected that SOD_Lip presented higher diameter values, the difference between the size of SOD_Lip and empty liposomes is within the variability with the variability among the batches. Both formulations presented a near zero ζ- potential value, as expected for PEG coated liposomes. The *EE* for SOD_Lip was 59 ± 6 % (Table 3.2). Previous works, using bulk methods for encapsulation of SOD in liposomes, have reported different and lower *EE*. Corvo *et al.* reported an *EE* of 21 ± 2 % for SOD_Lip (lipid concentration of 48 µmol/mL) with a mean size of 110 ± 10 nm [172], whereas Rengel *et al.* reported for a similar nanosytem an *EE* of about 13% for a mean size of 90 ± 60 nm [326]. Simões *et al.* also reported SOD_Lip with a mean size of 149 ± 9 nm and an *EE* of 34 ± 2 % [327] and, more recently, Marcelino *et al.* obtained enzyme-loaded liposomes with an *EE* of 9 ± 2 % for a mean size of 140 ± 20 nm [328]. Previous works have also demonstrated that neutral SOD_Lip formulations are stable over the time, at 4 ºC [308,329–331].

An important consideration in this system is the retention of SOD enzymatic activity after the microfluidic process. Although the mixing time is fast, in this method ethanol is used as solvent in the inner phase, which might represent a threat for the enzyme activity. In this way, the SOD activity was evaluated and an enzymatic activity of 82 ± 3 % was observed (previous works reported a activity between 90– 95 % for bulk methods [172,308,326]), attesting that the microfluidic technique does not compromise the activity of the enzyme [332]. As such, the

production of SOD_Lip through the glass-capillary microfluidic process represents a notable improvement on the encapsulation of the enzyme over the formulations (with similar physico-chemical properties) produced by bulk process.

Table 3.2- Physicochemical characterization of Liposomes, *EE* and retained enzymatic activity of SOD_Lip.

	Size [nm]	PdI	ζ-potential [mV]	$(Prot/Lip)_f$ [µg/µmol]	*EE* [%]	Ret. Act. [%]*
SOD_Lip	135 ± 41	0.13 ± 0.01	- 0.6 ± 0.2	0.92 ± 0.10	59 ± 6	82 ± 3
Liposomes	171 ± 14	0.14 ± 0.02	0.4 ± 0.8	-	-	-

The results are expressed as mean ± S.D (n = 3)
PdI: Polydispersity index
$(Prot/Lip)_f$: Final enzyme to lipid ratio considering the final lipid concentration value.
Ret. Act.: Retained enzymatic activity.*n= two independent batches.

To confirm the structure of the SOD_Lip, a Cryo-TEM analysis was performed (Figure 3.10). The image shows a thin single-wall structure enclosing a vesicle with a mean size of 158 ± 7 nm, determined by Gatan Microscopy Suite software.

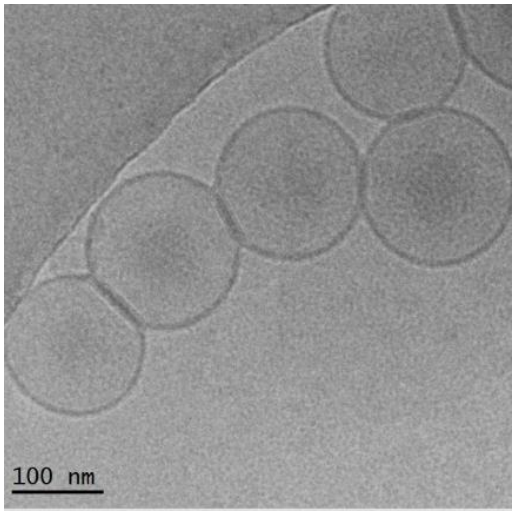

Figure 3.10- Cryo-TEM analysis of SOD-Lip (48.0 µmol/mL) vitrified in a 1:1 mixture of liquid ethane and propane at 180 °C.

3.2.4.2 In vitro cytotoxic studies

Cytotoxicity tests were performed using the CellTiter-Glo luminescence assay. Briefly, the Caco-2 and HT29-MTX cell lines (used in this work as a cellular model) were exposed to various concentrations of enzyme-loaded liposomes and empty liposomes, ranging from an equivalent concentration of the enzyme from 2.5 µg/mL to 15 µg/mL, for 6 h and 24 h. After 6 h, both cell lines presented higher viability for SOD_Lip than for empty liposomes, 13 ± 9 % and 14 ± 4 %, for Caco-2 and HT29-MTX cell lines, respectively (Figure 3.11). This was an expected result due to the antioxidant capacity of SOD. Since cancer cells can produce higher levels of ROS, leading to an oxidative stress, a consequent cell apoptosis might occur [333]. As such, upon action of SOD, the amount of ROS decrease, resulting also in a reduction of the oxidative stress. Therefore, it is expected an increase in the cell viability [334]. After 24 h, HT29-MTX cells presented a slight decrease of the cell viability at higher concentration. This can be related with the toxicity of the liposomes at high concentrations, as also observed before by Adamczak *et al.* [335]. For a lower concentration of neutral liposomes, a decrease of ~25 % was observed. Since the viability remained above 79 %, the liposomes are considered non-toxic, according to the guidelines from the regulatory authorities [336]. Moreover, SOD_Lip have already been used for longer treatment periods and no toxicity was observed [328]. Therefore, next the *in vivo* studies were pursued.

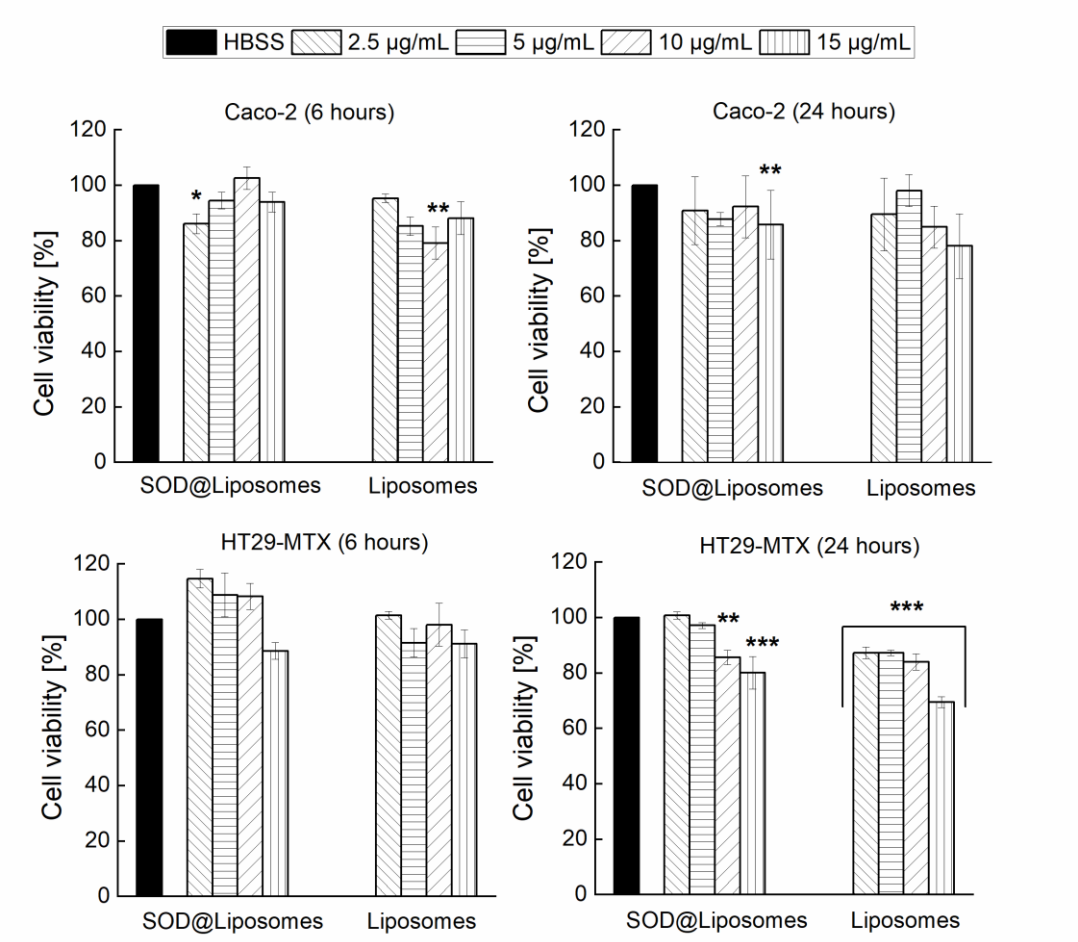

Figure 3.11- HT29-MTX and Caco-2 cells lines viability when exposed to different concentrations of SOD-Lip and empty liposomes, after 6 h and 24 h of incubation at 37 °C. All the data were compared to the negative control (HBSS-HEPES at pH 7.4). The level of significance was set at the probabilities of *p< 0.05, **p< 0.01 and ***p< 0.001. The results are expressed as mean ± S.D. (n = 3).

3.2.4.3 *In vivo* activity

The animal experiments using the anthralin ear edema model were conducted for 24 h to evaluate the anti-inflammatory effect of SOD formulated in liposomes, based on its antioxidant properties. Among the animal models available for the evaluation of anti-inflammatory agents, the anthralin (1,8- dihydroxy-9-anthrone)-induced ear swelling is an important tool to evaluate the relationship between anthralin-induced oxidative stress and ear swelling. The ear swelling assay was performed according to the method described by Lange *et al.* [324] also tested for topical antioxidants application [325,337]. In fact, oxidative stress plays an important role in chemically induced inflammation as occurring with anthralin contact with the skin, responsible

for the generation of ROS within the skin. Betamethasone was reported to reduce mice ear edema in this cutaneous inflammation model [325,337,338] and was used in this assay as a positive control to validate the model. The experimental inflammation evoked by the application of anthralin (epidermal hyperplasia and inflammatory cell infiltration) is remarkably reduced by betamethasone topical application. The work of Lange and co-workers presented systemic antioxidant administration to provide an opportunity to treat the oxidative stress generated at the site of anthralin application that can change the expression of dermal chemokines responsible for the recruitment of inflammatory cells [324]. In this work we have confirmed the usefulness of systemic SOD to treat local inflammation. The well-known biological activity of SOD has a bell-shape curve. It is known that doses ranging from 30 and 400 $\mu g\ kg^{-1}$ are in the high activity profile [309]. Thus, we administered 180 μL (7.3 μg) of SOD_Lip and SOD dissolved in the citrate buffer (free SOD), equivalent to a dose of 300 $\mu g\ kg^{-1}$ in each mouse. The i.v. and i.p. administrations were performed 1 h before the application of the challenge, since the inflammation onset occurs 24 h after the challenge. Figure 3.12 shows the edema inhibition percentage for each group. As expectable, it is possible to observe that SOD_Lip presented a higher edema inhibition (65 % ± 8 %), compared to SOD in its free form (20 % ± 13 %). This is due to the liposome's ability to improve the half-life of the enzyme, avoiding the fast SOD clearance [12,308] and the presence of PEG that can also increase the liposomes circulation in the bloodstream over 24 h, improving the therapeutic effect of SOD_Lip [172]. Moreover, the improvement of the therapeutic effect of the SOD_Lip is also related with the enhanced permeability and retention effect. This effect allows the extravasation and the accumulation of the PEGylated liposomes in the inflamed tissues, enabling a more efficient enzyme delivery [339,340]. The administration of SOD_Lip by different routes of administration was also assessed. Figure 3.12 shows a significant higher edema inhibition (*$p<0.05$) for SOD_Lip administered i.v. over the i.p. route. SOD_Lip (i.v.) showed an edema inhibition of 65 % ± 8 %, whereas SOD_Lip (i.p.) showed an edema inhibition of 33 % ± 13 %. Such difference is related with the different biodistribution of SOD_Lip, regarding the administration route. Previous studies have demonstrated that nanoparticles administrated by i.p. tend to accumulate in the local tissues in the abdominal cavity [341]. In addition, the peritoneal-blood barrier can limit the transport of the liposomes from the peritoneal cavity into the bloodstream [342]. Allen *et al.* also observed an increase of the half-life of the liposomes administered by i.p. of 9 h, contrasting with the half-life of 20.4 h from the liposomes administered by i.v. [343] As such, by i.v. administration, the distribution of the liposomes throughout the bloodstream is more effective than by

i.p., supporting the observed values. Both *in vitro* and *in vivo* studies highlight the superiority of the developed liposomal formulation over SOD in its free form.

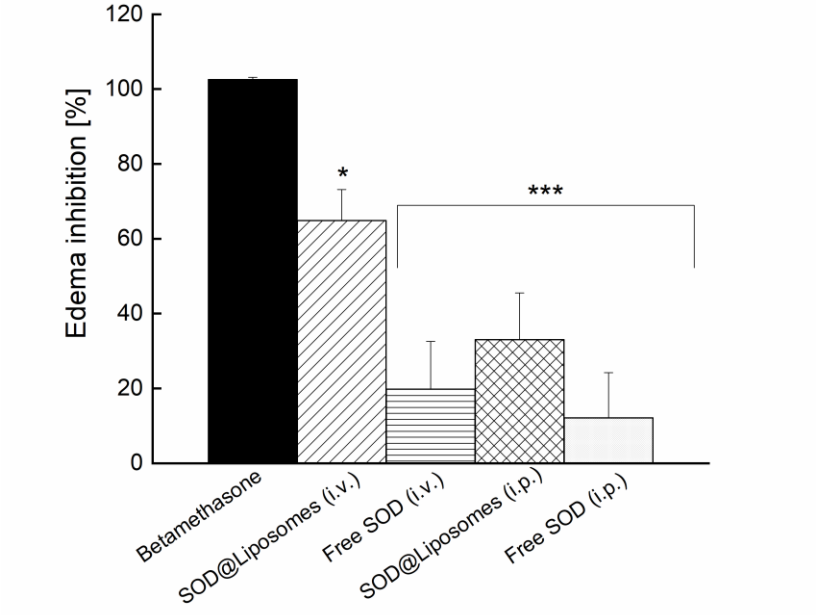

Figure 3.12- Effect of the treatment with i.v. administration of SOD-Lip (SOD-Liposomes (i.v.)), i.v. administration of SOD solution (Free SOD (i.v.)), i.p. administration of SOD-Lip (SOD- Liposomes (i.p.)), i.p. administration of SOD solution (Free SOD (i.p.)), topical application of betamethasone (positive control), 24 h after mice ear challenge with 10 mM of anthralin, expressed as percentage of ear edema inhibition. Each result represents the mean and SEM (n = 5), *p<0.05 and ***p<0.001.

Histological analyses of the ears, collected after 24 h of challenge application, confirmed the superior efficacy of the encapsulated SOD in inhibiting the edema formation, in comparison to the SOD administered in the free form (Figure 3.13). The negative control (anthralin applied on the ear, without treatment) showed mild acanthosis (increase of the cell layer), papillomatosis (external overgrowth of epidermis with elongation of dermal papillae) and epidermal hyperkeratosis (increase of the thickness of the cornified layer) (Figure 3.13.A). The free SOD (i.v.) treated animals (Figure 3.13.B) also presented a mixed focal inflammation (acanthosis, papillomatosis and hyperkeratosis), although the papillomatosis was not so evident. In addition, an epidermal reaction was also observed. Ears from animals treated with SOD_Lip (i.v.) (Figure 3.13.C) showed a focal ulceration of epidermis with underlying mixed inflammation. These observations are in accordance with the previous results from the percentage of the edema inhibition. A higher inflammation was observed for those mice that were treated with SOD solution, without liposomes. The images from SOD_Lip (i.p.) treated animals (Figure 3.13.D) showed only a slight focal epidermal hyperkeratosis and no other significant changes. Regarding the free

SOD (i.p.) treated mice (Figure 3.13.E) a mild epidermal hyperkeratosis was observed, corrobarationg the need of liposomes as a drug delivery system that enhances the therapeutic effect of the enzyme. Finally, as expected, the positive control (betamethasone) did not exhibit cellular infiltration or edema (Figure 3.13.F). The measurement of the ear edema pointed to the superiority of the i.v administration of SOD_Lip over the i.p. administration. However, the cellular events assessed by histological analysis do not corroborate these findings. In any case, the superiority of encapsulated SOD over free SOD to inhibit edema formation was confirmed.

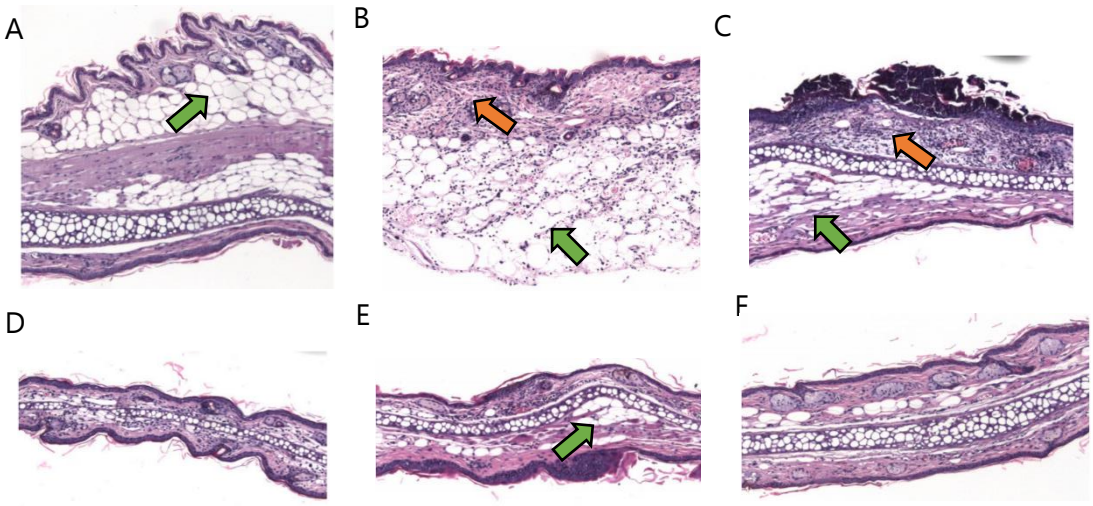

Figure 3.13- Representative microphotographs of longitudinal sections (100x) of the mouse ear pinna from (A) negative control; (B) free SOD (i.v.); (C) SOD_Lip (i.v.); (D) SOD_Lip (i.p.); (E) free SOD (i.p.); and (F) positive control (betamethasone), af after 24 h of challenge application. The edema is highlighted by the orange arrows, whereas the inflammatory cell infiltration is highlighted by the green arrows.

3.2.5 Conclusions

In this work, the microfluidic technique was used to encapsulate SOD in PEGylated liposomes (SOD_Lip). In this manner, SOD was efficiently encapsulated (59±6 %), showing higher *EE* than SOD_Lip with similar physicochemical properties from conventional processes. Although the process requires the use of an organic solvent, the SOD_Lip retains the enzymatic activity (82 ± 3 %). This work highlights the potential of the microfluidic technique to overcome the high loss of enzyme associated to the common batch production of liposomal formulations, which makes the process cheaper. The produced nanosystems also showed high cytocompatibility in the cells tested. In vivo experiments to test the anti-inflammatory properties of SOD_Lip showed the inhibition of 65 ± 8 % for animals treated with SOD_Lip administered i.v. The

histopathological studies also showed the effectiveness of the administration of the SOD_Lip, compared to the SOD administered on its free form, because of the decreased infiltration of inflammatory cells. Overall, microfluidics showed to be a suitable and efficient technique to encapsulate SOD into liposomes, which represent a promising approach to encapsulate therapeutic enzymes in liposomes anti-inflammatory applications *in vivo.*

4

INHALABLE HYDROPHILIC MOLECULE-LOADED LIPOSOMAL DRY POWDER FORMULATIONS USING SUPERCRITICAL CO_2 - ASSISTED SPRAY-DRYING

The contents of this chapter were published in a peer reviewed international journal:

C. Costa, B. Nobre, A.S. Matos, A.S. Silva, T. Casimiro, M. Luisa Corvo, A. Aguiar-Ricardo. Inhalable hydrophilic molecule-loaded liposomal dry powder formulations using supercritical CO_2 – assisted spray-drying. Journal of CO_2 Utilization, **2021**, 53, 101709.
(https://www.sciencedirect.com/science/article/pii/S2212982021002766)

Personal contribution

CC contributed to the design of the study, performed the experimental work and wrote the manuscript.

4.1 Abstract

Liposomes are known to be one of the most promising drug delivery systems for carrying and delivering biopharmaceuticals. Yet, both liposomes and biopharmaceuticals are susceptible to destabilization during storage, and thus require cold supply and efficient distribution chains. This drawback can be overcome, though, by converting liposomal suspension into solid form dosage capable of administration via different routes, including the lungs. In this work, we present a synergy between pharmaceutical and supercritical carbon dioxide technologies to assist in liposome drying. Liposomes, encapsulating 5(6)- carboxyfluorescein (CF) as a marker of the internal aqueous phase, were produced and then dried using supercritical CO_2 - assisted spray-drying. CF-loaded liposomal dry powder formulations were thus obtained. After resuspension in water to remove the trehalose, the liposomes maintained their structure and the CF encapsulation efficiency remained above 95 %. To optimize the process, a quality-by-design approach using the design of experiments tool was used. Then, the powders were submitted to storage stability assays at relative humidities of 4%, 50% and 78 % for 30 days. Results showed that the dry powder formulations were able to maintain liposome stability at relative humidities of 4 % and 50 % at 20 ºC for 30 days.

4.1 Introduction

Liposomes are a well-known, non-toxic, biodegradable and biocompatible drug delivery systems (DDS) [17,171]. Due to their physical and chemical features, liposomes are able to carry hydrophilic biopharmaceuticals in an inner aqueous medium [12]. Converting liposomal suspensions into solid form dosages not only offers the additional advantage of potential biopharmaceutical delivery to the lungs, but also enables the general access to the liposomal formulations despite the geographical and social conditions. Due to the lungs' physiognomy, pulmonary Lip-DPFs delivery has benefits over the parenteral and intravenous routes, like the direct targeting for local effect, which requires smaller doses, avoids the hepatic first-pass effect and is easily administered [344]. Different studies have described the use of $scCO_2$ to produce biopharmaceutical-loaded liposomes. Reverchon and co-workers [179,345] have reported on their use of supercritical $scCO_2$ to produce liposomes (supercritical assisted liposome formation – SuperLip) and successfully incorporated hydrophilic and hydrophobic compounds.

J. Merlo-Mas *et al.* [346] have also reported the use of the depressurization of an expanded liquid organic solution into aqueous solution (DELOS-susp) technique to encapsulate an enzyme into liposomes. More recently, Villanueva-Bermejo and Temelli [347] reported the encapsulation of Coenzyme Q_{10} in soy lecithin-based liposomes utilizing a single step $scCO_2$, without organic solvents. Nevertheless, it is important to highlight that the loaded liposomes are obtained in aqueous bulk [348] rather than in dried form.

Supercritical CO_2-assisted spray-drying (SASD) is a one-step process that produces dry powders [82], as $scCO_2$ is solubilized into the liquid solution containing the drug and/or carrier system. The resulting near-equilibrium mixture outflowing from the saturator/static mixer is then atomized through a nozzle to the precipitation chamber at near atmospheric pressure [94]. Compared to conventional methods, SASD offers numerous advantages, such as the opportunity to control both particle size and distribution [349], as well as to function at mild temperatures. Moreover, it is scalable, and can be used for both water-soluble and non-water-soluble compounds. For this reason, SASD is not only attractive for liposome drying, but it also provides suitable powders for liposome inhalation [54,200]. During drying processes, carbohydrates are often used to prevent liposome fusion, aggregation or even drug leakage [23]. Lactose is the only FDA-approved carbohydrate excipients for inhalation. Nonetheless, trehalose has being highlighted as a great promise [25]. It is a non-reducing sugar that offers various advantages over other carbohydrates, namely its low chemical reactivity, low hygroscopicity, high glass transition temperature (T_g) and lack of internal hydrogen bonds, all of which facilitate liposome interaction through the formation of new hydrogen bonds [350]. Moreover, the addition of amino acids, such as a L-Leucine (Leu), may provide moisture protection [80].

SASD optimization can be complex, due to the high number of variables affecting final liposome and powder properties including, temperature, pressure, CO_2 and liquid flow rates and the casting solution composition [351]. The quality-by-design (QbD) approach using the design of experiments (DoE) tool, followed by statistical analyses, is fundamental to obtain an efficient and low time- and cost-consuming optimization [25,82].

In this work, we first applied SASD to the liposomes. To monitor the process, a hydrophilic dye, 5(6)-carboxyfluorescein (CF), was encapsulated in PEGylated liposomes (CF_Lip), that were then dried in the SASD (CF_Lip-DPFs). Next, the QbD approach used the DoE tool and then statistical analyses were carried out. Finally, powder storage stability was assessed at different relative humidities to evaluate moisture impact on the CF_Lip and CF_Lip-DPFs, first at one week and then at a month. CF is a good model molecule for hydrophilic compounds, and it will enable

process optimization. This optimization will also serve to keep the encapsulated hydrophilic molecules (including biopharmaceuticals) in liposomal form during drying and storage. Therefore, our aim was to design an innovative, robust, upscaling and time-efficient technique for drying liposomes, keeping them stable during storage and overcoming the common drawbacks of current drying and storage methods. Moreover, we expected to obtain a green and patient-friendly DDS able to deliver biopharmaceuticals such as enzymes and siRNA to the lungs.

4.2 Experimental procedure

4.2.1 Materials

Egg-phosphatidylcholine (E-PC) (> 99 %) and distearoylphosphatidylethanolamine-poly(ethyleneglycol)$_{2000}$ (DSPE-PEG$_{2000)}$ (> 99 %) were obtained from Lipoid (Germany). Cholesterol (Chol) (> 99 %), 5-(6)-carboxyfluorescein (CF) (> 95 %), citric acid monohydrate (> 99 %) and L-leucine (98 %) were purchased from Sigma-Aldrich (USA). Trehalose dehydrated (> 98 %) were acquired from Tokyo Chemical Industry (China), chloroform (> 99 %) was purchased from Carlo Erba (Spain) and ethanol absolute anhydrous (99.9 %) was sourced from Scharlau (Spain). Air Liquide (Portugal) provided carbon dioxide (99.998 %). All components were used as received without further purification.

4.2.2 CF_loaded liposomes preparation (CF_Lip)

The liposomes were prepared using film hydration followed by extrusion [172]. Briefly, EPC, Chol and DSPE-PEG$_{2000}$ (molar ratio of 1.85:1:0.15, respectively) were dissolved in chloroform in a round bottom flask at a total lipid concentration of 32 µmol/mL. The mixture was then dried using a rotary evaporator (Rotavapor RE-111- Buchi, Swiss) and formed a lipid film. Next, the film was hydrated with a 10 mL of 5(6)-carboxyfluorescein, at a concentration of 0.05 mg/mL, that had previously been dissolved in a buffer solution (10 mM citric acid in 280 mM trehalose, at pH 6). It stood waiting for 1 hour (CF_Lip) at room temperature, occasionally shaken. Afterwards, a high-pressure extruder (Lipex TM Thermobarrel Extruder, Biomembranes Inc., Vancouver, BC, Canada) with a Nucleopore® Track-Etched Membranes (Whatman®, USA) with pore sizes of 600, 400 and 200 nm was applied. Finally, the suspension was extruded three times across a membrane filter of 100 nm. Then an Optima TM XL-90 Ultracentrifuge (Beckman

Coulter, USA) operated for two hours at 300,000 *g* and at 15 ºC to remove the non-encapsulated CF. The supernatant was then discarded and the pellets were resuspended at the desired concentration in the same buffer solution (10 mM citric acid and 280 mM trehalose, at pH 6). The so obtained formulations were sterilized by filtration through sterile filter with a pore size of 0.2 µm for SASD.

4.2.3 Dry powder liposomal formulations (Lip-DPFs)

In each assay, 4% (v/v) of the liposome suspensions were mixed with a solution at a total concentration of 300 mM of excipient. This solution was prepared with trehalose at varying ethanol (EtOH) percentages—0 %, 15 % and 30 % (v/v), and the L-leucine (Leu) mass percentages of 0 %, 10 % and 20 % w/w of trehalose. The final solution containing the liposomes suspension and all the excipients is referred as the casting solution from now on.

In each assay, the casting solution was fed into a laboratory scale SASD apparatus which was previously described in detail elsewhere [25]. Firstly, the CO_2 was liquified at -20 ºC (at 25 mL/min) by passing the feeding line of carbon dioxide in a cryogenic bath which was then pumped using a high-pressure pump (HPLC pump K-501, Knauer). The high-pressure CO_2 is then warmed using a heated bath (T_{CO_2} = 80 ºC) before being delivered to the static mixer. Simultaneously, the casting solution, containing the CF-loaded liposomes and the excipients, was put through a high-pressure pump (Smartline pump 1000, Knauer), at 3.5 mL/min, into a heated static mixer, at 80 ºC, (3/16 model 37-03-075 Chemieer) comprising a high-pressure column of 4.8 mm diameter, 191 mm length and 27 helical mixing elements that promoted CO_2 solubilization into the liquid solution, in order to obtain a near-equilibrium mixture (p_{SM} = 120 bar). The static mixer and the inlet streams were heated using tapes and a Shinko FCS-13A temperature controller (± 0.2 ºC resolution). Afterwards, the mixture was atomized into the precipitator through a 150 µm internal diameter nozzle where the solvent underwent accelerated evaporation by heated compressed air flow ($F_{Air,in}$ = 27 m^3/h and $T_{Air,in}$= 100 ºC). The particles were separated from the CO_2-solvent flow in a high-efficiency cyclone and collected in a glass vessel.

The process yield is defined as follows:

$$\eta_{SASD}\ (\%) = \frac{amount\ of\ excipients\ after\ SASD\ (g)}{amount\ of\ excipients\ before\ SASD\ (g)} \times 100 \quad (1)$$

4.2.4 Liposome characterization

Before and after SASD, the liposomes were characterized according to their average size and polydispersity index (PdI), as well as phospholipid concentration and CF encapsulation efficiency. A Zetasizer Nano S (Malvern Panalytical Ltd., Malvern, UK) determined the mean size (Z-average), and the polydispersity index as a measure of the particle size distribution that ranged from 0 (monodisperse) and 1.0 (polydisperse). The Rouser method [321] assessed the phospholipid quantification. The CF encapsulation into the aqueous phase of the liposomes was quantified using a fluorometer (F4010 Fluorescence Spectrophotometer, Hitachi, Japan). The EX and EM band passes were 5nm, with a time average of 0 sec and a response of 2 sec. To ensure that all the carboxyfluorescein had been released from the liposomes, the vesicles were destroyed by adding 1 mL of EtOH to 20 µL of the liposomal solution. The samples were vigorously agitated, and the liposomes were left to destroy. Posteriori, sample fluorescence was measured at an excitation wavelength of 456 nm and an emission wavelength of 520 nm. The CF yield (η_{CF}) was calculated as follows:

$$\eta_{CF}\ (\%) = \frac{amount\ of\ CF\ after\ SASD\ (\mu g)}{amount\ of\ CF\ before\ SASD\ (\mu g)} \times 100 \quad (2)$$

The lipid yield (η_{Lipid}) was calculated as follows:

$$\eta_{lipid}\ (\%) = \frac{amount\ of\ CF\ after\ SASD\ (\mu g)}{amount\ of\ CF\ before\ SASD\ (\mu g)} \times 100 \quad (3)$$

Moreover, the percentage of encapsulation efficiency (*EE*) of the dye is given by the following equation

$$EE\ (\%) = \frac{\left(\frac{\mu g_{CF}}{\mu mol_{Lip}}\right)_f}{\left(\frac{\mu g_{CF}}{\mu mol_{Lip}}\right)_i} \times 100 \quad (4)$$

where $\left(\frac{\mu g_{CF}}{\mu mol_{Lip}}\right)_i$ is the initial CF to lipid ratio and $\left(\frac{\mu g_{CF}}{\mu mol_{Lip}}\right)_f$ is the final one.

4.2.5 Characterization of liposomal dry powder formulations

4.2.5.1 Storage stability assays

The CF_Lip-DPFs obtained from SASD were stored in triplicate in desiccators at relative humidities (RH) of 4 ± 2 %, 50 ± 4 % and 78 ± 2% at 20 ºC. The different RHs were obtained using nitrogen and saturated solutions of potassium carbonate and sodium chloride, respectively. The temperature and the relative humidity were monitored using the Lasel® thermohygrometer data logger, model EL-USB-2, for one month. The samples were characterized firstly after one week and then after a month of storage.

4.2.5.2 Morphology and particle size distribution

The shape and morphology of Lip-DPFs particles were determined by scanning electron microscopy (SEM). The samples were coupled to adhesive carbon tapes, and the excess powder was removed by a jet of compressed air. Then a Hitachi S2400 with Bruker light elements EDS detector (Japan) analyzed the samples with an accelerating voltage set to 15 kV and at magnifications of 5 k and 10 k. The dry powder particle size and size distribution were determined using Morphologi G3 (Malvern, Paralab, Portugal) equipment. The width of the particle size distribution was evaluated by calculating the sample's span using the follow equation:

$$span = \frac{d_{v,90} - d_{v,10}}{d_{v,50}} \quad (5)$$

where the $d_{v,10}$, $d_{v,50}$ and $d_{v,90}$ are the volume mean diameters respective to 10 %, 50 % and 90 % of the sample population. Each sample characterization analyzed approximately 30,000 particles.

4.2.5.3 *In vitro* aerosolization study

The aerodynamic properties of the Lip-DPFs were determined using an eight-stage Andersen Cascade Impactor – ACI - (Copley Scientific). Soon thereafter, 30 mg of CF_Lip-DPFs were loaded into three hydroxypropylmethylcellulose capsules nº3 (Aerovaus). The capsules were individually placed into a previously weighed dry powder inhaler (DPI) that was coupled to the ACI device. Each plate of the cascade impactor was covered by a pre-weighed filter (Glass Microfiber filter MFV1080, Filter Lab). The DPI punctured the capsule prior to the inhalation, and a high capacity pump was turned on to simulate an intake of breath: an air flow rate of 60 L/min lasting 4 s, according to the European pharmacopoeia [352]. The amount of powder

deposited in each stage was calculated by weighing the filters before and after the test and calculating the difference. From this assay, several aerodynamic parameters were calculated—mass median aerodynamic diameter (MMAD), fine particle fraction (FPF), and geometric standard deviation (GSD). The MMAD characterizes the size of those particles that reached the impactor, excluding those deposited in the throat. The value is displayed below, which is the diameter of 50% of the particles. On the other hand, FPF is the portion of the delivered particles sized below 5 µm, as determined by the interpolation of the percentage of the particles with smaller sizes than this value. Finally, the GSD can be calculated using the following equation:

$$GSD = \sqrt{\frac{d_{84}}{d_{16}}} \quad (6)$$

where d_{84} and d_{16} are the diameters corresponding to 84 % and 16 % of the cumulative distribution, respectively.

4.2.5.4 Water content measurement

Powder water content was determined before and after storage using a Karl-Fischer titration. Approximately 15 mg of powder were dissolved in 5 mL of anhydrous EtOH. All samples were individually analyzed at room temperature using an 831 KF Titrino Coulometer (Metrohm Ltd, Antwerp, Belgium).

4.2.5.5 Differential Scanning Calorimetry (DSC)

The glass transition temperature (T_g) was determined by weighing approximately 5 mg of powder on a TA Instruments differential scanning calorimeter, DSC Q2000, within a temperature range from -90 ºC to 175.0 ºC, in two cycles.

X-ray powder diffraction (XRD)

The X-ray diffraction patterns were produced by analyzing the samples in a RIGAKU X-ray diffractometer, model Miniflex II using Cu radiation (30 KV/15 mA) with a 2θ angle ranging between 5 º and 40 º and a step size of 0.015 º.

4.2.5.6 Attenuated Total Reflectance Fourier Transform Infra-Red (ATR-FTIR)

A Spectrum Two FTIR spectrometer (PerkinElmer, Inc.) was used to perform the ATR-FTIR analyses. Enough amount of each sample was placed in a crystal diamond plate to completely cover the prism surface and each spectrum was recorded with 16 scans from 400 cm^{-1} to 4000 cm^{-1}.

4.2.5.7 Confocal Laser Scanning Microscopy (CLSM)

The CF_Lip location inside the CF_Lip-DPFs was observed using a CLSM (Zeiss LSM 880) with a laser wavelength of 488 nm and brightfield. Zen black software and Imaris Bitplane carried out additional image processing. All the CF_Lip-DPFs were placed on glass coverslips, and the particles were immediately observed.

4.2.6 Design of experiments and data analysis

A screening of replicated experiments (n=2) was planned, and the data were collected according to a full-factorial, two factor, three level design (Figure 4.1).

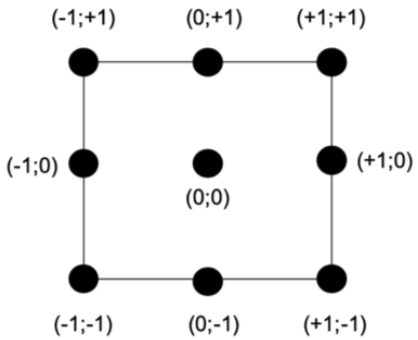

Figure 4.1 — Full factorial design of CF_Lip-DPFs, two factors at three levels (n = 1).The Leu and the EtOH percentages were the factors, and the three levels were 0, 10, 20 % ($w_{Leu}/w_{trehalose}$) and 0, 15, 30 % (v/v), respectively. The Leu concentrations are based on trehalose and were represented by L1 for 0% ($w_{Leu}/w_{trehalose}$), L2 for 10% ($w_{Leu}/w_{trehalose}$) and L3 for 20 % ($w_{Leu}/w_{trehalose}$).

The Leu and the EtOH percentages were the factors, and the three levels were 0, 10, 20 % ($w_{Leu}/w_{trehalose}$) and 0, 15, 30 % (v/v), respectively. The Leu concentrations are based on trehalose and were represented by L1 for 0% ($w_{Leu}/w_{trehalose}$), L2 for 10 % ($w_{Leu}/w_{trehalose}$) and L3 for 20 % ($w_{Leu}/w_{trehalose}$). Table 4.1 shows the SASD parameters used in the DoE. StatisticaTM software (StatSoft, TIBCO®, USA) quantified the impact of the input parameters (EtOH and Leu percentage in the casting solution) on the liposome structure (size, PdI, lipid yield and *EE* of CF), on the CF_Lip-DPFs properties (Dv_{50} and span), and on the process yield.

Table 4.1- The SASD parameters used in the DoE, and the combination of the three levels used for the two factors in each experiment: EtOH percentage in the casting solution (EtOH), Leu percentage in the casting solution (Leu), pressure at the static mixer (p_{SM}), inlet air temperature (T_{AirIn}), CO_2 temperature (T_{CO2}), temperature at the static mixer (T_{SM}), outlet temperature (T_{out}).

Assay	Leu [%]	EtOH [%]	p_{SM} [bar]	T_{AirIn} [ºC]	T_{CO_2} [ºC]	T_{SM} [ºC]	T_{out} [ºC]
L1_CF_EtOH0		0	120	97	79	80	65
L1_CF_EtOH15	0	15	120	100	72	87	62
L1_CF_EtOH30		30	121	90	72	95	59
L2_CF_EtOH0		0	122	93	78	93	52
L2_CF_EtOH15	10	15	121	99	73	87	63
L2_CF_EtOH30		30	121	90	74	92	52
L3_CF_EtOH0		0	121	100	78	93	56
L3_CF_EtOH15	20	15	121	100	75	86	65
L3_CF_EtOH30		30	121	91	73	91	55
L1_CF_EtOH0_R		0	120	101	75	88	66
L1_CF_EtOH15_R	0	15	121	91	76	80	59
L1_CF_EtOH30_R		30	119	98	77	95	55
L2_CF_EtOH0_R		0	121	104	74	89	60
L2_CF_EtOH15_R	10	15	121	103	72	81	64
L2_CF_EtOH30_R		30	120	90	78	89	63
L3_CF_EtOH0_R		0	121	104	75	91	58
L3_CF_EtOH15_R	20	15	120	105	74	88	65
L3_CF_EtOH30_R		30	120	94	75	91	59

R: REPLICATE

4.2.7 Statistical analysis

The statistical analysis was performed applying the two-way ANOVA, using the StatisticaTM software (StatSoft, TIBCO®, USA). When the overall result was statistically significant, the Tukey-Kramer multiple comparison test was conducted to identify which methods were significantly different. Differences were considered significant at a p-value below 0.05.

4.3 Results and discussion

To monitor the dynamic behavior of the liposomes during drying, a model hydrophilic drug, CF, was used to mark their internal space. Thus, if we were to observe a significant decrease in the EE_{CF}, we could assume that the liposomes had suffered disruption during SASD. Otherwise, the EE_{CF} would have been retained or be only slightly reduced. To optimize the process, a QbD study of SASD was carried out.

4.3.1 Design of Experiments

The QTTPs of the produced CF_Lip-DPFs focused on i) maintaining the CF_Lip structure during SASD; ii) retaining the encapsulated molecule; and iii) obtaining monodisperse powders. In the work from Moura *et al.* [25], conducted in the same apparatus, the process conditions, and the excipient formulation for the manufacturing of inhalable dry powders were optimized. These parameters were used as a guideline for the present work. It was demonstrated that within certain ranges neither the operating pressure (95 bar < p_{SM} < 120 bar) nor the operating temperatures (100 ºC < T_{SM} < 115 ºC and 60 ºC < T_{CO_2} < 80 ºC) have significant impact on the dried liposomes. Some impact was observed, however, with the variation of Leu and EtOH. For this reason, for the DoE, the chosen CPPs were the percentage of Leu and EtOH. Taking the QTTPs into consideration, the CQAs were the size and PdI of the liposomes, the lipid yield and the dye's *EE*. The CF_Lip-DPFs CQAs were the process yield, the volumetric diameter and span of the powders. CF_Lip-DPFs production is mainly divided into two distinct steps: i) production and characterization of CF_Lip; and ii) drying and characterizing CF_Lip and CF_Lip-DPFs after SASD. In the first step, film hydration yielded CF_Lip and was followed by extrusion. Excess CF was removed by ultracentrifugation, and the liposomes were resuspended and stored. The CF_Lips were characterized in terms of size, PdI and lipid and CF concentration (Table 4.2).

Table 4.2- Characterization of blank sample liposomes, and CF_Lip before SASD.

Assay	Size [nm]	PdI	[Lip] [μmol/mL]	[CF] [μg/mL]
Blank Sample*	145 ± 1	0.063 ± 0.012	26.1 ± 1.2	-
CF_Lip	134	0.068	30.0	0.594
CF_Lip_R**	140	0.074	30.0	0.578

*n=2; *CF_Lip_R: Replicated CF_Lip

The empty liposomes and CF_Lip were mixed with a casting solution (4% v/v) composed of trehalose (Tre) and Leu (300 mM) and processed in the SASD (mass balance in the Appendix B, Table B.1). It is important to highlight PEG presence in the liposomes. The PEGylation of liposomes creates a steric barrier that improves in vitro stability [353]. This steric effect (zeta potential near zero) forms a hydration cloud around the liposomes that prevents the opsonization with proteins and liposome uptake by the macrophage [354]. During drying, this hydration cloud assists synergistically in inhibiting liposome-liposome interaction and disruption. However, even the drying of PEGylated liposomes uses carbohydrates. Stark *et al.* [355] demonstrated that the presence of cryoprotectants is absolutely necessary during drying, even in the presence of liposome surface PEG. Van den Hoven *et al.* [30] reported the necessary stabilization of PEGylated liposomes during freeze-drying and spray-drying using cyclodextrins.

Next, the selected volume of CF_Lip-DPF was resuspended with deionized water to prevent osmotic shock to the liposomal formulations. Thus, the excipients were removed by dilution and ultracentrifugation, and the resulting CF_Lip were characterized in terms of their CQAs (Appendix B, Table B.2). The yield and morphology of the remaining CF_Lip-DPF powder were measured. The blank sample was produced without EtOH, Leu or CF.

For the blank sample, liposome size was found to increase from 145 ± 1 nm to 221 ± 20 nm and the PdI from 0.063 ± 0.012 to 0.480 ± 0.056. A similar trend was observed for the remaining formulations without Leu, suggesting that this amino acid played an important role in the liposome morphology. Several studies have suggested that amino acids can stabilize liposomes not only via hydrogen bonding but also through electrostatic interactions [356]. In our work, we suggest that the maintenance of the liposome size upon presence of Leu is due to the electrostatic interaction between the carboxyl group of the Leu and the E-PC amine group. More recently, Deber and Stone [357] have suggested that the hydrophobic interaction via van der Waals forces between the Leu and the lipids might lead to packing and thereby decrease liposome size. With this in mind, we observed that the higher the Leu, the smaller the liposome size. Moreover, interaction between the Leu and CF_Lip might result in the formation of a Leu layer on the liposome surface, capable of shielding them from the external forces they are exposed to during drying. Regarding the CF_Lip-DPFs, the higher the percentage of EtOH and Leu, the smaller the yield. Leu acts as a dispersibility enhancer due to its hydrophobic nature [33,161]. Previous work by Li *et al.* [358] have shown that Leu decreases the interaction between air moisture and particle surfaces. EtOH also has an important impact on dry powder properties. At low temperatures and pressures, CO_2 exhibits low water solubility, leading to inefficient

drying. The addition of EtOH as co-solvent contributes to an increase of CO_2 miscibility with water [94,359], leading to higher efficiency in the supercritical assisted atomization [94]. Thus, low Leu and EtOH percentages can yield higher levels of powder moisture powder and consequently to higher yield (Appendix B, Table B.2).

In respect to the volumetric diameter, the results showed that the absence of Leu can increase volumetric diameter, since the high moisture level might promote particle aggregation [360]. This phenomenon can also be explained by Leu interactions on the particle surface. Rabbani *et al.* [361] have suggested that Leu has surfactant-like properties. They defended this hypothesis on the grounds that, depending on the surface tension of the solvent system, Leu can migrate to the droplet surface during drying, leading to smaller volumetric diameters. On the other hand, a 20% Leu increase grew the volumetric particle diameter, as well. Similar observations were also reported by Rattanupatam *et al.* [362], who suggested that the substantial Leu increase produces a highly fine powder that can exhibit powder cohesion.

In order to understand the relation between the CPPs- Leu and EtOH percentages- on liposome and CF_Lip-DPF properties, a full factorial DoE was performed as shown in Figure 4.1. Table 4.3 evaluates the impact of the CPPs on the CQAs. All the ANOVA assumptions were validated by residual analysis.

Table 4.3- ANOVA testing the effects of the parameters on liposome CQAs (size, PdI, lipid yield and *EE* of CF) and CF_Lip-DPF CQAs (ηSASD, Dv_{50}, span, MMAD, GSD and FPF) for a 5% significance level.

	Assay	Effect	*p*-value	Equation
CF_Lip	Size	Leu (w/w)	0****	$z = 305 - 28.2\,x + 0.914x^2 - 2.17y + 0.321xy - 0.115x^2y$
		EtOH (v/v)	0.00526**	
		Leu*EtOH	0.00605**	
	PdI	Leu (w/w)	0.00053***	$z = 0.434 - 0.041\,x + 0.001x^2$
	Lipid yield	Leu (w/w)	0.00346**	$z = 67.3 - 0.641x$
	EE_{CF}	Leu (w/w)	0.78473	$z = 77.3 - 2.15x + 0.107x^2 - 1.72y + 0.0438y^2 + 1.03xy - 0.0325xy^2 - 0.0517x^2y + 0.00164x^2y^2$
		EtOH (v/v)	0.70419	
		Leu*EtOH	0.36024	
CF_Lip-DPFs	η_{SASD}	Leu (w/w)	0.00395**	$z = 67.1 - 0.414x - 0.241y$
		EtOH (v/v)	0.00945**	
	$Dv_{,50}$	Leu (w/w)	0.00314**	$z = 8.56 - 0.238x + 0.021x^2 - 0.009xy + 0.0002\,xy^2$
		Leu*EtOH	0.01622*	
	Span	Leu (w/w)	<0.00001****	$z = 2.61 - 0.121x$

p-value: *p < 0.05; **p < 0.01; ***p < 0.001; ****p < 0.0001.

Where x is Leu; y is EtOH; z is the different CQAs

Table 4.3 demonstrates that the CF_Lip size is significantly affected by Leu, EtOH or their combination. However, it is Leu that has a more significant effect on liposome size of (p < 0.0001). In addition, Figure 4.2.A also shows that increased EtOH concentration leads to a decrease of liposome size. A similar observation was reported by Hantz *et al.* [363], who offered two hypotheses. On the one hand, the addition of EtOH may disturb the osmotic pressure gradient between the external and the inner phase, leading to liposome shrinkage. On the other hand, it may be that the higher EtOH concentration enables more alcohol to interact with the membrane, altering the behavior of the variation of the cross-sectional area. More recently, findings

of Pal *et al.* [364] proved that, for nanoscale liposomes, the addition of EtOH can cause liposomes to shrink and significantly reduce their size. The authors suggested that EtOH leads to a reduction in the bending modulus of lipid membranes, causing membrane undulation and a consequent liposome area loss. Figure 4.2.A shows that for lower Leu concentrations, even with an increase in EtOH percentage, the liposome size remained above 200 nm. Similar liposome size distribution (PdI) behavior can be observed for Leu ($p < 0.001$) in Figure 4.2B whereas EtOH shows no significant effect.

With regards to the EE_{CF}, Table 4.3 shows that neither the Leu nor the EtOH (nor their combination) had significant effects (p -value > 0.05). Although, the model in Figure 4.2.C shows that, when Leu ranged between 8 % and 13 % and EtOH was between 12 % and 18 %, *EE* was maximized this observation cannot be statistically supported. This model prediction was not experimentally demonstrated since the encapsulation efficiency of a hydrophilic molecule *EE* depends mainly on the behavior saturation curve of the dye in the inner aqueous space. Moreover, a technical compromise took place between the encapsulation efficiency and liposome size [365]. Finally, Figure 4.2.D shows that the lipid yield was mainly influenced only by the Leu (p-value of 0.00346). As for the CF_Lip-DPFs, the SASD yield (Figure 4.2.E) was significantly influenced by the linear components—Leu and EtOH (p-value of 0.00395 and 0.00945, respectively). For this reason, there was no curvature in the respective OOS. In fact, the hydrophobic nature of the Leu and the properties of the ternary system of CO_2 + EtOH + water had a huge impact on the powder yield, as mentioned previously. Finally, Leu and their interaction also significantly (p-value of 0.00314 and 0.01622, respectively) impacted the powders' volumetric diameters (Figure 4.2.F). Curiously, it would have been expected that the powder size distribution (span) be influenced by the same CPPs as the D_{V50}. Still, Figure 4.2.G shows that the span is strongly influenced only by the amino acid (p-value <0.00001).

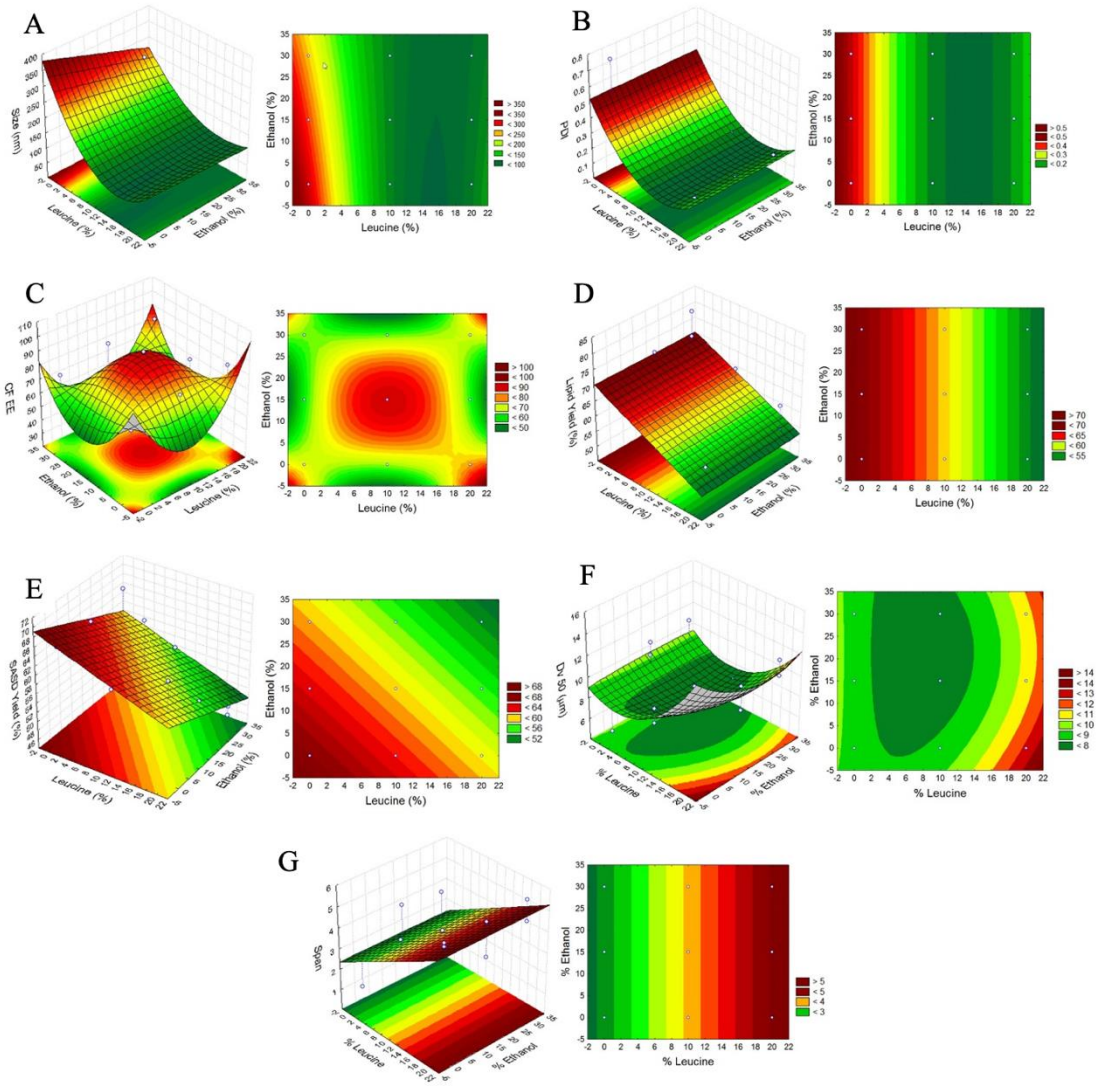

Figure 4.2- 3D response surface (OOS) and 2D DoE contour plots, showing the effects of Leu (%) and EtOH (%) on A) liposome size and B) PdI; C) EE of 5(6)- carboxyfluorescein; D) Lipid yield; E) CF_Lip-DPF process yield; F) volumetric diameter and G) CF_Lip-DPF span.

From the combined analysis of the ANOVA results summarized in Table 4.3 and plotted in Figure 4.2, we conclude that the liposome structure is successfully retained with Leu > 10 % whereas the properties of the liposomal dry powder formulations are optimized for low Leu percentages and 15 % < EtOH < 20 %. The overall selection of the optimum CPPs for the CQAs selected suggest that Leu composition should be around 10 % and EtOH 15 %. Thus, the liposomal formulation L2_CF_EtOH15 was selected for further experimental studies, namely, the stability assays.

4.3.2 Stability assays of CF_Lip-DPF

After OOS identification, the CF_Lip-DPF storage stability studies were carried out for L2_CF_EtOH15. Stability assays were conducted at three different relative humidities (RH= 4 ± 2 %, RH= 50 ± 4 % and RH= 78 ± 2 % to evaluate the moisture influence on the Tre and Leu-protected liposomes. Furthermore, this step was essential to understand the viability of powder inhalation at different points in time during storage (after 7 and 30 days). Triplicate batches of CF_Lip were produced, and CF excess was removed by dilution and ultra-centrifugation. The solution used to hydrate the lipid film had a concentration of carboxyfluorescein of 50 µg/mL, resulting in a saturated solution. The CF-lipid ratio after extrusion was 1.8 ± 0.1 µg/µmol. However, after extrusion and ultracentrifugation, the concentration decreased to approximately 1.6 µg/mL. This was expected due to the saturation curve of the dye in the liposomal inner aqueous volume [365]. Moreover, excess CF was removed during the two ultra-centrifugations with previous dilution. The CF-lipid ratio after centrifugation was 0.070 ± 0.031 µg/µmol. Next, the sterilized CF_Lips were divided into aliquots, stored at 4 °C and then processed by SASD. The experiment was carried out at $T\text{air}_{in}$ = 103 ± 2 °C; T_{CO_2} = 81 ± 6 °C; T_{SM} = 84 ± 2 °C; $T\text{air}_{out}$= 61 ± 1 °C; p_{SM} = 119 ± 1 bar. Table 4.4 shows the characterization of CF_Lip before and after SASD.

Table 4.4- Characterization of CF_Lip before and after SASD. The SASD process parameters were $T_{air,in}$ = 103 ± 2 °C, T_{CO2} = 81 ± 6 °C; T_{SM} = 84 ± 2 °C; $T_{air,out}$ = 61 ± 1 °C; p_{SM} = 119 ± 1 bar. The $[CF]_i$ was 0.057 ± 0.003 mg/mL and $[CF/Lip]_i$ = 1.8 ± 0.1 µg/µmol. The results are expressed as mean ± SD (n=3).

Assay*	Size [nm]	PdI	η_{Lipid} [%]	η_{CF} [%]	EE_{CF} [%]
CF_Lip (before SASD)	143 ± 1	0.053 ± 0.007	-	-	-
CF_Lip (after SASD)	94 ± 7	0.130 ± 0.005	69 ± 1	74 ± 7	> 95

*After ultra-centrifugation

Following SASD processing, CF_Lip-DPFs were resuspended in deionized water to maintain their osmolarity. The excipients were removed by ultra-centrifugation. Table 4.4 shows that liposome size decreased slightly, likely due to EtOH and Leu action. The *EE* of the CF in the liposomes was above 95 %. Interestingly, from the CF balance mass, lipid and excipients before

and after SASD (Appendix B, Table B C.3), we can observe that all the CF (100 ± 5 %) was recovered following SASD. These results showed that liposomes can be recovered without structural damage during this process. This observation is corroborated by the work from Elizondo *et al.* [139] that shows that a compressed fluid provides a more homogeneous path for the assembling of the lipids, leading to a supramolecular organization of the lipids in their membrane. This also represents a huge improvement in CF recovery over other techniques. In fact, previous work has demonstrated a CF retention of approximately 15 % for liposomes morphologically akin to those produced here but freeze-dried [193]. For air-dried liposomes, the CF retention was higher than that found in the literature (Sun *et al.* [366] reported a EE_{CF} of 78 % for a mean size of 102 nm, whereas Moore *et al.* [367] reported an *EE* of 44 %). However, our technique requires neither high shear nor heat stresses, and it is more time efficient. EDS quantitative analysis showed that the powders consist of 54.9 ± 0.2 % of carbon and 45.0 ± 0.2 % oxygen atoms. Research from Rudra *et al.* [368] and Kotouček *et al.* [369] showed the presence of phosphorous in the EDS liposome analysis. Moreover, due to the CF fluorescence properties and *EE* above 95 % revealed by confocal images (Appendix B, Figure B.1), that CF_Lips are encapsulated into the trehalose (represented by the yellow contour). Thus, this characterization suggests that liposomes are in fact encapsulated within the sugars, otherwise we would observe nitrogen and phosphate atoms in the EDS analysis.

The SASD powders were stored at different RHs at room temperature and storage stability was evaluated after 7 days and again after 30. Table 4.5 display the CF_Lip characterization of the CF_Lip-DPFs after seven and 30 days.

Table 4.5- Characterization of CF_Lip from CF_Lip-DPFs stored at relative humidities of 4 ± 2 %, 50 ± 4 % and 78 ± 2 %, on the 7th and 30th days, at 20 ºC. The results are expressed as mean ± SD (n=3).

	Assay	RH [%]	Size [nm]	PdI	η_{Lipid} [%]	η_{CF} [%]	EE_{CF} [%]
t= 7 days	CF_Lip from CF_Lip-DPFs	4 ± 2	99 ± 9	0.131 ± 0.011	85 ± 18	95 ± 14	95 - 100
		50 ± 4	105 ± 9	0.126 ± 0.020	93 ± 7	94 ± 11	
		78 ± 2	148 ± 18	0.215 ± 0.034	103 ± 17	94 ± 14	
t= 30 days	CF_Lip from CF_Lip-DPFs*	4 ± 2	95 ± 6	0.136 ± 0.001	95 ± 14	119 ± 8	> 95
		50 ± 4	99 ± 10	0.108 ± 0.004	88 ± 17	109 ± 7	
		78 ± 2	139 ± 20	0.205 ± 0.066	112 ± 13	106 ± 17	

*n= 2 independent assays

The most common theories about how liposomes are stabilized by carbohydrates during storage are the Water Replacement Theory (WRT) and Vitrification [193]. The former suggests that the carbohydrates contribute to liposome stability by replacing the water molecules' hydrogen bonding, meaning that carbohydrates interact directly with the polar head of the liposomes. In addition, the sugar increases the space between the liposome polar heads, leading to a dip in the gel-to-fluid phase transition temperature (*T*m) of phospholipid, and stabilizing the liposomes. Vitrification refers to sugars' ability to vitrify and potentially to stabilize the liposomes. During drying, the highly viscous glassy matrix surrounds the liposomes, reducing their molecular mobility [187]. The trehalose di-hydrate in this experiment has a glass transition temperature of 115 ºC (experimentally determined).

Table 4.5 shows that, after seven days, a moisture increase led to a growth in liposome size. In turn, PdI changed drastically at an RH of 78 %. Increasing moisture content would be expected to lead to a fall in trehalose's T_g [370]. In fact, Sun *et al.* [366] reported that the alteration of T_g can lead to liposome fusion and increase their size. The vitrification theory, thus, postulates that the increase in size and PdI, coupled with the rise in RH, is related to an increase in molecular mobility, itself caused by the lower glass transition temperature of the trehalose. However, DSC graphs in Figure 4.3.A show that the powder T_g at different RHs remained similar over time. Conversely, XRD analysis (Figure 4.3.B) showed that moisture increase led to a powder recrystallization, which assumed an amorphous structure following SASD. In fact, powders stored at an RH of 78 % showed a water content increase from approximately 6 % to 21 % after 7 days (Table 4.6). These observations corroborate findings by Chiou and Langrish [371], which

have shown that spray-dried amorphous particles tend to crystallize with greater moisture. Additionally, Buera *et al.* [372] have demonstrated that moisture increases are accompanied by limited hydrogen bonds between the sugars and membranes, leading to weak stabilization. Similar behavior was also recorded after 30 days. We observed a size growth and a rise in RH, whereas the size and PdI of the control remained unchanged throughout. It is interesting to note that a non-significant alteration in the liposome size and PdI of the CF_Lip-DPFs was found between day 7 and 30, suggesting that powder storage conditions over the first seven days had a greater impact on these morphological properties. The lipid yield, on the other hand, remained unchanged after both 7 and 30 days. In fact, at day seven, the CF yield measured 95 % for all RHs. Similarly, the EE_{CF} remained between 95 % and 100 % at different RHs. Moreover, the EE_{CF} was still above 95 % after 30 days of storage. These observations revealed that, regardless of moisture levels and storage time, drug leakage did not take place, corroborating the importance of the trehalose as a stabilizing agent, as noted in previous work [373,374], and highlighting, as well, that cold chains are unnecessary. We can also conjecture that encapsulated molecule retention inside the liposomes over time depends mainly on powder stability, since this has been shown to persist regardless of the powder's crystalline structure.

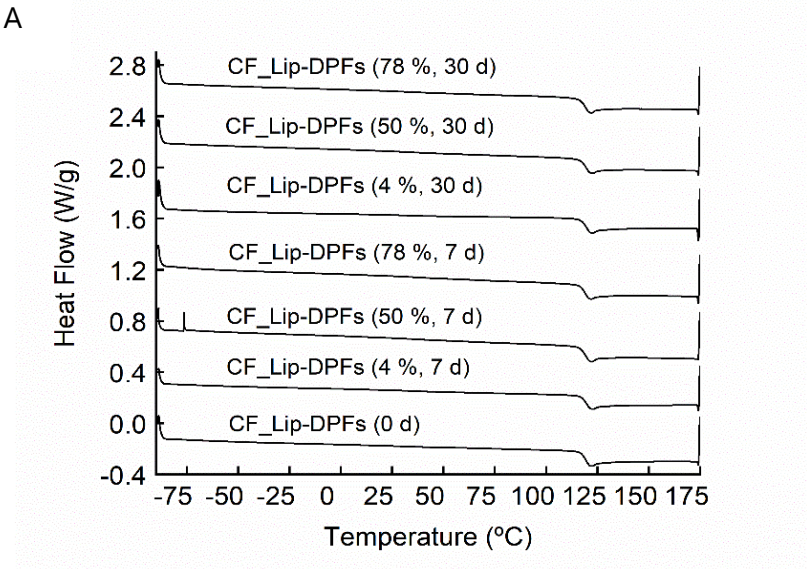

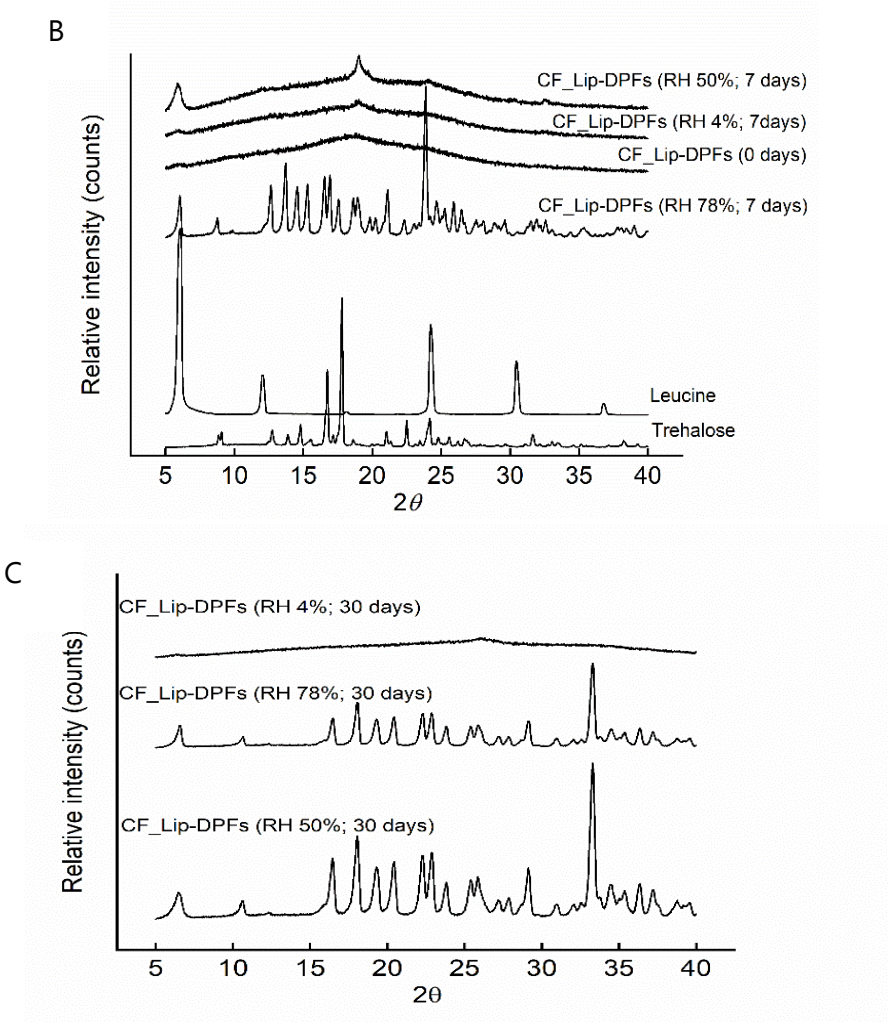

Figure 4.3- A) DSC analysis of CF_Lip-DPFs after SASD, after 7 and 30 days, at different relative humidites. XRD analysis of raw trehalose, leucine and CF_Lip-DPFs after SASD, after B) 7 and C) 30 days, at different relative humidities.

The morphological, chemical and aerosolization properties of CF_Lip-DPFs were also investigated. The CF_Lip encapsulation in an excipient has promising applications for pulmonary medication delivery. Table 4.6 shows the powder's evolution over time, at different RHs. Ensuring the survival of the physical-chemical properties of the powders throughout storage might be challenging [160] , since some powders tend to crystalize, especially at higher RHs [371]. The process yield was 69 ± 8 % and, after SASD, powders with a volumetric diameter around 7 µm were obtained. These powders also showed an MMAD of 1.8 µm and an FPF of 65%, which enables them to be deposited into alveolar airspaces [54,82,375]. After 7 days, despite a slight increase in the Dv_{50} and the MMAD for powders stored at RH of 4 ± 2 %, they continued to

have proportions that would ensure their delivery. Water content rose approximately 3 %, promoting a fall in FPF. The SEM image (Figure 4.4A) shows particle aggregation for those powders stored at RH of 4 ± 2 %. In contrast, for storage at RH of 50 ± 4 %, a higher difference was observed for MMAD and FPF, since the water content increased to 19 %. In Figure 4.4B, we can observe that for powders stored at RH of 50 ± 4 %, larger particle diameters were found. Even so, the parameters fulfill the requirement for successful lung delivery. The impact of moisture on powders stored at RH of 78 ± 2% was greater. The Dv_{50} increased from 7.1 µm to 19.9 µm, whereas the MMAD rose from 1.8 to 5.8 µm. The FPF dropped drastically to 14 %, indicating that 86 % of the affected powders are retained in stage 1 of the Andersen cascade impactor (Appendix B, Figure B.2) which simulates the upper region of the respiratory system [376]. As RH increased, the water molecules absorbed on the particle surface promoted attractive forces due to the capillary action of absorbed water layers, thereby increasing the cohesive forces between the particles (Figure 4.4C) [377]. Thus, a particle size increase and a fall in FPF, coupled with a RH increase were predictable. Table 4.6 shows that no significant changes (p-value > 0.05) were observed between day 7 and 30 for all the characterizations, excepting the water content percentages, for 50 % and 78 %. As shown in the Figure 4.3C, after 30 days the powders stored at 50 % and 78% are in crystalline form. Studies showed that when the water is absorbed by a glassy state trehalose, a stable crystalline dihydrate form is obtained for higher humidity percentages [378]. In the Figure 4.4D-F, SEM images display greater microparticles aggregation after 30 days. These results echo those of Sibum *et al.* [379]. At 3 % and 5 % of Leu, spray-dried microparticles exhibited a suitable FPF after at least one month. However, at higher RH, the powders only lasted 7 days. Higher percentages of Leu were not considered [379]. Work from Shetty *et al.* [160] showed a decrease in FPF of the spray-dried Ciprofloxacin dry powder inhaler formulations stored at RH of 55 % relative to that of 20 %. However, the addition of 10 % or 50 % of Leu improved the formulations, and, after ten days of storage, no significant alterations were observed at different RH. Table 4.6 also evidences the impact of the relative humidities on the powder's properties. The increase of RH from 4 to 50 % does not affect significantly the Dv_{50} and GSD, whereas the water content is significantly affected. In contrast, the aerodynamic properties (MMAD and FPF) are directly impacted as, for both time-points, the increase of the RH affects these parameters significantly. Regarding the particles size distribution, no significant changes were observed with the increase of the RH.

In terms of the chemical structure and intermolecular interactions of the powders, ATR-FTIR analysis (Appendix B, Figure B.3) suggested no structural modifications of the CF_Lip-DPFs upon the rise in RH at both points of time.

Table 4.6- Morphological characterization of CF_Lip-DPFs at 0 days, and then at 4 %, 50 % and 78 % of relative humidity on the 7th and 30th days at 20 ºC. The results are expressed as mean ± SD (n=3).

Assay	RH [%]	D_{V50} [µm]	span	MMAD [µm]	GSD	FPF [%]	Wc [%]
CF_Lip-DPFs (t=0 days)	-	7 ± 2	1.2 ± 0.1	1.75 ± 0.04	2.21 ± 0.03	65 ± 3	6 ± 1
CF_Lip-DPFs (t= 7 days)	4 ± 2	8^{a} ± 2	1.3 ± 0.1	1.95^{a} ± 0.07	2.24^{b} ± 0.01	63^{c} ± 2	9^{a} ± 3
	50 ± 4	9^{a} ± 1	2 ± 1	3.3^{b} ± 0.2	2.96^{b} ± 0.03	50^{b} ± 2	19^{b} ± 3
	78 ± 2	20^{b} ± 5	2.1 ± 0.1	5.8^{c} ± 0.6	1.46^{a} ± 0.01	14^{a} ± 7	21^{b} ± 1
CF_Lip-DPFs (t= 30 days)	4 ± 2	7^{a} ± 3	2 ± 1	1.8^{a} ± 0.1	2.21^{b} ± 0.01	65^{c} ± 5	8^{a} ± 5
	50 ± 4	14^{a} ± 3	3.1 ± 0.3	3.2^{b} ± 0.2	2.1^{b} ± 0.1	51^{b} ± 5	13^{b} ± 1
	78 ± 2	20^{b} ± 2	2.1 ± 0.1	6.3^{c} ± 0.5	1.43^{a} ± 0.07	10^{a} ± 4	14^{b} ± 4

For 7 and 30 days, within the columns, values with different letters are significantly different ($p < 0.05$). Values without letters, or with the same letter are not significantly different ($p > 0.05$).

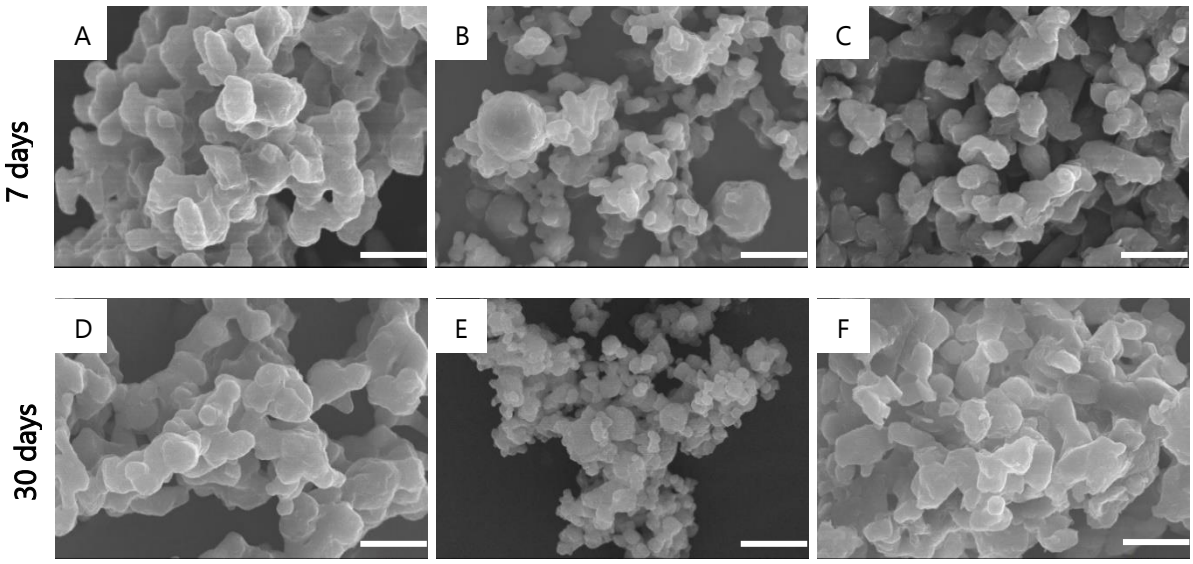

Figure 4.4- SEM images of CF_Lip-DPFs after 7 and 30 days stored at 4 ± 2 % (A and D); 50 ± 4 % (B and E) and 78 ± 2 % (C and F) of relative humidity, respectively (scale bar: 10 µm; magnitude: 3000 x; high-voltage: 20 kV).

4.4 Conclusions

This work is a proof-of-concept that highlights the innovative potential of supercritical CO_2-assisted spray-drying for drying liposomes and converting them into liposomal dry powder formulations, using trehalose and leucine as excipients. The major challenge in drying is maintaining the liposomal structure after processing, which was achieved here. Results showed that at determined concentrations of leucine and ethanol, liposomes kept their structure and the *EE* of the water-soluble dye above 95 %. The challenges faced with regards to the chemical and physical stability of hydrophilic loaded liposomal formulations were surmounted through the production of solid form dosages using the supercritical fluid drying method with optimized ratios of excipients. The QbD approach using the DoE showed that leucine, ethanol and their interactions have a significant impact on the morphological properties of the CF_Lip-DPFs. Through this optimization, correlations for different CQAs were obtained. Although XRD diffractograms showed powder recrystallization at a relative humidity of 78 % after 7 days and at 50 % after 30 days, liposome chemical and physical stabilities were maintained in those stored at relative humidities of 4 % and 50 % at 20 ºC. The aerodynamic performance of the dry powders was also investigated, showing that CF_Lip-DPFs stored at relative humidities of 4 % and 50 % kept those aerodynamic properties required for effective pulmonary liposomal delivery. Several challenges have been overcome in this work, including liposome structure maintenance during the drying and dye encapsulation. We were also successful at retaining the liposome structure following resuspension and excipient removal. This work, thus, contributes greater insight into powders and liposome behavior at different environmental humidity levels. Overall, our findings point to promising synergies between pharmaceutical and chemical technologies in the search for effective alternative liposome storage techniques that forgo the need for cold chain storage. Further studies with biopharmaceutical-loaded liposomes (e.g., RNA therapeutics, enzymes, etc.) are to be undertaken to ascertain the effects of the supercritical drying method on the solid-state properties and stability of biopharmaceutical-loaded liposomal dry powders.

5

Cu, Zn - Superoxide dismutase liposomal dry powder formulations using supercritical CO_2-assisted spray-drying: a proof-of-concept

The contents of this chapter were submitted in a peer reviewed international journal:

C. Costa, T. Casimiro, M. Luisa Corvo, A. Aguiar-Ricardo. Cu, Zn - Superoxide dismutase liposomal dry powder formulations production using supercritical CO_2-assisted spray-drying: a proof-of-concept. Submitted in The Journal of Supercritical Fluids

Personal contribution

CC contributed to the design of the study, performed the experimental work and wrote the manuscript.

5.1 Abstract

Enzyme-based inhalable therapeutics for chronic inflammatory lung disease has led to growing researcher interest essentially to overcome long-term treatments using inhaled corticosteroids. However, enzymes' poor pharmacokinetic profile hinders this goal. When encapsulated into liposomes, enzyme's *in vivo* fate modifies with an increased half-live and a modified biodistribution. Yet, both liposomes and enzymes are susceptible to destabilization during storage. This drawback can be surpassed, by converting liposomal suspension into solid dosage form capable of administration via different routes, including the lungs. In this proof-of-concept study, enzyme Cu, Zn- superoxide dismutase (SOD) was encapsulated into liposomes and then dried using the supercritical CO_2-assisted spray-drying, obtaining SOD-loaded liposomal dry powder formulations (SOD_Lip-DPFs). After resuspension in water, liposomes maintained their structure, and the SOD encapsulation efficiency was 99 %, with preserved enzymatic activity. Powders' stability studies showed that SOD_Lip-DPFs maintained both liposomal and enzyme stability, at a relative humidity of 40% for 50 days.

5.2 Introduction

Therapeutic proteins and namely enzymes have aroused interest for the treatment of chronic inflammatory diseases. Global protein therapeutics are predicted to reach a value of US$ 456.0 billion by 2027 [380]. However, therapeutic outputs face limitations including low physical and chemical stability, protein degradation and immunogenicity [381]. Different non-invasive administration routes for enzyme delivery have been studied to overcome those disadvantages. In particular, pulmonary administration of enzymes has gained particular attention, due to the lung characteristics namely the thin blood-barrier membrane (0.1 - 0.2 μm), large absorption area (> 100 m^2) from a highly vascularized alveolar epithelium constituted by a single layer of cells, elevated blood flow (5 L/min) [36,37], and bypass the hepatic first-pass of metabolism. Other positive properties include the fact that the physiological pH and reduced mucociliary clearance in the deep lungs avoid rapid clearance, poor absorption, and exposure to digestive enzymes [7]. Inhalable protein-based therapies have attracted attention as the range of biological candidates for treating a wide gamut of respiratory diseases has broadened [382].

Ibrahim *et al.* [383] developed a spray-dried inhalable powder formulation of basic fibroblast growth factor (bFGF) for treating asthma or chronic obstructive pulmonary disease. However, powders with a fine particle fraction (FPF) of 25.2 % resulted and limited delivery to the respiratory region. Wahjudi and co-workers [384] studied a formulation of spray-freeze dried acyl–homoserine lactone (AHL) acylase, using mannitol, trehalose, and inulin as excipients. The enzyme was observed to maintain its activity following drying. More recently, Fernandes *et al*. [26,385] reported the encapsulation of Cu, Zn- superoxide dismutase (SOD) in trehalose and leucine through spray-drying (SD). This work successfully addressed the impact of SD parameters on the aerodynamic performance, enzyme activity retention (EAR) and conformational stability SOD. SOD is an enzyme weighting 32.5 kDa that catalyzes the dismutation of anion superoxide radicals in molecular oxygen and hydrogen peroxide. This enzyme is used in broad disease models, such as inflammation [386,387], rheumatoid arthritis [9,339], and ischemia-reperfusion injury [388,389]. In its free form and after iv administration, SOD has a bloodstream half-life of approximately 6 min in rats and 25 min in humans [308,309], essentially due to its rapid renal filtration. Enzyme encapsulation in liposomes – a DDS known by its biocompatibility, non-toxicity, and ability to encapsulate and carry hydrophilic molecules in its inner aqueous core [14] – might be advantageous insofar as liposomes not only protect enzymes from degradation and but also act as vehicles, delivering them into the target site [390]. Corvo and co-workers [11,12,172] have demonstrated improvement of the enzyme biodistribution and its therapeutic effect in inflammatory processes, increasing its half-life up to 20 h when SOD is encapsulated into PEGylated liposomes. This research showed that small-sized (110 nm) SOD-loaded liposomes were preferable for targeting SOD to the arthritic lesions in rats with adjuvant arthritis [308].

Enzyme-loaded liposomes can be converted into dry powder formulations (Lip-DPFs) to ensure their stability during storage. This avoids the need to cold distributions chains and facilitates access to the procedure by irrespective of location or social class. Over recent years, several techniques like freeze-drying [28,210], spray-freeze drying [75,382], spray-drying [27,28] and supercritical fluids [167] have been proposed to produce Lip-DPFs. In a previous work, Aguiar-Ricardo and co-workers [167] used supercritical CO_2-assisted spray-drying (SASD) to convert PEGylated liposomes encapsulating a model hydrophilic dye molecule, (5(6)- carboxyfluorescein- CF) into Lip-DPFs. Different critical process parameters influenced certain critical quality attributes, such as size, polydispersity index (PdI), and encapsulation efficiency, which were evaluated using quality-by-design (QbD). After drying, liposomes maintained their structure

and integrity, while the dye remained encapsulated in the inner aqueous phase of liposomes. The CF-loaded liposomal dry powder formulations also remained stable for 30 days at relative humidities of 4 and 50 %. Translating the knowledge from this previous work, we herein investigate whether SOD-loaded liposomal dry powder (SOD_Lip-DPFs) formulations could be produced using SASD with adequate aerodynamic performance for pulmonary delivery while maintaining the enzyme's encapsulation efficiency and enzymatic activity. To our knowledge, no results have been published to date with liposomal dry powder formulations encapsulating enzymes, namely SOD, using SASD. Therefore, this is an innovative work focused on obtaining a robust, upscaling and time-efficient technique for achieving green, accessible, and patient-friendly inhalable protein delivery system.

5.3 Experimental procedure

5.3.1 Materials

Egg-phosphatidylcholine (E-PC) (> 99 %) and distearoylphosphatidylethanolamine-poly(ethyleneglycol)$_{2000}$ (DSPE-PEG$_{2000}$) (> 99 %) were obtained from Lipoid GmbH (Germany). Cholesterol (Chol) (> 99 %), bovine erythrocytes Cu, Zn-superoxide dismutase, (SOD), citric acid monohydrate (> 99 %) and L-leucine (98 %) were purchased from Sigma-Aldrich (USA). Trehalose dehydrated (> 98 %) were acquired from Tokyo Chemical Industry (China), chloroform (> 99 %) was purchased from Carlo Erba (Spain) and ethanol absolute anhydrous (99.9 %) was sourced from Scharlau (Spain). Air Liquide (Portugal) provided carbon dioxide (99.998 %). All components were used as received without further purification.

5.3.2 SOD-loaded liposomes preparation (SOD_Lip)

The liposomes were prepared using film hydration followed by extrusion methods [172]. Briefly, appropriate amount of EPC, Chol and DSPE-PEG$_{2000}$ (molar ratio of 1.85:1:0.15, respectively) were dissolved in chloroform. The mixture was then dried using a rotary evaporator (Rotavapor RE-111- Buchi, Swiss) to form a lipidic film. The obtained film was hydrated with a 10 mL of SOD, at a concentration of 0.5 mg/mL in a buffer solution (10 mM citric acid in 280 mM trehalose, at pH 6) at a total lipid concentration of 32 µmol/mL. The suspension rested for 1 hour (SOD_Lip) at room temperature, occasionally shaken. The so-formed liposomal suspension was extruded sequentially through membranes with pore sizes of 600, 400 and 200 nm using a

high-pressure extruder (Lipex TM Thermobarrel Extruder, Biomembranes Inc., Vancouver, BC, Canada) with a Nucleopore® Track-Etched Membranes (Whatman®, USA). Finally, the suspension was extruded three times through a membrane filter of 100 nm. Then, non-encapsulated SOD was removed by dilution and centrifugation using an Optima TM XL-90 Ultracentrifuge (Beckman Coulter, USA), for two hours at 300,000 *g* and at 4 ºC. The supernatant was then discarded, and the pellets were resuspended at the same concentration in the same buffer solution (10 mM citric acid and 280 mM trehalose, at pH 6). The so obtained formulations were sterilized by filtration through sterile filter with a pore size of 0.2 µm for SASD.

5.3.3 Dry powder liposomal formulations (Lip-DPFs)

In each assay, 4% (v/v) of the liposome suspensions were mixed with a solution at a total concentration of 300 mM of excipient, composed by trehalose and L-Leucine in a ratio of 9:1 (*w/w*). The final solution containing the liposomes suspension and all the excipients is referred as the casting solution from now on.

In each assay, the casting solution was fed into a laboratory scale SASD apparatus which was previously described in detail elsewhere [25]. Firstly, the CO_2 was liquified at -5 ºC (at 25 mL/min) by passing the feeding line of carbon dioxide in a cryogenic bath which was then pumped using a high-pressure pump (HPLC pump K-501, Knauer). The high-pressure CO_2 is then warmed using a heated bath (T_{CO_2} = 80 ºC) before being delivered to the static mixer. Simultaneously, the casting solution, containing the SOD-loaded liposomes and the excipients, was loaded through a high-pressure pump (Smartline pump 1000, Knauer), at 3.5 mL/min, into a heated static mixer, at 80 ºC, (3/16 model 37-03-075 Chemieer) comprising a high-pressure column of 4.8 mm diameter, 191 mm length and 27 helical mixing elements that promoted CO_2 solubilization into the liquid solution, in order to obtain a near-equilibrium mixture (ρ_{SM} = 120 bar). The static mixer and the inlet streams were heated using tapes and a Shinko FCS-13A temperature controller (± 0.2 ºC resolution). Afterwards, the mixture was atomized into the precipitator through a 150 µm internal diameter nozzle where the solvent underwent accelerated evaporation by heated compressed air flow ($F_{Air,in}$ = 30 m^3/h and $T_{Air,in}$= 100 ºC). The particles were separated from the CO_2-solvent flow in a high-efficiency cyclone and collected in a glass vessel.

The process yield is defined as follows:

$$\eta_{SASD}\ (\%) = \frac{amount\ of\ excipients\ after\ SASD\ (g)}{amount\ of\ excipients\ before\ SASD\ (g)} \times 100 \qquad (1)$$

5.3.4 Reconstitution of SOD_Lip after SASD

After the SASD, a selected mass equivalent to 1 mL of liposomal formulation of SOD_Lip-DPFs was resuspended with deionized water to prevent osmotic shock to the liposomal formulations (final osmolarity of 300 mM). The excipients were removed by dilution and ultracentrifugation, for two hours at 300,000 *g* and at 4 ºC. Then, the pellet was resuspended in 1 mL of the buffer solution (10 mM citric acid and 145 mM NaCl, at pH 6). The resulting SOD_Lip were characterized.

5.3.5 Liposome characterization

Before and after SASD, liposomes were characterized according to their average size and polydispersity index (PdI), as well as phospholipid and protein content to calculate SOD encapsulation efficiency (*EE*). A Zetasizer Nano S (Malvern Panalytical Ltd., Malvern, UK) was used to determine the mean size (Z-average), and the PdI, as a measure of the particle size distribution that ranged from 0 (monodisperse) and 1.0 (polydisperse). The concentration of phospholipids was determined by the Rouser's method [321]. The enzyme was quantified with a modified Lowry's method [322], where liposomes were previously disrupted with 2 % (v/v) Triton® X-100 and 20 % (v/v) of sodium dodecylsulphate (SDS) [323]. When needed and to avoid excipients interference in the protein quantification assay, trehalose and leucine were previously removed by enzyme precipitation with trichloroacetic acid at 10%. The SOD yield (η_{SOD}) was calculated as follows:

$$\eta_{SOD}\ (\%) = \frac{amount\ of\ SOD\ after\ SASD\ (\mu g)}{amount\ of\ SOD\ before\ SASD\ (\mu g)} \times 100 \qquad (2)$$

The lipid yield (η_{Lipid}) was calculated as follows:

$$\eta_{lipid}\ (\%) = \frac{mol\ of\ lipids\ after\ SASD\ (\mu mol)}{mol\ of\ lipids\ before\ SASD\ (\mu mol)} \times 100 \qquad (3)$$

Moreover, the percentage of encapsulation efficiency (*EE*) of SOD is given by the following equation:

$$EE\ (\%) = \frac{\left(\frac{\mu g_{SOD}}{\mu mol_{Lip}}\right)_f}{\left(\frac{\mu g_{SOD}}{\mu mol_{Lip}}\right)_i} \times 100 \quad (4)$$

where $\left(\frac{\mu g_{SOD}}{\mu mol_{Lip}}\right)_i$ is the initial SOD to lipid ratio and $\left(\frac{\mu g_{SOD}}{\mu mol_{Lip}}\right)_f$ is the final one.

The SOD enzymatic activity from SOD-Lip was evaluated using the SOD assay kit (19160 1KT-F, Sigma-Aldrich), where liposomes were previously disrupted with 2 % (v/v) Triton® X-100 and 20 % (v/v) of SDS. After 20 mins, absorbance was measured at 450 nm in a microplate reader Infinite® 200 (Tecan Trading AG, Männedorf, Switzerland).

5.3.6 Characterization of liposomal dry powder formulations

5.3.6.1 Storage stability assays

The SOD_Lip-DPFs obtained from SASD were stored in triplicate in a desiccator at relative humidity (RH) of 40 ± 5 % at 20℃. The RH was obtained using saturated solution of potassium carbonate. The temperature and the relative humidity were monitored using the Lasel® thermohygrometer data logger, model EL-USB-2, for 50 days, when the samples were characterized.

5.3.6.2 *In vitro* aerosolization study

The aerodynamic properties of the Lip-DPFs with and without SOD were determined using an eight-stage Andersen Cascade Impactor – ACI - (Copley Scientific). After 5 (due to the static electricity) and 50 days, due to e 30 mg of the powders were loaded into three hydroxypropylmethylcellulose capsules nº3 (Aerovaus). The capsules were individually placed into a previously weighed dry powder inhaler (DPI) that was coupled to the ACI device. Each plate of the cascade impactor was covered by a pre-weighed filter (Glass Microfiber filter MFV1080, Filter Lab). The DPI punctured the capsule prior to the inhalation, and a high capacity pump was turned on to simulate an intake of breath: an air flow rate of 60 L/min lasting 4 s, according to the European pharmacopoeia [352]. The amount of powder deposited in each stage was calculated by weighing the filters before and after the test and calculating the difference. From this assay, several aerodynamic parameters were calculated—mass median aerodynamic diameter (MMAD), fine particle fraction (FPF), emitted dose (ED) and geometric standard deviation (GSD). The MMAD characterizes the size of those particles that reached the impactor, excluding those deposited in the throat. The value is displayed below, which is the diameter of 50% of

the particles. On the other hand, FPF is the portion of the delivered particles sized below 5 µm, as determined by the interpolation of the percentage of the particles with smaller sizes than this value. Finally, the GSD can be calculated using the following equation:

$$GSD = \sqrt{\frac{d_{84}}{d_{16}}} \quad (5)$$

where d_{84} and d_{16} are the diameters corresponding to 84 % and 16 % of the cumulative distribution, respectively. The emitted dose was calculated as follows:

$$ED = \frac{m_{full} - m_{empty}}{m_{powder}} \; x\; 100 \quad (6)$$

where m_{full} and m_{empty} are the weights (mg) of the capsule before and after simulating the inhalation and m_{powder} is the initial weight (mg) of the powder in the capsule.

5.3.6.3 Differential scanning calorimetry (DSC)

The glass transition temperature (*T*g) was determined by weighing approximately 4 mg of powder on a TA Instruments differential scanning calorimeter, DSC Q2000, within a temperature range from -90 ℃ to 130.0 ℃, in two cycles.

5.3.6.4 Residual moisture content

Residual ethanol content was evaluated by high-performance liquid chromatography (HPLC) Dionex ICS3000 (Sunnyvale, CA, USA) with Pulsed Amperometric Detection (PAD). Briefly, Lip-DPFs with and without SOD were dissolved in Milli-Q water in a final concentration of 100 mg/mL. Then 10 µL of each sample was injected into a Thermo Carbopac PA10 250 x 4.6 mm with pre-column Thermo Aminotrap 50 x 4.6 mm (Waltham, Massachusetts, EUA). The analysis was conducted at a flowrate of 1 mL/min with NaOH (18mM).

5.3.6.5 2.7. Statistical analysis

All results are expressed as mean ± standard deviation (S.D.). To analyze the data, *t*-test with Welch's correction (GraphPadPrism, GraphPad software Inc., CA, USA) was used. The level of significance was set at the probabilities of *p< 0.05, and ** p < 0.01.

5.4 Results and Discussion

5.4.1 Production of SOD-loaded liposomal dry powder formulations

Costa *et al.* [167], produced inhalable hydrophilic molecule-loaded liposomal dry powder formulations using the design-of-experiments approach to optimize the percentage of trehalose and leucine in the casting solution, so , after SASD, liposomes were able to keep their structure, while retaining the dye ((5(6)-carboxyfluorescein)) encapsulated. In this work, we hypothesized that the same optimized percentages of trehalose and leucine could produce SOD_Lip-DPFs. Empty and SOD-loaded liposomes with neutral charge were produced. A slight size increase was observed upon SOD encapsulation (Table 5.1). The initial SOD/Lip ratio (in the film hydration step) was approximately 15 µg/µmol. During extrusion, however, when passing through filters with several cut-offs, liposomes reorder themselves to decrease their size, leading to encapsulated enzyme loss in the inner core, resulting in a final SOD/Lip of 5 µg/µmol (Table 5.1). Following ultracentrifugation, empty liposomal and SOD-loaded liposomal formulations were sterilized and divided into two aliquots, one for storage at 4℃ and the other one to be dried using SASD equipment. Considering the critical process parameters (percentage of leucine (Leu) and ethanol) and the process variables optimized in the previous study, empty liposomes, and SOD_Lip were mixed with a casting solution (4 %, v/v) composed of 90 % (w/w) of trehalose (Tre) and 10 % (w/w) of Leu (total solution osmolarity of 300 mM). The SASD experiment was carried out at $T_{air_{in}}$ = 100 ± 2 ℃; T_{CO_2} = 80 ± 2 ℃; T_{SM} = 84 ± 4 ℃; $T_{air_{out}}$ = 64 ± 1 ℃; p_{SM} = 120 ± 2 bar (three independent batches).

Table 5.1- Physicochemical characterization, encapsulation efficiency (*EE*) and retained enzymatic activity of liposomes and SOD_Lip, before and after SASD.

		Size [nm]	PdI	η_{Powder} [%]	η_{Lipid} [%]	η_{SOD} [%]	$[SOD/Lip]_f$ [µg/µmol]	*EE* [%]	Ret.Act. [%]
Before SASD	Empty liposomes	131 ± 1	0.048 ± 0.011	-	-	-	-	-	-
	SOD_Lip	136 ± 3	0.060 ± 0.007	-	-	-	5 ± 1	-	> 95
After SASD*	Empty liposomes	122 ± 3	0.174 ± 0.014	57 ± 6	58 ± 4	-	-	-	-
	SOD_Lip	117 ± 3	0.211 ± 0.009	65 ± 3	81 ± 2	99 ± 3	7 ± 1	> 95	80-100

*Liposomes which were resuspended from the powders

The results are expressed as mean ± S.D (n = 3).

PdI: Polydispersity index.

$[SOD/Lip]_f$: Final SOD to lipid ratio considering the final lipid concentration value

Table 5.1 shows a slight size decrease in the resuspended empty and loaded liposomes following drying. This might be related to two different phenomena. First, the water replacement theory suggests that during dehydration and in the solid state, the surrounding water molecules are replaced by hydrogen bonds with carbohydrates [24]. Second, as observed previously, leucine plays a role not only in moisture prevention but also in the maintenance of liposome structure. Electrostatic interaction between the carboxyl group of the Leu and the E-PC amine group might take place between leucine and liposomes, forming a layer on the liposome surface, capable of shielding them from external forces while drying [167]. Finally, the presence of ethanol in the casting solution can cause liposomes to shrink, resulting in a reduction of their size as studied by Pal and co-workers [364]. When compared to empty liposomes, the size decrease was more pronounced for SOD-Lip. It suggests possible interactions between the enzyme and the pegylated chain of DSPE-PEG_{2000} lipid. To confirm this assumption, further two-dimensional nuclear magnetic resonance studies must be performed [391]. Nonetheless, in our previous work [167] reconstituted CF-loaded liposomes from DPFs showed similar behavior, suggesting that the drying process and the casting solution composition might be the key critical process parameters to control the final liposome structure. Observations from Porras-Gomez and co-workers [392] showed that compression increase lipid alkyl chains disorder relative to the effect of cholesterol on gel (solid ordered) phases. In addition, Elizondo *et*

al. [139] argue that compressed CO_2 provides a more homogeneous path for the supramolecular organization of the lipids in their membrane. Consequently, during drying, liposomes kept their homogeneity (PdI ≈ 0.2). The SOD yield of 99 ± 3 % (with a respective *EE* over 95 %), reveals that liposomes maintained their structure, retaining the enzyme inside aqueous the inner core. Otherwise, a significant decrease in the SOD recovery would have been expected.
In addition to SASD enzyme yield, it is also worth considering SOD enzymatic activity retention. SOD activity was thereby assessed and percentages ranging from 80 and 100 % were observed, proving that SASD does not significantly affect enzyme integrity and consequent enzymatic activity. Lo *et al.* [198] produced spray-dried SOD-loaded liposomal formulations, in which the main phospholipid was DPPC and the excipient was sucrose. SOD enzymatic activity was 98 % preserved. Thereby, the SOD enzymatic activity retention highlighted the DDS role of liposomes. This work also overcomes the drawbacks associated with liposomal aerosols. It has been reported that the during nebulization, the shear applied to convert the aqueous liposomal suspensions into aerosol droplets may exert physical stress on liposome bilayers, leading to a loss of the entrapped drug [393].
Aerodynamic characterizations were then performed to verify if the SOD_Lip-DPFs were possible candidates for pulmonary delivery. Table 5.2 shows that SOD_Lip-DPFs presented an MMAD of 1.6 ± 0.4 μm and an FPF of 65 ± 5 %, indicating that particles can achieve deposition in the lower respiratory tract, reaching stage 5 which represents the terminal bronchi. The emitted dose indicates that 98.6 ± 0.4 % of the powder content can be fluidized by the airflow through the inhaler. Finally, HPLC analysis failed to detect ethanol peaks at powder concentrations up to 100 mg/mL. The regulated threshold for residual ethanol was 5000 ppm [394]. For this reason, SOD_Lip-DPFs are able not only to be inhaled but also to spare residual organic solvent has for patient.

Table 5.2- Aerodynamic and residual solvent characterization of Lip-DPFs and SOD_Lip-DPFs.

	MMAD [µm]	GSD	FPF [%]	ED [%]	Residual ethanol [ppm]
Lip-DPFs	1.7 ± 0.1	2.3 ± 0.1	59 ± 7	98 ± 1	n.d.
SOD_Lip-DPFs	1.6 ± 0.4	2.3 ± 0.1	65 ± 5	98.6 ± 0.4	n.d.

The results are expressed as mean ± S.D (n = 3).

n.d.- Not detected.

5.4.2 Stability assays of SOD_Lip-DPFs

Stability assays of the powders at a relative humidity of 40 ± 5 % at 20 ℃, were conducted for 50 days. As a control, SOD-Lip suspensions were stored at 4℃ for the same time. After 50 days, powders were ultracentrifuged to remove the excipients, and liposomes were resuspended and characterized. Table 5.3 shows a non-significant increase in liposome size which was expectable due to DSC studies. Increased liposome size is often related to the modification of trehalose glass transition temperature. Sun and co-workers [366] suggest that an increase in molecular mobility with the decrease of trehalose glass transition temperature results in an increase in liposome size increase. In this case, the T_g was not affected. DSC studies showed a T_g of 128 ℃ (the same before storage, data not shown). The *EE* remained above 95 %, highlighting that despite the storage in such relative humidity, trehalose was able to prevent drug leakage, reflecting its role as a stabilizing agent. Not only was *EE* maintained, but the SOD retained its enzymatic activity after 50 days storage. This demonstrates that, in terms of nanosystem, SOD_Lip-DPFs can prevent liposome fusion and rearrangement, keeping the enzyme in liposomes and protecting its enzymatic activity.

Table 5.3- Physicochemical characterization, encapsulation efficiency (*EE*) and retained enzymatic activity (Ret.Act.) of SOD_Lip after 50 days at RH of 40 ± 5 % at 20 ℃. SOD_Lip in suspension form was stored at 4℃ acting as control.

		Size [nm]	PdI	η_{Lipid} [%]	η_{SOD} [%]	[SOD/Lip] [µg/µmoL] $_f$	*EE* [%]	Ret.Act[¥] [%]
t= 0 days	SOD_Lip (suspension)	136 ± 3	0.060 ± 0.007	-	-	5 ± 1	-	> 95
	SOD_Lip From DPFs	117 ± 3	0.211 ± 0.009	81 ± 2	99 ± 3	7 ± 1	> 95	80-100
t= 50 days	SOD_Lip (suspension)	145 ± 5^{ns}	0.062 ± 0.020 ^{ns}	88 ± 1^{ns}	97 ± 5^{ns}	8 ± 1*	> 95^{ns}	> 95^{ns}
	SOD_Lip From DPFs	124 ± 2^{ns}	0.185 ± 0.008*	75 ± 6^{ns}	99 ± 9 ^{ns}	7 ± 1^{ns}	> 95^{ns}	90-100^{ns}

The results are expressed as mean ± S.D (n = 3).

[¥]n= 2 independent batches

ns: non-significant; *p-value < 0.05

Regarding the powders' aerodynamic properties, the MMAD increased from 1.6 ± 0.4 µm to 4 ± 1 µm (p-value< 0.05), while GSD presented a non-significant (p-value >0.05) decrease to 1.9 ± 0.4, indicating a falling distribution of the aerodynamic diameter. FPF fell from 65 ± 5 % to 28 ± 5 % (p-value< 0.01), while the ED maintained its percentage (p-value >0.05). The decrease in FPF indicates that only 28 % of the particle managed to reach the respiratory region. Therefore, future research must be developed to further protect the powder from moisturizing and to improve the aerosolization efficiency of the stored powder. Despite the fall in powder flowability, drying has been shown to protect SOD-loaded liposomal formulations from external moisture. This forgoes the need for supply and distribution cold chains at – 80 ℃ and – 20 ℃, which hinder easy access to people of all geographical and socio-economic conditions.

5.5 Conclusions

In this work, SOD was encapsulated into PEGylated liposomes and successfully dried in SASD, using trehalose and leucine as excipients. Considering previously optimized critical process parameters using a quality-by-design, following drying, resuspended liposomes from dry powder formulations were revealed to have maintained both their structure and integrity, while

preserving the enzymatic activity. Challenges regarding the chemical and physical stability of SOD-loaded liposomal formulations were surmounted by producing solid dosages form using the supercritical fluid drying method with optimized ratios of excipients. Moreover, the SOD_Lip-DPFs aerodynamic characterization proves that enzyme-loaded solid dosage form can reach the respiratory region, particularly the terminal bronchi. Stability studies showed that over 50 days, powders can protect liposomes and the encapsulated enzyme. However, decreased flowability suggests that more in-depth studies regarding stabilization agents (sugar) and moisture reduction (amino acid) must be carried out. Nonetheless, this work highlights the powder capacity to carry and protect enzyme-loaded liposomal formulations from moisture, with the same stability as those suspensions stored at 4°C, at least for 50 days, which represents a great advantage over the cold supply and distribution cold chains. Overall, this work represents an innovative and scalable alternative accessible to people of all geographic and socio-economic conditions.

6

QUERCETIN-LOADED LIPOSOMAL DRY POWDER FORMULATIONS USING SUPERCRITICAL CO_2 – ASSISTED SPRAY-DRYING FOR THE TREATMENT OF LUNG INFLAMMATORY DISEASES

Personal contribution

CC contributed to the design of the study, performed the experimental work, and wrote the manuscript.

6.1 Abstract

Quercetin – a natural polyphenolic flavonoid – presents remarkable anti-inflammatory properties. When incorporated in liposomes, quercetin's water solubility and permeability are improved, being a candidate for the treatment of inflammatory diseases. However, for local treatment, particles should be inhaled and, consequently comprise a diameter between 1 and 5 μm to reach the deep respiratory region. Here, we present quercetin-loaded liposomal dry powder formulations, obtained through the sustainable and green process – supercritical CO_2- assisted spray-drying (SASD). Different compositions of liposome membranes were studied considering the incorporation efficiency of quercetin after the drying process. Powders presented an MMAD of 1.7 μm and an FPF of 63 %, being suitable for inhalation. After resuspension in water to remove excipients, liposomes showed 57 % of quercetin incorporation efficiency.

6.2 Introduction

Chronic obstructive pulmonary disease (COPD) is one of the chronic inflammatory lung diseases, which was responsible in 2019 for 3.23 million deaths worldwide, according to the World Health Organization (WHO) [3]. This disease is characterized by a chronic inflammatory response, which leads to the production of reactive oxygen species (ROS) [2], resulting in tissue damage and consequent alterations of lung tissue structure [395], which may lead to emphysema with concomitant pulmonary fibrosis. Common COPD treatment is based on inhaled corticosteroids (ICS). Early randomized controlled trials (RCTs) have shown that ICS monotherapy has no significant effect on exacerbations of COPD. However, when conjugated with a bronchodilator a reduction of 25-35 % is obtained [5]. Nonetheless, there is evidence that a long-term therapy based on ICS can cause several adverse effects, like pneumonia [4–6], cataracts [4], and even the risk of fractures [4,396]. Quercetin (Quer) is a polyphenolic flavonoid found in vegetables and fruits with remarkable anti-inflammatory and antioxidant properties [7]. This polyphenol is reported to be an active oxygen scavenger and an estrogen receptor agonist. Mitani *et al.* [397] reported that quercetin increased AMPK activation and Nrf2 expression, and it also restored corticosteroid sensitivity suggesting that quercetin might be a potential new treatment for COPD. Recently, Derosa *et al.* [398] reported computation methods that showed quercetin's ability to interfere with the SARS-CoV-19 replication. Despite all the advantages of

a possible quercetin-based treatment, this flavonoid is a biopharmaceutical classification system (BCS) class IV [10,399], which restricts its therapeutic potential. Liposomes, known to be biodegradable, biocompatible, and non-toxic drug delivery systems (DDS) [15,400], due to their physicochemical properties, can accommodate hydrophobic compounds in their bilayer, being an excellent candidate for the carry and delivery of quercetin. Several studies have evaluated the antioxidant potential of quercetin-loaded liposomes [401–405]. Rezaei-Sadabady *et al.* [403] reported the production of liposomal formulations of quercetin, improving its solubility and bioavailability. Moreover, nano-sized quercetin encapsulated by liposomes enhanced cellular uptake. Ferreira-Silva *et al.* [405] studied the efficacy of quercetin liposomal nanoformulation, with an incorporation efficiency of 96 ± 3 %, for ischemia and reperfusion injury treatment. Despite the successful studies of quercetin-loaded liposomes on inflammatory processes, COPD acts in the respiratory region, therefore a pulmonary drug delivery is a more effective and suitable treatment. Several works have reported quercetin in solid dosage forms. Recently, Alhajj *et al.* [406] reported a ciprofloxacin-quercetin co-amorphous system for the treatment of cystic fibrosis. Powders with a mass median aerodynamic diameter between 2.51 ± 0.05 and 3.51 ± 0.60 μm were obtained. However, due to the poor water solubility of the drugs, 75 % of ethanol is used during the process. In the end, powders with a residual moisture content between 2.95 ± 0.14 and 3.59 ± 0.13 % are obtained, which are above the regulated threshold for ethanol [394]. Freeze and spray-dried solid dispersions constituted by quercetin and polymers, such as polyvinylpyrrolidone, hydroxypropyl methylcellulose, poloxamer 400, polyethylene glycol 8000 towards the increase of quercetin solubility have been also reported [407,408]. Scalia *et al.* [409] obtained solid lipid microparticles composed of tristearin as the lipid component and phosphatidylcholine as the emulsifier with a fine particle fraction of 20.5 ± 3.3 %, whereas Papakyriakopoulou and co-workers reported quercetin-β-cyclodextrin derivatives complexes with mannitol/lecithin microparticles for the treatment of Alzheimer disease, through the nasal delivery [410]. Supercritical fluids have been also applied to the drying of quercetin. Lévai *et al*. [192] produced quercetin suspensions using soybean lecithin and Pluronic L64® using Supercritical Fluid Extraction of Emulsion. Then, microparticles of quercetin suspensions were produced through Particles from Gas Saturated Solutions (PGSS)-drying technology. The authors observed a significant improvement in quercetin permeability through a transdermal membrane into the simulated intestinal fluid. More recently, liposomal formulations with a hydrophilic dye were converted into liposomal dry powder formulations (Lip-DPFs) suitable for inhalation, using the supercritical CO_2-assisted spray-drying (SASD) process [167].

SASD is a one-step process that produces dry powders [35], as $scCO_2$ is solubilized into the liquid solution containing the drug and/or carrier system. The resulting near-equilibrium mixture outflowing from the saturator/static mixer is then atomized through a nozzle to the precipitation chamber at near atmospheric pressure [31]. Compared to conventional methods, SASD offers numerous advantages, such as the opportunity to control both particle size and distribution [411], as well as to function at mild temperatures. SASD is also scalable. Therefore, this CO_2-assisted process is not only attractive for liposome drying, but it also provides suitable powders for liposome inhalation [411]. To date, no study has been conducted to produce quercetin-loaded liposomal dry powder formulations using SASD. Thereby, the objective of this work is to process quercetin-loaded liposomal dry powder formulations (Quer_Lip-DPFs) for inhalation purposes. To achieve this, considering a previous SASD optimization to produce Lip-DPFs [167], different liposomal formulations (with different surface charges and lipid: quercetin molar ratio) were produced to maximize the quercetin incorporation efficiency of resuspended liposomes, after SASD processing. Regarding the drying process, different leucine and ethanol percentages were also studied. Here, the quercetin's crystalline form and solubility-related issues are overcome, since after drying process, upon resuspension in Milli-Q water, quercetin remained loaded into the liposomal bilayer. In sum, we aim to design a promising work for suitable, patient-friendly, green, and efficient lipid-based dry powder formulations for the treatment of lung inflammatory diseases, overcoming the drawbacks of long-term ICS therapy.

6.3 Experimental procedure

6.3.1 Materials

1,2-Dimyristoyl-sn-glycero-3-phosphocholine (DMPC), 1,2-dimyristoyl-sn-glycero-3-phosphorylglycerol sodium salt (DMPG), and egg-phosphatidylcholine (E-PC) were obtained from Lipoid (Germany). Cholesterol (Chol), stearylamine (SA) (99%), L-leucine (98%), citric acid and sodium chloride were purchased from Sigma-Aldrich (USA). Quercetin (>97%) was purchased from Alfa Aesar. Trehalose dehydrated (> 98 %) was acquired from Tokyo Chemical Industry (China), chloroform (> 99 %) was purchased from Carlo Erba (Spain) and ethanol absolute anhydrous (99.9 %) was sourced from Scharlau (Spain). Methanol (HPLC gradient grade) was purchased from Merck (Germany). Air Liquide (Portugal) provided carbon dioxide (99.998 %). All components were used as received without further purification.

6.3.2 Preparation of liposomes and quercetin-loaded liposomes (Quer_Lip)

Liposomes were prepared using the film hydration method followed by extrusion [167]. Briefly, for neutral liposomes, EPC and Chol (molar ratio of 9:1, respectively) were dissolved in chloroform in a round bottom flask, whereas for cationic liposomes, EPC, Chol and SA a molar ratio of 8:1:1 as applied. Finally, for negative liposomes, DMPC and DMPG were dissolved at a molar ratio of 7:3. All the formulations were prepared at a total lipid concentration of 32 µmol/mL (final hydration volume). For the preparation of quercetin-loaded liposomes (Quer_Lip), in parallel quercetin was dissolved in methanol and then added to the lipid components dissolved in chloroform (molar ratio of 1:10,). The mixture was then dried using a rotary evaporator (Rotavapor RE-111- Buchi, Swiss) and formed a lipidic film. The film was then hydrated with 10 mL of a buffer solution (10 mM citric acid in 280 mM trehalose, at pH 6), resting for 1 hour (Quer_Lip) at room temperature, with occasional agitation. A high-pressure extruder (Lipex TM Thermobarrel Extruder, Biomembranes Inc., Vancouver, BC, Canada) with a Nucleopore® Track-Etched Membranes (Whatman®, USA) with pore sizes of 600, 400 and 200 nm was applied to the obtained suspension with three passes across a membrane filter of 100 nm. Finally, the non-incorporated Quer was separated from the liposomal formulation by size exclusion chromatography using a desalting column with a 1000 Dalton cut-off (Econo-Pac®, BIO-RAD, Hercules, CA, USA) and sterilized by filtration through syringe 0.2 µm PTFE sterile filters.

6.3.3 Preparation of quercetin-loaded dry powder liposomal formulations (Quer_Lip-DPFs)

In each assay, 4% (v/v) of the liposome suspensions were mixed with a solution at a total concentration of 300 mM of trehalose (Tre) and 10 % (w/w) of leucine (Leu). This suspension was prepared as a mixture of water:ethanol (85:15, % v/v). The final suspension containing the liposomes suspension and all the excipients is referred to as the casting solution from now on. In each assay, the casting solution was fed into a laboratory-scale SASD apparatus which was previously described in detail elsewhere [31]. Firstly, the CO_2 was liquified (at 25 mL/min) by passing the feeding line of carbon dioxide in a cryogenic bath which was then pumped using a high-pressure pump (HPLC pump K-501, Knauer). The high-pressure CO_2 is then warmed using a heated bath (T_{CO_2} = 80 °C) before being delivered to the static mixer. Simultaneously, the casting solution, containing the liposomes or Quer_Lip and the excipients, was put through

a high-pressure pump (Smartline pump 1000, Knauer), at 3.5 mL/min, into a heated static mixer, at 80 °C, (3/16 model 37-03-075 Chemieer) comprising a high-pressure column of 4.8 mm diameter, 191 mm length and 27 helical mixing elements that promoted CO_2 solubilization into the liquid solution, to obtain a near-equilibrium mixture (p_{SM} = 120 bar). The static mixer and the inlet streams were heated using tapes and a Shinko FCS-13A temperature controller (± 0.2°C resolution). Afterwards, the mixture was atomized into the precipitator through a 150 µm internal diameter nozzle where the solvent underwent accelerated evaporation by heated compressed air flow ($F_{Air,in}$ = 30 m^3/h and $T_{Air,in}$= 100 °C). The particles were separated from the CO_2-solvent flow in a high-efficiency cyclone and collected in a glass vessel.

The process yield is defined as follows:

$$\eta_{SASD}\ (\%) = \frac{amount\ of\ excipients\ after\ SASD\ (g)}{amount\ of\ excipients\ before\ SASD\ (g)} \times 100 \qquad (1)$$

6.3.4 Characterization of liposomal formulations

Before and after SASD processing, liposomes were characterized according to their average size and polydispersity index (PdI), as well as phospholipid and quercetin content used to calculate the incorporation efficiency (*IE*). A Zetasizer Nano S (Malvern Panalytical Ltd., Malvern, UK) determined the mean size (Z-average), and the polydispersity index as a measure of the particle size distribution that ranged from 0 (monodisperse) and 1.0 (polydisperse). The Rouser method [321] assessed the phospholipid quantification. Quercetin quantification was performed by high-performance liquid chromatography (HPLC) in a Purospher® STAR RP-18 end-capped (5 µm) HPLC column, 4.6 × 250 mm (Merck, Darmstadt, Germany), using a Beckman System Gold HPLC (Beckman Coulter, Carlsbad, CA, USA). Liposomes containing the drug were disrupted with methanol, with the concomitant solubilization of quercetin, and filtered through a PTFE membrane with 0.2 µm pore diameter before quantification at 360 nm with a mobile phase consisting of methanol/water acidified with 0.1% (v/v) trifluoroacetic acid (70:30, v/v).

The quercetin yield (η_{Quer}) was calculated as follows:

$$\eta_{Quer}\ (\%) = \frac{amount\ of\ Quer\ after\ SASD\ (\mu g)}{amount\ of\ Quer\ before\ SASD\ (\mu g)} \times 100 \qquad (2)$$

The lipid yield (η_{Lipid}) was calculated as follows:

$$\eta_{lipid}\ (\%) = \frac{amount\ of\ CF\ after\ SASD\ (\mu g)}{amount\ of\ CF\ before\ SASD\ (\mu g)} \times 100 \qquad (3)$$

Moreover, the percentage of incorporation efficiency (*IE*) of the quercetin is given by the following equation

$$IE\ (\%) = \frac{\left(\frac{\mu g_{Quer}}{\mu mol_{Lip}}\right)_f}{\left(\frac{\mu g_{Quer}}{\mu mol_{Lip}}\right)_i} \times 100 \quad (4)$$

where $\left(\frac{\mu g_{Quer}}{\mu mol_{Lip}}\right)_i$ is the initial quercetin-to-lipid ratio and $\left(\frac{\mu g_{Quer}}{\mu mol_{Lip}}\right)_f$ is the final one.

6.3.5 Characterizations of liposomal dry powder formulations

6.3.5.1 In vitro aerosolization study

The aerodynamic properties of the Lip-DPFs and Quer_Lip-DPFs were determined using an eight-stage Andersen Cascade Impactor – ACI - (Copley Scientific). Soon thereafter, 30 mg of Quer_Lip-DPFs were loaded into three hydroxypropylmethylcellulose capsules nº3 (Aerovaus). The capsules were individually placed into a previously weighed dry powder inhaler (DPI) that was coupled to the ACI device. Each plate of the cascade impactor was covered by a pre-weighed filter (Glass Microfiber filter MFV1080, Filter Lab). The DPI punctured the capsule before the inhalation, and a high-capacity pump was turned on to simulate an intake of breath: an airflow rate of 60 L/min lasting 4 s, according to the European pharmacopoeia [352]. The amount of powder deposited in each stage was calculated by weighing the filters before and after the test and calculating the difference. From this assay, several aerodynamic parameters were calculated—mass median aerodynamic diameter (MMAD), fine particle fraction (FPF), and geometric standard deviation (GSD). The MMAD characterizes the size of those particles that reached the impactor, excluding those deposited in the throat. The value is displayed below, which is the diameter of 50 % of the particles. On the other hand, FPF is the portion of the delivered particles sized below 5 µm, as determined by the interpolation of the percentage of the particles with smaller sizes than this value. Finally, the GSD can be calculated using the following equation:

$$GSD = \sqrt{\frac{d_{84}}{d_{16}}} \quad (5)$$

where d_{84} and d_{16} are the diameters corresponding to 84 % and 16 % of the cumulative distribution, respectively. The emitted dose was calculated as follows:

$$ED = \frac{m_{full} - m_{empty}}{m_{powder}}\ x\ 100 \quad (6)$$

where m_{full} and m_{empty} are the weights (mg) of the capsule before and after simulating the inhalation and m_{powder} is the initial weight (mg) of the powder in the capsule.

6.3.5.2 Scanning electron microscopy

The shape and morphology of Lip-DPFs particles were determined by scanning electron microscopy (SEM). The samples were coupled to adhesive carbon tapes, and the excess powder was removed by a jet of compressed air. Then a Hitachi S2400 with Bruker light elements EDS detector (Japan) analyzed the samples with an accelerating voltage set to 15 kV and at magnifications of 5 k and 10 k.

6.3.5.3 Residual moisture content

Residual ethanol content was evaluated by high-performance liquid chromatography (HPLC) Dionex ICS3000 (Sunnyvale, CA, USA) with Pulsed Amperometric Detection (PAD). Briefly, Lip-DPFs with and without quercetin were dissolved in Milli-Q water at a final concentration of 100 mg/mL. Then 10 µL of each sample was injected into a Thermo Carbopac PA10 250 x 4.6 mm with pre-column Thermo Aminotrap 50 x 4.6 mm (Waltham, Massachusetts, EUA). The analysis was conducted at a flow rate of 1 mL/min with NaOH (18 mM).

6.4 Results and Discussion

The biggest challenge faced in the drying of liposomes is to keep the associated drug (Quer) incorporated upon liposome resuspension. Therefore, preliminary studies where different membranes' composition, surface charge, and different molar ratios of lipid/quercetin were performed (Appendix C). Negative, neutral, and cationic quercetin-loaded liposomes were produced through the thin-film method followed by extrusion. Molar ratios of 10:0.5 and 10:1 lipid/quercetin were studied. The results showed that negatively charged liposomes presented a lower *IE* (13-14 %) than neutral (37-32 %) and cationic liposomes (28-69 %). It was also observed that liposomes with molar ratios of 10:1 presented higher *IE* than those with molar ratios of 10:0.5. Therefore, further experiments were carried out with cationic liposomes.

6.4.1 Preparation of neutral and cationic liposomes and quercetin-loaded liposomes (Quer_Lip)

During the preparation, liposomes with and without the cationic amphipathic molecule (SA) were prepared. Stearylamine was added to the liposomes components to induce a cationic charge in lipid nanoparticles [14], to improve further interaction with lung cells in *in vitro* studies. Therefore, in this work, neutral liposomes act as a control. Table 6.1 shows the physicochemical characterization of neutral and cationic liposomes and Quer_Lip.

na

Table 6.1- Physicochemical characterization and incorporation efficiency (IE) of neutral and cationic liposomes and Quer_Lip, before SASD.

	Size [nm]	PdI	ζ- potential [mV]	$(Quer/Lip)_f$ [µg/µmol]	*IE* [%]
Neutral liposomes	136 ± 1	0.098 ± 0.016	- 1 ± 1	-	-
Neutral Quer_Lip	138 ± 2	0.148 ± 0.030	- 1 ± 1	37 ± 4	96 ± 10
Cationic liposomes	137 ± 5	0.080 ± 0.006	11 ± 1	-	-
Cationic Quer_Lip	153 ± 10	0.123 ± 0.064	12 ± 1	40 ± 3	98 ± 2

The results are expressed as mean ± S.D (n = 3).

PdI: Polydispersity index.

$(Quer/Lip)_f$: Final quercetin to lipid ratio considering the final lipid concentration value

Table 6.1 shows that no major differences between the size of cationic and neutral liposomes were observed. However, for those incorporated with quercetin, a slight increase was observed. Similar observations were reported by Eid *et al.* [412] for liposomes composed of PC, Chol and quercetin. Through atomic force microscopy and molecular dynamics measurements, Eid and co-workers observed that with the increase in quercetin concentration, they observed larger distances between the lipid molecules, explaining the increase in the size. Moreover, the diffusion coefficients of lipid molecules are also increased [412]. The ζ- potential increased significantly for those liposomes with SA, proving a successful SA distribution into the liposome's bilayer. Finally, 96-98 % of quercetin was incorporated in the liposome's bilayer. Liposomes

and Quer_Lip were then sterilized, divided into two aliquots, and stored at 4℃, for further processing in SASD.

6.4.2 Preparation of liposomal dry powder formulation (Lip-DPFs) and quercetin-loaded liposomal dry powder formulation (Quer_Lip-DPFs)

The main challenge of liposomes drying is the maintenance of their structure during and after SASD processing, as well as the keeping of the incorporated molecule. A previous work in which a model hydrophilic dye was encapsulated in liposomes and then processed in SASD showed that liposomes with hydrophilic molecules encapsulated in their aqueous core can keep their structure after a $scCO_2$-based process [167].

In this work, neutral and cationic liposomes and quercetin-loaded liposomes were processed in SASD. The pressure and temperatures at which the experiments were carried out as well as the respective process yield are described in Table 6.2.

Table 6.1- SASD process parameters.

	$T_{air,in}$ [℃]	T_{CO2} [℃]	T_{SM} [℃]	$T_{air,out}$ [℃]	p_{SM} [bar]	η_{SASD} [%]
Neutral liposomes	98 ± 2	80 ± 1	96 ± 2	57 ± 3	119 ± 1	64 ± 2
Neutral Quer_Lip	99 ± 3	80 ± 1	93 ± 1	58 ± 2	120 ± 1	64 ± 1
Cationic liposomes	97 ± 4	80 ± 1	92 ± 1	56 ± 3	118 ± 1	60 ± 6
Cationic Quer_Lip	99 ± 6	79 ± 1	89 ± 5	59 ± 2	120± 1	61 ± 1

The results are expressed as mean ± S.D (n = 3).

$T_{air,in}$: Temperature of heated compressed air; $T_{CO2:}$ Temperature of heated CO_2; $T_{air,out:}$ Outlet air temperature; T_{SM}: Temperature at the static-mixer; p_{SM}: Pressure at the static-mixer.

The process yield was between 60 and 65 % of the recovered powder. Liposomes were successfully encapsulated in trehalose. Through EDS analysis, it was possible to observe 49.4 ± 0.1 % of carbon atoms, 47 ± 1 % of oxygen atoms and a residual presence of nitrogen atoms (3 ±

1 %), probably from liposomes present on the sugar surface. Following SASD processing, cationic Lip-DPFs, Quer_Lip-DPFs and respective controls were resuspended in deionized water to maintain their osmolarity. The excipients were removed by ultra-centrifugation. Then, the resuspended liposomes were characterized in terms of their morphological and physical and chemical properties as shown in Table 6.3.

Table 6.2- Physicochemical characterization and incorporation efficiency (*IE*) of resuspended neutral and cationic liposomes and Quer_Lip, after SASD.

	Size [nm]	PdI	ζ- potential [mV]	η_{Lipid} [%]	η_{Quer} [%]	*IE* [%]
Neutral liposomes	121 ± 2	0.229 ± 0.009	- 0.8 ± 0.3	55 ± 10	-	-
Neutral Quer_Lip	143 ± 3	0.378 ± 0.008	0.6 ± 0.4	67 ± 1	44 ± 1	66 ± 3
Cationic liposomes	260 ± 2	0.412 ± 0.006	10.6 ± 0.2	82 ± 7	-	-
Cationic Quer_Lip	316 ± 29	0.428 ± 0.013	9 ± 1	100 ± 5	59 ± 4	57 ± 10

The results are expressed as mean ± S.D (n = 3).

Neutral liposomes showed a smaller size than before supercritical processing. Similar results were observed in a previous work [167]. According to the water replacement theory, during drying water molecules are replaced by carbohydrates which establish hydrogen bonding with the phospholipids' polar head [24]. Leucine also plays an important role on the maintenance of the liposomes' size. It is expectable an electrostatic interaction between the carboxyl group of the Leu and the E-PC amine group which contribute for a liposomal stabilization [356]. Moreover, studies of Pal *et al.* [364] showed that an increase of ethanol concentration contributes for liposomes shrinking, due to a reduction in the bending modulus of lipid membranes. However, the polydisperse index increased from 0.098 ± 0.016 to 0.229 ± 0.009, suggesting an increase in the size heterogeneity from liposomes rearrangement, during the processing. A similar result was observed for neutral Quer_Lip. Nonetheless, an increase in their size was observed. This might be related to the quercetin presence in the lipidic bilayer, since its addition in lipidic bilayers contributes to larger distances between the lipid molecules [412]. Studies

from Movileanu *et al.* [413] showed that quercetin molecules penetrate the lipid bilayer by intercalating between the flexible acyl chains of the phospholipids. Therefore, $scCO_2$ diffusion might increase during the drying process leading to an increase in polydispersity index and liposomes' rearrangement.

Regarding the cationic liposomes, it was observed that the SA insertion in the lipidic bilayer led to a higher increase in terms of size and PdI compared to neutral liposomes. Toopkanloo *et al.* [414] suggested that highly lipophilic agents induced structural changes in liposomes' membrane and vesicle stability, changing the fluidity and packing density of the polar-nonpolar interface of the phospholipid head group area at the surface of the liposomes, like the cholesterol effect. Therefore, under thermal and shear stress, it is expectable an increase of their size. Regarding quercetin's *IE*, similar values were obtained for both formulations. The decrease in incorporation efficiency might be related to the thermal and air-interface-related stresses. The shear rate imposed on liposomes resulted in the unfolding and exposing of the hydrophobic bilayer [415]. Thermodynamic studies of the solubility of quercetin in CO_2 + ethanol system from Chafer and co-workers [416] have shown that solvating power of CO_2 becomes greater, and more solute is transferred to the supercritical phase, with increasing pressure. Thereby, it is suggested that quercetin is being dragged with CO_2. Studies with quercetin/trehalose/leucine system (without liposomes) were performed. We observed that only 25 ± 3 % of quercetin remained in the final powders, suggesting that CO_2 dragged quercetin.

The ζ- potential of resuspended liposomes decreased to 9 ± 1 mV. Liposomal cationic surface contributes to a better interaction with the cells' negative surface. A higher interaction promotes endocytosis and quercetin diffusion through the liposome's bilayer to cells. Besides, higher liposomal sizes increase surface area contact with cells, with a consequent increase of delivered quercetin. Even so, an additional experiment where the leucine percentage was increased to 15 % and ethanol to 30 % was performed, to understand if this increase in the size of the resuspended liposomes would decrease and the incorporation efficiency would be higher than 58 %. In fact, cationic Quer_Lips decrease their size to 225 ± 27, whereas PdI was 0.426 ± 0.029. However, the *IE* decrease to 32 ± 8 %.

Aerodynamic, and morphological characterization of cationic liposomal dry powder formulations were then performed. Table 6.4 shows the values obtained for Quer_Lip-DPFs and Lip-DPFs with cationic liposomal surface charge.

Table 6.3- Aerodynamic and chemical characterization of Lip-DPFs and Quer_Lip-DPFs.

	MMAD [µm]	GSD	FPF [%]	*ED [%]*	*Residual ethanol [ppm]*
Lip-DPFs	1.7 ± 0.1	2.3 ± 0.1	59 ± 7	96 ± 2	< 5000
Quer_Lip-DPFs	1.7 ± 0.1	2.2 ± 0.1	63 ± 4	98 ± 1	< 5000

The results are expressed as mean ± S.D (n = 3).

Quercetin-loaded liposomal dry powder formulations showed an MMAD between of 1.68 µm and a fine particle fraction of 63 %, which enables them to reach the respiratory region, being deposited in the alveolar airspaces. SEM images (Figure 6.1) corroborate these observations. Figure 6.1A shows Lip-DPFs bigger than Quer_Lip-DPFs (Figure 6.1B).

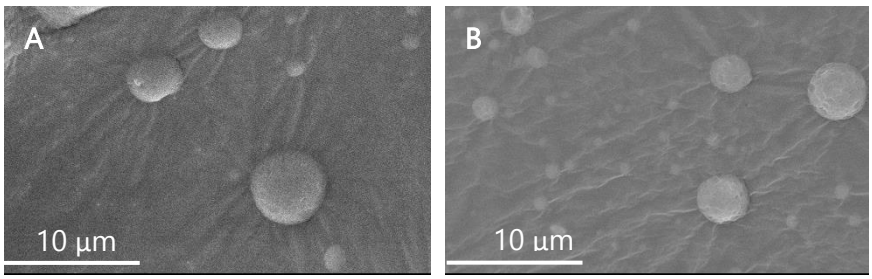

Figure 6.1- SEM images of (A) Lip-DPFs and (B) Quer_Lip-DPFs (scale bar: 10 µm; magnitude: 3000 x; high-voltage: 15 kV).

According to the aerodynamic studies, 57 ± 2 mg of powder reaches the respiratory tract, which results in 5.2 ± 0.4 µg of delivered quercetin from liposomes. Once classified by the BCS as a class IV drug, higher amounts of quercetin in its free form are required for an efficient treatment. Work from Mamani-Matsuda *et al.* [417] reports that five oral administrations of quercetin with a dose of 160 mg/kg to arthritic rats resulted in an anti-arthritic effect compared to untreated control. Similar results were obtained for those treated with five cycles of 60 mg/kg administered by the intra-peritoneal route. However, studies from Priprem and co-workers [418] showed that when incorporated in liposomes and administrated by the intranasal route, the administration of quercetin for anti-inflammatory purposes decrease drastically. Their study compared the oral intake of 300 mg/kg/day of free quercetin in rats with the in-tranasal administration of 20 µg/day of quercetin-loaded liposomes. The results showed that

a lower dose and a faster rate of anxiolytic effects were observed for liposomes administrated via intranasal route over oral administration. To understand if the delivered dose has a potential therapeutic effect, *in vitro* cell viability assays and antioxidant activity studies of quercetin from Quer_Lip- DPFs, will be performed in the future.

6.5 Conclusions

This work is a proof-of-concept that highlights the potential of supercritical CO_2-assisted spray-drying to convert liposomal suspensions loaded with hydrophobic compounds, converting them into liposomal dry powder formulations. The major challenge of this study was to keep the liposomes' structure and the incorporation efficiency over 80 %, after the drying process. Different compositions of liposomes membrane, as well as different molar ratios of lipid/quercetin, were also studied considering the increase of the incorporation efficiency. Studies with quercetin-loaded cationic liposomes were performed, considering the cellular interaction and better incorporation efficiency among others. Thermal and air-interface-related stresses during the SASD, might result in the unfolding and exposing of the hydrophobic bilayer. Moreover, it is suggested that CO_2 dragged quercetin during the process. Notwithstanding, *IE* of 57 ± 10 % (n=3) was obtained. The incorporated quercetin along with the aerodynamic performance of the dry powders shows that Quer_Lip-DPFs present aerodynamic properties required for effective pulmonary liposomal delivery of the drug. For a better understanding related to toxicity and quercetin's antioxidant activity after SASD and from powders, *in vitro* cellular assays will be performed in the future. Moreover, future research to obtain a deep knowledge of how quercetin interacts with lipids under supercritical conditions will be crucial to optimize the obtained results.

7

Conclusion and future perspectives

7.1 Final overview

At the beginning of this dissertation, the major aims were pointed out towards the development of a green integrated manufacturing process to produce liposomal dry powder formulations (Lip-DPFs) for encapsulation of high-and-low molecular weight anti-inflammatory drugs for the treatment of lung inflammatory diseases. It was proposed to produce solid dosage forms of SOD and quercetin using green methodologies, combining microfluidics coupled to supercritical CO_2-assisted spray-drying (SASD) continuous production, with optimized process parameters using the quality-by-design approach. In this way, at the end of Chapter 1, several questions related to this work were proposed as follows: ´

1. Is it possible to process a biopharmaceutical using microfluidics, while the conformational structure and enzymatic activity are preserved?
2. Is it possible to obtain empty Lip-DPFs using SASD? Does their structure remain? What are the variables that must be considered?
3. Can hydrophilic molecules with high and low molecular weight present similar encapsulation efficiency?
4. Can Lip-DPFs keep liposomes and hydrophilic molecules stable upon storage?
5. Is it possible to process liposomal dry powder formulations with hydrophilic and hydrophobic loaded molecules, while keeping their size, encapsulation/incorporation efficiency, and activity retention?

Throughout this doctoral dissertation, a synergy between pharmaceutical technology and chemical engineering was essential to achieve most of the established goals, answering all the questions that were settled. Thereby, the first question was addressed in *Chapter 3*, where proteins with different molecular weights were encapsulated into liposomes, using microfluidics. The first step was to assemble a glass-capillary microfluidic device and optimize microfluidic process parameters in terms of flow rate ratio, total flow rate, and lipid composition. The optimization was performed considering the desired liposomes' size and polydispersity index (PdI), and encapsulation efficiency (*EE*) of protein. For this reason, the first work was performed using insulin as a model protein. Thereby, insulin-loaded liposomes (InsLip) with an *EE* of 91 ± 4 % were obtained. Facing the potential application of the results, the studies were pursued, and nano-in-microparticles were produced for oral protein delivery. In this way, InsLip were coated with chitosan and then, through a microfluidic glass-capillary-based double-emulsion, coated by an enteric polymer to confer total protection from the harsh gastric conditions. Insulin

permeability and circular dichroism studies showed a strong improvement in insulin permeation across the intestinal epithelium without compromising its activity, respectively. Moreover, the low cytotoxicity of the nano-in-microparticles in the intestinal cells was observed. After obtaining interesting results with insulin, the studies were pursued considering Cu, Zn- superoxide dismutase (SOD), an enzyme weighing 32.5 kDa. Small adaptations in the microfluidic device were performed. SOD was efficiently encapsulated (59±6 %) in liposomes with preserved enzymatic activity (82 ± 3 %). *In vivo* experiments to test the anti-inflammatory properties of SOD_Lip showed the inhibition of 65 ± 8 % for animals treated with SOD_Lip administered i.v. The histopathological studies also showed the effectiveness of the administration of the SOD_Lip, compared to the SOD administered in its free form.

After successful SOD_Lip production using microfluidics, the work was conducted towards the supercritical CO_2-assisted spray-drying (SASD) optimization considering the liposomal structure maintenance during and after the process (*Chapter 4*), where the questions ii) to iv) were addressed. To monitor the dynamic behavior of the liposomes during drying, a model hydrophilic drug, 5(6)-carboxyfluorescein (CF), was used to mark their internal space. CF-loaded liposomal dry powder formulations CF_Lip-DPFs were produced using SASD. A quality-by-design approach followed by the design of experiments showed that leucine, ethanol, and their interactions have a significant impact not only on the morphological properties of the CF_Lip-DPFs but also on the liposomes structure and encapsulation efficiency of CF. It was observed that leucine had a more significant effect on liposome size, PdI, lipid yield, and powders' span. The SASD yield was shown to be significantly influenced by leucine and ethanol. From the combined analysis of the ANOVA results it was concluded that the liposome structure would be successfully retained with a casting solution composed of 10 % of leucine and 15 % of ethanol. Considering these observations, CF_Lip-DPFs suitable for inhalation were produced. Thus, after excipients removal, liposome structure was maintained as well as the dye encapsulation efficiency (*EE* > 95 %). Powders' stability studies showed that CF_Lip-DPFs maintained liposomes stability when stored at relative humidities of 4 % and 50 % at 20 ºC. The aerodynamic performance of the dry powders showed that CF_Lip-DPFs stored at relative humidities of 4 % and 50 %, for 30 days, kept those aerodynamic properties required for effective pulmonary liposomal delivery.

In *Chapter 5*, in which questions iii) to v) were addressed, it was hypothesized that the same optimized percentages of trehalose and leucine could produce SOD-loaded liposomal dry powder formulations (SOD_Lip-DPFs). Thereby, considering the optimized percentages, SOD was encapsulated into PEGylated liposomes and successfully dried in SASD (*EE* > 95 %). After resuspension, reconstituted liposomes from dry powder formulations were revealed to have maintained both their structure and integrity, while preserving the enzymatic activity (80-100 %). Aerodynamic characterizations of SOD_Lip-DPFs showed an MMAD of 1.6 ± 0.4 μm and an FPF of 65 ± 5 %, indicating that particles can achieve deposition in the lower respiratory tract, reaching stage 5 which represents the terminal bronchi. Finally, storage stability assays were conducted at a relative humidity of 40 %, for 50 days. SOD_Lip-DPFs have shown to be effective in maintaining both liposomal and enzyme stability. However, the MMAD increased from 1.6 ± 0.4 μm to 4 ± 1 μm and FPF fell from 65 ± 5 % to 28 ± 5 %. From the work developed in *Chapters 4 and 5*, it was possible to confirm that independent of the molecular weight of the encapsulated molecule, its encapsulation efficiency will be kept. The works suggested that the drying process and the casting solution composition might be the key critical process parameters to control the final liposome structure.

Finally, the outputs from the *Chapter 4* were considered and in *Chapter 6* quercetin-loaded liposomal dry powder formulations (Quer_Lip-DPFs) were produced. Quercetin is a flavonoid and is classified as a class IV drug in the BC system. The major challenge of this study was to keep the liposomes' structure and the incorporation efficiency over 80 %, after the drying process. For this, different compositions of liposome membranes (anionic and neutral lipids and stearylamine) and the ratio quercetin/lipid were studied considering the increase of the incorporation efficiency (*IE*). Prelaminar studies showed that liposomes with stearylamine (positively charged liposomes) showed higher *IE* (*IE* of 69 % over 32 % of neutral and 13 % of anionic liposomes). Besides, a cationic surface might promote better interaction with cells. Quer_Lip-DPFs with an *IE* of 57 ± 10 % (*n*=3) were obtained. Yet, after resuspension, reconstituted liposomes showed an increase in size from 153 ± 10 nm to 316 ± 29 nm, suggesting a change in the fluidity and packing density at the surface of the liposomes. Finally, Quer_Lip-DPFs showed an MMAD between 1.7 ± 0.1 μm and an FPF of 63 ± 4 % %, presenting aerodynamic properties required for effective pulmonary liposomal delivery of the drug.

Ultimately, the investigation conducted in this thesis and the findings that resulted from it enabled the successful development of potential liposomal dry powder formulations using SASD, for lung delivery. Here, different challenges were surpassed resulting in the achievement of the established goals and bringing new insights for the use of pulmonary delivery in chronic inflammatory situations.

7.2 Future perspectives

A Ph.D. work is a world full of possibilities and this one is not an exception. Although the main questions were answered, several side questions were raised. This is why science is so beautiful and exciting. Thereby, forthcoming works that can arise from this thesis and be implemented in a near future include:

1. Integration of microfluidics and SASD would result in a continuous process to manufacture liposomal dry powder formulations (in fact this was what motivated this work).
2. Study of different amino acids not only as dispersibility enhancers but also as a liposomal stabilizing agent.
3. A deeper understanding of how biopharmaceuticals interact with polar heads of liposomes, using characterization techniques like NMR.
4. In vitro cellular assays with 3D human tissue model of lung inflammation to study the cytotoxicity of the Quer_Lip and Quer_Lip-DPFs and the quercetin's antioxidant activity.
5. Computational modeling approaches to study the interaction of hydrophobic molecules and lipidic bilayer under supercritical conditions.

8 REFERENCES

[1] H. Suer, H. Bayram, Liposomes as potential nanocarriers for theranostic applications in chronic inflammatory lung diseases, Biomed Biotechnol Res J. 1 (2017) 1-8. https://doi.org/10.4103/bbrj.bbrj_54_17.

[2] B. Patel, R. Priefer, Impact of chronic obstructive pulmonary disease, lung infection, and/or inhaled corticosteroids use on potential risk of lung cancer, Life Sci. 294 (2022) 120374. https://doi.org/10.1016/j.lfs.2022.120374.

[3] Chronic obstructive pulmonary disease (COPD), (2022). https://www.who.int/news-room/fact-sheets/detail/chronic-obstructive-pulmonary-disease-(copd) (accessed October 6, 2022).

[4] K. Mattishent, M. Thavarajah, P. Blanco, D. Gilbert, A.M. Wilson, Y.K. Loke, Meta-Review: Adverse Effects of Inhaled Corticosteroids Relevant to Older Patients, Drugs. 74 (2014) 539–547. https://doi.org/10.1007/s40265-014-0202-z.

[5] A. Agusti, L.M. Fabbri, D. Singh, J. Vestbo, B. Celli, F.M.E. Franssen, K.F. Rabe, A. Papi, Inhaled corticosteroids in COPD: friend or foe?, Eur Respir J. 52 (2018) 1801219. https://doi.org/10.1183/13993003.01219-2018.

[6] S. Pascoe, N. Barnes, G. Brusselle, C. Compton, G.J. Criner, M.T. Dransfield, D.M.G. Halpin, M.K. Han, B. Hartley, P. Lange, S. Lettis, D.A. Lipson, D.A. Lomas, F.J. Martinez, A. Papi, N. Roche, R.J.P. van der Valk, R. Wise, D. Singh, Blood eosinophils and treatment response with triple and dual combination therapy in chronic obstructive pulmonary disease: analysis of the IMPACT trial, Lancet Respir. Med. 7 (2019) 745–756. https://doi.org/10.1016/S2213-2600(19)30190-0.

[7] B. Salehi, L. Machin, L. Monzote, J. Sharifi-Rad, S.M. Ezzat, M.A. Salem, R.M. Merghany, N.M. El Mahdy, C.S. Kılıç, O. Sytar, M. Sharifi-Rad, F. Sharopov, N. Martins, M. Martorell, W.C. Cho, Therapeutic Potential of Quercetin: New Insights and Perspectives for Human Health, ACS Omega. 5 (2020) 11849–11872. https://doi.org/10.1021/acsomega.0c01818.

[8] M.L. Corvo, H.S. Marinho, M.B.F. Martins, Nanomedicine as a strategy for the therapeutic use of Superoxide Dismutases, in: N.H. Philips (Ed.), Superoxide Dismutase (SOD): Sources, Therapeutic Uses and Health Benefits, Nova Science Publishers, 2016: p. 135-170.

[9] M.E.M. Cruz, M.M. Gaspar, M.B.F. Martins, M.L. Corvo, Liposomal superoxide dismutases and their use in the treatment of experimental arthritis, Meth. Enzymol. 391 (2005) 395–413. https://doi.org/10.1016/S0076-6879(05)91022-7.

[10] C.-E. Chang, C.-M. Hsieh, S.-C. Huang, C.-Y. Su, M.-T. Sheu, H.-O. Ho, Lecithin-Stabilized Polymeric Micelles (LsbPMs) for Delivering Quercetin: Pharmacokinetic Studies and Therapeutic Effects of Quercetin Alone and in Combination with Doxorubicin, Sci Rep. 8 (2018) 17640. https://doi.org/10.1038/s41598-018-36162-0.

[11] M.L. Corvo, O.C. Boerman, W.J.G. Oyen, L. Van Bloois, M.E.M. Cruz, D.J.A. Crommelin, G. Storm, Intravenous administration of superoxide dismutase entrapped in long circulating liposomesII. In vivo fate in a rat model of adjuvant arthritis, Biochim Biophys Acta - Biomembranes. 1419 (1999) 325–334. https://doi.org/10.1016/S0005-2736(99)00081-4.

[12] M.L. Corvo, M.B. Martins, A.P. Francisco, J.G. Morais, M.E.M. Cruz, Liposomal formulations of Cu,Zn-superoxide dismutase: Physicochemical characterization and activity assessment in an inflammation model, J. Control. Release. 43 (1997) 1–8. https://doi.org/10.1016/S0168-3659(96)01473-3.

[13] R.M. Lopes, M.L. Corvo, C.V. Eleutério, M.C. Carvalheiro, E. Scoulica, M.E.M. Cruz, Formulation of oryzalin (ORZ) liposomes: In vitro studies and in vivo fate, Eur J Pharm Biopharm. 82 (2012) 281–290. https://doi.org/10.1016/j.ejpb.2012.06.013.

[14] G. Gregoriadis, Drug entrapment in liposomes, FEBS Letters. 36 (1973) 292–296. https://doi.org/10.1016/0014-5793(73)80394-1.

[15] A.D. Bangham, M.M. Standish, J.C. Watkins, Diffusion of univalent ions across the lamellae of swollen phospholipids, J. Mol. Biol. 13 (1965) 238-IN27. https://doi.org/10.1016/S0022-2836(65)80093-6.

[16] P. Trucillo, R. Campardelli, E. Reverchon, Supercritical CO_2 assisted liposomes formation: Optimization of the lipidic layer for an efficient hydrophilic drug loading, J. CO_2 Util.18 (2017) 181–188. https://doi.org/10.1016/j.jcou.2017.02.001.

[17] G. Gregoriadis, Liposomes in Drug Delivery: Present and Future, Liposome Dermatics. 45 (1992) 346–352. https://doi.org/10.1007/978-3-642-48391-2_37.

[18] Liposome Drug Delivery Market, (2020). https://www.transparencymarketresearch.com/liposome-drug-delivery-market.html (accessed January 30, 2023).

[19] M. Sedighi, S. Sieber, F. Rahimi, M.-A. Shahbazi, A.H. Rezayan, J. Huwyler, D. Witzigmann, Rapid optimization of liposome characteristics using a combined microfluidics and design-of-experiment approach, Drug Deliv. and Transl. Res. 9 (2019) 404–413. https://doi.org/10.1007/s13346-018-0587-4.

[20] W. Li, L. Zhang, X. Ge, B. Xu, W. Zhang, L. Qu, C.H. Choi, J. Xu, A. Zhang, H. Lee, D.A. Weitz, Microfluidic fabrication of microparticles for biomedical applications, Chem Soc Rev. 47 (2018) 5646–5683. https://doi.org/10.1039/c7cs00263g.

[21] D. Liu, S. Cito, Y. Zhang, C.F. Wang, T.M. Sikanen, H.A. Santos, A versatile and robust microfluidic platform toward high throughput synthesis of homogeneous nanoparticles with tunable properties, Adv Mater. 27 (2015) 2298–2304. https://doi.org/10.1002/adma.201405408.

[22] Microfluidics Market Growth Drivers & Opportunities, MarketsandMarkets. (2021). https://www.marketsandmarkets.com/Market-Reports/microfluidics-market-1305.html (accessed January 30, 2023).

[23] A. Misra, K. Jinturkar, D. Patel, J. Lalani, M. Chougule, Recent advances in liposomal dry powder formulations: preparation and evaluation, Expert Opin Drug Deliv. 6 (2009) 71–89. https://doi.org/10.1517/17425240802652309.

[24] P.T. Ingvarsson, M. Yang, H.M. Nielsen, J. Rantanen, C. Foged, Stabilization of liposomes during drying, Expert Opin Drug Deliv. 8 (2011) 375–388. https://doi.org/10.1517/17425247.2011.553219.

[25] C. Moura, T. Casimiro, E. Costa, A. Aguiar-Ricardo, Optimization of supercritical CO_2-assisted spray drying technology for the production of inhalable composite particles using quality-by-design principles, Powder Technol. 357 (2019) 387–397. https://doi.org/10.1016/j.powtec.2019.08.090.

[26] D.A. Fernandes, P. Leandro, E. Costa, M.L. Corvo, Dry powder inhaler formulation of Cu,Zn-superoxide dismutase by spray drying: A proof-of-concept, Powder Technol. 389 (2021) 131–137. https://doi.org/10.1016/j.powtec.2021.05.008.

[27] A.S. Silva, M.T. Tavares, A. Aguiar-Ricardo, Sustainable strategies for nano-in-micro particle engineering for pulmonary delivery, J Nanopart Res. 16 (2014) 2602. https://doi.org/10.1007/s11051-014-2602-0.

[28] D. Lu, A.J. Hickey, Liposomal dry powders as aerosols for pulmonary delivery of proteins, AAPS PharmSciTech. 6 (2005) E641–E648. https://doi.org/10.1208/pt060480.

[29] M.E. Ali, A. Lamprecht, Spray freeze drying as an alternative technique for lyophilization of polymeric and lipid-based nanoparticles, Int. J. Pharm. 516 (2017) 170–177. https://doi.org/10.1016/j.ijpharm.2016.11.023.

[30] J.M. van den Hoven, J.M. Metselaar, G. Storm, J.H. Beijnen, B. Nuijen, Cyclodextrin as membrane protectant in spray-drying and freeze-drying of PEGylated liposomes, Int. J. Pharm. 438 (2012) 209–216. https://doi.org/10.1016/j.ijpharm.2012.08.046.

[31] C. Moura, T. Casimiro, E. Costa, A. Aguiar-Ricardo, Optimization of supercritical CO_2-assisted spray drying technology for the production of inhalable composite particles using quality-by-design principles, Powder Technol. 357 (2019) 387–397. https://doi.org/10.1016/j.powtec.2019.08.090.

[32] Food and Drug Administration, Metered Dose Inhaler (MDI) and Dry Powder Inhaler (DPI) Products - Quality Considerations Guidance for Industry, (2018).

[33] M. Tavares, R.P. Cabral, C. Costa, P. Martins, A.R. Fernandes, T. Casimiro, A. Aguiar-Ricardo, Development of PLGA dry powder microparticles by supercritical CO_2 -assisted spray-drying for potential vaccine delivery to the lungs, J Supercrit Fluids. 128 (2017) 235–243. https://doi.org/10.1016/j.supflu.2017.06.004.

[34] S. Ohtake, C. Schebor, J.J. de Pablo, Effects of trehalose on the phase behavior of DPPC–cholesterol unilamellar vesicles, Biochim Biophys Acta-Biomembranes. 1758 (2006) 65–73. https://doi.org/10.1016/j.bbamem.2006.01.002.

[35] J. Grossman, The Evolution of Inhaler Technology, J Asthma, 31 (1994) 55-64. https://doi.org/10.3109/02770909409056770.

[36] J.C. Sung, B.L. Pulliam, D.A. Edwards, Nanoparticles for drug delivery to the lungs, TRENDS in Biotechnol. 25 (2007) 563-57. https://doi.org/10.1016/j.tibtech.2007.09.005.

[37] G. Pilcer, K. Amighi, Formulation strategy and use of excipients in pulmonary drug delivery, Int. J. Pharm. 392 (2010) 1–19. https://doi.org/10.1016/j.ijpharm.2010.03.017.

[38] B. Pulliam, J.C. Sung, D.A Edwards, Design of nanoparticle-based dry powder pulmonary vaccines, Expert Opin. Drug Deliv. 4 (2007) 651-663. https://doi.org/10.1517/17425247.4.6.651

[39] E.W.X. Leong, R. Ge, Lipid Nanoparticles as Delivery Vehicles for Inhaled Therapeutics, Biomedicines. 10 (2022) 2179. https://doi.org/10.3390/biomedicines10092179.

[40] W. Tang, Y. Zhang, G. Zhu, Pulmonary delivery of mucosal nanovaccines, Nanoscale. 14 (2022) 263–276. https://doi.org/10.1039/D1NR06512B.

[41] A.R. Martin, W.H. Finlay, Nebulizers for drug delivery to the lungs, Expert Opin Drug Deliv. 12 (2015) 889–900. https://doi.org/10.1517/17425247.2015.995087.

[42] B. Aggarwal, J. Gogtay, Use of pressurized metered dose inhalers in patients with chronic obstructive pulmonary disease: review of evidence, Expert Rev. Respir. Med. 8 (2014) 349–356. https://doi.org/10.1586/17476348.2014.905916.

[43] H.-G. Lee, D.-W. Kim, C.-W. Park, Dry powder inhaler for pulmonary drug delivery: human respiratory system, approved products and therapeutic equivalence guideline, J. Pharm. Investig. 48 (2018) 603–616. https://doi.org/10.1007/s40005-017-0359-z.

[44] T. Iwanaga, The Respimat® Soft Mist Inhaler: Implications of Drug Delivery Characteristics for Patients, Clin Drug Investig. 9 (2019) 1021-1030. https://doi.org/ 10.1007/s40261-019-00835-z

[45] J.B. Fink, G.L. Colice, R. Hodder, Inhaler Devices for Patients with COPD, COPD: J. Chronic Obstr. Pulm. Dis 10 (2013) 523-535. https://doi.org/ 10.3109/15412555.2012.761960

[46] S. Stegemann, S. Kopp, G. Borchard, V.P. Shah, S. Senel, R. Dubey, N. Urbanetz, M. Cittero, A. Schoubben, C. Hippchen, D. Cade, A. Fuglsang, J. Morais, L Borgström, F. Farshi, K.H. Seyfang, R. Hermann, A. van de Putte, I. Klebovich, A. Hincal, Developing and advancing dry powder inhalation towards enhanced therapeutics, Eur J Pharm Sci. 48 (2013) 181-194. https://doi.org/10.1016/j.ejps.2012.10.021.

[47] C. Moura, Improved particle engineering and DPI formulation for optimal pulmonary delivery, Universidade Nova de Lisboa, 2017.

[48] Q. Liu, J. Guan, L. Qin, X. Zhang, S. Mao, Physicochemical properties affecting the fate of nanoparticles in pulmonary drug delivery, Drug Discov. 25 (2020) 150–159. https://doi.org/10.1016/j.drudis.2019.09.023.

[49] M. García-Díaz, D. Birch, F. Wan, H.M. Nielsen, The role of mucus as an invisible cloak to transepithelial drug delivery by nanoparticles, Adv. Drug Deliv. Rev. 124 (2018) 107–124. https://doi.org/10.1016/j.addr.2017.11.002.

[50] S.-H. Yu, F. Possmayer, Lipid compositional analysis of pulmonary surfactant monolayers and monolayer-associated reservoirs, J. Lipid Res. 44 (2003) 621–629. https://doi.org/10.1194/jlr.M200380-JLR200.

[51] W. Yang, J.I. Peters, R.O. Williams, Inhaled nanoparticles—A current review, Int. J. Pharm. 356 (2008) 239–247. https://doi.org/10.1016/j.ijpharm.2008.02.011.

[52] C. Darquenne, Deposition Mechanisms, J. Aerosol Med. Pulm. 33 (2020) 181–185. https://doi.org/10.1089/jamp.2020.29029.cd.

[53] M.J. Mitchell, M.M. Billingsley, R.M. Haley, M.E. Wechsler, N.A. Peppas, R. Langer, Engineering precision nanoparticles for drug delivery, Nat Rev Drug Discov. 20 (2021) 101–124. https://doi.org/10.1038/s41573-020-0090-8.

[54] A.H.L. Chow, H.H.Y. Tong, P. Chattopadhyay, B.Y. Shekunov, Particle engineering for pulmonary drug delivery, Pharm. Res. 24 (2007) 411–37. https://doi.org/10.1007/s11095-006-9174-3.

[55] M. Lau, P.M. Young, D. Traini, A review of co-milling techniques for the production of high dose dry powder inhaler formulation, Drug Dev. Ind. Pharm. 43 (2017) 1229–1238. https://doi.org/10.1080/03639045.2017.1313858.

[56] I.Y. Saleem, H.D.C. Smyth, Micronization of a Soft Material: Air-Jet and Micro-Ball Milling, AAPS PharmSciTech. 11 (2010) 1642–1649. https://doi.org/10.1208/s12249-010-9542-5.

[57] H. Al-Obaidi, A. Granger, T. Hibbard, S. Opesanwo, Pulmonary Drug Delivery of Antimicrobials and Anticancer Drugs Using Solid Dispersions, Pharmaceutics. 13 (2021) 1056. https://doi.org/10.3390/pharmaceutics13071056.

[58] A.D. Brunaugh, S.U. Jan, S. Ferrati, H.D.C. Smyth, Excipient-Free Pulmonary Delivery and Macrophage Targeting of Clofazimine via Air Jet Micronization, Mol. Pharm. 14 (2017) 4019–4031. https://doi.org/10.1021/acs.molpharmaceut.7b00690.

[59] T.R. Desai, R.E.W. Hancock, W.H. Finlay, Delivery of liposomes in dry powder form: aerodynamic dispersion properties, Eur J Pharm Sci. 20 (2003) 459–467. https://doi.org/10.1016/j.ejps.2003.09.008.

[60] M. Joshi, A.N. Misra, Pulmonary disposition of budesonide from liposomal dry powder inhaler, Methods Find Exp Clin Pharmacol. 23 (2001) 531–536. https://doi.org/10.1358/mf.2001.23.10.677118.

[61] H. Steckel, H.G. Brandes, A novel spray-drying technique to produce low density particles for pulmonary delivery, Int. J. Pharm. 278 (2004) 187–195. https://doi.org/10.1016/j.ijpharm.2004.03.010.

[62] X. Cai, Y. Yang, X. Xie, F. Yu, Y. Yang, Z. Yang, T. Zhang, X. Mei, Preparation, characterization, and pulmonary pharmacokinetics of a new inhalable zanamivir dry powder, Drug Deliv. 23 (2016) 1962–1971. https://doi.org/10.3109/10717544.2015.1037968.

[63] P.C. Seville, H. Li, T.P. Learoyd, Spray-Dried Powders for Pulmonary Drug Delivery, Crit. Rev. Ther. Drug Carr. 24 (2007) 307-360. https://doi.org/ 10.1615/CritRevTherDrugCarrierSyst.v24.i4.10

[64] D. Santos, A.C. Maurício, V. Sencadas, J.D. Santos, M.H. Fernandes, P.S. Gomes, Spray Drying: An Overview, in: R. Pignatello, T. Musumeci (Eds.), Biomaterials - Physics and Chemistry - New Edition, InTech, 2018. https://doi.org/10.5772/intechopen.72247.

[65] K. Cal, K. Sollohub, Spray Drying Technique. I: Hardware and Process Parameters, J. Pharm. Sci. 99 (2010) 575–586. https://doi.org/10.1002/jps.21886.

[66] R. Vehring, Pharmaceutical Particle Engineering via Spray Drying, Pharm Res. 25 (2008) 999–1022. https://doi.org/10.1007/s11095-007-9475-1.

[67] S. Pardeshi, P. Patil, R. Rajput, A. Mujumdar, J. Naik, Preparation and characterization of sustained release pirfenidone loaded microparticles for pulmonary drug delivery: Spray drying approach, Dry. Technol. 39 (2021) 337–347. https://doi.org/10.1080/07373937.2020.1833213.

[68] D. Charnvanich, N. Vardhanabhuti, P. Kulvanich, Effect of Cholesterol on the Properties of Spray-Dried Lysozyme-Loaded Liposomal Powders, AAPS PharmSciTech. 11 (2010) 832–842. https://doi.org/10.1208/s12249-010-9442-8.

[69] M.B. Chougule, B.K. Padhi, A. Misra, Nano-Liposomal Dry Powder Inhaler of Amiloride Hydrochloride, J Nanosci Nanotechnol. 6 (2006) 3001–3009. https://doi.org/10.1166/jnn.2006.405.

[70] M.B. Chougule, B.K. Padhi, A. Misra, Development of Spray Dried Liposomal Dry Powder Inhaler of Dapsone, AAPS PharmSciTech. 9 (2008) 47–53. https://doi.org/10.1208/s12249-007-9024-6.

[71] B.C. Huck, D. Thiyagarajan, A. Bali, A. Boese, K.F.W. Besecke, C. Hozsa, R.K. Gieseler, M. Furch, C. Carvalho-Wodarz, F. Waldow, D. Schwudke, O. Metelkina, A. Titz, H. Huwer, K. Schwarzkopf, J. Hoppstädter, A.K. Kiemer, M. Koch, B. Loretz, C.M. Lehr. Nano-in-Microparticles for Aerosol Delivery of Antibiotic-Loaded, Fucose-Derivatized, and Macrophage-Targeted Liposomes to Combat Mycobacterial Infections: In Vitro Deposition, Pulmonary Barrier Interactions, and Targeted Delivery. Adv Healthc Mater. 11 (2022) 2102117. https://doi.org/10.1002/adhm.202102117.

[72] L.G. Sweeney, Z. Wang, R. Loebenberg, J.P. Wong, C.F. Lange, W.H. Finlay, Spray-freeze-dried liposomal ciprofloxacin powder for inhaled aerosol drug delivery, Int. J. Pharm. 305 (2005) 180–185. https://doi.org/10.1016/j.ijpharm.2005.09.010.

[73] M.E. Ali, A. Lamprecht, Spray freeze drying for dry powder inhalation of nanoparticles, Eur J Pharm Biopharm. 87 (2014) 510–517. https://doi.org/10.1016/j.ejpb.2014.03.009.

[74] W. Liang, A.Y.L. Chan, M.Y.T. Chow, F.F.K. Lo, Y. Qiu, P.C.L. Kwok, J.K.W. Lam, Spray freeze drying of small nucleic acids as inhaled powder for pulmonary delivery, Asian J. Pharm. Sci. 13 (2018) 163–172. https://doi.org/10.1016/j.ajps.2017.10.002.

[75] R. Bi, W. Shao, Q. Wang, N. Zhang, Spray-freeze-dried dry powder inhalation of insulin-loaded liposomes for enhanced pulmonary delivery, J. Drug Target. 16 (2008) 639–648. https://doi.org/10.1080/10611860802201134.

[76] M.B. Adali, A.A. Barresi, G. Boccardo, R. Pisano, Spray Freeze-Drying as a Solution to Continuous Manufacturing of Pharmaceutical Products in Bulk, Processes. 8 (2020) 709. https://doi.org/10.3390/pr8060709.

[77] F. Zhang, X. Ma, X. Wu, Q. Xu, W. Tian, Z. Li, Inert particles as process aid in spray-freeze drying, Dry. Technol. 38 (2020) 71–79. https://doi.org/10.1080/07373937.2019.1623246.

[78] Hannay, J.B.; Hogarth, J., On the Solubility of Solids in Gases, Philos. Trans. Royal Soc. 29 (1879) 324–326. https://doi.org/10.1098/rspl.1879.0054.

[79] N. Jovanovic, A. Bouchard, G.W. Hofland, G.-J. Witkamp, D.J.A Crommelin, W. Jiskoot, Stabilization of proteins in dry powder formulations using supercritical fluid technology, Pharm Res. 21 (2004) 1955–1969. https://doi.org/10.1023/B:PHAM.0000048185.09483.e7

[80] M. Tavares, R.P. Cabral, C. Costa, P. Martins, A.R. Fernandes, T. Casimiro, A. Aguiar-Ricardo, Development of PLGA dry powder microparticles by supercritical CO_2-assisted spray-drying for potential vaccine delivery to the lungs, J Supercrit Fluids. 128 (2017) 235–243. https://doi.org/10.1016/j.supflu.2017.06.004.

[81] A. Aguiar-Ricardo, V.B.D. Bonifácio, T. Casimiro, V.G. Correia VG. Supercritical carbon dioxide design strategies: from drug carriers to soft killers. Phil. Trans. R. Soc. A 373 (2015) 20150009. http://dx.doi.org/10.1098/rsta.2015.0009

[82] A. Aguiar-Ricardo, Building dry powder formulations using supercritical CO_2 spray drying, Curr. Opin. Green Sustain. Chem. 5 (2017) 12–16. https://doi.org/10.1016/j.cogsc.2017.03.005.

[83] P. Anastas, N. Eghbali, Green Chemistry: Principles and Practice. Chem. Soc. Rev. 39 (2010) 301–312. https://doi.org/10.1039/B918763B

[84] G.D. Porta, C. De Vittori, E. Reverchon, Supercritical assisted atomization: A novel technology for microparticles preparation of an asthma-controlling drug, AAPS PharmSciTech. 6 (2005) E421–E428. https://doi.org/10.1208/pt060352.

[85] A.V.M. Nunes, C.M.M. Duarte, Dense CO_2 as a Solute, Co-Solute or Co-Solvent in Particle Formation Processes: A Review, Materials. 4 (2011) 2017–2041. https://doi.org/10.3390/ma4112017.

[86] Petersen, R.C.; Matson, D.W.; Smith, R.D. Rapid Precipitation of Low Vapor Pressure Solids from Supercritical Fluid Solutions: The Formation of Thin Films and Powders. J. Am. Chem. Soc. 108 (1986) 2100–2102. https://doi.org/10.1021/ja00268a066

[87] D.W. Matson, J.L. Fulton, R.C Petersen, R.D. Smith, Rapid Expansion of Supercritical Fluid Solutions: Solute Formation of Powders, Thin Films, and Fibers. Ind. Eng. Chem. Res. 26 (1987) 2298–2306. https://doi.org/10.1021/ie00071a021

[88] D.W. Matson, J.L. Fulton, R.C Petersen, R.D. Smith, Production of Powders and Films by the Rapid Expansion of Supercritical Solutions. J. Mater. Sci. 22 (1987) 1919–1928. https://doi.org/10.1007/BF01132917

[89] E. Reverchon, R. Adami, Rev Nanomaterials and Supercritical Fluids. J. Supercrit. Fluids 37 (2006) 1–22. https://doi.org/10.1016/j.supflu.2005.08.003

[90] A. Aguiar-Ricardo, E. Costa, Supercritical Fluid Manufacture, in: Pharmaceutical Inhalation Aerosol Technology, 3rd ed., CRC Press, 2019.

[91] R.B. Gupta, J.-J. Shim, Solubility in Supercritical Carbon Dioxide, 1st ed.; CRC Press: Boca Raton, USA, 2007; p. 1–18.

[92] E. Reverchon, G. Donsi, D. Gorgoglione, Salicylic Acid Solubilization in Supercritical CO_2 and Its Micronization by RESS, J Supercrit Fluids. 6 (1993) 241-248. https://doi.org/10.1016/0896-8446(93)90034-U

[93] N. Yildiz, S. Tuna, O. Döker, A. Çalimli, Micronization of Salicylic Acid and Taxol (Paclitaxel) by Rapid Expansion of Supercritical Fluids (RESS). J. Supercrit. Fluids 41 (2007) 440–451. https://doi.org/10.1016/j.supflu.2006.12.012

[94] C. Costa, T. Casimiro, A. Aguiar-Ricardo, Optimization of Supercritical CO_2-Assisted Atomization: Phase Behavior and Design of Experiments, J. Chem. Eng. Data. 63 (2018) 885–896. https://doi.org/10.1021/acs.jced.7b00820.

[95] K. Mishima, K. Matsuyama, D. Tanabe, S. Yamauchi, T.J. Young, K.P. Johnston, Microencapsulation of proteins by rapid expansion of supercritical solution with a nonsolvent, AIChE Journal. 46 (2000) 857–865. https://doi.org/10.1002/aic.690460418

[96] K. Matsuyama, K. Mishima, K.-I. Hayashi, H. Ishikawa, H. Matsuyama, T. Harada, Formation of microcapsules of medicines by the rapid expansion of a supercritical solution with a nonsolvent, J. Appl. Polym. Sci. 89 (2003) 742–752. https://doi.org/10.1002/app.12201

[97] P. Pathak, M.J. Meziani, T. Desai, Y.-P. Sun, Nanosizing Drug Particles in Supercritical Fluid Processing, J. Am. Chem. Soc. 126 (2004) 10842–10843. https://doi.org/10.1021/ja046914t

[98] S.T. Xiang, B.Q. Chen, R.K. Kankala, S.B. Wang, A.Z. Chen, Solubility Measurement and RESOLV-Assisted Nanonization of Gambogic Acid in Supercritical Carbon Dioxide for Cancer Therapy. J. Supercrit. Fluids 150 (2019) 147–155. https://doi.org/10.1016/j.supflu.2019.04.008

[99] E. Weidner, Ž. Knez, Z. Novak, Process for Preparing Particles or Powders. WO Patent 1995/021688, 1995.

[100] J. Kerc, S. Srcic, Ž. Knez, P. Sencar-Božic, Micronization of drugs using supercritical carbon dioxide, Int. J. Pharm. 182 (1999) 33–39. https://doi.org/10.1016/S0378-5173(99)00063-0.

[101] J. Hao, M.J. Whitaker, B. Wong, G. Serhatkulu, K.M. Shakesheff, S.M. Howdle, Plasticization and spraying of poly (DL-lactic acid) using supercritical carbon dioxide: control of particle size, J. Pharm. Sci. 93 (2004) 1083–1090. https://doi.org/10.1002/jps.20002.

[102] Y.-T. Shieh, J.-H. Su, G. Manivannan, P.H.C. Lee, S.P. Sawan, W.D. Spall, Interaction of supercritical carbon dioxide with polymers. I. Crystalline polymers, J. Appl. Polym. Sci. 59 (1996) 695–705. https://doi.org/10.1002/(SICI)1097-4628(19960124)59:4<695::AID-APP15>3.0.CO;2-P.

[103] D.R. Perinelli, G. Bonacucina, M. Cespi, A. Naylor, M. Whitaker, G.F. Palmieri, G. Giorgioni, L. Casettari, Evaluation of P(L)LA-PEG-P(L)LA as processing aid for biodegradable particles from gas saturated solutions (PGSS) process, Int. J. Pharm. 468 (2014) 250–257. https://doi.org/10.1016/j.ijpharm.2014.04.031.

[104] J. Hao, M. J. Whitaker, G. Serhatkulu, K. M. Shakesheff, S. M. Howdle, Supercritical fluid assisted melting of poly(ethylene glycol): a new solvent-free route to microparticles, J. Mater. Chem. 15 (2005) 1148. https://doi.org/10.1039/b411187g.

[105] F. Jordan, A. Naylor, C.A. Kelly, S.M. Howdle, A. Lewis, L. Illum, Sustained release hGH microsphere formulation produced by a novel supercritical fluid technology: In vivo studies, J. Control. Release. 141 (2010) 153–160. https://doi.org/10.1016/j.jconrel.2009.09.013.

[106] M. Rodrigues, N. Peiriço, H. Matos, E. Gomes de Azevedo, M.R. Lobato, A.J. Almeida, Microcomposites theophylline/hydrogenated palm oil from a PGSS process for controlled drug delivery systems, J Supercrit Fluids. 29 (2004) 175–184. https://doi.org/10.1016/S0896-8446(03)00034-2.

[107] S. Tokunaga, K. Ono, S. Ito, T. Sharmin, T. Kato, K. Irie, K. Mishima, T. Satho, T. Harada, T.M. Aida, K. Mishima, Microencapsulation of drug with enteric polymer Eudragit L100 for

controlled release using the particles from gas saturated solutions (PGSS) process, J Supercrit Fluids. 167 (2021) 105044. https://doi.org/10.1016/j.supflu.2020.105044.
[108] R.E. Sievers, U. Karst, Methods for Fine Particle Formation. US Patent 5639441, 1997.
[109] R.E. Sievers, Formation of Aqueous Small Droplet Aerosols Assisted by Supercritical Carbon Dioxide, Aerosol Sci Technol. 30 (1999) 3–15. https://doi.org/10.1080/713834046.
[110] C. Xu, B.A. Watkins, R.E. Sievers, X. Jing, P. Trowga, C.S. Gibbons, A. Vecht, Submicron-sized spherical yttrium oxide-based phosphors prepared by supercritical CO_2-assisted aerosolization and pyrolysis, Appl. Phys. Lett. 71 (1997) 1643–1645. https://doi.org/10.1063/1.120004.
[111] S.P. Sellers, G.S. Clark, R.E. Sievers, J.F. Carpenter, Dry powders of stable protein formulations from aqueous solutions prepared using supercritical CO_2-assisted aerosolization, J. Pharm. Sci. 90 (2001) 785–797. https://doi.org/10.1002/jps.1032.
[112] R.E. Sievers, B.P. Quinn, S.P. Cape, J.A. Searles, C.S. Braun, P. Bhagwat, L.G. Rebits, D.H. McAdams, J.L. Burger, J.A. Best, L. Lindsay, M.T. Hernandez, K.O. Kisich, T. Iacovangelo, D. Kristensen, D. Chen, Near-critical fluid micronization of stabilized vaccines, antibiotics and antivirals, J Supercrit Fluids. 42 (2007) 385–391. https://doi.org/10.1016/j.supflu.2007.03.001.
[113] K.O. Kisich, M.P. Higgins, I. Park, S.P. Cape, L. Lindsay, D.J. Bennett, S. Winston, J. Searles, R.E. Sievers, Dry powder measles vaccine: Particle deposition, virus replication, and immune response in cotton rats following inhalation, Vaccine. 29 (2011) 905–912. https://doi.org/10.1016/j.vaccine.2010.10.020.
[114] J.L. Burger, S.P. Cape, C.S. Braun, D.H. McAdams, J.A. Best, P. Bhagwat, P. Pathak, L.G. Rebits, R.E. Sievers, Stabilizing Formulations for Inhalable Powders of Live-Attenuated Measles Virus Vaccine, Journal of Aerosol Medicine and Pulmonary Drug Deliv. 21 (2008) 25–34. https://doi.org/10.1089/jamp.2007.0658.
[115] W.-H. Lin, D.E. Griffin, P.A. Rota, M. Papania, S.P. Cape, D. Bennett, B. Quinn, R.E. Sievers, C. Shermer, K. Powell, R.J. Adams, S. Godin, S. Winston, Successful respiratory immunization with dry powder live-attenuated measles virus vaccine in rhesus macaques, Proc. Natl. Acad. Sci. U. S. A. 108 (2011) 2987–2992. https://doi.org/10.1073/pnas.1017334108.
[116] J.R. Manion, S.P. Cape, D.H. McAdams, L.G. Rebits, R.E. Sievers, Inhalable Antibiotics Manufactured Through Use of Near-Critical or Supercritical Fluids, Aerosol Sci. Technol. 46 (2012) 403–410. https://doi.org/10.1080/02786826.2011.634453
[117] E. Reverchon, Process For The Production Of Micro And/Or Nano Particles, U.S. Patent 7276190, 2001.

[118] R. Adami, L.S. Osséo, E. Reverchon, Micronization of lysozyme by supercritical assisted atomization, Biotechnol. Bioeng. 104 (2009) 1162–1170. https://doi.org/10.1002/bit.22470.
[119] O. Adeoye, C. Costa, T. Casimiro, A. Aguiar-Ricardo, H. Cabral-Marques, Preparation of ibuprofen/hydroxypropyl-γ-cyclodextrin inclusion complexes using supercritical CO_2-assisted spray drying, J Supercrit Fluids. 133 (2018) 479–485. https://doi.org/10.1016/j.supflu.2017.11.009.
[120] E. Reverchon, Supercritical-Assisted Atomization To Produce Micro- and/or Nanoparticles of Controlled Size and Distribution, Ind. Eng. Chem. Res. 41 (2002) 2405–2411. https://doi.org/10.1021/ie010943k.
[121] E. Reverchon, G.D. Porta, A. Spada, Ampicillin micronization by supercritical assisted atomization, Journal of Pharmacy and Pharmacology. 55 (2003) 1465–1471. https://doi.org/10.1211/0022357022043.
[122] E. Reverchon, G. Della Porta, Micronization of antibiotics by supercritical assisted atomization, J Supercrit Fluids. 26 (2003) 243–252. https://doi.org/10.1016/S0896-8446(02)00162-6.
[123] E. Reverchon, A. Spada, Erythromycin micro-particles produced by supercritical fluid atomization, Powder Technol. 141 (2004) 100–108. https://doi.org/10.1016/j.powtec.2004.02.017.
[124] E. Reverchon, A. Antonacci, Chitosan Microparticles Production by Supercritical Fluid Processing, Ind. Eng. Chem. Res. 45 (2006) 5722–5728. https://doi.org/10.1021/ie060233k.
[125] E. Reverchon, A. Antonacci, Polymer microparticles production by supercritical assisted atomization, J Supercrit Fluids. 39 (2007) 444–452. https://doi.org/10.1016/j.supflu.2006.03.005.
[126] E. Reverchon, A. Antonacci, Drug–polymer microparticles produced by supercritical assisted atomization, Biotechnol. Bioeng. 97 (2007) 1626–1637. https://doi.org/10.1002/bit.21370.
[127] R.P. Cabral, A.M.L. Sousa, A.S. Silva, A.I. Paninho, M. Temtem, E. Costa, T. Casimiro, A. Aguiar-Ricardo, Design of experiments approach on the preparation of dry inhaler chitosan composite formulations by supercritical CO_2-assisted spray-drying, J Supercrit Fluids. 116 (2016) 26–35. https://doi.org/10.1016/j.supflu.2016.04.001.
[128] R.B. Restani, R.F. Pires, A. Tolmatcheva, R. Cabral, P.V. Baptista, A.R. Fernandes, T. Casimiro, V.D.B. Bonifácio, A. Aguiar-Ricardo, POxylated Dendrimer-Based Nano-in-Micro Dry Powder Formulations for Inhalation Chemotherapy, ChemistryOpen. 7 (2018) 772–779. https://doi.org/10.1002/open.201800093.

[129] A.S. Silva, A.M. Sousa, R.P. Cabral, M.C. Silva, C. Costa, S.P. Miguel, V.D.B. Bonifácio, T. Casimiro, I.J. Correia, A. Aguiar-Ricardo, Aerosolizable gold nano-in-micro dry powder formulations for theragnosis and lung delivery, Int. J. Pharm. 519 (2017) 240–249. https://doi.org/10.1016/j.ijpharm.2017.01.032.

[130] M. Silva, A. Silva, J. Fernandez-Lodeiro, T. Casimiro, C. Lodeiro, A. Aguiar-Ricardo, Supercritical CO_2-Assisted Spray Drying of Strawberry-Like Gold-Coated Magnetite Nanocomposites in Chitosan Powders for Inhalation, Materials. 10 (2017) 74. https://doi.org/10.3390/ma10010074.

[131] M.-Q. Cai, Y.-X. Guan, S.-J. Yao, Z.-Q. Zhu, Supercritical fluid assisted atomization introduced by hydrodynamic cavitation mixer (SAA-HCM) for micronization of levofloxacin hydrochloride, J Supercrit Fluids. 43 (2008) 524–534. https://doi.org/10.1016/j.supflu.2007.07.008.

[132] I.E. Santo, R. Campardelli, E.C. Albuquerque, S.V. de Melo, G. Della Porta, E. Reverchon, Liposomes preparation using a supercritical fluid assisted continuous process, J. Chem. Eng. 249 (2014) 153–159. https://doi.org/10.1016/j.cej.2014.03.099.

[133] R. Campardelli, I. Espirito Santo, E.C. Albuquerque, S.V. de Melo, G. Della Porta, E. Reverchon, Efficient encapsulation of proteins in submicro liposomes using a supercritical fluid assisted continuous process, J Supercrit Fluids. 107 (2016) 163–169. https://doi.org/10.1016/j.supflu.2015.09.007.

[134] P. Trucillo, R. Campardelli, E. Reverchon, A versatile supercritical assisted process for the one-shot production of liposomes, J Supercrit Fluids. 146 (2019) 136–143. https://doi.org/10.1016/j.supflu.2019.01.015.

[135] N. Ventosa, S. Sala, J. Veciana, J. Torres, J. Llibre, Depressurization of an Expanded Liquid Organic Solution (DELOS): A New Procedure for Obtaining Submicron- or Micron-Sized Crystalline Particles, Cryst. Growth Des. 1 (2001) 299–303. https://doi.org/10.1021/cg0155090.

[136] N. Ventosa, S. Sala, J. Veciana, DELOS Process: A Crystallization Technique Using Compressed Fluids-1. Comparison to the GAS Crystallization Method. J. Supercrit. Fluids 26 (2003) 33–45. https://doi.org/10.1016/S0896-8446(02)00189-4

[137] M. Muntó, N. Ventosa, S. Sala, J. Veciana, Solubility behaviors of ibuprofen and naproxen drugs in liquid "CO_2–organic solvent" mixtures, J Supercrit Fluids. 47 (2008) 147–153. https://doi.org/10.1016/j.supflu.2008.07.013.

[138] S. Sala, A. Córdoba, E. Moreno-Calvo, E. Elizondo, M. Muntó, P.E. Rojas, M.À. Larrayoz, N. Ventosa, J. Veciana, Crystallization of Microparticulate Pure Polymorphs of Active

Pharmaceutical Ingredients Using CO_2 -Expanded Solvents, Cryst. Growth Des. 12 (2012) 1717–1726. https://doi.org/10.1021/cg200356x.
[139] E. Elizondo, J. Larsen, N.S. Hatzakis, I. Cabrera, T. Bjørnholm, J. Veciana, D. Stamou, N. Ventosa, Influence of the Preparation Route on the Supramolecular Organization of Lipids in a Vesicular System, J. Am. Chem. Soc. 134 (2012) 1918–1921. https://doi.org/10.1021/ja2086678.
[140] E. Elizondo, J. Veciana, N. Ventosa, Nanostructuring molecular materials as particles and vesicles for drug delivery, using compressed and supercritical fluids, Nanomedicine. 7 (2012) 1391–1408. https://doi.org/10.2217/nnm.12.110.
[141] M. Cano-Sarabia, N. Ventosa, S. Sala, C. Patiño, R. Arranz, J. Veciana, Preparation of Uniform Rich Cholesterol Unilamellar Nanovesicles Using CO_2 -Expanded Solvents, Langmuir. 24 (2008) 2433–2437. https://doi.org/10.1021/la7032109.
[142] J. Merlo-Mas, J. Tomsen-Melero, J.-L. Corchero, E. González-Mira, A. Font, J.N. Pedersen, N. García-Aranda, E. Cristóbal-Lecina, M. Alcaina-Hernando, R. Mendoza, E. Garcia-Fruitós, T. Lizarraga, S. Resch, C. Schimpel, A. Falk, D. Pulido, M. Royo, S. Schwartz, I. Abasolo, J.S. Pedersen, D. Danino, A. Soldevila, J. Veciana, S. Sala, N. Ventosa, A. Córdoba, Application of Quality by Design to the robust preparation of a liposomal GLA formulation by DELOS-susp method, J Supercrit Fluids. 173 (2021) 105204. https://doi.org/10.1016/j.supflu.2021.105204.
[143] L. Ballell-Hosa, E. González-Mira, H. Santana, J. Morla-Folch, M. Moreno-Masip, Y. Martínez-Prieto, A. Revuelta, P.P. Di Mauro, J. Veciana, S. Sala, L. Ferrer-Tasies, N. Ventosa, DELOS Nanovesicles-Based Hydrogels: An Advanced Formulation for Topical Use, Pharmaceutics. 14 (2022) 199. https://doi.org/10.3390/pharmaceutics14010199.
[144] O.R. Davies, A.L. Lewis, M.J. Whitaker, H. Tai, K.M. Shakesheff, S.M. Howdle, Applications of supercritical CO2 in the fabrication of polymer systems for drug delivery and tissue engineering, Adv. Drug Deliv. Rev. 60 (2008) 373–387. https://doi.org/10.1016/j.addr.2006.12.001.
[145] M. Kalani, R. Yunus, Application of supercritical antisolvent method in drug encapsulation: a review, Int. J. Nanomed. 6 (2011) 1429–1442. https://doi.org/10.2147/IJN.S19021.
[146] N. Elvassore, A. Bertucco, P. Caliceti, Production of Protein-Loaded Polymeric Microcapsules by Compressed CO_2 in a Mixed Solvent, Ind. Eng. Chem. Res. 40 (2001) 795–800. https://doi.org/10.1021/ie0004904.
[147] P. Franco, I. De Marco, Supercritical Antisolvent Process for Pharmaceutical Applications: A Review, Processes. 8 (2020) 938. https://doi.org/10.3390/pr8080938.

[148] S.-D. Yeo, G.-B. Lim, P.G. Debendetti, H. Bernstein, Formation of microparticulate protein powder using a supercritical fluid antisolvent, Biotechnol. Bioeng. 41 (1993) 341–346. https://doi.org/10.1002/bit.260410308.

[149] S. Yeo, P.G. Debenedetti, S.Y. Patro, T.M. Przybycien, Secondary Structure Characterization of Microparticulate Insulin Powders†, J. Pharm. Sci. 83 (1994) 1651–1656. https://doi.org/10.1002/jps.2600831203.

[150] J. Bleich, P. Kleinebudde, B.W. Müller, Influence of gas density and pressure on microparticles produced with the ASES process, Int. J. Pharm. 106 (1994) 77–84. https://doi.org/10.1016/0378-5173(94)90278-X.

[151] S. Palakodaty, P.York, J. Pritchard, Supercritical fluid processing of materials from aqueous solutions: the application of SEDS to lactose as a model substance, Pharm. Res. 15 (1998) 1835–43. https://doi.org/10.1023/A:1011949805156

[152] F. Fusaro, J. Kluge, M. Mazzotti, G. Muhrer, Compressed CO_2 antisolvent precipitation of lysozyme, J Supercrit Fluids. 49 (2009) 79–92. https://doi.org/10.1016/j.supflu.2008.12.005.

[153] R.K. Kankala, Y.S. Zhang, S.-B. Wang, C.-H. Lee, A.-Z. Chen, Supercritical Fluid Technology: An Emphasis on Drug Delivery and Related Biomedical Applications, Adv. Healthcare Mater. 6 (2017) 1700433. https://doi.org/10.1002/adhm.201700433.

[154] J.C. Evans, B.D. Scherzer, C.D. Tocco, G.B. Kupperblatt, J.N. Becker, D.L. Wilson, S.A. Saghir, E.J. Elder, Preparation of nanostructured particles of poorly water-soluble drugs via a novel ultra-rapid freezing technology, in: Svenson, S. (Ed.), Polymeric Drug Delivery – Polymeric Matrices and Drug Particle Engineering, American Chemical Society, Washington, DC, 2006.

[155] S.G. Thakkar, T.B. Ruwona, R.O. Williams, Z. Cui, The immunogenicity of thin-film freeze-dried, aluminum salt-adjuvanted vaccine when exposed to different temperatures, Hum. Vaccines Immunother. 13 (2017) 936–946. https://doi.org/10.1080/21645515.2016.1259042.

[156] M. Zhang, H. Li, B. Lang, K. O'Donnell, H. Zhang, Z. Wang, Y. Dong, C. Wu, R.O. Williams, Formulation and delivery of improved amorphous fenofibrate solid dispersions prepared by thin film freezing, Eur J Pharm Biopharm. 82 (2012) 534–544. https://doi.org/10.1016/j.ejpb.2012.06.016.

[157] J.D. Engstrom, E.S. Lai, B.S. Ludher, B. Chen, T.E. Milner, R.O. Williams, G.B. Kitto, K.P. Johnston, Formation of Stable Submicron Protein Particles by Thin Film Freezing, Pharm Res. 25 (2008) 1334–1346. https://doi.org/10.1007/s11095-008-9540-4.

[158] X. Li, S.G. Thakkar, T.B. Ruwona, R.O. Williams, Z. Cui, A method of lyophilizing vaccines containing aluminum salts into a dry powder without causing particle aggregation or

decreasing the immunogenicity following reconstitution, J. Control. Release. 204 (2015) 38–50. https://doi.org/10.1016/j.jconrel.2015.02.035.

[159] K. AboulFotouh, H. Xu, C. Moon, R.O. Williams, Z. Cui, Development of (Inhalable) Dry Powder Formulations of AS01B-Containing Vaccines Using Thin-Film Freeze-Drying, Int. J. Pharm. 622 (2022) 121825. https://doi.org/10.1016/j.ijpharm.2022.121825.

[160] N. Shetty, D. Cipolla, H. Park, Q.T. Zhou, Physical stability of dry powder inhaler formulations, Expert Opin Drug Deliv. 17 (2020) 77–96. https://doi.org/10.1080/17425247.2020.1702643.

[161] L. Chen, T. Okuda, X.-Y. Lu, H.-K. Chan, Amorphous powders for inhalation drug delivery, Adv. Drug Deliv. Rev. 100 (2016) 102–115. https://doi.org/10.1016/j.addr.2016.01.002.

[162] R. Heida, W.L. Hinrichs, H.W. Frijlink, Inhaled vaccine delivery in the combat against respiratory viruses: a 2021 overview of recent developments and implications for COVID-19, Expert Rev. Vaccines 21 (2022) 957–974. https://doi.org/10.1080/14760584.2021.1903878.

[163] Y. He, Y. Liang, R. Han, W.-L. Lu, J.C.W. Mak, Y. Zheng, Rational particle design to overcome pulmonary barriers for obstructive lung diseases therapy, J. Control. Release. 314 (2019) 48–61. https://doi.org/10.1016/j.jconrel.2019.10.035.

[164] D. Zillen, M. Beugeling, W.L.J. Hinrichs, H.W. Frijlink, F. Grasmeijer, Natural and bioinspired excipients for dry powder inhalation formulations, COCIS. 56 (2021) 101497. https://doi.org/10.1016/j.cocis.2021.101497.

[165] C. Costa, T. Casimiro, M.L. Corvo, A. Aguiar-Ricardo, Solid Dosage Forms of Biopharmaceuticals in Drug Delivery Systems Using Sustainable Strategies, Molecules. 26 (2021) 7653. https://doi.org/10.3390/molecules26247653.

[166] C.J. Bailey, A.H. Barnett, Why is Exubera being withdrawn?, BMJ. 335 (2007) 1156–1156. https://doi.org/10.1136/bmj.39409.507662.94.

[167] C. Costa, B. Nobre, A.S. Matos, A.S. Silva, T. Casimiro, M.L. Corvo, A. Aguiar-Ricardo, Inhalable hydrophilic molecule-loaded liposomal dry powder formulations using supercritical CO_2 – assisted spray-drying, J. CO_2 Util. 53 (2021) 101709. https://doi.org/10.1016/j.jcou.2021.101709.

[168] C.A. Hobbs, K. Saigo, M. Koyanagi, S. Hayashi, Magnesium stearate, a widely-used food additive, exhibits a lack of in vitro and in vivo genotoxic potential, Toxicol. Rep. 4 (2017) 554–559. https://doi.org/10.1016/j.toxrep.2017.10.003.

[169] J. Weers, T. Tarara, The PulmoSphere™ platform for pulmonary drug delivery, Ther. Deliv. 5 (2014) 277–295. https://doi.org/10.4155/tde.14.3.

[170] Y. Wu, Y. Xiong, L. Wang, Q. Zhou, L. Li, P.A. Levkin, G. Davidson, L. Gao, W. Deng, Development of new self-assembled cationic amino liposomes for efficient gene delivery, Biomater. Sci. 8 (2020) 3021–3025. https://doi.org/10.1039/d0bm00331j.

[171] A.D. Bangham, M.M. Standish, J.C. Watkins, Diffusion of univalent ions across the lamellae of swollen phospholipids, J. Mol. Biol. 13 (1965) 238–252. https://doi.org/10.1016/S0022-2836(65)80093-6.

[172] M. L. Corvo, J.C.S. Jorge, R. Van't Hof, M.E.M. Cruz, D.J.A. Crommelin, G. Storm, Superoxide dismutase entrapped in long-circulating liposomes: Formulation design and therapeutic activity in rat adjuvant arthritis, Biochim Biophys Acta. 1564 (2002) 227–236. https://doi.org/10.1016/S0005-2736(02)00457-1.

[173] I. Takeuchi, N. Kishi, K. Shiokawa, H. Uchiro, K. Makino, Polyborane encapsulated liposomes prepared using pH gradient and reverse-phase evaporation for boron neutron capture therapy : biodistribution in tumor-bearing mice, Colloid Polym Sci. 296 (2018) 1137–1144. https://doi.org/10.1007/s00396-018-4331-x

[174] D. Szoka, F.; Olson, F.; Heath, T.; Vail, W.; Mayhew, E.; Papahadjopoulos, Preparation of unilamellar liposomes of intermediate size (0.1-0.2 μm) by a combination of reverse phase evaporation and extrusion through polycarbonate membranes, Biochim Biophys Acta. 601 (1980) 559–571. https://doi.org/10.1016/0005-2736(80)90558-1

[175] C. Charcosset, A. Juban, J.P. Valour, S. Urbaniak, H. Fessi, Preparation of liposomes at large scale using the ethanol injection method: Effect of scale-up and injection devices, Chem Eng Res Des. 94 (2015) 508–515. https://doi.org/10.1016/j.cherd.2014.09.008.

[176] G.T. Vladisavljevic, A. Laouini, C. Charcosset, H. Fessi, H.C.H. Bandulasena, R.G. Holdich, Production of liposomes using microengineered membrane and co-flow microfluidic device, Colloids Surf. A Physicochem. Eng. 458 (2014) 168–177. https://doi.org/10.1016/j.colsurfa.2014.03.016.

[177] S. Joshi, M.T. Hussain, C.B. Roces, G. Anderluzzi, E. Kastner, S. Salmaso, D.J. Kirby, Y. Perrie, Microfluidics based manufacture of liposomes simultaneously entrapping hydrophilic and lipophilic drugs, Int. J. Pharm. 514 (2016) 160–168. https://doi.org/10.1016/j.ijpharm.2016.09.027.

[178] L. Maja, K. Željko, P. Mateja, Sustainable technologies for liposome preparation, J Supercrit Fluids. 165 (2020) 104984. https://doi.org/10.1016/j.supflu.2020.104984.

[179] P. Trucillo, R. Campardelli, E. Reverchon, A versatile supercritical assisted process for the one-shot production of liposomes, J Supercrit Fluids. 146 (2019) 136–143. https://doi.org/10.1016/j.supflu.2019.01.015.

[180] Y. Özer, H. Talsma, D.J.A. Crommelin, A. Hincal, Influence of freezing and freeze-drying on the stability of liposomes dispersed in aqueous media. Acta Pharm.Technol., 34 (1988) 129–139.

[181] M. Grit, D.J.A. Crommelin, Chemical stability of liposomes: implications for their physical stability, Chem Phys Lipids. 64 (1993) 3–18. https://doi.org/10.1016/0009-3084(93)90053-6

[182] F. Krammer, SARS-CoV-2 vaccines in development, Nature. 586 (2020) 516–527. https://doi.org/10.1038/s41586-020-2798-3.

[183] E.M.G. Van Bommel, D.J.A. Crommelin, Stability of doxorubicin-liposomes on storage: as an aqueous dispersion, frozen or freeze-dried, Int. J. Pharm. 22 (1984) 299–310. https://doi.org/10.1016/0378-5173(84)90030-9.

[184] L.M. Crowe, J.H. Crowe, A. Rudolph, Preservation of freeze-dried liposomes by trehalose. Arch Biochem Biophys. 242 (1985) 240-247. https://doi.org/ 10.1016/0003-9861(85)90498-9

[185] A.F. Ourique, P. S. Chaves, G.D. Souto, A.R. Pohlmann, S.S. Guterres, R.C.R. Beck, Redispersible liposomal-N-acetylcysteine powder for pulmonary administration: Development, in vitro characterization and antioxidant activity, Eur J Pharm Sci . 65 (2014) 174–182. https://doi.org/10.1016/j.ejps.2014.09.017.

[186] P.T. Ingvarsson, M. Yang, H. Mulvad, H.M. Nielsen, J. Rantanen, C. Foged, Engineering of an inhalable dda/tdb liposomal adjuvant: A quality-by-design approach towards optimization of the spray drying process, Pharmaceutical Research. 30 (2013) 2772–2784. https://doi.org/10.1007/s11095-013-1096-2.

[187] P.T. Ingvarsson, M. Yang, H.Mø. Nielsen, J. Rantanen, C. Foged, Stabilization of liposomes during drying, Expert Opin Drug Deliv. 8 (2011) 375–388. https://doi.org/10.1517/17425247.2011.553219.

[188] J. Gómez-Estaca, A. Pérez-García, A. Alemán, M.C. Gómez-Guillén, P. Montero, Drying soy phosphatidylcholine liposomal suspensions in alginate matrix: Effect of drying methods on physico-chemical properties and stability, Food Hydrocoll. 111 (2021) 106357. https://doi.org/10.1016/j.foodhyd.2020.106357.

[189] J.-Y. Chun, F. C. Godoi, N. Bansal, M. Morand, B. Bhandari, Investigation of nanovesicle liposome powder production from soy lecithin by spray drying, Dry. Technol., 35 (2017) 1020-1028. https://doi.org/10.1080/07373937.2016.1229333

[190] X. Zhu, Y. Kong, Q. Liu, Y. Lu, H. Xing, X. Lu, Y. Yang, J. Xu, N. Li, D. Zhao, X. Chen, Y. Lu, Inhalable dry powder prepared from folic acid-conjugated docetaxel liposomes alters pharmacodynamic and pharmacokinetic properties relevant to lung cancer chemotherapy, Pulm. Pharmacol. 55 (2019) 50–61. https://doi.org/10.1016/j.pupt.2019.02.001.

[191] S. Kunastitchai, L. Pichert, N. Sarisuta, B.W. Müller, Application of aerosol solvent extraction system (ASES) process for preparation of liposomes in a dry and reconstitutable form, Int. J. Pharm. 316 (2006) 93–101. https://doi.org/10.1016/j.ijpharm.2006.02.051.

[192] G. Lévai, Á. Martín, A. Moro, A.A. Matias, V.S.S. Gonçalves, M.R. Bronze, C.M.M. Duarte, S. Rodríguez-Rojo, M.J. Cocero, Production of encapsulated quercetin particles using supercritical fluid technologies, Powder Technol. 317 (2017) 142–153. https://doi.org/10.1016/j.powtec.2017.04.041.

[193] J.H. Crowe, F.A. Hoekstra, K.H.N. Nguyen, L.M. Crowe, Is vitrification involved in depression of the phase transition temperature in dry phospholipids?, Biochim Biophys Acta. 1280 (1996) 187–196. https://doi.org/10.1016/0005-2736(95)00287-1.

[194] K.L. Koster, M.S. Webb, G. Bryant, D.V. Lynch, Interactions between soluble sugars and POPC (1-palmitoyl-2-oleoylphosphatidylcholine) during dehydration: vitrification of sugars alters the phase behavior of the phospholipid, Biochim Biophys Acta. 1193 (1994) 143–150. https://doi.org/10.1016/0005-2736(94)90343-3.

[195] G.F. Boafo, K.T. Magar, M.D. Ekpo, W. Qian, S. Tan, C. Chen, The Role of Cryoprotective Agents in Liposome Stabilization and Preservation, IJMS. 23 (2022) 12487. https://doi.org/10.3390/ijms232012487.

[196] L. Jorgensen, H.M. Nielson, Delivery Technologies for Biopharmaceuticals: Peptides, Proteins, Nucleic Acids and Vaccines, in: L. Jorgensen, H.M. Nielsen (Eds.), John Wiley & Sons, 2009.

[197] M. Joshi, A. Misra, Disposition kinetics of ketotifen from liposomal dry powder for inhalation in rat lung, Clin Exp Pharmacol Physiol. 30 (2003) 153–156. https://doi.org/10.1046/j.1440-1681.2003.03813.x.

[198] Y. Lo, J. Tsai, J. Kuo, Liposomes and disaccharides as carriers in spray-dried powder formulations of superoxide dismutase, J. Control. Release. 94 (2004) 259–272. https://doi.org/10.1016/j.jconrel.2003.09.019.

[199] M. Chougule, B. Padhi, A. Misra, Nano-liposomal dry powder inhaler of tacrolimus: Preparation, characterization, and pulmonary pharmacokinetics, Int J Nanomedicine. 2 (2007) 675-688. *Doi not found*

[200] J.M. Van Den Hoven, J.M. Metselaar, G. Storm, J.H. Beijnen, B. Nuijen, Cyclodextrin as membrane protectant in spray-drying and freeze-drying of PEGylated liposomes, Int. J. Pharm. 438 (2012) 209–216. https://doi.org/10.1016/j.ijpharm.2012.08.046.

[201] P.T. Ingvarsson, S.T. Schmidt, D. Christensen, N.B. Larsen, W.L.J. Hinrichs, P. Andersen, J. Rantanen, H.M. Nielsen, M. Yang, C. Foged, Designing CAF-adjuvanted dry powder vaccines: Spray drying preserves the adjuvant activity of CAF01, J. Control. Release. 167 (2013) 256–264. https://doi.org/10.1016/j.jconrel.2013.01.031.

[202] M. Gandhi, T. Pandya, R. Gandhi, S. Patel, R. Mashru, A. Misra, H. Tandel, Inhalable liposomal dry powder of gemcitabine-HCl: Formulation, in vitro characterization and in vivo studies, Int. J. Pharm. 496 (2015) 886–895. https://doi.org/10.1016/j.ijpharm.2015.10.020.

[203] T. Ye, J. Yu, Q. Luo, S. Wang, H.-K. Chan, Inhalable clarithromycin liposomal dry powders using ultrasonic spray freeze drying, Powder Technol. 305 (2017) 63–70. https://doi.org/10.1016/j.powtec.2016.09.053.

[204] T. Zhang, Y. Chen, Y. Ge, Y. Hu, M. Li, Y. Jin, Inhalation treatment of primary lung cancer using liposomal curcumin dry powder inhalers, Acta Pharm. Sin. B.8 (2018) 440–448. https://doi.org/10.1016/j.apsb.2018.03.004.

[205] S. Chennakesavulu, A. Mishra, A. Sudheer, C. Sowmya, C. Suryaprakash Reddy, E. Bhargav, Pulmonary delivery of liposomal dry powder inhaler formulation for effective treatment of idiopathic pulmonary fibrosis, AJPS. 13 (2018) 91–100. https://doi.org/10.1016/j.ajps.2017.08.005.

[206] J. Xu, X. Lu, X. Zhu, Y. Yang, Q. Liu, D. Zhao, Y. Lu, J. Wen, X. Chen, N. Li, Formulation and Characterization of Spray-Dried Powders Containing Vincristine-Liposomes for Pulmonary Delivery and Its Pharmacokinetic Evaluation From In Vitro and In Vivo, J. Pharm. Sci. 108 (2019) 3348–3358. https://doi.org/10.1016/j.xphs.2019.05.009.

[207] S. Honmane, A. Hajare, H. More, R.A.M. Osmani, S. Salunkhe, Lung delivery of nanoliposomal salbutamol sulfate dry powder inhalation for facilitated asthma therapy, J. Liposome Res. 29 (2019) 332–342. https://doi.org/10.1080/08982104.2018.1531022.

[208] I. Khatib, W.-R. Ke, D. Cipolla, H.-K. Chan, Storage stability of inhalable, controlled-release powder formulations of ciprofloxacin nanocrystal-containing liposomes, Int. J. Pharm. 605 (2021) 120809. https://doi.org/10.1016/j.ijpharm.2021.120809.

[209] D. Thiyagarajan, B. Huck, B. Nothdurft, M. Koch, D. Rudolph, M. Rutschmann, C. Feldmann, C. Hozsa, M. Furch, K.F.W. Besecke, R.K. Gieseler, B. Loretz, C.-M. Lehr, Spray-dried lactose-leucine microparticles for pulmonary delivery of antimycobacterial nanopharmaceuticals, Drug Deliv. and Transl. Res. 11 (2021) 1766–1778. https://doi.org/10.1007/s13346-021-01011-7.

[210] J.D. Vanza, D.M. Shah, R.B. Patel, M.R. Patel, Afatinib liposomal dry powder inhaler: Targeted pulmonary delivery of EGFR inhibitor for the management of lung cancer, J Drug Deliv Sci Technol. 74 (2022) 103506. https://doi.org/10.1016/j.jddst.2022.103506.

[211] Quality by design, European Medicines Agency. (2018). https://www.ema.europa.eu/en/human-regulatory/research-development/quality-design (accessed December 20, 2022).

[212] M. Altekar, C.A. Homon, M.A. Kashem, S.W. Mason, R.M. Nelson, L.A. Patnaude, J. Yingling, P.B. Taylor, Assay Optimization: A Statistical Design of Experiments Approach, JALA. 11 (2006) 33–41. https://doi.org/10.1016/j.jala.2005.11.001.

[213] M. Temtem, C. Moura, T. Casimiro, E. Costa, A. Aguiar-Ricardo, Benchmarking Supercritical CO_2-assisted Spray Drying with Conventional Spray Drying for the Manufacture of Inhalation Formulations, RDD Europe 1 (2017) 153-166.

[214] M. Malamatari, S. Somavarapu, K. Kachrimanis, G. Buckton, K.M.G. Taylor, Preparation of respirable nanoparticle agglomerates of the low melting and ductile drug ibuprofen: Impact of formulation parameters, Powder Technol. 308 (2017) 123–134. https://doi.org/10.1016/j.powtec.2016.12.007.

[215] Y. Yang, Z. Yang, Y. Ren, X. Mei, Effects of formulation and operating variables on Zanamivir dry powder inhalation characteristics and aerosolization performance, Drug Deliv. 21 (2014) 480–486. https://doi.org/10.3109/10717544.2014.883113.

[216] M. Goldberg, I. Gomez-Orellana, Challenges for the oral delivery of macromolecules, Nat. Rev. Drug Discov. 2 (2003) 289–295. https://doi.org/10.1038/nrd1067.

[217] J. Huang, Q. Shu, L. Wang, H. Wu, A.Y. Wang, H. Mao, Layer-by-Layer Assembled Milk Protein Coated Magnetic Nanoparticle Enabled Oral Drug Delivery with High Stability in Stomach and Enzyme-Responsive Release in Small Intestine, Biomaterials. 39 (2015) 105–113. https://doi.org/10.1161/CIRCULATIONAHA.110.956839.

[218] T.X. Nguyen, L. Huang, M. Gauthier, G. Yang, Q. Wang, Recent advances in liposome surface modification for oral drug delivery, Nanomedicine. 11 (2016) 1169–1185. https://doi.org/10.2217/nnm.16.9.

[219] A. Banerjee, K. Ibsen, T. Brown, R. Chen, C. Agatemor, S. Mitragotri, Ionic liquids for oral insulin delivery, Proc. Natl. Acad. Sci. U. S. A. 115 (2018) 7296–7301. https://doi.org/10.1073/pnas.1722338115.

[220] L.N. Thwala, V. Préat, N.S. Csaba, Emerging delivery platforms for mucosal administration of biopharmaceuticals: a critical update on nasal, pulmonary and oral routes, Expert Opin Drug Deliv. 14 (2017) 23–36. https://doi.org/10.1080/17425247.2016.1206074.

[221] P. Batista, P.M. Castro, A.R. Madureira, B. Sarmento, M. Pintado, Recent insights in the use of nanocarriers for the oral delivery of bioactive proteins and peptides, Peptides. 101 (2018) 112–123. https://doi.org/10.1016/j.peptides.2018.01.002.

[222] E.M. Pridgen, F. Alexis, O.C. Farokhzad, Polymeric nanoparticle drug delivery technologies for oral delivery applications, Expert Opin Drug Deliv. 12 (2015) 1459–1473. https://doi.org/10.1517/17425247.2015.1018175.

[223] N. Shrestha, F. Araújo, M.A. Shahbazi, E. Mäkilä, M.J. Gomes, B. Herranz-Blanco, R. Lindgren, S. Granroth, E. Kukk, J. Salonen, J. Hirvonen, B. Sarmento, H.A. Santos, Thiolation and Cell-Penetrating Peptide Surface Functionalization of Porous Silicon Nanoparticles for Oral Delivery of Insulin, Adv. Funct. Mater. 26 (2016) 3405–3416. https://doi.org/10.1002/adfm.201505252.

[224] Y. Xu, Y. Zheng, L. Wu, X. Zhu, Z. Zhang, Y. Huang, Novel Solid Lipid Nanoparticle with Endosomal Escape Function for Oral Delivery of Insulin, ACS Appl. Mater. Interfaces. 10 (2018) 9315–9324. https://doi.org/10.1021/acsami.8b00507.

[225] P. Fonte, F. Araújo, S. Reis, B. Sarmento, Oral insulin delivery: How far are we?, JDST. 7 (2013) 520–531. https://doi.org/10.1177/193229681300700228.

[226] W. Fan, D. Xia, Q. Zhu, X. Li, S. He, C. Zhu, S. Guo, L. Hovgaard, M. Yang, Y. Gan, Functional nanoparticles exploit the bile acid pathway to overcome multiple barriers of the intestinal epithelium for oral insulin delivery, Biomaterials. 151 (2018) 13–23. https://doi.org/10.1016/j.biomaterials.2017.10.022.

[227] A. Abramson, E. Caffarel-Salvador, M. Khang, D. Dellal, D. Silverstein, Y. Gao, M.R. Frederiksen, A. Vegge, F. Hubálek, J.J. Water, A. V. Friderichsen, J. Fels, R.K. Kirk, C. Cleveland, J. Collins, S. Tamang, A. Hayward, T. Landh, S.T. Buckley, N. Roxhed, U. Rahbek, R. Langer, G. Traverso, An ingestible self-orienting system for oral delivery of macromolecules, Science. 363 (2019) 611–615. https://doi.org/10.1126/science.aau2277.

[228] G. Sharma, K. Wilson, C.F. van der Walle, N. Sattar, J.R. Petrie, M.N.V. Ravi Kumar, Microemulsions for oral delivery of insulin: Design, development and evaluation in streptozotocin

induced diabetic rats, Eur J Pharm Biopharm. 76 (2010) 159–169. https://doi.org/10.1016/j.ejpb.2010.07.002.

[229] Y. Li, W. Yokoyama, S. Xu, S. Zhu, J. Ma, F. Zhong, Formation and stability of W/O microemulsion formed by food grade ingredients and its oral delivery of insulin in mice, JFF. 30 (2017) 134–141. https://doi.org/10.1016/j.jff.2017.01.006.

[230] F. Araújo, N. Shrestha, M.A. Shahbazi, D. Liu, B. Herranz-Blanco, E.M. Mäkilä, J.J. Salonen, J.T. Hirvonen, P.L. Granja, B. Sarmento, H.A. Santos, Microfluidic Assembly of a Multifunctional Tailorable Composite System Designed for Site Specific Combined Oral Delivery of Peptide Drugs, ACS Nano. 9 (2015) 8291–8302. https://doi.org/10.1021/acsnano.5b02762.

[231] K. Sonaje, Y.J. Chen, H.L. Chen, S.P. Wey, J.H. Juang, H.N. Nguyen, C.W. Hsu, K.J. Lin, H.W. Sung, Enteric-coated capsules filled with freeze-dried chitosan/poly(γ-glutamic acid) nanoparticles for oral insulin delivery, Biomaterials. 31 (2010) 3384–3394. https://doi.org/10.1016/j.biomaterials.2010.01.042.

[232] J.P. Martins, R.D. Auria, D. Liu, F. Fontana, M.P.A. Ferreira, A. Correia, M. Kemell, K. Moslova, E. Mäkilä, J. Salonen, L. Casettari, J. Hirvonen, B. Sarmento, H.A. Santos, Engineered Multifunctional Albumin-Decorated Porous Silicon Nanoparticles for FcRn Translocation of Insulin, Small. 1800462 (2018) 1–11. https://doi.org/10.1002/smll.201800462.

[233] T. Andreani, C.P. Kiill, A.L.R. de Souza, J.F. Fangueiro, L. Fernandes, S. Doktorovová, D.L. Santos, M.L. Garcia, M.P.D. Gremião, E.B. Souto, A.M. Silva, Surface engineering of silica nanoparticles for oral insulin delivery: Characterization and cell toxicity studies, Colloids Surf. B 123 (2014) 916–923. https://doi.org/10.1016/j.colsurfb.2014.10.047.

[234] C.Y. Wong, H. Al-Salami, C.R. Dass, Recent advancements in oral administration of insulin-loaded liposomal drug delivery systems for diabetes mellitus, Int. J. Pharm. 549 (2018) 201–217. https://doi.org/10.1016/j.ijpharm.2018.07.041.

[235] M. Niu, Y. Tan, P. Guan, L. Hovgaard, Y. Lu, J. Qi, R. Lian, X. Li, W. Wu, Enhanced oral absorption of insulin-loaded liposomes containing bile salts: A mechanistic study, Int. J. Pharm. 460 (2014) 119–130. https://doi.org/10.1016/j.ijpharm.2013.11.028.

[236] J. Parmentier, M.M.M. Becker, U. Heintz, G. Fricker, Stability of liposomes containing bio-enhancers and tetraether lipids in simulated gastro-intestinal fluids, Int. J. Pharm. 405 (2011) 210–217. https://doi.org/10.1016/j.ijpharm.2010.12.005.

[237] H.M. Patel, B.E. Ryman, Oral administration of insulin by encapsulation within liposomes, FEBS Letters. 62 (1976) 10–13. https://doi.org/10.1016/0014-5793(76)80016-6

[238] G. Gregoriadis P.D. Leathwood Brenda E. Ryman, Enzyme Entrapment in Liposomes, FEBS Letters. 14 (1971) 95–99. https://doi.org/10.1016/S0076-6879(76)44019-3.

[239] S. Hu, M. Niu, F. Hu, Y. Lu, J. Qi, Z. Yin, W. Wu, Integrity and stability of oral liposomes containing bile salts studied in simulated and ex vivo gastrointestinal media, Int. J. Pharm. 441 (2013) 693–700. https://doi.org/10.1016/j.ijpharm.2012.10.025.

[240] H. He, Y. Lu, J. Qi, Q. Zhu, Z. Chen, W. Wu, Adapting liposomes for oral drug delivery, Acta Pharm. Sin. B. 9 (2019) 36–48. https://doi.org/10.1016/j.apsb.2018.06.005.

[241] M. Niu, Y. Lu, L. Hovgaard, W. Wu, Liposomes containing glycocholate as potential oral insulin delivery systems: preparation, in vitro characterization, and improved protection against enzymatic degradation, Int J Nanomedicine. 6 (2011) 1155–66. https://doi.org/10.2147/ijn.s19917.

[242] J. Yu, Y. Zhang, J. Wang, D. Wen, A.R. Kahkoska, J.B. Buse, Z. Gu, Glucose-responsive oral insulin delivery for postprandial glycemic regulation, Nano Res. 12 (2019) 1539–1545. https://doi.org/10.1007/s12274-018-2264-9

[243] K. Iwanaga, S. Ono, K. Narioka, K. Morimoto, M. Kakemi, S. Yamashita, M. Nango, N. Oku, Oral delivery of insulin by using surface coating liposomes. Improvement of stability of insulin in GI tract, Int. J. Pharm. 157 (1997) 73–80. https://doi.org/10.1016/S0378-5173(97)00237-8.

[244] A. Wang, T. Yang, W. Fan, Y. Yang, Q. Zhu, S. Guo, Protein Corona Liposomes Achieve Efficient Oral Insulin Delivery by Overcoming Mucus and Epithelial Barriers, Adv. Healthcare Mater. 8 (2019) 1801123. https://doi.org/10.1002/adhm.201801123

[245] A. Bigdeli, S. Palchetti, D. Pozzi, M.R. Hormozi-Nezhad, F. Baldelli Bombelli, G. Caracciolo, M. Mahmoudi, Exploring Cellular Interactions of Liposomes Using Protein Corona Fingerprints and Physicochemical Properties, ACS Nano. 10 (2016) 3723–3737. https://doi.org/10.1021/acsnano.6b00261.

[246] H. Elsana, T.O.B. Olusanya, J. Carr-wilkinson, S. Darby, A. Faheem, A.A. Elkordy, Evaluation of novel cationic gene based liposomes with cyclodextrin prepared by thin film hydration and microfluidic systems, Sci. Rep. 9 (2019) 1–17. https://doi.org/10.1038/s41598-019-51065-4.

[247] R. Ran, A.P.J. Middelberg, C.X. Zhao, Microfluidic synthesis of multifunctional liposomes for tumour targeting, Colloids Surf. B. 148 (2016) 402–410. https://doi.org/10.1016/j.colsurfb.2016.09.016.

[248] N. Dimov, E. Kastner, M. Hussain, Y. Perrie, N. Szita, Formation and purification of tailored liposomes for drug delivery using a module-based micro continuous-flow system, Sci. Rep. 7 (2017) 1–13. https://doi.org/10.1038/s41598-017-11533-1.

[249] P.M. Valencia, O.C. Farokhzad, R. Karnik, R. Langer, Microfluidic technologies for accelerating the clinical translation of nanoparticles, Nat. Nanotechnol. 7 (2012) 623–629. https://doi.org/10.1038/nnano.2012.168.

[250] J.P. Rolland, R.M. Van Dam, D.A. Schorzman, S.R. Quake, J.M. DeSimone, Solvent-Resistant Photocurable "Liquid Teflon" for Microfluidic Device Fabrication, J. Am. Chem. Soc.126 (2004) 2322–2323. https://doi.org/10.1021/ja031657y.

[251] J.P. Martins, G. Torrieri, H.A. Santos, The importance of microfluidics for the preparation of nanoparticles as advanced drug delivery systems, Expert Opin Drug Deliv. 15 (2018) 1–11. https://doi.org/10.1080/17425247.2018.1446936.

[252] D. Bodas, C. Khan-Malek, Hydrophilization and hydrophobic recovery of PDMS by oxygen plasma and chemical treatment-An SEM investigation, Sens. Actuators B Chem. 123 (2007) 368–373. https://doi.org/10.1016/j.snb.2006.08.037.

[253] D. Liu, H. Zhang, F. Fontana, J.T. Hirvonen, H.A. Santos, Microfluidic-assisted fabrication of carriers for controlled drug delivery, Lab Chip. 17 (2017) 1856–1883. https://doi.org/10.1039/c7lc00242d.

[254] D. Carugo, E. Bottaro, J. Owen, E. Stride, C. Nastruzzi, Liposome production by microfluidics: Potential and limiting factors, Sci. Rep. 6 (2016) 1–15. https://doi.org/10.1038/srep25876.

[255] V.M. Shah, D.X. Nguyen, P. Patel, B. Cote, A. Al-Fatease, Y. Pham, M.G. Huynh, Y. Woo, A.W. Alani, Liposomes produced by microfluidics and extrusion: A comparison for scale-up purposes, Nanomed-Nanotechnol 18 (2019) 146–156. https://doi.org/10.1016/j.nano.2019.02.019.

[256] D. Van Swaay, A. Demello, Microfluidic methods for forming liposomes, Lab Chip. 13 (2013) 752–767. https://doi.org/10.1039/c2lc41121k.

[257] R.K. Shah, H.C. Shum, A.C. Rowat, D. Lee, J.J. Agresti, A.S. Utada, L.Y. Chu, J.W. Kim, A. Fernandez-Nieves, C.J. Martinez, D.A. Weitz, Designer emulsions using microfluidics, Mater. Today Commun. 11 (2008) 18–27. https://doi.org/10.1016/S1369-7021(08)70053-1.

[258] W. Li, L. Zhang, X. Ge, B. Xu, W. Zhang, L. Qu, C.H. Choi, J. Xu, A. Zhang, H. Lee, D.A. Weitz, Microfluidic fabrication of microparticles for biomedical applications, Chem Soc Rev. 47 (2018) 5646–5683. https://doi.org/10.1039/c7cs00263g.

[259] W. Li, D. Liu, H. Zhang, A. Correia, E. Mäkilä, J. Salonen, J. Hirvonen, H.A. Santos, Microfluidic assembly of a nano-in-micro dual drug delivery platform composed of halloysite nanotubes and a pH-responsive polymer for colon cancer therapy, Acta Biomater. 48 (2017) 238–246. https://doi.org/10.1016/j.actbio.2016.10.042.

[260] C.Y. Wong, H. Al-salami, C.R. Dass, Microparticles, microcapsules and microspheres: a review of recent developments and prospects for oral delivery of insulin, Int. J. Pharm. 537 (2017) 223–244. https://doi.org/10.1016/j.ijpharm.2017.12.036.

[261] F.L. Lopez, T.B. Ernest, C. Tuleu, M.O. Gul, Formulation approaches to pediatric oral drug delivery: Benefits and limitations of current platforms, Expert Opin Drug Deliv. 12 (2015) 1727–1740. https://doi.org/10.1517/17425247.2015.1060218.

[262] E.T.L. Lau, K.J. Steadman, M. Mak, J.A.Y. Cichero, L.M. Nissen, Prevalence of swallowing difficulties and medication modification in community pharmacy customers, Aust. J. Pharm. 96 (2015) 68–71. https://doi.org/10.1002/jppr.1052.

[263] J.P. Martins, D. Liu, F. Fontana, M.P.A. Ferreira, A. Correia, S. Valentino, M. Kemell, K. Moslova, E. Mäkilä, J. Salonen, J. Hirvonen, B. Sarmento, H.A. Santos, Microfluidic Nanoassembly of Bioengineered Chitosan-Modified FcRn-Targeted Porous Silicon Nanoparticles @ Hypromellose Acetate Succinate for Oral Delivery of Antidiabetic Peptides, ACS Appl. Mater. Interfaces 10 (2018) 44354–44367. https://doi.org/10.1021/acsami.8b20821.

[264] W. Li, Y. Li, Z. Liu, N. Kerdsakundee, M. Zhang, F. Zhang, X. Liu, T. Bauleth-Ramos, W. Lian, E. Mäkilä, M. Kemell, Y. Ding, B. Sarmento, R. Wiwattanapatapee, J. Salonen, H. Zhang, J.T. Hirvonen, D. Liu, X. Deng, H.A. Santos, Hierarchical structured and programmed vehicles deliver drugs locally to inflamed sites of intestine, Biomaterials. 185 (2018) 322–332. https://doi.org/10.1016/j.biomaterials.2018.09.024.

[265] J.M. Zook, W.N. Vreeland, Effects of temperature, acyl chain length, and flow-rate ratio on liposome formation and size in a microfluidic hydrodynamic focusing device, Soft Matter. 6 (2010) 1352–1360. https://doi.org/10.1039/b923299k.

[266] D.L. and Y.P. Elisabeth Kastner, Varun Verma, Microfluidic-controlled manufacture of liposomes for the solubilisation of a poorly water soluble drug., Int. J. Pharm. 485 (2015) 122–130.

[267] A. Jahn, W.N. Vreeland, D.L. Devoe, L.E. Locascio, M. Gaitan, Microfluidic directed formation of liposomes of controlled size, Langmuir. 23 (2007) 6289–6293. https://doi.org/10.1021/la070051a.

[268] D.D. Lasic, F.J. Martin, On the mechanism of vesicle formation, J. Membr. Sci. 50 (1990) 215–222. https://doi.org/10.1016/S0376-7388(00)80317-8.

[269] K. Muramatsu, Y. Maitani, T. Nagai, Dipalmitoylphosphatidylcholine Liposomes with Soybean-Derived Sterols and Cholesterol as a Carrier for the Oral Administration of Insulin in Rats, Chem. Pharm. Bull. 19 (1996) 1055–1058. https://doi.org/10.1248/bpb.19.1055

[270] O. Mertins, R. Dimova, Binding of chitosan to phospholipid vesicles studied with isothermal titration calorimetry, Langmuir. 27 (2011) 5506–5515. https://doi.org/10.1021/la200553t.

[271] J.D. Fisher, A.P. Acharya, S.R. Little, Micro and nanoparticle drug delivery systems for preventing allotransplant rejection, J. Clin. Immunol. 160 (2015) 24–35. https://doi.org/10.1016/j.clim.2015.04.013.

[272] M.F. Ukasawa, S.C. Co, S. Chemicals, Molecular Weight Determination of Hypromellose Acetate Succinate (HPMCAS) Using Size Exclusion Chromatography with a Multi-Angle Laser Light Scattering Detector, Chem. Pharm. Bull. 52 (2004) 1391–1393. https://doi.org/10.1248/cpb.52.1391

[273] D.T. Friesen, R. Shanker, M. Crew, D.T. Smithey, W.J. Curatolo, J.A.S. Nightingale, Hydroxypropyl Methylcellulose Acetate Succinate-Based Spray-Dried Dispersions: An Overview, Mol Pharm. 5 (2008) 1003–1019. https://doi.org/10.1021/mp8000793

[274] A.A.P. Mansur, H.S. Mansur, Quantum dot/glycol chitosan fluorescent nanoconjugates, Nanoscale Res. Lett. 10 (2015). https://doi.org/10.1186/s11671-015-0879-2.

[275] S. Bertoni, Z. Liu, A. Correia, J.P. Martins, A. Rahikkala, F. Fontana, M. Kemell, D. Liu, B. Albertini, N. Passerini, W. Li, H.A. Santos, pH and Reactive Oxygen Species-Sequential Responsive Nano-in-Micro Composite for Targeted Therapy of Inflammatory Bowel Disease, Adv. Funct. Mater. 28 (2018) 1–11. https://doi.org/10.1002/adfm.201806175.

[276] N. Shrestha, M.A. Shahbazi, F. Araújo, E. Mäkilä, J. Raula, E.I. Kauppinen, J. Salonen, B. Sarmento, J. Hirvonen, H.A. Santos, Multistage pH-responsive mucoadhesive nanocarriers prepared by aerosol flow reactor technology: A controlled dual protein-drug delivery system, Biomaterials. 68 (2015) 9–20. https://doi.org/10.1016/j.biomaterials.2015.07.045.

[277] E.L. McConnell, A.W. Basit, S. Murdan, Measurements of rat and mouse gastrointestinal pH, fluid and lymphoid tissue, and implications for in-vivo experiments, JPP. 60 (2008) 63–70. https://doi.org/10.1211/jpp.60.1.0008.

[278] A.L. Sarode, S. Obara, F.K. Tanno, H. Sandhu, R. Iyer, N. Shah, Stability assessment of hypromellose acetate succinate (HPMCAS) NF for application in hot melt extrusion (HME), Carbohydr. Polym. 101 (2014) 146–153. https://doi.org/10.1016/j.carbpol.2013.09.017.

[279] Y. Sambuy, I. De Angelis, G. Ranaldi, M.L. Scarino, A. Stammati, F. Zucco, The Caco-2 cell line as a model of the intestinal barrier: Influence of cell and culture-related factors on Caco-2 cell functional characteristics, Cell Biol. Toxicol. 21 (2005) 1–26. https://doi.org/10.1007/s10565-005-0085-6.

[280] E. Leteurtre, V. Gouyer, K. Rousseau, O. Moreau, A. Barbat, D. Swallow, G. Huet, T. Lesuffleur, Differential mucin expression in colon carcinoma HT-29 clones with variable resistance to 5-fluorouracil and methotrexate, Mol. Biol. Cell. 96 (2004) 145–151. https://doi.org/10.1016/j.biolcel.2003.12.005.

[281] P. Opanasopit, P. Aumklad, J. Kowapradit, T. Ngawhiranpat, A. Apirakaramwong, T. Rojanarata, S. Puttipipatkhachorn, Effect of salt forms and molecular weight of chitosans on in vitro permeability enhancement in intestinal epithelial cells (Caco-2), Pharm Dev Technol. 12 (2007) 447–455. https://doi.org/10.1080/10837450701555901.

[282] S.Y. Chae, M.K. Jang, J.W. Nah, Influence of molecular weight on oral absorption of water soluble chitosans, J. Control. Release. 102 (2005) 383–394. https://doi.org/10.1016/j.jconrel.2004.10.012.

[283] X. Boulenc, T. Breul, J. Gautier, H. Joyeux, C. Roques, Y. Berger, G. Fabre, Sodium lauryl sulphate increases tiludronate paracellular transport using human epithelial Caco-2 monolayers, Int. J. Pharm. 123 (1995) 71–83. https://doi.org/10.1016/0378-5173(95)00041-G

[284] B. Srinivasan, A.R. Kolli, M.B. Esch, H.E. Abaci, M.L. Shuler, J.J. Hickman, TEER Measurement Techniques for In Vitro Barrier Model Systems, J. Lab. Autom.20 (2015) 107–126. https://doi.org/10.1177/2211068214561025.

[285] L.W. Hsu, P.L. Lee, C.T. Chen, F.L. Mi, J.H. Juang, S.M. Hwang, Y.C. Ho, H.W. Sung, Elucidating the signaling mechanism of an epithelial tight-junction opening induced by chitosan, Biomaterials. 33 (2012) 6254–6263. https://doi.org/10.1016/j.biomaterials.2012.05.013.

[286] Y.H. Chen, Q. Lu, E.E. Schneeberger, D.A. Goodenough, Restoration of tight junction structure and barrier function by down- regulation of the mitogen-activated protein kinase pathway in Ras-transformed Madin-Darby canine kidney cells, Mol. Biol. Cell. 11 (2000) 849–862. https://doi.org/10.1091/mbc.11.3.849.

[287] J.M. Smith, M. Dornish, E.J. Wood, Involvement of protein kinase C in chitosan glutamate-mediated tight junction disruption, Biomaterials. 26 (2005) 3269–3276. https://doi.org/10.1016/j.biomaterials.2004.06.020.

[288] Collado-González, González Espinosa, Goycoolea, Interaction Between Chitosan and Mucin: Fundamentals and Applications, Biomimetics. 4 (2019) 32. https://doi.org/10.3390/biomimetics4020032.

[289] N. Greenfield, G.D. Fasman, Computed Circular Dichroism Spectra for the Evaluation of Protein Conformation, Biochemistry. 8 (1969) 4108–4116. https://doi.org/10.1021/bi00838a031.

[290] V.A. Ivancic, C.A. Krasinski, Q. Zheng, R.J. Meservier, N.D. Lazo, Enzyme kinetics from circular dichroism of insulin reveals mechanistic insights into the regulation of insulin-degrading enzyme, Biosci Rep. 38 (2018) BSR20181555. https://doi.org/10.1042/bsr20181555.

[291] D. Pozzi, V. Colapicchioni, G. Caracciolo, S. Piovesana, A.L. Capriotti, S. Palchetti, S. De Grossi, A. Riccioli, H. Amenitsch, A. Laganà, Effect of polyethyleneglycol (PEG) chain length on the bio-nano- interactions between PEGylated lipid nanoparticles and biological fluids: From nanostructure to uptake in cancer cells, Nanoscale. 6 (2014) 2782–2792. https://doi.org/10.1039/c3nr05559k.

[292] N. Dan, Effect of liposome charge and PEG polymer layer thickness on cell-liposome electrostatic interactions, Biochim Biophys Acta - Biomembranes. 1564 (2002) 343–348. https://doi.org/10.1016/S0005-2736(02)00468-6.

[293] C.R. Miller, B. Bondurant, S.D. McLean, K.A. McGovern, D.F. O'Brien, Liposome-cell interactions in vitro: Effect of liposome surface charge on the binding and endocytosis of conventional and sterically stabilized liposomes, Biochemistry. 37 (1998) 12875–12883. https://doi.org/10.1021/bi980096y.

[294] M. Lopes, N. Shrestha, A. Correia, M.A. Shahbazi, B. Sarmento, J. Hirvonen, F. Veiga, R. Seiça, A. Ribeiro, H.A. Santos, Dual chitosan/albumin-coated alginate/dextran sulfate nanoparticles for enhanced oral delivery of insulin, J. Control. Release. 232 (2016) 29–41. https://doi.org/10.1016/j.jconrel.2016.04.012.

[295] I.A. Sogias, A.C. Williams, V. V. Khutoryanskiy, Why is chitosan mucoadhesive?, Biomacromolecules. 9 (2008) 1837–1842. https://doi.org/10.1021/bm800276d.

[296] M. Bjelošević, A. Zvonar Pobirk, O. Planinšek, P. Ahlin Grabnar, Excipients in freeze-dried biopharmaceuticals: Contributions toward formulation stability and lyophilisation cycle optimisation, Int. J. Pharm. 576 (2020) 119029. https://doi.org/10.1016/j.ijpharm.2020.119029.

[297] M. Kesik-Brodacka, Progress in biopharmaceutical development, Biotechnol. Appl. Biochem. 65 (2018) 306–322. https://doi.org/10.1002/bab.1617.
[298] J. Swaminathan, C. Ehrhardt, Liposomal delivery of proteins and peptides, Expert Opin Drug Deliv. 9 (2012) 1489–1503. https://doi.org/10.1517/17425247.2012.735658.
[299] M.L. Van Slooten, O. Boerman, K. Romøren, E. Kedar, D.J.A. Crommelin, G. Storm, Liposomes as sustained release system for human interferon-γ: Biopharmaceutical aspects, Biochim Biophys Acta - MOL CELL BIOL L. 1530 (2001) 134–145. https://doi.org/10.1016/S1388-1981(00)00174-8.
[300] S. jun Cao, S. Xu, H. ming Wang, Y. Ling, J. Dong, R. dong Xia, X. hong Sun, Nanoparticles: Oral Delivery for Protein and Peptide Drugs, AAPS PharmSciTech. 20 (2019) 1–11. https://doi.org/10.1208/s12249-019-1325-z.
[301] S. Mitragotri, P.A. Burke, R. Langer, Overcoming the challenges in administering biopharmaceuticals: formulation and delivery strategies, Nat Rev Drug Discov. 13 (2014) 655–672. https://doi.org/10.1016/j.physbeh.2017.03.040.
[302] M.E.M. Cruz, S. Simões, M.L. Corvo, M.B.F. Martins, M.M. Gaspar, Formulation of NPDDS for macromolecules, in: Y. Pathaar, D. Thassu (Eds.) Drug Delivery Nanoparticles Formulation and Characterization, 2009, CRC Press, Boca Raton, FL, pp. 35–49. https://doi.org/10.3109/9781420078053-4.
[303] Y. Barenholz, Doxil® - The first FDA-approved nano-drug: Lessons learned, J. Control. Release. 160 (2012) 117–134. https://doi.org/10.1016/j.jconrel.2012.03.020.
[304] U. Bulbake, S. Doppalapudi, N. Kommineni, W. Khan, Liposomal formulations in clinical use: An updated review, Pharmaceutics. 9 (2017) 1–33. https://doi.org/10.3390/pharmaceutics9020012.
[305] A.A. Mokhtarieh, J. Lee, S. Kim, M.K. Lee, Preparation of siRNA encapsulated nanoliposomes suitable for siRNA delivery by simply discontinuous mixing, Biochim Biophys Acta-Biomembranes. 1860 (2018) 1318–1325. https://doi.org/10.1016/j.bbamem.2018.02.027.
[306] V. V. Shuvaev, R.Y. Kiseleva, E. Arguiri, C.H. Villa, S. Muro, M. Christofidou-Solomidou, R. V. Stan, V.R. Muzykantov, Targeting superoxide dismutase to endothelial caveolae profoundly alleviates inflammation caused by endotoxin, J. Control. Release. 272 (2018) 1–8. https://doi.org/10.1016/j.jconrel.2017.12.025.
[307] Q. Zhang, H. Tao, Y. Lin, Y. Hu, H. An, D. Zhang, S. Feng, H. Hu, R. Wang, X. Li, J. Zhang, A superoxide dismutase/catalase mimetic nanomedicine for targeted therapy of inflammatory

bowel disease, Biomaterials. 105 (2016) 206–221. https://doi.org/10.1016/j.biomaterials.2016.08.010.

[308] M.L. Corvo, O.C. Boerman, W.J.G. Oyen, J.C.S. Jorge, M.E.M. Cruz, D.J.A. Crommelin, G. Storm, Subcutaneous administration of superoxide dismutase entrapped in long circulating liposomes: In vivo fate and therapeutic activity in an inflammation model, Pharm. Res. 17 (2000) 600–606. https://doi.org/10.1023/A:1007577101964.

[309] G. Jadot, A. Vaille, J. Maldonado, P. Vanelle, Clinical Pharmacokinetics and Delivery of Bovine Superoxide Dismutase, Clin. Pharmacokinet. 28 (1995) 17–25. https://doi.org/10.2165/00003088-199528010-00003.

[310] V.P. Torchilin, M.I. Papisov, Why Do Polyethylene Glycol-Coated Liposomes Circulate So Long?, J. Liposome Res. 4 (1994) 725–739.

[311] O.K. Nag, V. Awasthi, Surface engineering of liposomes for stealth behavior, Pharmaceutics. 5 (2013) 542–569. https://doi.org/10.3390/pharmaceutics5040542.

[312] A.S. Ghatorae, G. Bell, P.J. Halling, Inactivation of enzymes by organic solvents: New technique with well-defined interfacial area, Biotechnol. Bioeng. 43 (1994) 331–336. https://doi.org/10.1002/bit.260430410.

[313] D.D. Lasic, Novel applications of liposomes, Trends Biotechnol. 16 (1998) 307–321. https://doi.org/10.1016/S0167-7799(98)01220-7.

[314] M.J. York-Duran, M. Godoy-Gallardo, M.M.T. Jansman, L. Hosta-Rigau, A dual-component carrier with both non-enzymatic and enzymatic antioxidant activity towards ROS depletion, Biomater. Sci. 7 (2019) 4813–4826. https://doi.org/10.1039/c9bm00913b.

[315] E.A. Morozova, V. V. Kulikova, N. V. Anufrieva, A.N. Minakov, A.S. Chernov, G.B. Telegin, S. V. Revtovich, V.S. Koval, T. V. Demidkina, Methionine γ-lyase in enzyme prodrug therapy: An improvement of pharmacokinetic parameters of the enzyme, Int. J. Biol. Macromol. 140 (2019) 1277–1283. https://doi.org/10.1016/j.ijbiomac.2019.08.224.

[316] Z. Liu, F. Fontana, A. Python, J.T. Hirvonen, H.A. Santos, Microfluidics for Production of Particles: Mechanism, Methodology, and Applications, Small. 16 (2020) 1–24. https://doi.org/10.1002/smll.201904673.

[317] F. Fontana, J.P. Martins, G. Torrieri, H.A. Santos, Nuts and Bolts: Microfluidics for the Production of Biomaterials, Adv. Mater. Technol. 4 (2019) 1–21. https://doi.org/10.1002/admt.201800611.

[318] D. Liu, H. Zhang, F. Fontana, J.T. Hirvonen, H.A. Santos, Microfluidic-assisted fabrication of carriers for controlled drug delivery, Lab Chip. 17 (2017) 1856–1883. https://doi.org/10.1039/c7lc00242d.

[319] F. Bally, D.K. Garg, C.A. Serra, Y. Hoarau, N. Anton, C. Brochon, D. Parida, T. Vandamme, G. Hadziioannou, Improved size-tunable preparation of polymeric nanoparticles by microfluidic nanoprecipitation, Polymer. 53 (2012) 5045–5051. https://doi.org/10.1016/j.polymer.2012.08.039.

[320] C. Costa, Z. Liu, J.P. Martins, A. Correia, P. Figueiredo, A. Rahikkala, W. Li, J. Seitsonen, J. Ruokolainen, S.-P. Hirvonen, A. Aguiar-Ricardo, M.L. Corvo, H.A. Santos, All-in-one microfluidic assembly of insulin-loaded pH-responsive nano-in-microparticles for oral insulin delivery, Biomater. Sci. (2020) 3270–3277. https://doi.org/10.1039/d0bm00743a.

[321] G. Rouser, S. Fleischer, A. Yamamoto, Two dimensional thin layer chromatographic separation of polar lipids and determination of phospholipids by phosphorus analysis of spots, Lipids. 5 (1970) 494–496. https://doi.org/10.1007/BF02531316.

[322] O.H. Lowry, N.J. Rosebrough, A. Lewis Farr, R.J. Randall, Protein measurement with the folin phenol reagent, Journal of Biological Chemistry. 193 (1951) 265–275. *DOI not found*

[323] C.-S. Wang, R.L. Smith, Lowry Determination of Protein in the Presence of Triton X- 100, Anal. Biochem. 63 (1975) 414–417. https://doi.org/10.1016/0003-2697(75)90363-2.

[324] R.W. Lange, D.R. Germolec, J.F. Foley, M.I. Luster, Antioxidants attenuate anthralin-induced skin inflammation in BALB/c mice: Role of specific proinflammatory cytokines, J. Leukoc. Biol. 64 (1998) 170–176. https://doi.org/10.1002/jlb.64.2.170.

[325] A. Ascenso, S. Pinho, C. Eleutério, F.G. Praça, M.V.L.B. Bentley, H. Oliveira, C. Santos, O. Silva, S. Simões, Lycopene from tomatoes: Vesicular nanocarrier formulations for dermal delivery, J. Agric. Food Chem. 61 (2013) 7284–7293. https://doi.org/10.1021/jf401368w.

[326] R. Galovi Rengel, K. Bariši, E. Paveli, T. Ani Grubiši, I. Epelak, J. Filipovi-Grči, High efficiency entrapment of superoxide dismutase into mucoadhesive chitosan-coated liposomes, Eur J Pharm Sci. 15 (2002) 441–448. https://doi.org/10.1016/S0928-0987(02)00030-1.

[327] S. Simões, C. Marques, M.E. Cruz, M.B. Figueira Martins, Anti-inflammatory effects of locally applied enzyme-loaded ultradeformable vesicles on an acute cutaneous model, J. Microencapsul. 26 (2009) 649–658. https://doi.org/10.3109/02652040802630403.

[328] P. Marcelino, H.S. Marinho, M.C. Campos, A.R. Neves, C. Real, F.S. Fontes, A. Carvalho, G. Feio, M.B.F. Martins, M.L. Corvo, Therapeutic activity of superoxide dismutase-containing

enzymosomes on rat liver ischaemia-reperfusion injury followed by magnetic resonance microscopy, Eur J Pharm Sci. 109 (2017) 464–471. https://doi.org/10.1016/j.ejps.2017.09.008.
[329] A. Carvalho, M.B.F. Martins, M.L. Corvo, G. Feio, Enhanced contrast efficiency in MRI by PEGylated magnetoliposomes loaded with PEGylated SPION: Effect of SPION coating and micro-environment, Mater. Sci. Eng. 43 (2014) 521–526. https://doi.org/10.1016/j.msec.2014.07.055.
[330] T. Hernández-Caselles, J. Villalaín, J.C. Gómez-Fernández, Stability of Liposomes on Long Term Storage, JPP. 42 (1990) 397–400. https://doi.org/10.1111/j.2042-7158.1990.tb06578.x.
[331] J. Cauzzo, M. Nystad, A.M. Holsæter, P. Basnet, N. Škalko-Basnet, Following the fate of dye-containing liposomes in vitro, Int. J. Mol. Sci. 21 (2020) 1–17. https://doi.org/10.3390/ijms21144847.
[332] M.M. Gaspar, M.B. Martins, M.L. Corvo, M.E.M. Cruz, Design and characterization of enzymosomes with surface-exposed superoxide dismutase, Biochim Biophys Acta.- Biomembranes. 1609 (2003) 211–217. https://doi.org/10.1016/S0005-2736(02)00702-2.
[333] G. Liou, P. Storz, Reactive oxygen species in cancer, Free Radic. Res. 44 (2010) 479–496. https://doi.org/10.3109/10715761003667554.
[334] E.A. Hileman, G. Achanta, P. Huang, Superoxide dismutase: an emerging target for cancer therapeutics, Expert Opin. Ther. Targets. 5 (2001) 697–710. https://doi.org/10.1517/14728222.5.6.697
[335] M.I. Adamczak, E. Hagesaether, G. Smistad, M. Hiorth, An in vitro study of mucoadhesion and biocompatibility of polymer coated liposomes on HT29-MTX mucus-producing cells, Int. J. Pharm. 498 (2016) 225–233. https://doi.org/10.1016/j.ijpharm.2015.12.030.
[336] G.K. Srivastava, M.L. Alonso-Alonso, I. Fernandez-Bueno, M.T. Garcia-Gutierrez, F. Rull, J. Medina, R.M. Coco, J.C. Pastor, Comparison between direct contact and extract exposure methods for PFO cytotoxicity evaluation, Sci. Rep. 8 (2018) 1–9. https://doi.org/10.1038/s41598-018-19428-5.
[337] T.P. Pivetta, S. Simões, M.M. Araújo, T. Carvalho, C. Arruda, P.D. Marcato, Development of nanoparticles from natural lipids for topical delivery of thymol: Investigation of its anti-inflammatory properties, Colloids Surf. B 164 (2018) 281–290. https://doi.org/10.1016/j.colsurfb.2018.01.053.

[338] M.M.A. Abdel-Mottaleb, B. Moulari, A. Beduneau, Y. Pellequer, A. Lamprecht, Nanoparticles enhance therapeutic outcome in inflamed skin therapy, Eur J Pharm Biopharm. 82 (2012) 151–157. https://doi.org/10.1016/j.ejpb.2012.06.006.

[339] M.L. Corvo, H.S. Marinho, P. Marcelino, R.M. Lopes, C.A. Vale, C.R. Marques, L.C.D. Martins, P. Laverman, G. Storm, M.B.A.F. Martins, Superoxide dismutase enzymosomes: Carrier capacity optimization, in vivo behaviour and therapeutic activity, Pharm. Res. 32 (2015) 91–102. https://doi.org/10.1007/s11095-014-1447-7.

[340] Y. Nakamura, A. Mochida, P.L. Choyke, H. Kobayashi, Nanodrug Delivery: Is the Enhanced Permeability and Retention Effect Sufficient for Curing Cancer?, Bioconjug. Chem. 27 (2016) 2225–2238. https://doi.org/10.1021/acs.bioconjchem.6b00437.

[341] Y. Gao, X. Zhu, Y. Zhang, X. Chen, L. Wang, W. Feng, C. Huang, F. Li, In vivo biodistribution and passive accumulation of upconversion nanoparticles in colorectal cancer models via intraperitoneal injection, RSC Advances. 7 (2017) 31588–31596. https://doi.org/10.1039/c7ra04349j.

[342] P. Jacquet, P.H. Sugarbaker Peritoneal-plasma barrier. In: Sugarbaker, P.H. (Eds) Peritoneal Carcinomatosis: Principles of Management. Cancer Treatment and Research, vol 82. Springer, Boston, MA, 2016. https://doi.org/10.1007/978-1-4613-1247-5_4

[343] T.M. Allen, C.B. Hansen, L.S.S. Guo, Subcutaneous administration of liposomes: a comparison with the intravenous and intraperitoneal routes of injection, Biochim Biophys Acta - Biomembranes. 1150 (1993) 9–16. https://doi.org/10.1016/0005-2736(93)90115-G.

[344] T. Sou, R.T. Forbes, J. Gray, R.J. Prankerd, L.M. Kaminskas, M.P. McIntosh, D.A.V. Morton, Designing a multi-component spray-dried formulation platform for pulmonary delivery of biopharmaceuticals: The use of polyol, disaccharide, polysaccharide and synthetic polymer to modify solid-state properties for glassy stabilisation, Powder Technol. 287 (2016) 248–255. https://doi.org/10.1016/j.powtec.2015.10.008.

[345] R. Campardelli, I. Espirito Santo, E.C. Albuquerque, S.V. De Melo, G. Della Porta, E. Reverchon, Efficient encapsulation of proteins in submicro liposomes using a supercritical fluid assisted continuous process, J Supercrit Fluids. 107 (2016) 163–169. https://doi.org/10.1016/j.supflu.2015.09.007.

[346] J. Merlo-Mas, J. Tomsen-Melero, J.L. Corchero, E. González-Mira, A. Font, J.N. Pedersen, N. García-Aranda, E. Cristóbal-Lecina, M. Alcaina-Hernando, R. Mendoza, E. Garcia-Fruitós, T. Lizarraga, S. Resch, C. Schimpel, A. Falk, D. Pulido, M. Royo, S. Schwartz, I. Abasolo, J.S. Pedersen, D. Danino, A. Soldevila, J. Veciana, S. Sala, N. Ventosa, A. Córdoba, Application of Quality

by Design to the robust preparation of a liposomal GLA formulation by DELOS-susp method, J Supercrit Fluids. 173 (2021) 105204. https://doi.org/10.1016/j.supflu.2021.105204.
[347] D. Villanueva-bermejo, F. Temelli, Optimization of coenzyme Q10 encapsulation in liposomes using supercritical carbon dioxide, J. CO_2 Util. 38 (2020) 68–76. https://doi.org/10.1016/j.jcou.2020.01.011.
[348] P. Trucillo, P.F. Ferrari, R. Campardelli, E. Reverchon, P. Perego, A supercritical assisted process for the production of amoxicillin loaded liposomes for anti-microbial applications, J Supercrit Fluids. 163 (2020) 104842. https://doi.org/10.1016/j.supflu.2020.104842.
[349] L.X. Yu, G. Amidon, M.A. Khan, S.W. Hoag, J. Polli, G.K. Raju, J. Woodcock, Understanding pharmaceutical quality by design, AAPS PharmSciTech. 16 (2014) 771–783. https://doi.org/10.1208/s12248-014-9598-3.
[350] X. Li, H.M. Mansour, Physicochemical characterization and water vapor sorption of organic solution advanced spray-dried inhalable trehalose microparticles and nanoparticles for targeted dry powder pulmonary inhalation delivery, AAPS PharmSciTech. 12 (2011) 1420–1430. https://doi.org/10.1208/s12249-011-9704-0.
[351] R.P. Cabral, A.M.L. Sousa, A.S. Silva, A.I. Paninho, M. Temtem, E. Costa, T. Casimiro, A. Aguiar−Ricardo, Design of experiments approach on the preparation of dry inhaler chitosan composite formulations by supercritical CO_2−assisted spray−drying, J Supercrit Fluids 116 (2016) 26-35. https://doi.org/10.1016/j.supflu.2016.04.001.
[352] Council of Europe, Preparations for Inhalation: Aerodynaminc Assessment of Fine Particles, in: European Pharmacopeia 5.0, 2010: pp. 274-285.
[353] W.L.J. Hinrichs, F.A. Manceñido, N.N. Sanders, K. Braeckmans, S.C. De Smedt, J. Demeester, H.W. Frijlink, The choice of a suitable oligosaccharide to prevent aggregation of PEGylated nanoparticles during freeze thawing and freeze drying, Int. J. Pharm. 311 (2006) 237–244. https://doi.org/10.1016/j.ijpharm.2005.12.032.
[354] P. Muralidharan, E. Mallory, M. Malapit, D. Hayes, H. Mansour, Inhalable PEGylated Phospholipid Nanocarriers and PEGylated Therapeutics for Respiratory Delivery as Aerosolized Colloidal Dispersions and Dry Powder Inhalers, Pharmaceutics. 6 (2014) 333–353. https://doi.org/10.3390/pharmaceutics6020333.
[355] B. Stark, G. Pabst, R. Prassl, Long-term stability of sterically stabilized liposomes by freezing and freeze-drying: Effects of cryoprotectants on structure, Eur. J. Pharm. Sci. 3 41 (2010) 546–555. https://doi.org/10.1016/j.ejps.2010.08.010.

[356] A.R. Mohammed, A.G.A. Coombes, Y. Perrie, Amino acids as cryoprotectants for liposomal delivery systems, Eur. J. Pharm. Sci. 30 (2007) 406–413. https://doi.org/10.1016/j.ejps.2007.01.001.

[357] C.M. Deber, T.A. Stone, Relative role(s) of leucine versus isoleucine in the folding of membrane proteins, Pept, Sci. 111 (2019) e24075. https://doi.org/10.1002/pep2.24075.

[358] L. Li, S. Sun, T. Parumasivam, J.A. Denman, T. Gengenbach, P. Tang, S. Mao, H., K. Chan, L-Leucine as an excipient against moisture on in vitro aerosolization performances of highly hygroscopic spray-dried powders, Eur. J. Pharm. Biopharm. 102 (2016) 132–141. https://doi.org/10.1016/j.ejpb.2016.02.010.

[359] I. Dalmolin, E. Skovroinski, A. Biasi, M.L. Corazza, C. Dariva, J.V. Oliveira, Solubility of carbon dioxide in binary and ternary mixtures with ethanol and water, Fluid Phase Equilib. 245 (2006) 193–200.

[360] I. Alfagih, N. Kunda, F. Alanazi, S.R. Dennison, S. Somavarapu, G.A. Hutcheon, I., Y. Saleem, Pulmonary delivery of proteins using nanocomposite microcarriers, J. Pharm. Sci. 104 (2015) 4386–4398. https://doi.org/10.1002/jps.24681.

[361] R. Rabbani, P.C. Seville, The influence of formulation components on the aerosolisation properties of spray-dried powders, J. Control. Release. (2005).

[362] T. Rattanupatam, T. Srichana, Budesonide dry powder for inhalation: effects of leucine and mannitol on the efficiency of delivery, Drug Deliv. 21 (2014) 397–405. https://doi.org/10.3109/10717544.2013.868555.

[363] E. Hantz, A. Cao, E. Taillandier, Effect of ethanol on dimyristoylphosphatidylcholine large unilamellar vesicles investigated by quasi-elastic light scattering and vibrational spectroscopy, Chem. Phys. Lipids 49 (1988) 143–151. https://doi.org/10.1016/0009-3084(88)90001-1.

[364] A. Pal, P. Sunthar, D. V. Khakhar, Effects of Ethanol Addition on the Size Distribution of Liposome Suspensions in Water, Ind. Eng. Chem. Res.. 58 (2019) 7511–7519. https://doi.org/10.1021/acs.iecr.8b05028.

[365] X. Xu, A. Costa, D.J. Burgess, Protein encapsulation in unilamellar liposomes: High encapsulation efficiency and a novel technique to assess lipid-protein interaction, Pharm. Res. 29 (2012) 1919–1931. https://doi.org/10.1007/s11095-012-0720-x.

[366] W.Q. Sun, A.C. Leopold, L.M. Crowe, J.H. Crowe, Stability of dry liposomes in sugar glasses, Biophys. J. 70 (1996) 1769–1776. https://doi.org/10.1016/S0006-3495(96)79740-0.

[367] D.S. Moore, R. Hansen, S.C. Hand, Liposomes with diverse compositions are protected during desiccation by LEA proteins from Artemia franciscana and trehalose, Biochim. Biophys.

Acta Biomembr. 1858 (2016) 104–115. https://doi.org/5, https://doi. org/10.1016/j.bbamem.2015.10.019.
[368] A. Rudra, R.M. Deepa, M.K. Ghosh, S. Ghosh, B. Mukherjee, Doxorubicin-loaded phosphatidylethanolamine-conjugated nanoliposomes: in vitro characterization and their ac-cumulation in liver, kidneys, and lungs in rats, Int. J. Nanomed. 5 (2010) 811–823. https://doi.org/10.2147/IJN.S13031.
[369] J. Kotoucek, F. Hubatka, J. Masek, P. Kulich, K. Velínska, J. Bezdekova, M. Fojtíkov, a, E. Bartheldyova,A. Tomeckov, a, J. Straska, D. Hrebík, S. Macaulay, I. Kratochvílova, M. Raska, J. Turanek, Preparation of nanoliposomes by microfluidic mixing in herring-bone channel and the role of membrane fluidity in liposomes formation, Sci. Rep. 10 (2020) 1-11. https://doi.org/10.1038/s41598- 020-62500-2.
[370] A.C. Drake, Y. Lee, E.M. Burgess, J.O.M. Karlsson, A. Eroglu, A.Z. Higgins, Effect of water content on the glass transition temperature of mixtures of sugars, polymers, and penetrating cryoprotectants in physiological buffer, PLoS One. 13 (2018) 1–15. https://doi.org/10.1371/journal.pone.0190713.
[371] D. Chiou, T.A.G. Langrish, D. Chiou, T.A.G. Langrish, Crystallization of Amorphous Components in Spray-Dried Powders Crystallization of Amorphous Components in Spray-Dried Powders, Dry. Technol. 3937 (2007) 1427–1435. https://doi.org/10.1080/ 07373930701536718.
[372] P. Buera, C. Schebor, B. Elizalde, Effects of carbohydrate crystallization on stability of dehydrated foods and ingredient formulations, J. Food Eng. 67 (2005) 157–165. https://doi.org/10.1016/j.jfoodeng.2004.05.052.
[373] J.H. Crowe, B.J. Spargo, L.M. Crowe, Preservation of dry liposomes does not require retention of residual water, Proc. Natl. Acad. Sci. U. S. A. 84 (1987) 1537–1540. https://doi.org/10.1073/pnas.84.6.1537.
[374] Y. Xu, Y. Guo, Y. Yang, Y. Meng, X. Xia, Y. Liu, Stabilization of deformable nanovesicles based on insulin-phospholipid complex by freeze-drying, Pharmaceutics. 11 (2019) 539. https://doi.org/10.3390/pharmaceutics11100539.
[375] J.F. Pontes, A. Grenha, Multifunctional nanocarriers for lung drug delivery, Nanomaterials. 10 (2020) 183. https://doi.org/10.3390/nano10020183.
[376] A. Cripps, M. Riebe, M. Schulze, R. Woodhouse, Pharmaceutical transition to non-CFC pressurized metered dose inhalers, Respir. Med. 94 (2000) 3–9. https://doi. org/10.1016/S0954-6111(00)80143-2.

[377] P.M. Young, R. Price, M.J. Tobyn, M. Buttrum, F. Dey, Effect of humidity on aerosolization of micronized drugs, Drug Dev. Ind. Pharm. 29 (2003) 959–966. https://doi.org/g Dev. Indhttps://doi.org/10.1081/DDC-120025453.

[378] N.E. Hunter, C.S. Frampton, D.Q.M. Craig, P.S. Belton, The use of dynamic vapour sorption methods for the characterisation of water uptake in amorphous trehalose, Carbohydr. Res. 345 (2010) 1938–1944. https://doi.org/10.1016/j. carres.2010.06.011.

[379] I. Sibum, P. Hagedoorn, M.P.G. Kluitman, M. Kloezen, H.W. Frijlink, F. Grasmeijer, Dispersibility and storage stability optimization of high dose isoniazid dry powder inhalation formulations with L-leucine or trileucine, Pharmaceutics. 12 (2020) 1–14. https://doi.org/10.3390/pharmaceutics12010024.

[380] Protein Therapeutics Market Share, Size, Growth, Opportunity and Forecast 2022-2027, (2022). https://www.imarcgroup.com/protein-therapeutics-market (accessed January 16, 2023).

[381] S. Cao, S. Xu, H. Wang, Y. Ling, J. Dong, R. Xia, X. Sun, Nanoparticles: Oral Delivery for Protein and Peptide Drugs, AAPS PharmSciTech. 20 (2019) 190. https://doi.org/10.1208/s12249-019-1325-z.

[382] J.C.K. Lo, H.W. Pan, J.K.W. Lam, Inhalable Protein Powder Prepared by Spray-Freeze-Drying Using Hydroxypropyl-β-Cyclodextrin as Excipient, Pharmaceutics. 13 (2021) 615. https://doi.org/10.3390/pharmaceutics13050615.

[383] B.M. Ibrahim, S.W. Jun, M.Y. Lee, S.H. Kang, Y. Yeo, Development of inhalable dry powder formulation of basic fibroblast growth factor, Int. J. Pharm. 385 (2010) 66–72. https://doi.org/10.1016/j.ijpharm.2009.10.029.

[384] M. Wahjudi, S. Murugappan, R. van Merkerk, A.C. Eissens, M.R. Visser, W.L.J. Hinrichs, W.J. Quax, Development of a dry, stable and inhalable acyl–homoserine–lactone–acylase powder formulation for the treatment of pulmonary Pseudomonas aeruginosa infections, Eur J Pharm Sci .48 (2013) 637–643. https://doi.org/10.1016/j.ejps.2012.12.015.

[385] D.A. Fernandes, E. Costa, P. Leandro, M.L. Corvo, Formulation of spray dried enzymes for dry powder inhalers: An integrated methodology, Int. J. Pharm. 615 (2022) 121492. https://doi.org/10.1016/j.ijpharm.2022.121492.

[386] C. Costa, Z. Liu, S.I. Simões, A. Correia, A. Rahikkala, J. Seitsonen, J. Ruokolainen, A. Aguiar-Ricardo, H.A. Santos, M.L. Corvo, One-step microfluidics production of enzyme-loaded liposomes for the treatment of inflammatory diseases, Colloids Surf. B. 199 (2021) 111556. https://doi.org/10.1016/j.colsurfb.2020.111556.

[387] V.V. Shuvaev, R.Yu. Kiseleva, E. Arguiri, C.H. Villa, S. Muro, M. Christofidou-Solomidou, R.V. Stan, V.R. Muzykantov, Targeting superoxide dismutase to endothelial caveolae profoundly alleviates inflammation caused by endotoxin, J. Control. Release. 272 (2018) 1–8. https://doi.org/10.1016/j.jconrel.2017.12.025.

[388] K. Tanaka, M. Shimoda, M. Kubota, A. Takafuji, M. Kawahara, T. Mizushima, Novel pharmacological effects of lecithinized superoxide dismutase on ischemia/reperfusion injury in the kidneys of mice, Life Sci. 288 (2022) 120164. https://doi.org/10.1016/j.lfs.2021.120164.

[389] M. Danková, I. Domoráková, Z. Fagová, M. Stebnický, A. Kunová, E. Mechírová, Bradykinin and noradrenaline preconditioning influences level of antioxidant enzymes SOD, CuZn-SOD, Mn-SOD and catalase in the white matter of spinal cord in rabbits after ischemia/reperfusion, Eur J Histochem. 63 (2019), 197-203. https://doi.org/10.4081/ejh.2019.3045.

[390] M.E.M. Cruz, M.L. Corvo, M.B. Martins, S. Simões, M.M. Gaspar, Liposomes as Tools to Improve Therapeutic Enzyme Performance, Pharmaceutics. 14 (2022) 531. https://doi.org/10.3390/pharmaceutics14030531.

[391] C. Doyen, E. Larquet, P.-D. Coureux, O. Frances, F. Herman, S. Sablé, J.-P. Burnouf, C. Sizun, E. Lescop, Nuclear Magnetic Resonance Spectroscopy: A Multifaceted Toolbox to Probe Structure, Dynamics, Interactions, and Real-Time In Situ Release Kinetics in Peptide-Liposome Formulations, Mol. Pharmaceutics. 18 (2021) 2521–2539. https://doi.org/10.1021/acs.molpharmaceut.1c00037.

[392] M. Porras-Gómez, H. Kim, M.T. Dronadula, N. Kambar, C.J.B. Metellus, N.R. Aluru, A. van der Zande, C. Leal, Multiscale compression-induced restructuring of stacked lipid bilayers: From buckling delamination to molecular packing, PLoS ONE. 17 (2022) e0275079. https://doi.org/10.1371/journal.pone.0275079.

[393] Elhissi, Abdelbary, Liposomes for Pulmonary Drug Delivery: The Role of Formulation and Inhalation Device Design, Curr Pharm Des. 23 (2017) 362–372. https://doi.org/10.2174/1381612823666161116114732

[394] Committee for Human Medicinal Products, ICH guideline Q3C (R6) on impurities: guideline for residual solvents, (2017).

[395] F.J. Martinez, J.F. Donohue, S.I. Rennard, The future of chronic obstructive pulmonary disease treatment—difficulties of and barriers to drug development, The Lancet. 378 (2011) 1027–1037. https://doi.org/10.1016/S0140-6736(11)61047-7.

[396] C. Janson, Inhaled corticosteroids in COPD: risk and benefits, Thorax. 77 (2022) 530–531. https://doi.org/10.1136/thoraxjnl-2021-217930.

[397] A. Mitani, A. Azam, C. Vuppusetty, K. Ito, N. Mercado, P.J. Barnes, Quercetin restores corticosteroid sensitivity in cells from patients with chronic obstructive pulmonary disease, Exp. Lung Res. 43 (2017) 417–425. https://doi.org/10.1080/01902148.2017.1393707.
[398] G. Derosa, P. Maffioli, A. D'Angelo, F. Di Pierro, A role for quercetin in coronavirus disease 2019 (COVID-19), Phytother Res. 35 (2021) 1230–1236. https://doi.org/10.1002/ptr.6887.
[399] H. Abdelkader, Z. Fathalla, Investigation into the Emerging Role of the Basic Amino Acid L-Lysine in Enhancing Solubility and Permeability of BCS Class II and BCS Class IV Drugs, Pharm. Res. 35 (2018) 160. https://doi.org/10.1007/s11095-018-2443-0.
[400] G. Gregoriadis, Liposomes in Drug Delivery: Present and Future, in: O. Braun-Falco, H.C. Korting, H.I. Maibach (Eds.), Liposome Dermatics, Springer Berlin Heidelberg, Berlin, Heidelberg, 1992: pp. 346–352. https://doi.org/10.1007/978-3-642-48391-2_37.
[401] M.H. Gordon, A. Roedig-Penman, Antioxidant activity of quercetin and myricetin in liposomes, Chem. Phys. Lipids. 97 (1998) 79–85. https://doi.org/10.1016/S0009-3084(98)00098-X.
[402] E. Alexopoulou, A. Georgopoulos, K.A. Kagkadis, C. Demetzos, Preparation and Characterization of Lyophilized Liposomes with Incorporated Quercetin, J. Liposome Res. 16 (2006) 17–25. https://doi.org/10.1080/08982100500528594.
[403] R. Rezaei-Sadabady, A. Eidi, N. Zarghami, A. Barzegar, Intracellular ROS protection efficiency and free radical-scavenging activity of quercetin and quercetin-encapsulated liposomes, Artif Cells Nanomed Biotechnol. 44 (2016) 128–134. https://doi.org/10.3109/21691401.2014.926456.
[404] J. Azzi, A. Jraij, L. Auezova, S. Fourmentin, H. Greige-Gerges, Novel findings for quercetin encapsulation and preservation with cyclodextrins, liposomes, and drug-in-cyclodextrin-in-liposomes, Food Hydrocoll. 81 (2018) 328–340. https://doi.org/10.1016/j.foodhyd.2018.03.006.
[405] M. Ferreira-Silva, C. Faria-Silva, M.C. Carvalheiro, S. Simões, H.S. Marinho, P. Marcelino, M.C. Campos, J.M. Metselaar, E. Fernandes, P.V. Baptista, A.R. Fernandes, M.L. Corvo, Quercetin Liposomal Nanoformulation for Ischemia and Reperfusion Injury Treatment, Pharmaceutics. 14 (2022) 104. https://doi.org/10.3390/pharmaceutics14010104.
[406] N. Alhajj, N.J. O'Reilly, H. Cathcart, Development and characterization of a spray-dried inhalable ciprofloxacin-quercetin co-amorphous system, Int. J. Pharm. 618 (2022) 121657. https://doi.org/10.1016/j.ijpharm.2022.121657.

[407] P. Indra, E. Zaini, F. Ismed, H. Lucida, Preparation and characterization of quercetin-polyvinylpyrrolidone K-30 spray dried solid dispersion, J. Pharm. Pharmacogn. Res. 8 (2020) 127-134.

[408] Park, S. H., Song, I., & Choi, M., Preparation and Characterization of Quercetin-Loaded Solid Dispersion by Solvent Evaporation and Freeze-Drying Method, Mass Spectrom. Lett. 7 (2016) 79–83. https://doi.org/10.5478/MSL.2016.7.3.79.

[409] S. Scalia, M. Haghi, V. Losi, V. Trotta, P.M. Young, D. Traini, Quercetin solid lipid microparticles: A flavonoid for inhalation lung delivery, Eur J Pharm Sci. 49 (2013) 278–285. https://doi.org/10.1016/j.ejps.2013.03.009.

[410] P. Papakyriakopoulou, K. Manta, C. Kostantini, S. Kikionis, S. Banella, E. Ioannou, E. Christodoulou, D.M. Rekkas, P. Dallas, M. Vertzoni, G. Valsami, G. Colombo, Nasal powders of quercetin-β-cyclodextrin derivatives complexes with mannitol/lecithin microparticles for Nose-to-Brain delivery: In vitro and ex vivo evaluation, Int. J. Pharm. 607 (2021) 121016. https://doi.org/10.1016/j.ijpharm.2021.121016.

[411] L.X. Yu, G. Amidon, M.A. Khan, S.W. Hoag, J. Polli, G.K. Raju, J. Woodcock, Understanding Pharmaceutical Quality by Design, AAPS PharmSciTech. 16 (2014) 771–783. https://doi.org/10.1208/s12248-014-9598-3.

[412] J. Eid, A. Jraij, H. Greige-Gerges, L. Monticelli, Effect of quercetin on lipid membrane rigidity: assessment by atomic force microscopy and molecular dynamics simulations, Biochim Biophys Acta Advances. 1 (2021) 100018. https://doi.org/10.1016/j.bbadva.2021.100018.

[413] L. Movileanu, I. Neagoe, M.L. Flonta, Interaction of the antioxidant flavonoid quercetin with planar lipid bilayers, Int. J. Pharm. 205 (2000) 135–146. https://doi.org/10.1016/S0378-5173(00)00503-2.

[414] S.P. Toopkanloo, T.B. Tan, F. Abas, F.A. Alharthi, I.A. Nehdi, C.P. Tan, Impact of Quercetin Encapsulation with Added Phytosterols on Bilayer Membrane and Photothermal-Alteration of Novel Mixed Soy Lecithin-Based Liposome, Nanomaterials. 10 (2020) 2432. https://doi.org/10.3390/nano10122432.

[415] U. Sadiq, H. Gill, J. Chandrapala, F. Shahid, Influence of Spray Drying on Encapsulation Efficiencies and Structure of Casein Micelles Loaded with Anthraquinones Extracted from Aloe vera Plant, Appl. Sci. 13 (2022) 110. https://doi.org/10.3390/app13010110.

[416] A. Chafer, T. Fornari, A. Berna, R.P. Stateva, Solubility of quercetin in supercritical CO_2 + ethanol as a modifier: measurements and thermodynamic modelling, J Supercrit Fluids. 32 (2004) 89–96. https://doi.org/10.1016/j.supflu.2004.02.005.

[417] M. Mamani-Matsuda, T. Kauss, A. Al-Kharrat, J. Rambert, F. Fawaz, D. Thiolat, D. Moynet, S. Coves, D. Malvy, M.D. Mossalayi, Therapeutic and preventive properties of quercetin in experimental arthritis correlate with decreased macrophage inflammatory mediators, Biochem. Pharmacol. 72 (2006) 1304–1310. https://doi.org/10.1016/j.bcp.2006.08.001.

[418] A. Priprem, J. Watanatorn, S. Sutthiparinyanont, W. Phachonpai, S. Muchimapura, Anxiety and cognitive effects of quercetin liposomes in rats, Nanomed-Nanotechnol 4 (2008) 70–78. https://doi.org/10.1016/j.nano.2007.12.001.

A

APPENDIX

The information in this appendix is related to Chapter 3.

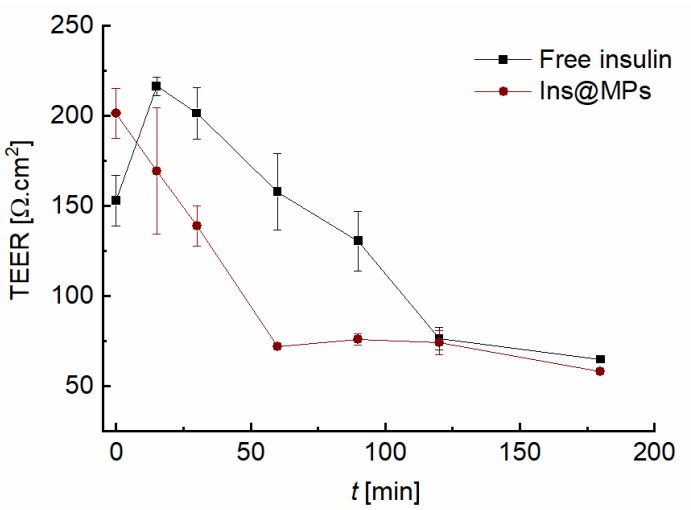

Figure A 1- TEER values, at different time-points, for Caco-2/HT29-MTX monolayer after incubation, at 37°C and for 3 hours, with insulin-loaded nano-in-microparticles (Ins@MPs) and free insulin. The results are expressed as mean ± S.D. (n = 3).

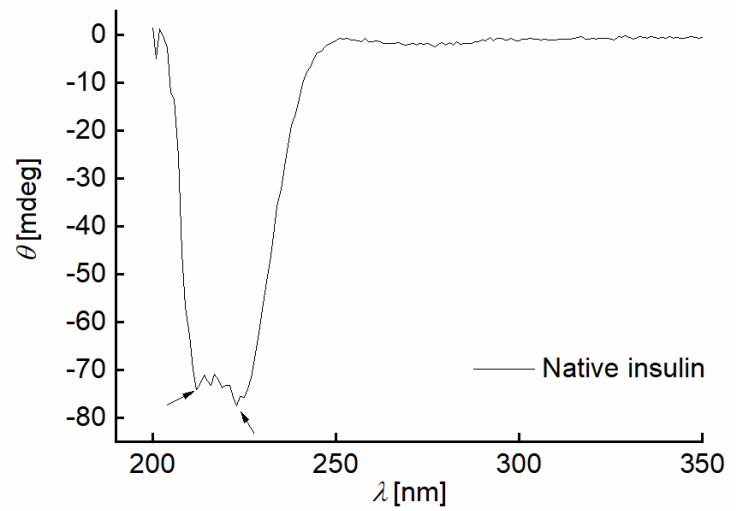

Figure A 2- Circular Dichroism of insulin in its native form at 1.0 mg/mL, in HBSS-HEPES (pH 7.4). The results are expressed as mean ± S.D (n = 3).

B

APPENDIX

The information in this appendix is related to Chapter 4.

Table B 1- Mass balance of CF, lipids and casting solution before and after SASD, for the DoE.

Assay	Before SASD		After SASD	
	CF/Lip (µg/ µmol)	Lip/Exc (µmol/g)	CF/Lip (µg/ µmol)	Lip/Exc (µmol/g)
Blank Sample	-	8.39	-	3.35
L1_CF_EtOH0	0.444	9.20	0.074	6.03
L1_CF_EtOH15		10.6	0.058	7.75
L1_CF_EtOH30		10.6	0.055	8.46
L2_CF_EtOH0		12.4	0.054	7.43
L2_CF_EtOH15	0.099	12.4	0.086	7.43
L2_CF_EtOH30		12.4	0.045	8.46
L3_CF_EtOH0		13.9	0.069	8.10
L3_CF_EtOH15		13.9	0.050	7.64
L3_CF_EtOH30		13.9	0.052	8.80
Blank Sample_R	-	9.50	-	5.86
L1_CF_EtOH0_R		9.50	0.068	6.17
L1_CF_EtOH15_R		10.6	0.061	6.70
L1_CF_EtOH30_R		10.6	0.073	7.58
L2_CF_EtOH0_R	0.096	12.4	0.076	7.64
L2_CF_EtOH15_R		12.4	0.090	6.40
L2_CF_EtOH30_R		12.4	0.080	6.40
L3_CF_EtOH0_R		13.9	0.082	7.18

L3_CF_EtOH15_R		13.9	0.070	6.95
L3_CF_EtOH30_R		13.9	0.083	7.64

CF: 5(6)- carboxyfluorescein; Exc: Trehalose and L-Leu; R: Replicate

Table B 2- Liposomal and Lip-DPFs responses obtained for each DoE experiment: liposome size, polydispersity index (PdI), lipid yield (η_{Lipid}), encapsulation efficiency (EE_{CF}), CF_Lip-DPFs process yield (η_{SASD}), mean volumetric diameters (Dv_{50}) and span.

Assays	Liposomes characterization				Lip-DPFs characterization		
	Size (nm)	PdI	η_{Lipid} (%)	EE_{CF} (%)	η_{SASD} (%)	Dv_{50} (µm)	Span
Blank Sample	236	0.52	40	-	68	13.3	3.31
L1_CF_EtOH0	311	0.76	66	71	65	4.54	1.04
L1_CF_EtOH15	276	0.28	73	58	65	9.86	4.11
L1_CF_EtOH30	265	0.44	80	55	67	7.47	3.82
L2_CF_EtOH0	116	0.18	60	54	60	7.69	3.60
L2_CF_EtOH15	117	0.15	60	86	56	9.06	4.00
L2_CF_EtOH30	112	0.16	68	45	58	7.63	3.45
L3_CF_EtOH0	104	0.16	58	70	58	12.1	5.35
L3_CF_EtOH15	106	0.16	55	51	56	11.3	5.51
L3_CF_EtOH30	101	0.17	63	52	49	11.7	5.61
Blank Sample_R	206	0.44	62	-	76	17.2	2.99
L1_CF_EtOH0_R	313	0.43	65	70	65	7.21	5.65
L1_CF_EtOH15_R	242	0.29	63	63	61	11.1	5.44
L1_CF_EtOH30_R	228	0.41	72	75	58	11.3	4.85
L2_CF_EtOH0_R	111	0.18	62	79	61	9.08	4.50
L2_CF_EtOH15_R	115	0.15	52	93	69	6.89	3.55
L2_CF_EtOH30_R	112	0.18	52	83	54	6.01	3.13
L3_CF_EtOH0_R	109	0.20	52	85	66	12.3	5.51

L3_CF_EtOH15_R	103	0.19	50	73	55	9.08	3.90
L3_CF_EtOH30_R	98	0.20	55	87	47	10.2	4.61

Table B 3- Mass balance of CF, lipids and casting solution before and after SASD, for the stability assays.

Assay	CF/Lip (µg /µmol)	Lip/Exc (µmol/g)	CF/Exc (µg/g)
CF_Lip (before SASD)	0.05 ± 0.01	9.8 ± 0.6	0.51 ± 0.03
CF_Lip (after SASD)	0.07 ± 0.01	6.8 ± 0.6	0.51 ± 0.06

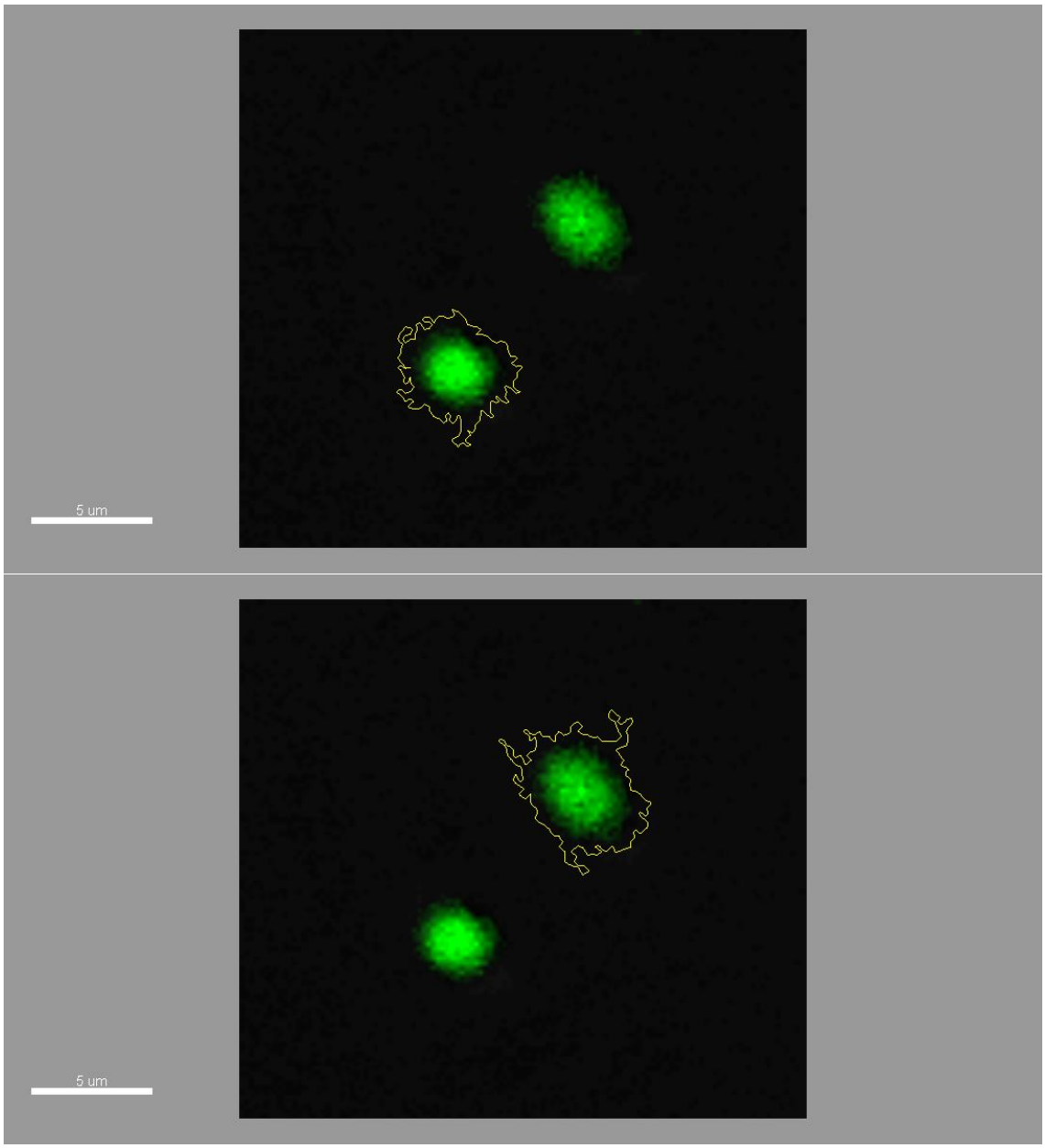

Figure B 1- Confocal fluorescence microscope images of CF_Lip localization inside the CF_Lip-DPFs, using a 10x objective (scale bar: 5 µm).

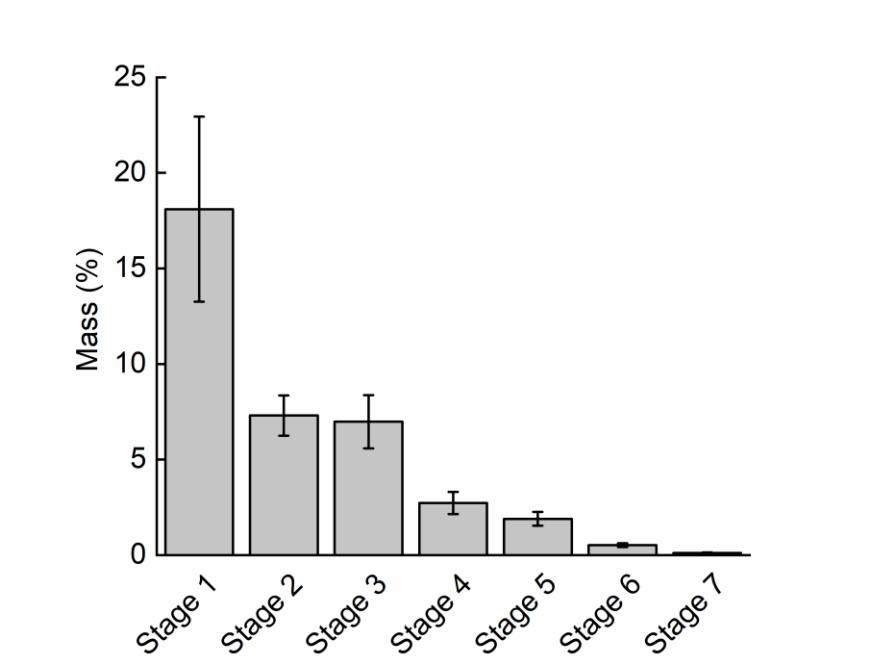

Figure B 2- ACI tests for the powders stored at RH of 78 %, after 7 days, at 20ºC.

A

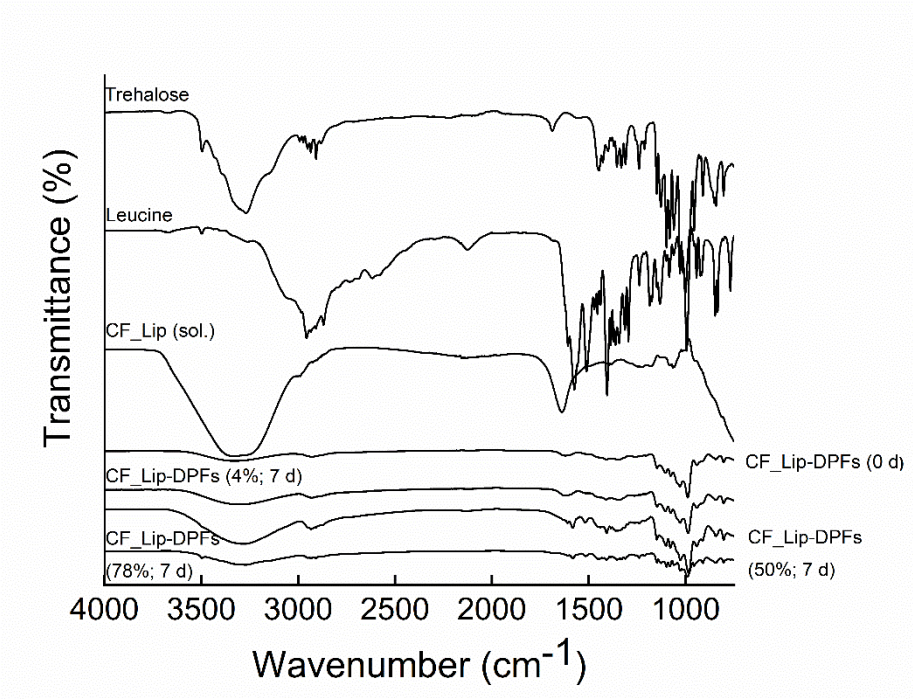

B

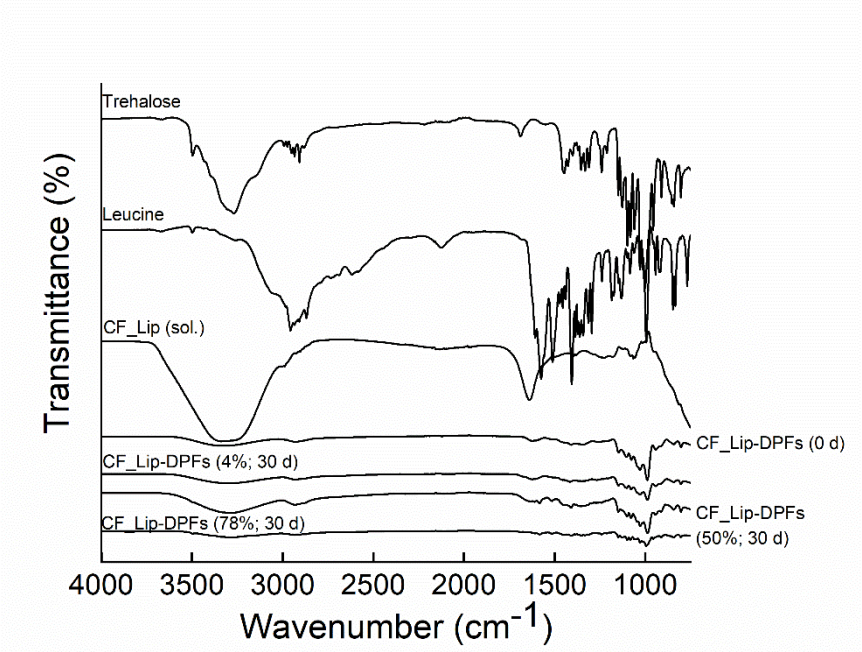

Figure B 3- ATR- FTIR analysis of the raw materials, liposomes in suspension form and CF_Lip-DPFs after SASD and after A) 7 days and B) 30 days.

C

APPENDIX

The information in this appendix is related to Chapter 6.

Table C 1 - Physicochemical characterization and incorporation efficiency *(IE)* of negative, neutral, and cationic

		Size [nm]	PdI	ζ- potential [mV]	Lipid [µmol/mL]	$(Quer/Lip)_f$ [µg/µmol]	*IE* [%]	
Negative*	10:0.5	137 ± 14		0.089 ± 0.048	- 24 ± 2	101 ± 6	12 ± 5	92 ± 3
Quer_Lip	10:1	147 ± 1		0.114 ± 0.017	- 28 ± 1	100 ± 2	35 ± 6	89 ± 1
Neutral§	10:0.5	150 ± 5		0.113 ± 0.029	- 1.1 ± 0.2	95 ± 3	19 ± 4	99 ± 15
Quer_Lip	10:1	153 ± 7		0.152 ± 0.023	- 1.0 ± 0.1	96 ± 5	34 ± 5	72 ± 5
Cationic¥	10:0.5	195 ± 2		0.093 ± 0.016	14 ± 1	92 ± 7	15 ± 3	99 ± 5
Quer_Lip	10:1	188 ± 10		0.122 ± 0.057	14 ± 2	100 ± 4	28 ± 1	88 ± 10

Quer_Lip, before SASD.

The results are expressed as mean ± S.D (n = 3).
*Liposomes components: DMPC: DMPG in a molar ratio of 7:3
§Liposomes components: E-PC:Chol in a molar ratio of 9:1
¥Liposomes components: E-PC:Chol:SA in a molar ratio of 8:1:1

Table C 2- SASD process parameters.

		p_{SM} [bar]	T_{SM} [°C]	T_{in} [°C]	T_{out} [°C]	Yield Process [%]	Water content [%]
Negative* Quer_Lip	10:0.5	121 ± 1	91 ± 4	99 ± 7	66 ± 5	58	6
	10:1	120 ± 1	84 ± 10	101 ± 8	66 ± 5	65	6
Neutral§ Quer_Lip	10:0.5	121 ± 1	92 ± 3	93 ± 2	63± 0.2	66	6
	10:1	121 ± 2	83 ± 7	98± 4	66 ± 5	48	7
Cationic¥ Quer_Lip	10:0.5	120 ± 1	83 ± 7	102 ± 7	68 ± 1	65	5
	10:1	121 ± 1	80 ± 5	101 ± 8	66 ± 1	56	6

Table C 3- Physicochemical characterization and incorporation efficiency (IE) of resuspended neutral and cationic liposomes and Quer_Lip, after SASD.

		Size [nm]	PdI	ζ- potential [mV]	Lipid [µmol/mL]	$(Quer/Lip)_f$ [µg/µmol]	*IE* [%]
Negative Quer_Lip	10:0.5	117	0.139	-7.2	71	0.9	14
	10:1	150	0.240	-12.2	65	2.7	13
Neutral Quer_Lip	10:0.5	146	0.240	-2.7	45	13	37
	10:1	293	0.401	-2.1	38	22	32
Cationic Quer_Lip	10:0.5	240	0.376	4.1	60	9	28
	10:1	276	0.490	7.7	43	8	69

2023

CLARINDA ISABEL DA SILVA E COSTA SEQUEIRA

INTEGRATED MANUFACTURE OF LIPOSOMAL DRY POWDER FORMULATIONS